UNIVERSITEIT VAN PRETORIA
UNIVERSITY OF PRETORIA
YUNIBESITHI YA PRETORIA

LOUBSER, CHRISTA

FLUORINATED FERROELECTRIC LIQUID CRYSTALS: SYNTHESIS, PROPERTIES AND FLUORINE-19 NMR.

DPhil (Chemistry) UP 1993

Digitised by the Department of Library Services in support of open access to information, University of Pretoria, 2021.

UNIVERSITEIT VAN PRETORIA
UNIVERSITY OF PRETORIA
YUNIBESITHI YA PRETORIA

Fluorinated ferroelectric liquid crystals: Synthesis, properties and fluorine-19 nmr.

A dissertation submitted by

CHRISTA LOUBSER

Hons (BSc), MSc

in partial fulfilment of the requirements
for the degree of

DOCTOR OF PHILOSOPHY

in

CHEMISTRY

in the Faculty of Natural Sciences of the

UNIVERSITY OF PRETORIA

August 1993

Digitised by the Department of Library Services in support of open access to information, University of Pretoria, 2021.

UNIVERSITEIT VAN PRETORIA
UNIVERSITY OF PRETORIA
YUNIBESITHI YA PRETORIA

Fluorinated ferroelectric liquid crystals: Synthesis, properties and fluorine-19 nmr.

Candidate: Christa Loubser
Supervisor: Prof. P.L. Wessels
Department of Chemistry, University of Pretoria
Degree: PhD (Chemistry)

ABSTRACT

A series of new laterally fluorinated liquid crystals containing a single chiral centre on the terminal chain, was synthesised. All the compounds, with a single exception, exhibit a ferroelectric smectic C* phase. Their liquid crystalline properties were investigated using optical polarising microscopy and differential scanning calorimetry, while ferroelectric properties were studied electro-optically.

The number / position of the lateral fluoro-substituents greatly influence the incidence and range of the liquid crystalline phases. The 2,3 - difluorophenyl unit stabilises the cholesteric and smectic C* phases, but suppresses the formation of the smectic A phase. The 2',3 - difluorobiphenyl unit, in contrast, discourages the formation of helical phases.

A helix inversion occurs in the cholesteric phase of (S)-4-n-octyloxy-2,3-difluorobiphenyl-4'-yl 3-fluoro-4-(2-fluorooctanoyloxy)benzoate. Due to certain structural features, the phenomenon could not be explained in terms of the conventional model. Instead, competing conformer species created through interaction between fluoro-substituents on the core and at the chiral centre, are suggested.

The influence of the lateral fluoro-substituents on the ferroelectric properties was investigated. Two of the compounds exhibit unusual tilt angle behaviour - the tilt angle decreases with decreasing temperature. A helix inversion takes place in the smectic C* phase of (S)-4-n-octyloxy-2',3-difluorobiphenyl-4'-yl 2-fluoro-4-(2-fluorooctanoyloxy)benzoate and is thought to be due to the presence of the 2',3-difluorobiphenyl unit.

The orientational ordering of several of the liquid crystals was investigated using ^{19}F nmr. A new technique was developed for this purpose and used to determine the order parameter as a function of temperature of (S)-4-n-octyloxy-2,3-difluorobiphenyl-4'-yl 4-(2-chloro-4-methylpentanoyl-oxy)benzoate from the dipolar coupling constant, D_{FF}.

Digitised by the Department of Library Services in support of open access to information, University of Pretoria, 2021.

The question of possible coupling between dipoles on the core and the chiral centre was addressed. For the first time it is experimentally shown that such an interaction does exist for two fluoro-substituents (^{19}F - ^{19}F dipolar coupling). Conformational analysis revealed a transverse electrostatic gradient.

The conformation of the 2',3-difluorobiphenyl unit was investigated by using ^{19}F nmr in conjunction with crystal structure data. It appears that the net dipole moment as well as the effective size of this unit play an important role.

Digitised by the Department of Library Services in support of open access to information, University of Pretoria, 2021.

SAMEVATTING

'n Reeks nuwe sywaarts-gefluorineerde vloeikristalle, met 'n enkele chirale sentrum op die terminale ketting, is gesintetiseer. Al die verbindings, met 'n enkele uitsondering, beskik oor 'n ferroëlektriese smektiese C* fase. Hul vloeikristallyne eienskappe is ondersoek deur van optiese polariserende mikroskopie en differensiële skandeerkalorimetrie gebruik te maak, terwyl die ferroëlektriese eienskappe elektro-opties bestudeer is.

Die aantal / posisie van die sywaartse fluoro-substituente beïnvloed die voorkoms en strekking van die vloeikristalfases aansienlik. Die 2,3-difluorofeniel-eenheid stabiliseer die cholesteriese en smektiese C* fases, maar onderdruk die vorming van die smektiese A fase. In teenstelling hiermee ontmoedig die 2',3-difluorobifeniel-eenheid die vorming van heliese fases.

'n Ommekeer van die heliks vind in die cholesteriese fase van (S)-4-n-oktieloksi-2,3-difluorobifeniel-4'-iel 3-fluoro-4-(2-fluoro-oktanoïel-oksi)bensoaat plaas. A.g.v. sekere strukturele kenmerke, kan die verskynsel nie in terme van die konvensionele model verklaar word nie. In plaas daarvan word kompeterende konformeerspesies, geskep d.m.v. 'n interaksie tussen fluoro-substituente op die kerngedeelte en die chirale sentrum, voorgestel.

Die invloed van die sywaartse fluoro-substuente op die ferroëlektriese eienskappe is ondersoek. Twee van die verbindings toon ongewone gedrag - die hoek waarteen die molekules oorhel neem af met afnemende temperatuur. 'n Ommekeer van die heliks vind in die smektiese C* fase van (S)-4-n-oktieloksi-2',3-difluorobifeniel-4'-iel 2-fluoro-4-(2-fluoro-oktanoïel-oksi)bensoaat plaas en word aan die invloed van die 2',3-difluorobifeniel-eenheid toegeskryf.

Die geörienteerde orde van verskeie van die vloeikristalle is ondersoek deur van ^{19}F kmr gebruik te maak. 'n Nuwe tegniek is vir hierdie doel ontwikkel en gebruik om die ordeparameter as 'n funksie van temperatuur van (S)-4-n-oktieloksi-2,3-difluorobifeniel-4'-iel 4-(2-chloro-4-metielpentanoïel-oksi) bensoaat vanaf die dipolare koppellingskonstante, D_{FF}, te bepaal.

Die vraagstuk aangaande moontlike koppelling tussen dipole op die kern en die chirale sentrum is aangespreek. Vir die eerste keer is daar eksperimenteel aangetoon dat so 'n interaksie wel tussen twee fluoro-substituente bestaan (^{19}F - ^{19}F dipolare koppelling). Konformasie-analise het aan die lig gebring dat 'n transverse elektrostatiese gradiënt bestaan.

Die konformasie van die 2',3-difluorobifeniel-eenheid is ondersoek deur van ^{19}F kmr tesame met kristalstruktuurdata gebruik te maak. Dit word aan die hand gedoen dat die netto dipoolmoment asook die effektiewe grootte van hierdie eenheid 'n belangrike rol speel.

Digitised by the Department of Library Services in support of open access to information, University of Pretoria, 2021.

UNIVERSITEIT VAN PRETORIA
UNIVERSITY OF PRETORIA
YUNIBESITHI YA PRETORIA

PUBLICATIONS

Sections of the work presented in this dissertation have been / will be published as follows...

1. *The synthesis and crystal structure of a liquid-crystalline ester of 4-carboxyphenylferrocene.* C. Loubser, C. Imrie and P.H. van Rooyen; *Adv. Mater.* **5** (1993) 45.

2. *Observing molecular motions of a fluorinated ferroelectric liquid crystal using fluorine-19 nmr.* C. Loubser, P.L. Wessels, J.W. Goodby and P. Styring; *Liq. Cryst.* **15** (1993); in press.

3. *Liquid crystals, materials and devices.* J.W. Goodby, C.Loubser and P. Styring. British Patent 9312095.4.

4. *A helix inversion in the chiral nematic phase of a ferroelectric liquid crystal containing a single chiral centre.* C. Loubser, P.L. Wessels, P.Styring and J.W. Goodby; accepted by *J. Mater. Chem.*

5. *Inversion phenomena in chiral liquid crystals.* J.W. Goodby, P.Styring, J.D. Vuijk, A.J. Slaney, J.S. Patel and C. Loubser. *Ferroelectrics* 1994; accepted for publication.

6. Ferroelectric liquid crystals with an (S)-2-fluorooctanoyloxy unit: synthesis and properties. C. Loubser, J.W. Goodby and P. Styring; manuscript in preparation.

7. *Orientational properties of fluorinated ferroelectric liquid crystals: a spectroscopic study using ^{19}F - ^{19}F dipolar coupling.* C. Loubser, J.W. Goodby and P.L. Wessels; submitted.

8. *^{19}F nmr data of fluorinated ferroelectric liquid crystals.* C. Loubser and P.L Wessels; manuscript in preparation.

... while some of the work was presented at the following international conference:

*European Conference on Liquid Crystals. Science and Technology (***ECLC 93**).
7 - 12 March 1993, Flims, Switzerland. Poster **MB-1**.

Digitised by the Department of Library Services in support of open access to information, University of Pretoria, 2021.

UNIVERSITEIT VAN PRETORIA
UNIVERSITY OF PRETORIA
YUNIBESITHI YA PRETORIA

ACKNOWLEDGEMENT

I would like to express my sincere gratitude towards the following without whose efforts a project as diverse could not have been completed:

My supervisor, prof. P.L. Wessels, for assistance with various aspects of the work involving nmr;

Prof. John W. Goodby, of the University of Hull in England for allowing me to work in his laboratory during the period February 1991 - October 1991 and again in March 1993. My sincere appreciation for his assistance, enthusiasm for the project and cheerfulness and also for realising that South Africans can be quite normal.

The following persons who, each one in some way or another, also contributed to the successful completion of the work:
Prof. Peet van Rooyen (UP), dr Peter Styring (UoH), prof. Robert Vleggaar (UP), dr Tony Chalmers (CSIR), dr Ken Toyne (UoH), dr Mike Hird (UoH), dr Christien Strydom (UP) and also the technical staff at both the University of Pretoria and the University of Hull.

The chemical information specialist at the Merensky Library, mrs. Leonora Wydeman, whose dedicated assistance throughout the years remains much appreciated. The librarian at the Science Library of the University of South Africa, mrs. Verheem, for her relentless efforts to locate books / journals.

My fellow-students for support and friendship in moments of both joy and despair.

A special friend, dr Christopher Imrie, for his interest in the work and encouragement throughout.

The University of Pretoria (in particular the Carl and Emily Fuchs Institute for Microelectronics) and the Foundation for Research Development (FRD, Pretoria) for financial support.

Finally, I would like to dedicate this dissertation to the memory of my late mother, who passed away in August 1991 while I was in Hull, and who would have been so proud ....

Digitised by the Department of Library Services in support of open access to information, University of Pretoria, 2021.

UNIVERSITEIT VAN PRETORIA
UNIVERSITY OF PRETORIA
YUNIBESITHI YA PRETORIA

LIST OF LIQUID CRYSTALS

34 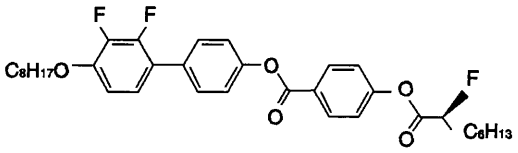

35 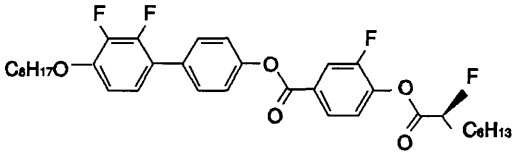

36 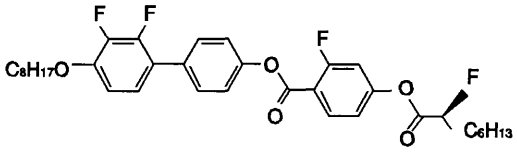

37 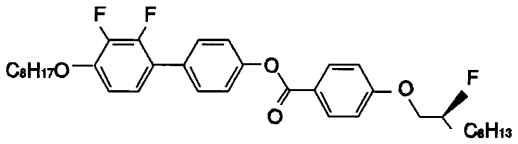

38 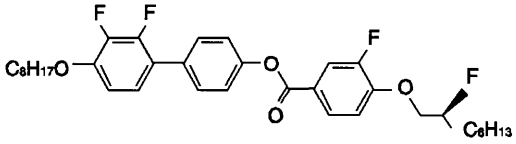

39 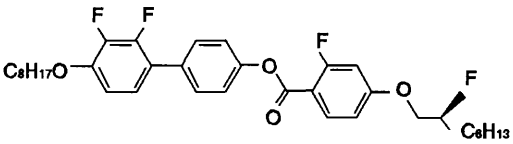

48 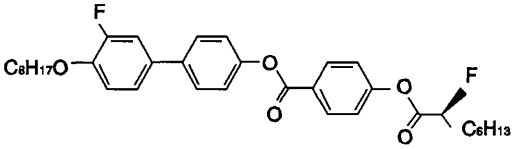

49 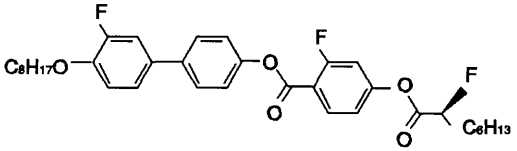

50 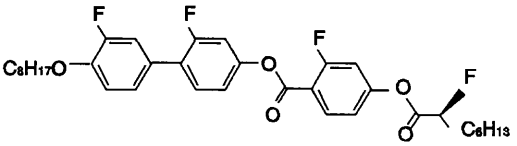

Digitised by the Department of Library Services in support of open access to information, University of Pretoria, 2021.

UNIVERSITEIT VAN PRETORIA
UNIVERSITY OF PRETORIA
YUNIBESITHI YA PRETORIA

LIST OF LIQUID CRYSTALS (CONTINUED)

51 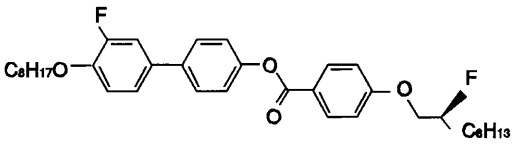

52 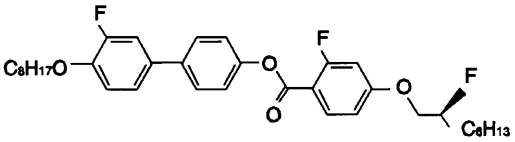

53 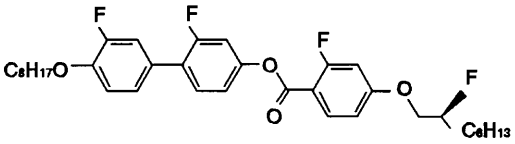

54 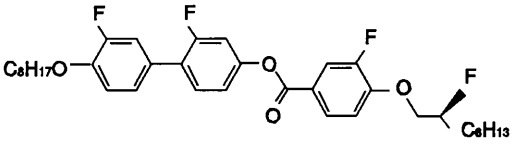

55 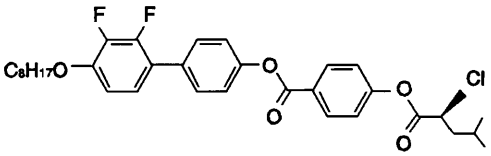

56 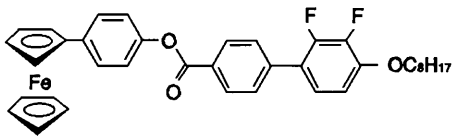

Digitised by the Department of Library Services in support of open access to information, University of Pretoria, 2021.

UNIVERSITEIT VAN PRETORIA
UNIVERSITY OF PRETORIA
YUNIBESITHI YA PRETORIA

CONTENTS

Digitised by the Department of Library Services in support of open access to information, University of Pretoria, 2021.

UNIVERSITEIT VAN PRETORIA
UNIVERSITY OF PRETORIA
YUNIBESITHI YA PRETORIA

Digitised by the Department of Library Services in support of open access to information, University of Pretoria, 2021.

UNIVERSITEIT VAN PRETORIA
UNIVERSITY OF PRETORIA
YUNIBESITHI YA PRETORIA

Digitised by the Department of Library Services in support of open access to information, University of Pretoria, 2021.

UNIVERSITEIT VAN PRETORIA
UNIVERSITY OF PRETORIA
YUNIBESITHI YA PRETORIA

CHAPTER 1

GENERAL INTRODUCTION

1.1 Introduction and outline of project

The ferroelectric display device has received much attention in recent years because of its great potential as a fast switching device with a high multiplexability[1-4]. Although there are several physical properties and requirements which are important in formulating materials for use in this device, a fundamental understanding of the behaviour of the molecules in a liquid crystalline phase (and particularly the ferroelectric smectic C* phase) and correlating this with the molecular structure is of great importance. In this regard nuclear magnetic resonance spectroscopy (nmr) can reveal more information than any other physical technique because of its ability to probe each nucleus *via* its distinct signal.

The work described in this dissertation is the result of a collaborative project between the Nuclear Magnetic Resonance Group at the University of Pretoria and the Liquid Crystal Group at the University of Hull in England. The project arose from the need to design and synthesise new chiral smectic liquid crystals that would at the same time be suitable for nmr investigation. To this effect it was decided to exploit the advantageous properties of the fluorine atom.

Fluorine is often incorporated into liquid crystalline molecules for a variety of reasons and its relatively small size makes fluorination the ideal way of building a small probe into a particular section of a molecule. Furthermore, for nmr studies, the fluorine-19 nucleus (spin = ½) has several advantages over other commonly used nuclei such as carbon-13 or deuterium.

Thus, the project commenced with the design of a basic molecular framework which would be conducive to the stabilization of the smectic C phase (fig. 1.1). Chirality was then introduced to this structure by way of attachment of a second terminal chain containing a single chiral centre.

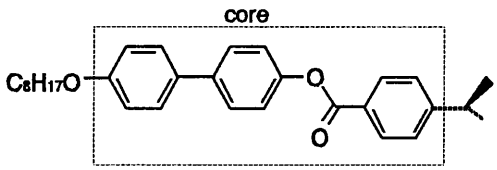

Figure 1.1

Digitised by the Department of Library Services in support of open access to information, University of Pretoria, 2021.

UNIVERSITEIT VAN PRETORIA
UNIVERSITY OF PRETORIA
YUNIBESITHI YA PRETORIA

A range of compounds was synthesised by combining this basic structure with lateral fluorination. Several of the resulting liquid crystals proved suitable for nmr work and were subsequently used in the investigation of the orientational order. These results were combined with those obtained from polarising microscopy, thermal analysis and selected electro-optical measurements to complete the picture.

In this chapter an attempt is made to provide the necessary background information for the results presented in chapters 2 to 7. More specific information is provided in the introduction to each of these chapters.

1.2 Nmr of liquid crystals

When a strong magnetic field is applied to a liquid crystal in its nematic phase, the long axes of the molecules tend to align themselves with the direction of the magnetic field. A high degree of orientation results, which makes it possible to measure the direct dipolar coupling (D_{ij}) between two nuclei (fig. 1.2).

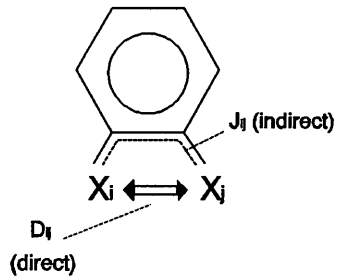

Figure 1.2 Direct coupling between two dipoles (D_{ij}) as opposed to indirect coupling *via* the electronic system (J_{ij}).

The magnitude of D_{ij} is dependent on the internuclear distance r_{ij} as well as on the degree of orientation by a factor of $3\cos^2\theta - 1$. Molecules in a smectic phase can also align with their long axes parallel to one another in the magnetic field, but the structure contains an additional degree of order, namely layering. Here the molecular motion is relatively slow, which means that intermolecular dipolar coupling becomes significant and can cause broadening of the spectral lines. In contrast to this, molecular motion in the nematic phase is sufficiently rapid to average out intermolecular interactions and spectra are largely determined by intramolecular effects.

Digitised by the Department of Library Services in support of open access to information, University of Pretoria, 2021.

UNIVERSITEIT VAN PRETORIA
UNIVERSITY OF PRETORIA
YUNIBESITHI YA PRETORIA

In the cholesteric and chiral smectic C phases the helical structure is often unwound by the magnetic field, causing them to behave like nematic and smectic C phases respectively.

The unique features of the oriented phase can thus be exploited in order to obtain direct dipolar coupling constants and hence information about the orientational order of each phase.

It is important to note that the discussion in this section refers to cases in which the molecules actually constituting the phase are studied. This should be seen as distinct from work in which small molecules dissolved in a liquid crystal (usually nematic) are observed. Studies of the latter kind are well-documented[5,6], but fall beyond the scope of this dissertation.

The first nmr study of a liquid crystal was reported in 1953 by Spence, Moses and Jain[7] who observed the ^{1}H nmr spectrum of p-azoxyanisole in its nematic phase. The spectrum was however, very poorly resolved as a result of the large number of intramolecular ^{1}H dipolar interactions. In order to overcome this problem, Phillips *et al*[8,9] selectively replaced some of the protons with deuterons (in order to restrict the number of dipolar interactions) to produce analysable spectra in which splittings could be specifically assigned. This technique has found many applications[10] and remains useful[11,12], although the replacement of protons by nuclei or groups other than ^{2}H has received little attention.

More recently, ^{13}C nmr has also found use in the study of liquid crystals[13]. This nucleus is present naturally in the molecule and there is no dipolar coupling between like spins because of its low isotopic abundance - this results in well-resolved spectra when proton spins are decoupled[13,14].

Earlier studies using ^{2}H and ^{13}C nmr were often restricted to nematogenic liquid crystals, particularly members of the well-known cyanobiphenyl class[15 - 20]:

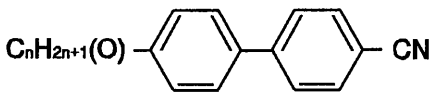

Figure 1.3

Compounds with smectic phases[14,21,22] and more specifically ferroelectric liquid crystals have not received as much attention. Consequently, as the latter form the subject of this dissertation, a concise summary of work carried out to date will be given.

Digitised by the Department of Library Services in support of open access to information, University of Pretoria, 2021.

UNIVERSITEIT VAN PRETORIA
UNIVERSITY OF PRETORIA
YUNIBESITHI YA PRETORIA

The first nmr study of a ferroelectric liquid crystal was reported by Luzar *et al*[23,24] who investigated the temperature dependence of the ^{13}C chemical shifts in the isotropic, smectic A and smectic C* phases of DOBAMBC and HOBACPC (fig. 1.4).

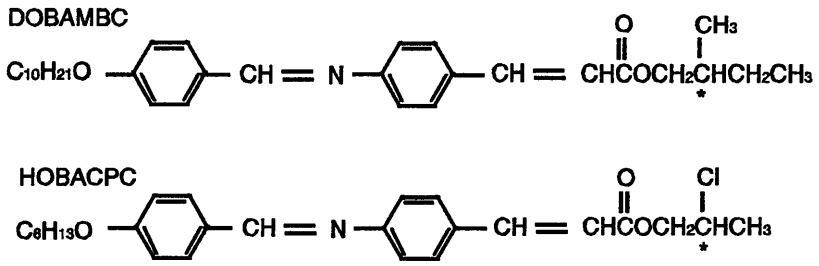

Figure 1.4

In 1989 Poon and Fung[25] published a study of the orientational ordering of the liquid crystal

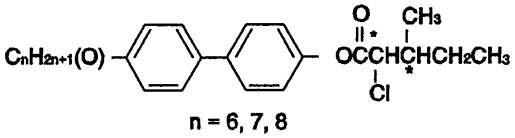

Figure 1.5

(n = 6, fig. 1.5) which has a high spontaneous polarisation. The compound was studied in its smectic A and smectic C* phases using ^{13}C 2D nmr together with the technique separated local-field spectroscopy. By obtaining carbon-proton dipolar coupling constants the order parameters were calculated for the different molecular segments. The order parameters of the core were found to increase with temperature. This is the first time the dipolar coupling constants were used to calculate the order parameters - in previous cases[24] the chemical shift data was used. Additionally, the carbon-13 chemical shifts were measured as a function of temperature and a discussion of their relation with the order parameter is given. The authors conclude that the molecular directors are oriented parallel to the magnetic field as a result of the smectic C* helix being unwound.

Subsequently, a more detailed study of the orientational ordering of two other homologues (n = 7, 8, fig.1.5), also in their smectic A and smectic C* phases, was carried out[26]. By comparing the results obtained for all three of the compounds, they concluded that while the smectic C* helix of two of the

Digitised by the Department of Library Services in support of open access to information, University of Pretoria, 2021.

UNIVERSITEIT VAN PRETORIA
UNIVERSITY OF PRETORIA
YUNIBESITHI YA PRETORIA

compounds (n = 6, 8) is unwound by the magnetic field (B_0 = 7.05 T), the helical structure of the remaining compound (n = 7) is preserved, but failed to offer any explanation.

The same technique was then used to study the orientational ordering of a series of ferroelectric thiobenzoate liquid crystals[27], shown in fig. 1.6.

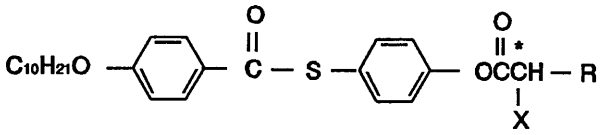

R = Me, Et, Pr, ^{i}Pr, Bu

X = Cl, CH_3

Figure 1.6

Once again the order parameters were calculated for different molecular segments from both dipolar coupling constants and chemical shift data. The order parameters of the cores of the molecules were found to increase with decreasing temperature and it is claimed that the helical structures of all the compounds are destroyed by the magnetic field. Very recently, a similar study by the same group[28] of three esters of α - chloro acids and 4-heptyloxy-4'-hydroxybiphenyl once again led to the calculation of the order parameters of the different molecular segments. The authors claimed that the helical structures of all three of the compounds are preserved in the magnetic field and were thus forced to use the racemates in order to obtain resolvable spectra.

Independently from the abovementioned work, the molecular motions (particularly around the smectic A - smectic C* transition) of the compound shown in fig. 1.7 (n = 9) were investigated by Yoshizawa *et al*[29,30] who similarly used variable temperature ^{13}C solid state cross polarization magic angle spinning nmr.

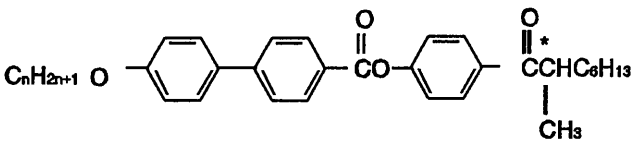

Figure 1.7

Digitised by the Department of Library Services in support of open access to information, University of Pretoria, 2021.

UNIVERSITEIT VAN PRETORIA
UNIVERSITY OF PRETORIA
YUNIBESITHI YA PRETORIA

Although their results enabled them to make conclusions concerning the motional behaviour of various molecular segments, these were deduced from relaxation measurements rather than calculation of the order parameters. More recently, they reported the ^{13}C nmr spectra of the antiferroelectric homologue[31] (n = 8, fig. 1.7) and they discussed the motional behaviour by observing the changes in the linewidth of some of the peaks. None of their compounds have a cholesteric phase (i.e. the desirable cholesteric - smectic A - smectic C* phase sequence for alignment purposes is absent) and they do not comment on the alignment of the molecules. In a subsequent investigation by them[32] the solid state ^{13}C nmr spectra of the compound shown in fig. 1.8 were recorded and this time they used the chemical shifts to estimate the order parameters of some of the carbons at a single temperature in the smectic A phase. The spectral resolution in the smectic C* phase did not permit the extraction of chemical shift data and hence no order parameters could be obtained and the authors assumed that the molecules are oriented with their directors parallel to the magnetic field.

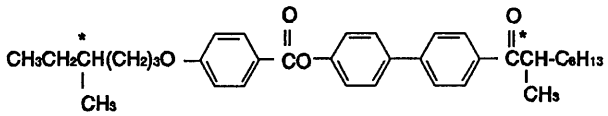

Figure 1.8

This short overview of nmr investigations of ferroelectric liquid crystals raises the following points:

1. recent efforts mainly relied on ^{13}C nmr (particularly solid state nmr), whereas earlier work involved the use of ^{1}H and ^{2}H magnetic resonance - other nuclei have generally been avoided;
2. the uncertainty surrounding the preservation / destruction of helical structures of ferroelectric compounds;
3. the uncertainty regarding the orientation of the molecular directors in the magnetic field.

Fluorine is often incorporated into mesogenic molecules for a variety of reasons (see section 1.3) and from an nmr point of view the ^{19}F nucleus offers some important advantages over ^{2}H and ^{13}C nuclei, in particular:

1. a much enhanced sensitivity which would lead to shorter accumulation times;
2. a much larger chemical shift range (over 1000 ppm) which means that the slightest change in the environment of a ^{19}F nucleus would be reflected in the spectrum;
3. the ease of introduction of a fluoro-substituent into a molecule due to improved synthetic methods (synthesising partially deuterated mesogens can be difficult and time consuming).

Digitised by the Department of Library Services in support of open access to information, University of Pretoria, 2021.

UNIVERSITEIT VAN PRETORIA
UNIVERSITY OF PRETORIA
YUNIBESITHI YA PRETORIA

Realising the potential advantages of the ^{19}F nucleus, Avent *et al*[33] used ^{19}F nmr to investigate the orientational ordering of two liquid crystals (fig. 1.9) in their smectic A and nematic phases using the spin echo technique.

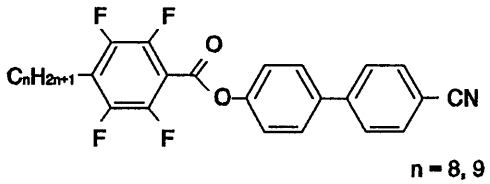

Figure 1.9

Their results are discussed more extensively in chapter 5. To date therefore, the obvious advantages of ^{19}F nmr have not been put to use in the investigation of ferroelectric liquid crystals.

1.3 Fluorinated liquid crystals

Fluorine is a small and highly electronegative substituent with a Van der Waals radius not much greater than that of hydrogen (hydrogen: 1.20Å, fluorine:1.47Å). It is those two properties that make fluorination the ideal way of introducing some changes to the physical properties of a molecule without completely disrupting the phase transition temperatures[34].

The majority of fluorinated liquid crystals can conveniently be divided into two types on the grounds of the different reasons for which fluorination is implemented:

I Compounds with fluoro-substituents on the core (referred to as laterally fluorinated liquid crystals)

II Compounds with fluoro-substituents on the terminal chain, or more specifically, on the chiral centre.

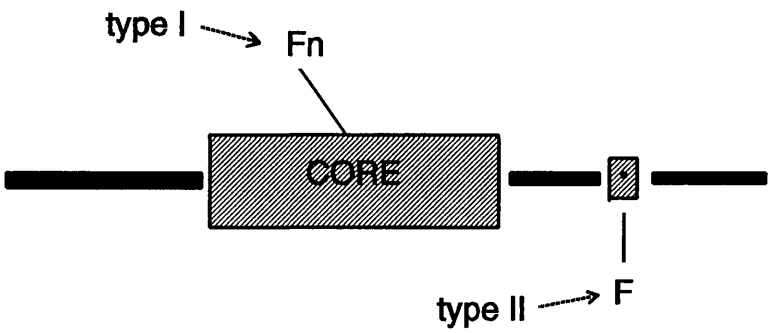

Figure 1.10

Digitised by the Department of Library Services in support of open access to information, University of Pretoria, 2021.

UNIVERSITEIT VAN PRETORIA
UNIVERSITY OF PRETORIA
YUNIBESITHI YA PRETORIA

Fluorination of the core units of liquid crystalline compounds has found numerous applications[35,36]. Interest in type **I** compounds has increased considerably during the past decade and several useful trends have been identified[37 - 44]. By placing lateral fluoro-substituents in various positions on the core, certain properties can be conferred on a liquid crystal. Some of those applicable to this work are:

(i) reduction of the clearing point of a liquid crystal;

(ii) reduction of the thermal stability of the nematic phases in favour of smectic phases[37] (or the opposite[45]);

(iii) suppression of highly ordered smectic phases;

(iv) stabilization of the tilted phases[44].

A fluoro-substituent on the terminal chain (type **II** compounds) is useful for introducing a dipole onto the chiral centre in order to increase the magnitude of the spontaneous polarisation (and reduce the response time)[46 - 55].

A combination of types **I** and **II** can lead to compounds with interesting properties. For instance, the effect of a high negative dielectric anisotropy (brought about by lateral fluorination) on the ferroelectric behaviour of a liquid crystal has yet to be investigated. Some work has been published, such as the use of a single fluoro-substituent on the core in conjunction with one on the chiral centre in an attempt to further enhance the spontaneous polarisation[56,57]. The influence of lateral fluorination on the macromolecular chirality of compounds with a single methyl-containing chiral centre has recently been investigated[58].

1.4 The ferroelectric smectic C* phase[59]

In 1975 Meyer[1] recognised that a tilted smectic phase made up of chiral molecules can be ferroelectric, owing to a reduction in the overall symmetry of the material. This has since formed the basis for the design of conventional ferroelectric liquid crystals.

The tilted smectic C phase of a non-optically active material has the following bulk symmetry elements: a centre of symmetry, a twofold axis normal to the tilt direction and a mirror plane perpendicular to the tilt direction (see fig. 1.11). When the material is optically active, the symmetry elements of the bulk are reduced to a single C_2 axis normal to the tilt direction of the phase and parallel to the layers (fig. 1.11, bottom left). Therefore, an optically active molecule (i.e. molecular chirality) results in layers of molecules each with a reduced symmetry, which collectively leads to a chiral phase (i.e. form chirality) as depicted in fig 1.11 (right). Hence, an individual layer has a spontaneous polarisation (Ps) and is ferroelectric. However, a helical arrangement exists in the bulk of the material and it causes a rotation of the spontaneous polarisation from one layer to the next.

Digitised by the Department of Library Services in support of open access to information, University of Pretoria, 2021.

UNIVERSITEIT VAN PRETORIA
UNIVERSITY OF PRETORIA
YUNIBESITHI YA PRETORIA

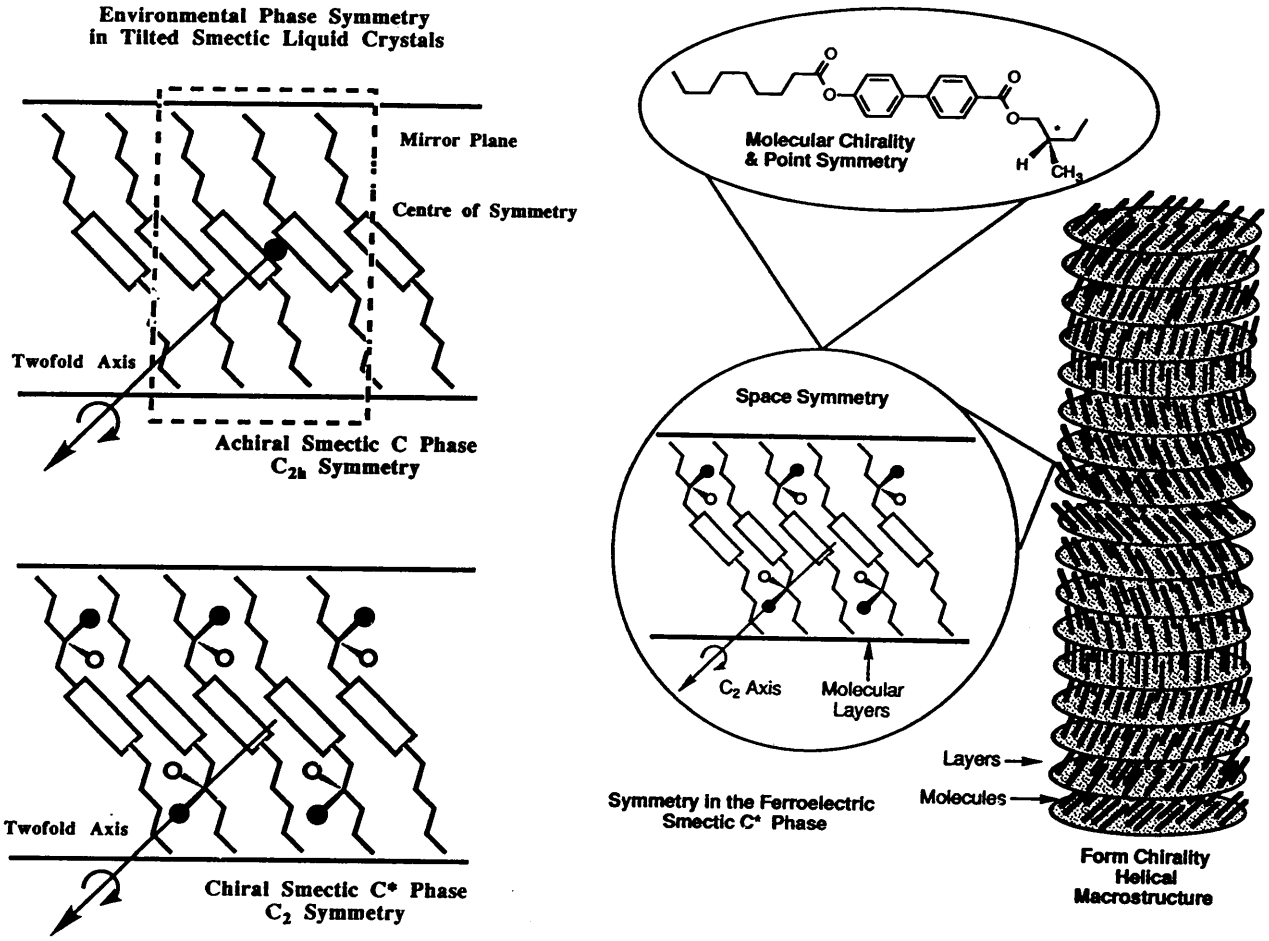

Figure 1.11

This means that the bulk is not ferroelectric as such, but that it can become ferroelectric on application of an electric field. Changing the polarity of the applied field causes the molecules to rotate through twice the tilt angle as shown in fig. 1.12.

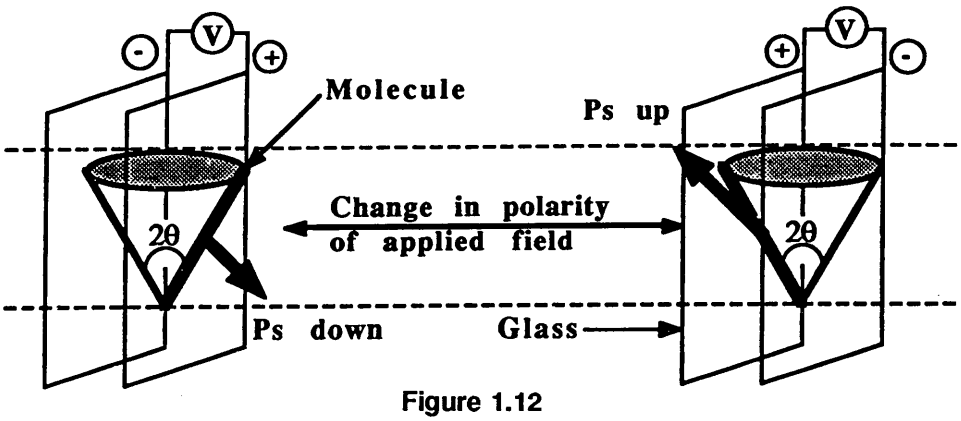

Figure 1.12

Digitised by the Department of Library Services in support of open access to information, University of Pretoria, 2021.

UNIVERSITEIT VAN PRETORIA
UNIVERSITY OF PRETORIA
YUNIBESITHI YA PRETORIA

There are two main types of smectic C* phases, those that form when a smectic A phase is cooled and those that form from a cholesteric phase. A smectic C* phase belonging to the first type usually shows a modest tilt of the molecules, increasing from 0° at the smectic A - smectic C* transition to seldom more than 25°. A smectic C* phase resulting from a cholesteric phase tends to have a fairly constant tilt that could approach 45°.

Ferroelectricity in a neat liquid crystal has conventionally been achieved by the incorporation of one or more chiral centres in the molecule and this is the approach followed in this work. It has since been discovered that achiral molecules can form a noncentrosymmetric packing arrangement and by doing so the smectic phase becomes ferroelectric[60].

1.5 Aims of project

The first objective was to design and synthesise new thermotropic liquid crystals with a smectic C* phase and to investigate and characterise their ferroelectric properties. An added requirement was that they should be suitable for study by nmr, i.e. they should be thermally stable and have sufficiently low clearing points.

Secondly, as the first objective was partially achieved by introducing a 2,3-difluorophenyl unit, the choice of method for investigating the orientational properties fell upon ^{19}F nmr. As no suitable technique existed, an experimental method had to be devised which would allow the acquisition of well-resolved ^{19}F nmr spectra using the available equipment.

Thirdly, it was hoped to investigate the possible existence[56,57] of interaction between dipoles on the core and at the chiral centre by the strategic placement of fluoro-substituents.

In a broader sense, it was hoped that a meaningful comparison could be made between the microscopic properties (nmr) and those measured macroscopically (thermal analysis, electro-optical measurements).

1.6 Outline

The necessary background information for the work is provided in this chapter. The synthesis and characterization of all the precursory compounds as well as the liquid crystals is given in chapter 2. Chapter 3 concerns measurements of the properties of the liquid crystals - the characterization of their phases and transition temperatures by optical polarising microscopy as well as thermal analysis

Digitised by the Department of Library Services in support of open access to information, University of Pretoria, 2021.

UNIVERSITEIT VAN PRETORIA
UNIVERSITY OF PRETORIA
YUNIBESITHI YA PRETORIA

and selected electrooptic measurements. One of the compounds with unusual ferroelectric properties was investigated more extensively and is discussed in chapter 4.

In chapter 5 the development of the experimental technique in order to obtain ^{19}F nmr spectra of the liquid crystals, is discussed on the basis of an example.

Chapters 6 and 7 are devoted to the application of ^{19}F nmr to specific problems, together with conformational analysis (chapter 6) and selected thermal and electrooptic measurements.

The results and most important conclusions are summarised in chapter 8.

----- # -----

Digitised by the Department of Library Services in support of open access to information, University of Pretoria, 2021.

UNIVERSITEIT VAN PRETORIA
UNIVERSITY OF PRETORIA
YUNIBESITHI YA PRETORIA

CHAPTER 2

SYNTHESIS

2.1 Experimental

Molecules were synthesised in a stepwise manner by the successive addition of fluorinated or non-fluorinated phenyl rings. This approach meant that the expensive fluorinated chiral acid or alcohol could conveniently be attached in the final step.

Reagents

Fluorinated aromatic starting materials were obtained as follows:

1,2-difluorobenzene (Aldrich), 4-bromo-2-fluorophenol (Aldrich or Fluorochem (UK)), 1-bromo-3-fluoro-4-iodobenzene (Aldrich), 2-fluoro-4-hydroxybenzoic acid (Merck), 2-fluoro-anisole (Fluka).

(*S*)-2-fluoro-octanoic acid ($[\alpha]_D^{30}$ = +10.6°; 96% ee) and (*S*)-2-fluoro-octanol ($[\alpha]_D^{30}$ = -10.0°) were obtained from the University of Hull (prepared according to the method of Nohira *et al*[53]).

$Pd(PPh_3)_4$ was prepared according to a published method[61] using $PdCl_2$ purchased from the Osmium Corporation, Johannesburg.

(*S*)-2-chloro-4-methylpentanoic acid was kindly donated by dr AJ Slaney (University of Hull) and 4-Carboxyphenylferrocene was a gift from dr C Imrie.

^{1}H nmr spectra were recorded on a JEOL JNM-GX270 spectrometer (University of Hull) or a Bruker AC300 instrument (University of Pretoria) as solutions in $CDCl_3$ unless otherwise stated.

Infrared spectra were obtained on a Perkin-Elmer 457 grating spectrometer (Hull) or a Bomem Michelson 100 FTIR instrument (Pretoria).

Mass spectra were recorded on a Finnigan-MAT 1020 GC/MS instrument (Hull) or a Perkin-Elmer RMU-6H instrument operating at 70 eV (Rand Afrikaans University, Johannesburg) except for six of the spectra which were obtained on a VG 7070H instrument (70 eV) (Pretoria).

Optical rotation measurements were done on an Atago Polax-D instrument (Pretoria) or an Optical Activity AA-10 automatic polarimeter (Hull) using 30mg/ml $CHCl_3$.

Purification. Final products were rigorously purified by column and/or flash chromatography. Products were subsequently recrystallised sequentially until constant transition temperatures were obtained.

Digitised by the Department of Library Services in support of open access to information, University of Pretoria, 2021.

UNIVERSITEIT VAN PRETORIA
UNIVERSITY OF PRETORIA
YUNIBESITHI YA PRETORIA

Melting points were determined on a Gallenkamp melting point aparatus and are uncorrected.

Phase transitions. Some of the precursor compounds to the final liquid crystals exhibited liquid crystalline properties. Their phases and transition temperatures are included in this chapter, but those of the final products will be discussed in chapter 3. Phases given in this chapter were identified by optical microscopy (Leitz Laborlux microscope fitted with polarisers and heating stage). Transition temperatures given are those obtained from microscopy.

Absolute configuration. The absolute configuration of the final products was inferred from those of the starting chiral alcohol and carboxylic acid.

Optical purity. The optical purity of one of the esters and one of the ethers was checked using the chiral shift reagent D-3-heptafluorobutyrylcamphorate (Lancaster Synthesis, UK). In both cases it was found that ee > 90% as there was no detectable amount of the other enantiomer. The proton on the chiral centre was affected the most and shifted downfield by 0.3 - 0.5 ppm.

Digitised by the Department of Library Services in support of open access to information, University of Pretoria, 2021.

UNIVERSITEIT VAN PRETORIA
UNIVERSITY OF PRETORIA
YUNIBESITHI YA PRETORIA

SCHEME 1

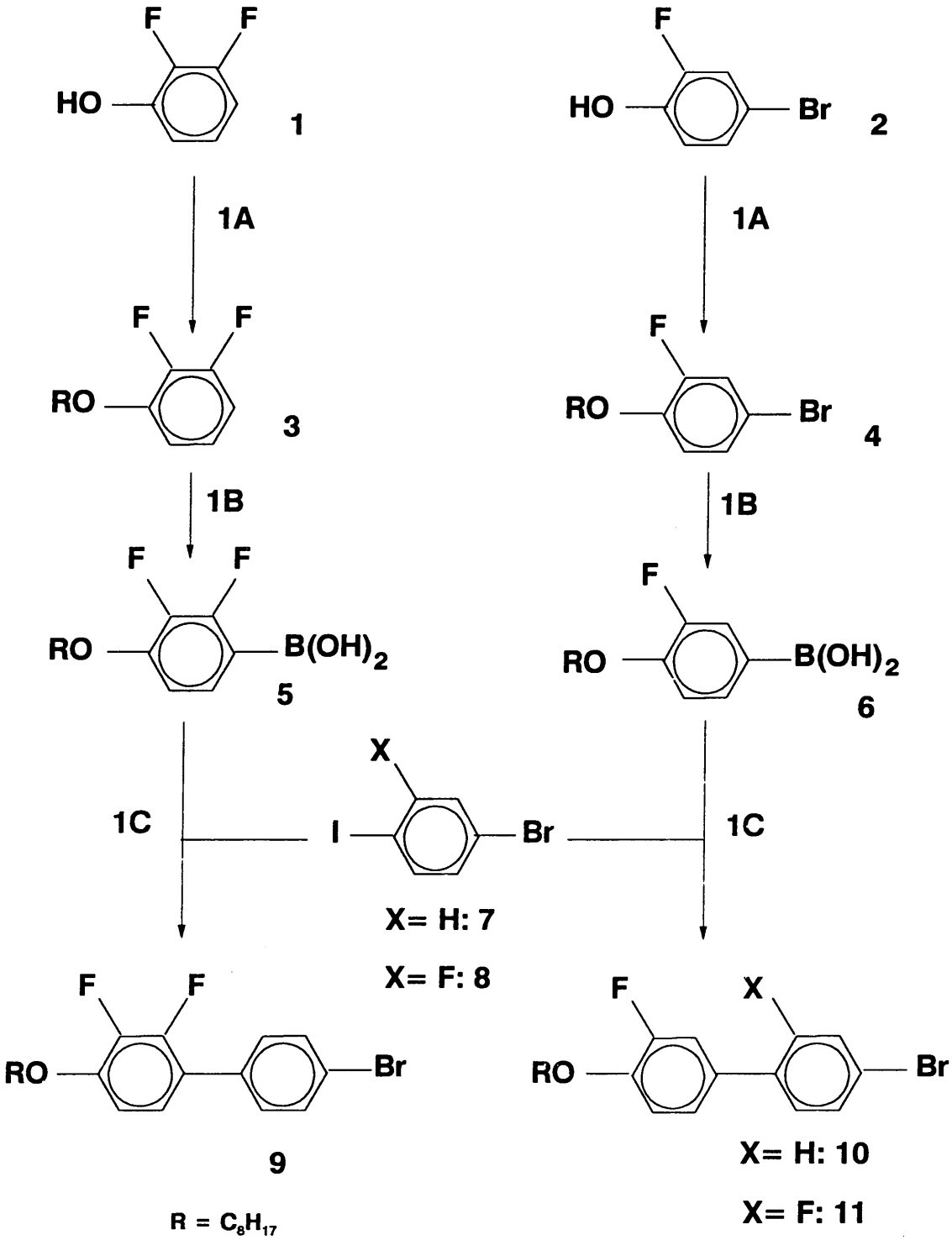

R = C_8H_{17}

1A : K_2CO_3 , RBr, acetone

1B : (i) BuLi, $(^iPrO)_3B$, THF; (ii) 10% HCl

1C : $Pd(PPh_3)_4$, DME, 2M Na_2CO_3

Digitised by the Department of Library Services in support of open access to information, University of Pretoria, 2021.

UNIVERSITEIT VAN PRETORIA
UNIVERSITY OF PRETORIA
YUNIBESITHI YA PRETORIA

SCHEME 2

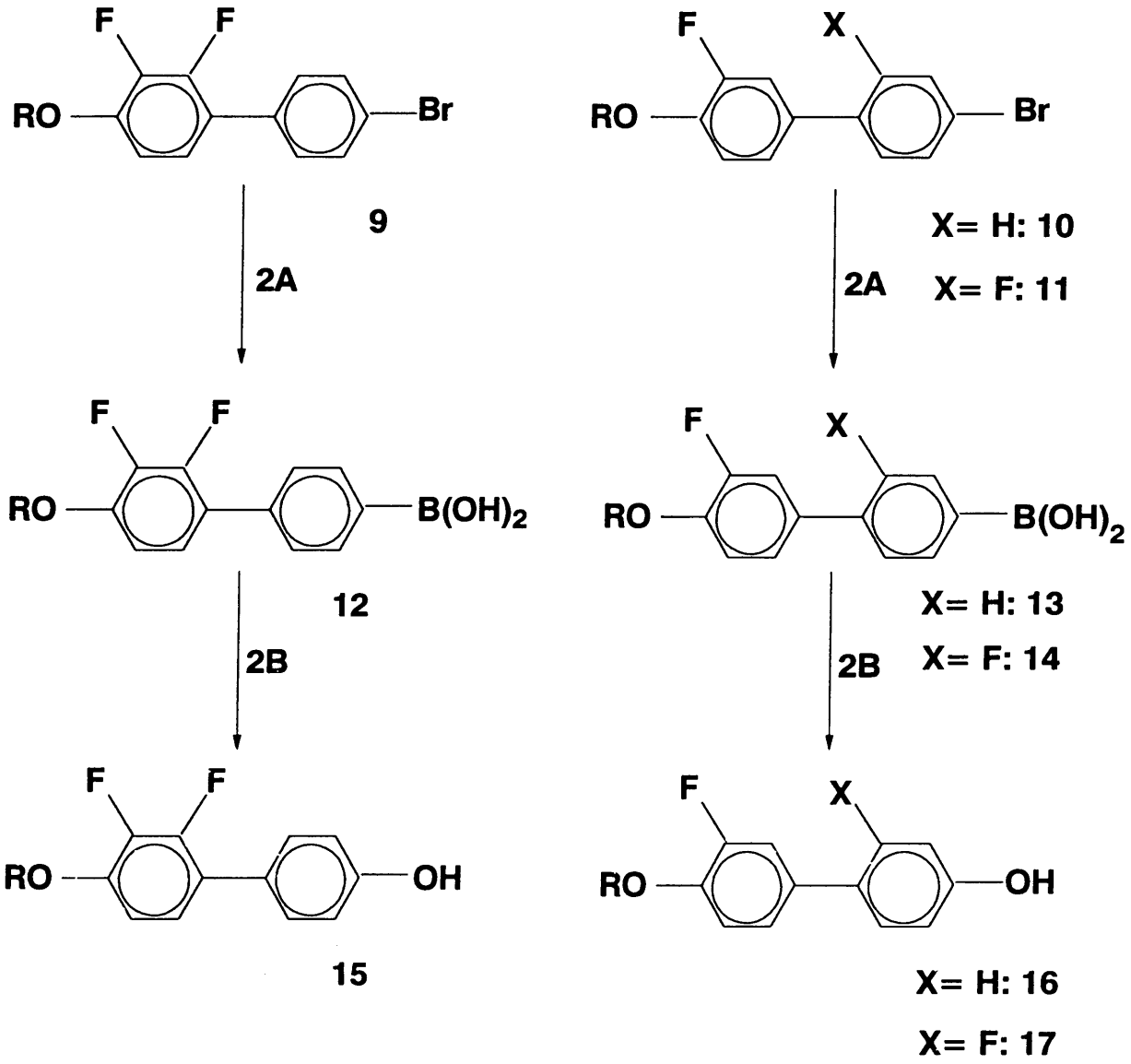

R = C_8H_{17}

2A : (i) BuLi, $(^iPrO)_3B$, THF; (ii) 10% HCl

2B : 10% H_2O_2 , Et_2O

Digitised by the Department of Library Services in support of open access to information, University of Pretoria, 2021.

UNIVERSITEIT VAN PRETORIA
UNIVERSITY OF PRETORIA
YUNIBESITHI YA PRETORIA

SCHEME 3

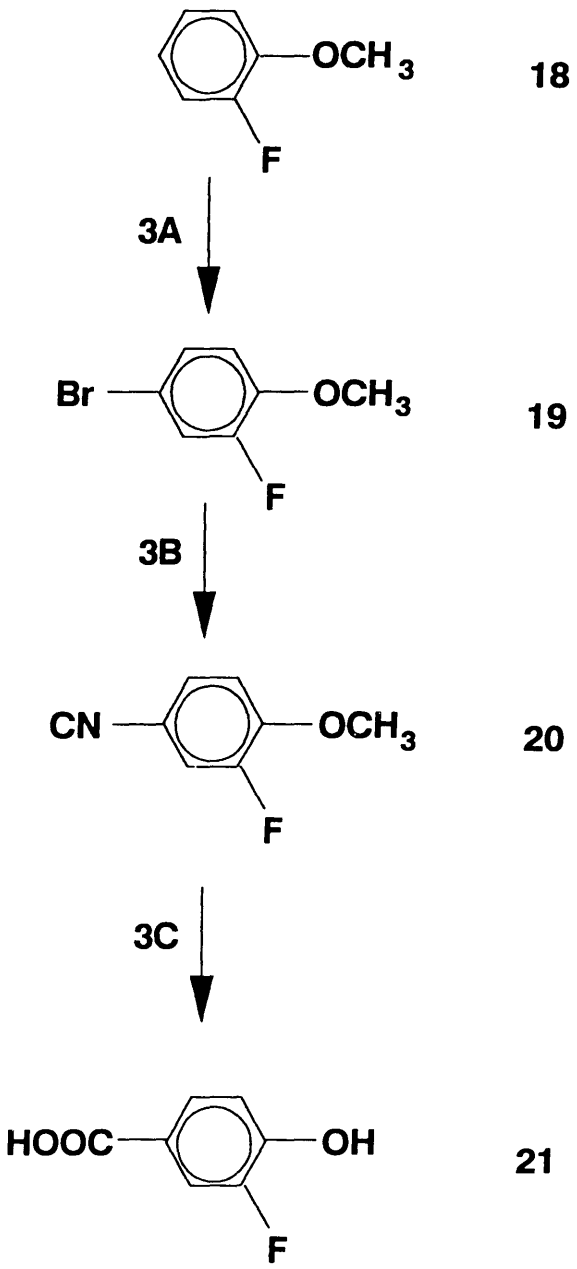

3A : Br_2 , $CHCl_3$

3B : CuCN, DMF

3C : HOOAc / HBr (aq)

Digitised by the Department of Library Services in support of open access to information, University of Pretoria, 2021.

UNIVERSITEIT VAN PRETORIA
UNIVERSITY OF PRETORIA
YUNIBESITHI YA PRETORIA

SCHEME 4

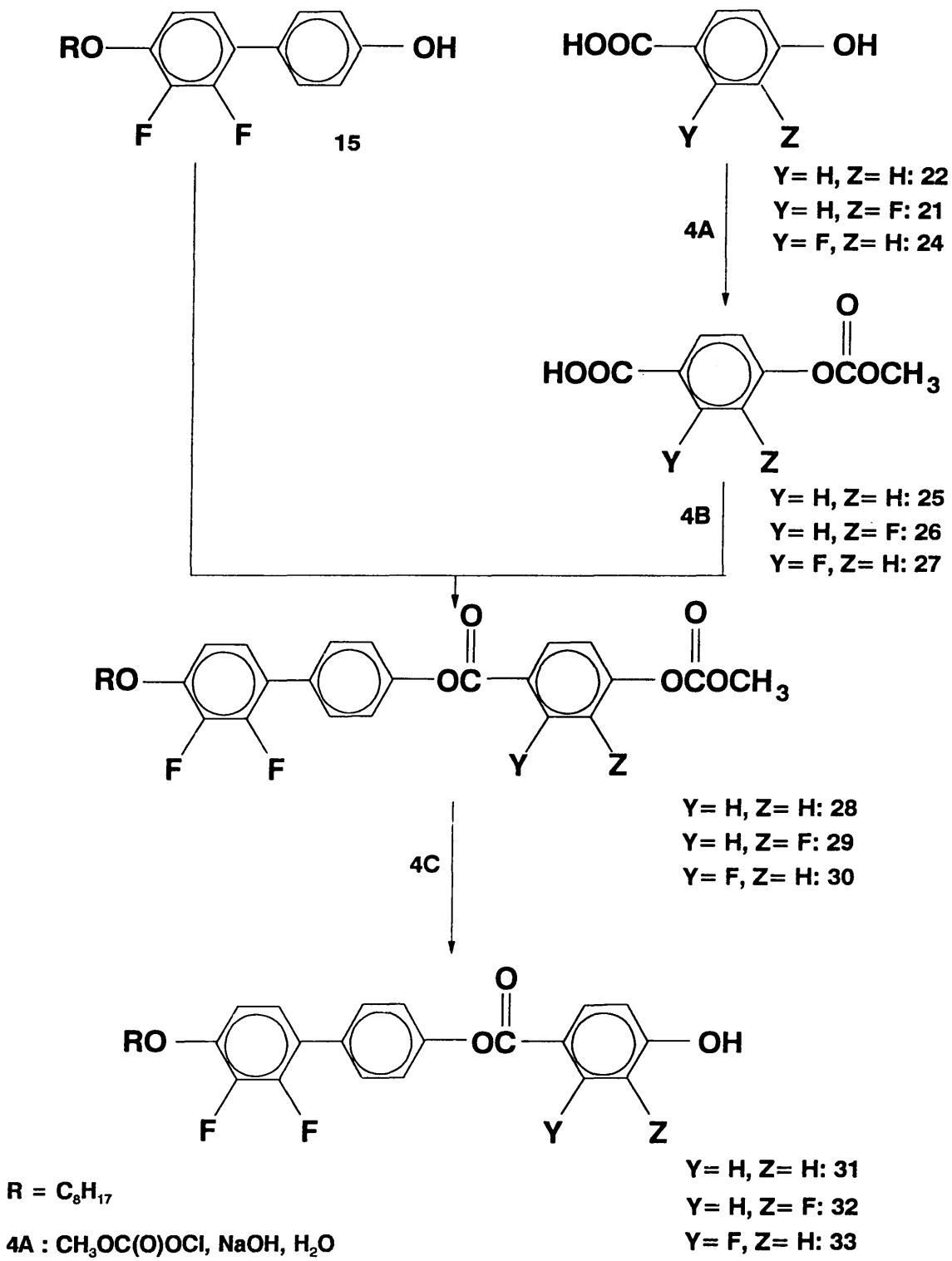

R = C_8H_{17}

4A : $CH_3OC(O)OCl$, NaOH, H_2O

4B : DEAD, PPh_3

4C : 35% NH_3 , EtOH

Digitised by the Department of Library Services in support of open access to information, University of Pretoria, 2021.

SCHEME 5

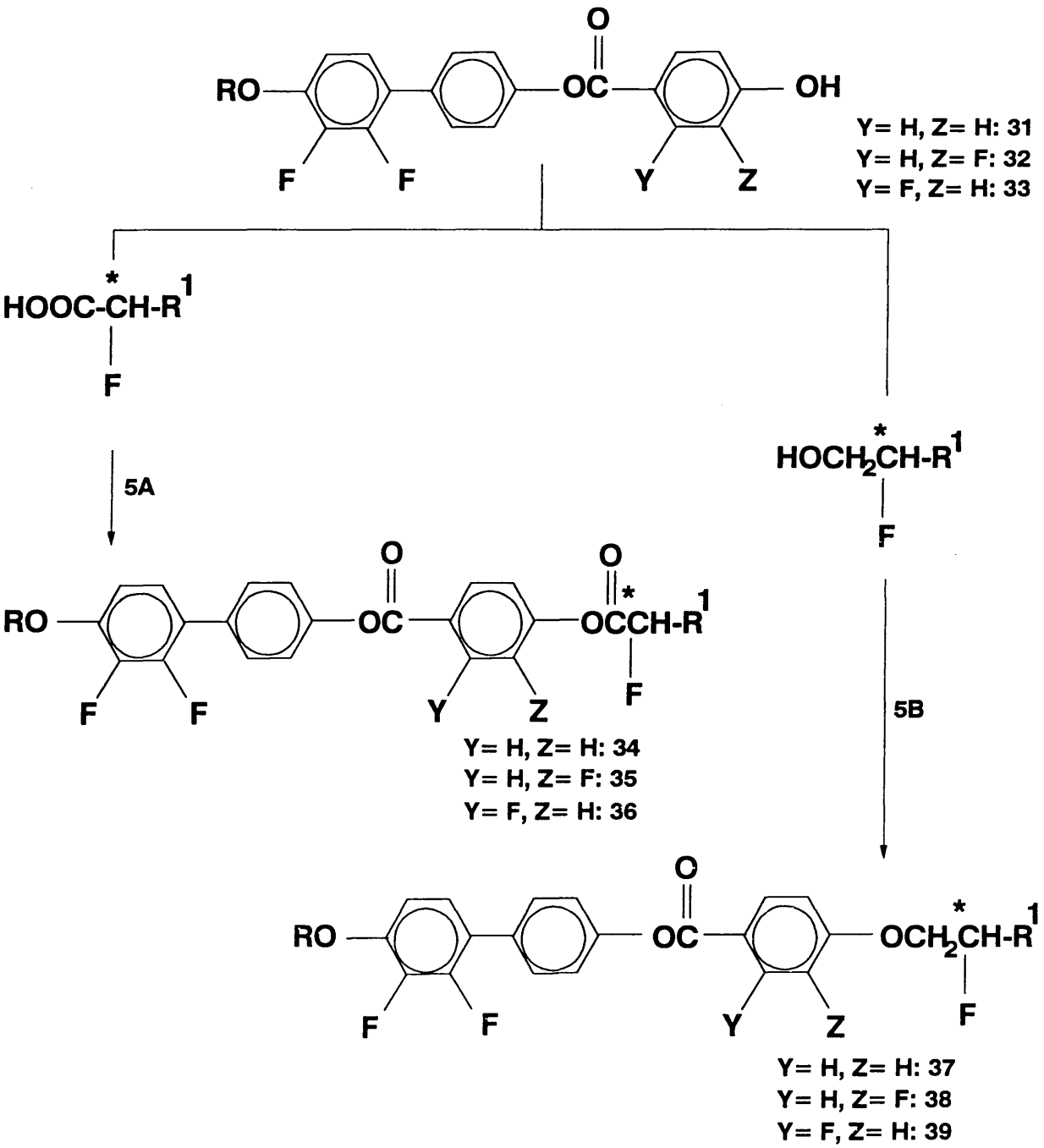

R = C_8H_{17} R^1 = C_6H_{13}

5A : DCC, CH_2Cl_2

5B : DEAD, PPh_3 , THF

Digitised by the Department of Library Services in support of open access to information, University of Pretoria, 2021.

UNIVERSITEIT VAN PRETORIA
UNIVERSITY OF PRETORIA
YUNIBESITHI YA PRETORIA

SCHEME 6

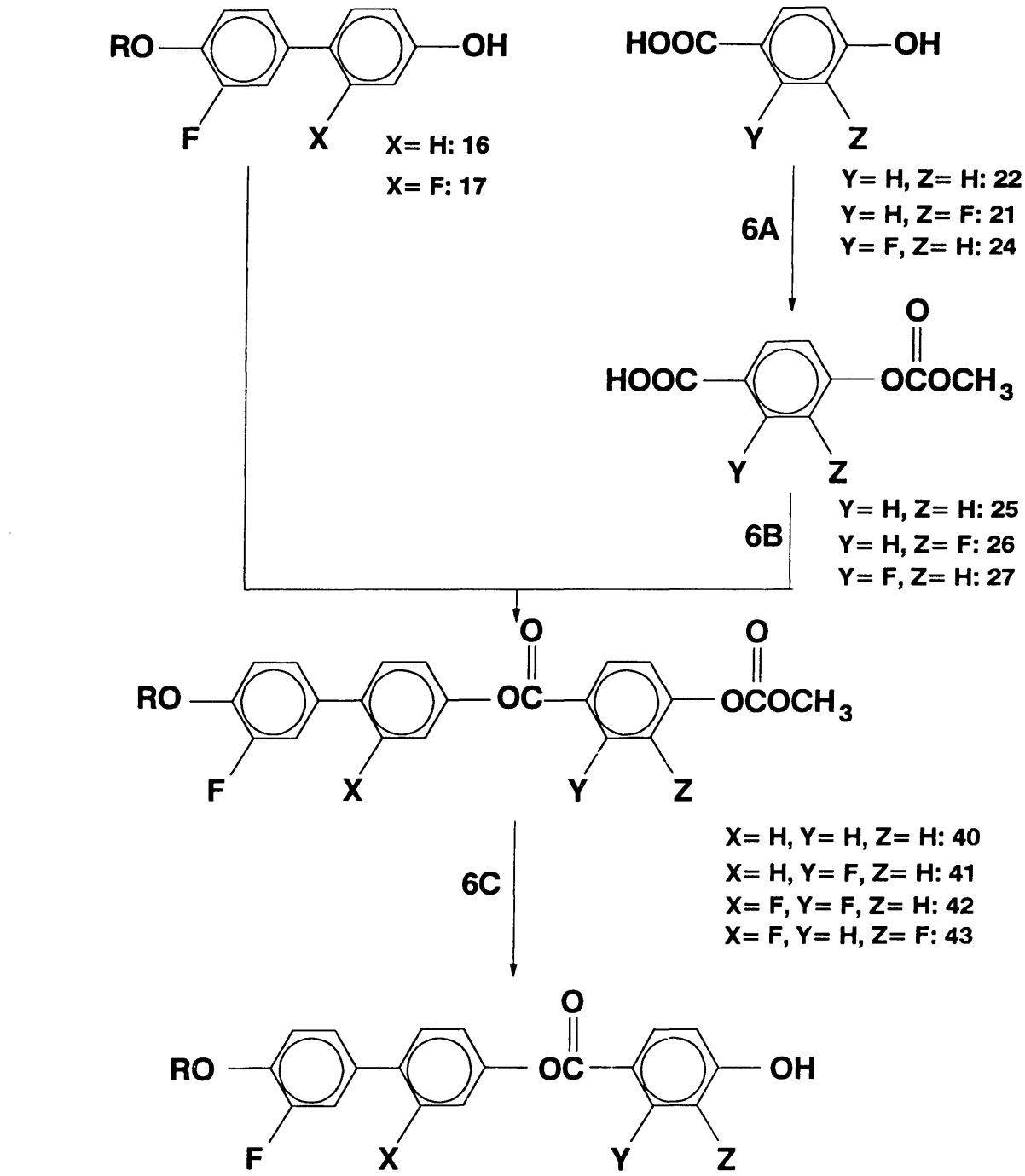

R = C_8H_{17}

6A : $CH_3OC(O)OCl$, NaOH, H_2O

6B : DEAD, PPh_3 ,THF

6C : 35% NH_3 , EtOH

Digitised by the Department of Library Services in support of open access to information, University of Pretoria, 2021.

SCHEME 7

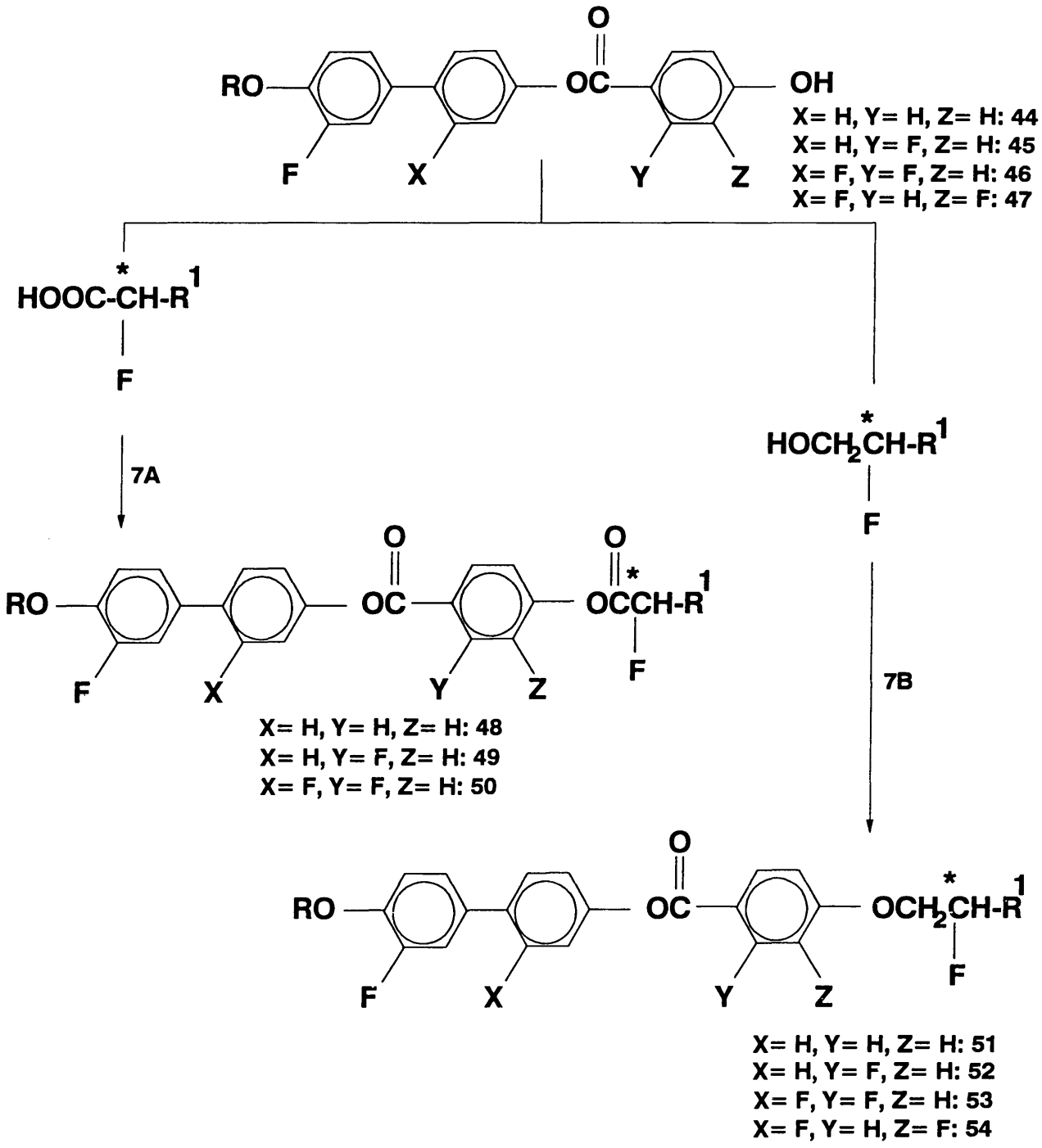

R = C_8H_{17} R^1 = C_6H_{13}

7A : DCC, CH_2Cl_2

7B : DEAD, PPh_3 , THF

Digitised by the Department of Library Services in support of open access to information, University of Pretoria, 2021.

UNIVERSITEIT VAN PRETORIA
UNIVERSITY OF PRETORIA
YUNIBESITHI YA PRETORIA

SCHEME 8

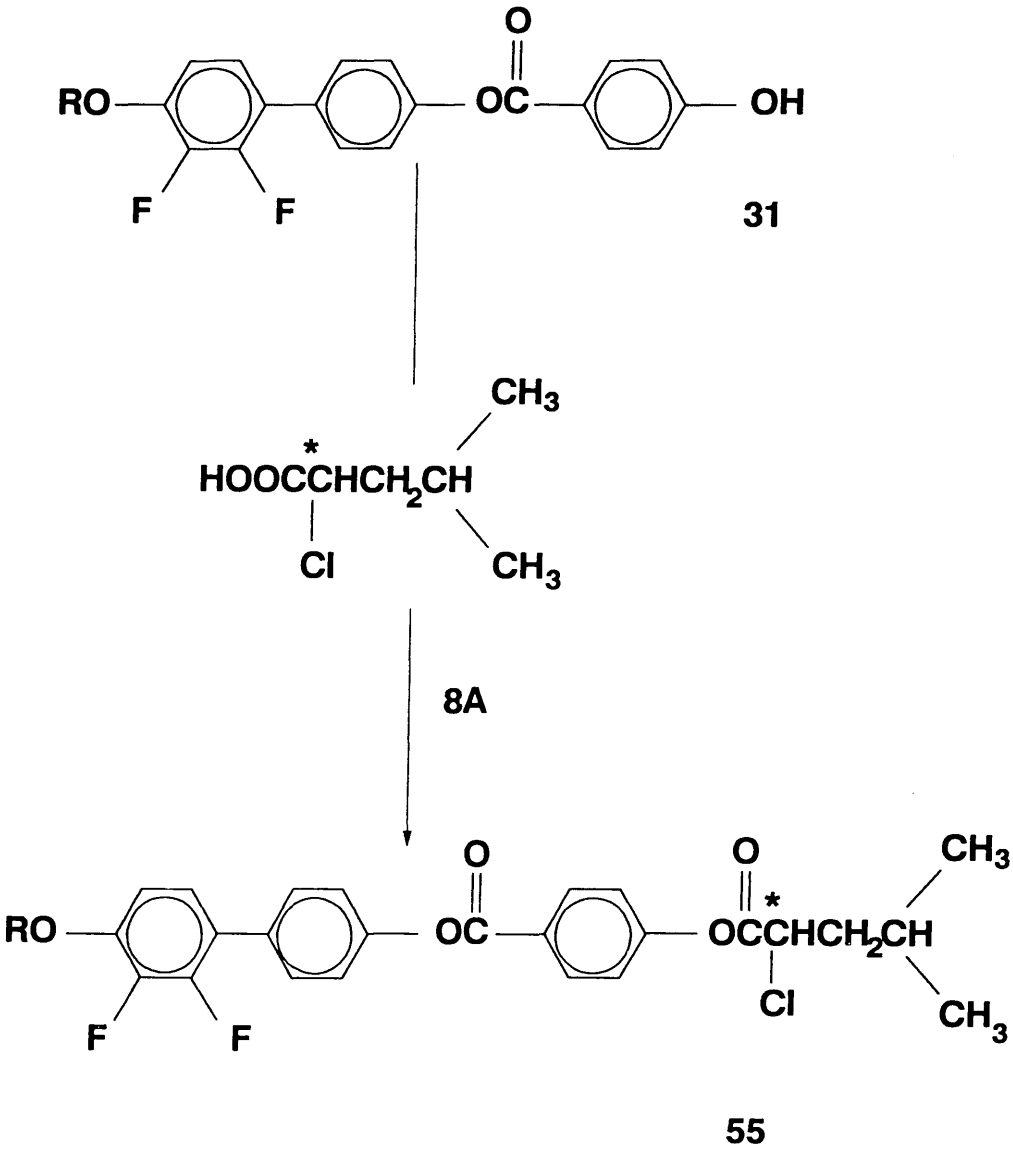

R = C_8H_{17}

8A : DCC, CH_2Cl_2

Digitised by the Department of Library Services in support of open access to information, University of Pretoria, 2021.

UNIVERSITEIT VAN PRETORIA
UNIVERSITY OF PRETORIA
YUNIBESITHI YA PRETORIA

SCHEME 9

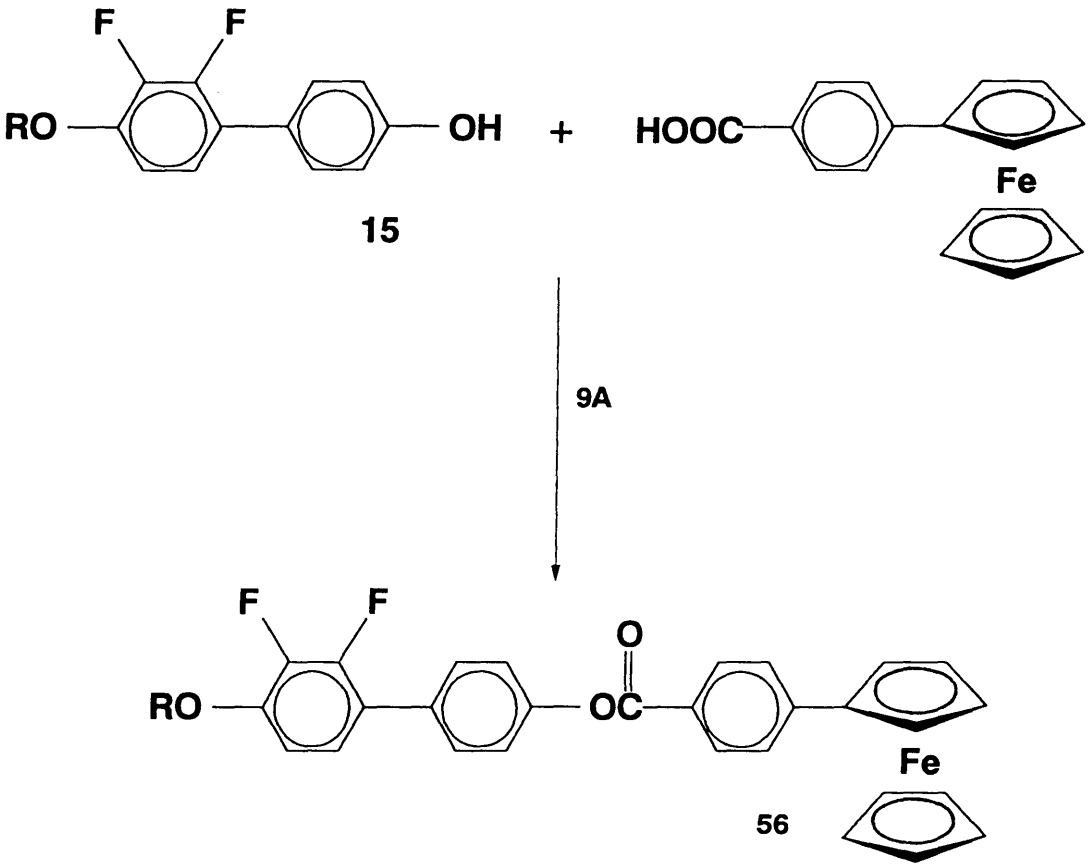

R = C_8H_{17}

9A : DCC, CH_2Cl_2

Digitised by the Department of Library Services in support of open access to information, University of Pretoria, 2021.

UNIVERSITEIT VAN PRETORIA
UNIVERSITY OF PRETORIA
YUNIBESITHI YA PRETORIA

1,2-Difluoro-3-octyloxybenzene (**3**)[42]

A solution of 1-bromo-octane (25.1 g, 0.13 mol) in acetone (30 ml) was added to a stirred refluxing mixture of 2,3-difluorophenol (**1**) (14 g, 0.108 mol) and potassium carbonate (20.0 g, 0.144 mol) in acetone (300 ml). The stirred mixture was heated under reflux for 24h or until tlc analysis revealed complete reaction. The potassium carbonate was filtered off and most of the acetone removed *in vacuo*. The residue was dissolved in ether, water was added, and the layers separated. This was followed by a second extraction of the aqueous layer with ether. The combined organic layers were washed with water, 5% sodium hydroxide, water and dried ($MgSO_4$). The solvent was removed under vacuum. The crude product was distilled to give a colourless oil.

yield	17.1 g (65%)
bp	78-81°C (3×10^{-3} mmHg)
	(lit.[42] 150°C / 15 mmHg)
^{1}H nmr ($CDCl_3$) δ	6.97 (1H,m), 6.71 (2H,m), 4.00 (2H,t), 1.82 (2H, quintet), 1.45 (2H,quintet), 1.27 (8H,m), 0.85 (3H,t).

1-Bromo-3-fluoro-4-octyloxybenzene (**4**)[45]

Quantities: 4-bromo-2-fluorophenol (10.0 g, 0.052 mol), 1-bromo-octane (12.0 g, 0.062 mol), potassium carbonate (14.5 g, 0.105 mol).

The experimental procedure was as for the preparation of compound **3** and the crude product was distilled.

yield	11.16 g (71%)
bp	112-114°C (0.01 mmHg)
	(lit.[45] 120-122°C / 0.1 mmHg)
^{1}H nmr ($CDCl_3$) δ	7.22 (1H,quintet), 7.13 (1H,m), 6.80 (1H,t), 4.01 (2H,t), 1.81 (2H, quintet), 1.44 (2H,quintet), 1.30 (8H,m), 0.90 (3H,t).

2,3-Difluoro-4-octyloxyphenyl boronic acid (**5**)[42]

A solution of 1,2-difluoro-3-octyloxybenzene (**3**) (6.94 g, 0.029 mol) in dry THF (100 ml) was cooled to -78°C. n-Butyllithium (3.0 ml, 10M in hexane, 0.029 mol) was added dropwise. The reaction mixture was maintained under these conditions for 2.5h and then a solution of tri-isopropylborate (10.91 g, 0.058 mol) in dry THF (30 ml) was added dropwise at -78°C. The reaction mixture was allowed to warm to room temperature overnight and then stirred for 1h with 10% hydrochloric acid (30 ml). The product was extracted into ether (twice) and the combined ethereal extracts were washed with water and dried ($MgSO_4$). The solvent was removed *in vacuo* to give a colourless solid.

yield	7.97 g (96%)

Digitised by the Department of Library Services in support of open access to information, University of Pretoria, 2021.

UNIVERSITEIT VAN PRETORIA
UNIVERSITY OF PRETORIA
YUNIBESITHI YA PRETORIA

^{1}H nmr ($CDCl_3$) δ	7.83 (1H,t), 6.80 (1H,t), 4.03 (2H,t), 1.80 (2H,quintet), 1.45 (2H,quintet), 1.30 (8H,m), 0.89 (3H,t), no OH resonance.
ir (KBr) ν_{max} cm^{-1}	3650-3130, 2980, 2940, 2880, 1642, 1530, 1474, 1365, 1319, 1232, 1090, 1035

3-Fluoro-4-octyloxyphenyl boronic acid (**6**)

Quantities: 1-bromo-3-fluoro-4-octyloxybenzene (**4**) (15 g, 0.05 mol), n-butyllithium (5 ml, 10M in hexane, 0.05 mol), tri-isopropylborate (18.8 g, 0.1 mol).

The experimental procedure was as described for compound **5**.

yield	7.5 g (56%)
^{1}H nmr ($CDCl_3$) δ	7.85 (2H,m), 7.47-6.88 (1H,m), 4.10 (2H,t), 1.85 (2H,quintet), 1.57-1.20 (10H,m), 0.90 (3H,t), no obvious OH resonance.
ir (KBr) ν_{max} cm^{-1}	3640-3100, 2960, 2930, 2860, 1617, 1428, 1385, 1350, 1307, 1275, 1134, 1100, 1028, 668.

4'-Bromo-2,3-difluoro-4-octyloxybiphenyl (**9**)[42]

A solution of 2,3-difluoro-4-octyloxyphenyl boronic acid (**5**) (8.29 g, 0.029 mol) in dimethoxyethane (40 ml) was added to a solution of 4-bromo-iodobenzene (6.80 g, 0.024 mol) and tetrakis(triphenylphosphine)palladium(0) (1.48 g, 1.29 mmol) in dimethoxyethane (40 ml) under nitrogen. To this, 2M sodium carbonate (60 ml) was added. The stirred mixture was gently heated under reflux. Progress of the reaction was carefully monitored using tlc until the boronic acid had reacted completely (usually 4-5h). The layers were separated and the aqueous layer extracted with ether (twice). The combined organic layers were washed with brine and dried ($MgSO_4$). The solvent was removed *in vacuo* and the residue purified by column chromatography [silica gel / petroleum ether (40-60°C) - ethyl acetate (9:1)] to give a white solid which was recrystallised from pentane (-20°C) to yield colourless crystals.

yield	5.28 g (61%)
mp	39-40°C (lit.42 ~30°C)
^{1}H nmr ($CDCl_3$) δ	7.53 (2H,d), 7.36 (2H,q), 7.00 (1H,sextet), 6.79 (1H,sextet), 4.05 (2H,t), 1.79 (2H,quintet), 1.45 (2H,quintet), 1.26 (8H,quintet), 0.90 (3H,t).
ir (KBr) ν_{max} cm^{-1}	2960, 2940, 2860, 1637, 1515, 1498, 1470, 1392, 1314, 1308, 1203, 1075, 1011, 1002, 900, 833, 803.
ms (m/z)	398(M^+), 396(M^+), 286, 284.

Digitised by the Department of Library Services in support of open access to information, University of Pretoria, 2021.

UNIVERSITEIT VAN PRETORIA
UNIVERSITY OF PRETORIA
YUNIBESITHI YA PRETORIA

4'-Bromo-3-fluoro-4-octyloxybiphenyl (**10**)

Quantities: 3-fluoro-4-octyloxyphenyl boronic acid (7.0 g, 0.026 mol), 4-bromo-iodobenzene (5.88 g, 0.021 mol), tetrakis(triphenylphosphine)palladium(0) (0.8 g, 0.7 mmol).

The experimental procedure was as described for compound **9**.

yield	5.09 g (64%)
mp	42-44°C
^{1}H nmr ($CDCl_3$) δ	7.53 (2H,m), 7.38 (2H,m), 7.32-6.96 (3H,m), 4.06 (2H,t), 1.84 (2H,quintet), 1.54-1.22 (10H,m), 0.89 (3H,t).
ir (KBr) ν_{max} cm^{-1}	2960, 2924, 2855, 1618, 1583, 1535, 1490, 1475, 1393, 1320, 1308, 1277, 1185, 1135, 1036, 1008, 997, 827, 810, 722.
ms (m/z)	378(M^+), 266.

3-Fluoro-4-octyloxy-4'-bromo-2'-fluorobiphenyl (**11**)

Quantities: 3-fluoro-4-octyloxyphenyl boronic acid (**6**) (6.83 g, 0.026 mol), 1-bromo-3-fluoro-4-iodobenzene (6.92 g, 0.023 mol), tetrakis(triphenylphosphine)palladium(0) (1 g, 0.87 mmol).

The experimental procedure was as described for the preparation of compound **9**.

The product is a low melting solid and was used without further purification.

yield	4.27 g (47%)
^{1}H nmr ($CDCl_3$) δ	7.33-7.18 (5H,m), 6.99 (1H,t), 4.05 (2H,t), 1.82 (2H,quintet), 1.47 (2H,quintet),
1.27	(8H,m), 0.88 (3H,t).
ir (neat) ν_{max} cm^{-1}	2931, 2857, 1604, 1583, 1562, 1524, 1490, 1392, 1310, 1274, 1234, 1213, 1186, 1132, 1074, 1027, 903, 859, 806, 724.
ms (m/z)	397(M^+), 396, 286, 284, 190, 175, 157, 112.

2,3-Difluoro-4-octyloxybiphenyl-4'-yl boronic acid (**12**)

Quantities: compound **9** (3.18 g, 8.0 mmol), n-butyllithium (3.2 ml, 2.5M in hexane, 8.0 mmol), tri-isopropylborate (3.01 g, 16.0 mmol).

The experimental procedure was as described for compound **5**.

yield	2.9 g (100%)
^{1}H nmr ($CDCl_3$) δ	8.32 (1H,d), 7.53 (3H,m), 7.03 (1H,m), 6.97 (1H,m), 4.09 (2H,t), 1.57 (2H,quintet), 1.65-1.20 (10H,m), 0.90 (3H,t), no obvious OH resonance.
ir (KBr) ν_{max} cm^{-1}	3620-3110, 2950, 2918, 2845, 1612, 1530, 1515, 1470, 1405-1345, 1323, 1309, 1200, 1115, 1080, 1025, 1004, 800, 732.
ms (m/z)	324, 318, 254, 222, 208, 206, 138, no M^+.

Digitised by the Department of Library Services in support of open access to information, University of Pretoria, 2021.

UNIVERSITEIT VAN PRETORIA
UNIVERSITY OF PRETORIA
YUNIBESITHI YA PRETORIA

3-Fluoro-4-octyloxybiphenyl-4'-yl boronic acid (**13**)

Quantities: compound **10** (4.95 g, 0.013 mol), n-butyllithium (5 ml, 2.5M in hexane, 0.013 mol), tri-isopropylborate (4.7 g, 0.026 mol).

The experimental procedure was the same as was described for compound **5**.

yield	4.40 g (98%)
^{1}H nmr (DMSO-d_6) δ	7.83 (1H,d), 7.54-7.19 (4H,m), 6.96 (2H,m), 3.59 (2H,t), 1.55 (2H,m), 1.50-1.10 (10H,m), 0.56 (3H,m), no obvious OH resonance.
ir (KBr) ν_{max} cm^{-1}	3640-3160, 2960, 2925, 2856, 1606, 1553, 1538, 1508, 1470, 1400-1330, 1306, 1278, 1190, 1135, 998, 835, 810, 741.
ms (m/z)	404, 398, 327, 298, 256, 186, 184, 157, 121, 55, no M^+.

3-Fluoro-4-octyloxy-2'-fluorobiphenyl-4'-yl boronic acid (**14**)

Quantities: compound **11** (4.25 g, 0.011 mol), n-butyllithium (4.5 ml, 2.5M in hexane, 0.011 mol), trimethylborate (2.22 g, 0.021 mol).

The experimental procedure was as described for the preparation of compound **5**.

yield	2.5 g (51%)
^{1}H nmr ($CDCl_3$) δ	8.01 (1H,d), 7.91 (1H,d), 7.36 (3H,m), 7.03 (1H,t), 4.70 (2H,br), 4.07 (2H,t), 1.84 (2H,quintet), 1.48 (2H,quintet), 1.29 (8H,m), 0.87 (3H,t).
ir (KBr) ν_{max} cm^{-1}	3348, 2924, 2853, 1614, 1579, 1533, 1399, 1315, 1282, 1191, 1134, 1019, 919, 868, 802, 736, 676.

2,3-Difluoro-4-octyloxy-4'-hydroxybiphenyl (**15**)

Hydrogen peroxide (10%, 10.5 ml, 0.023 mol) was added dropwise to a stirred refluxing solution of 2,3-difluoro-4-octyloxybiphenyl-4'-yl-boronic acid (**12**) (2.9 g, 8.0 mmol) in diethyl ether (40 ml). The stirred mixture was heated under reflux until tlc showed the reaction to be complete. The ether layer was separated and the aqueous layer extracted with ether. The combined ethereal layers were washed with water, dried ($MgSO_4$) and the solvent removed under reduced pressure. The crude product was purified on a flash column [silica gel/ petroleum ether (40-60° C) - ethyl acetate (2:1)] to give a white solid which was recrystallised from pentane - ethyl acetate mixtures.

yield	2.1 g (78%)
mp	112.5-113.5° C
^{1}H nmr ($CDCl_3$) δ	7.39 (2H,m), 7.04 (1H,td), 6.90 (2H,m), 6.77 (1H,td), 4.80 (1H,s), 4.06 (2H,t), 1.83 (2H,m), 1.45 (2H,m), 1.30 (8H,m), 0.90 (3H,t).
ir (KBr) ν_{max} cm^{-1}	3500-3390, 2925, 2868, 2854, 1611, 1508, 1474, 1292, 1079, 833, 812.
ms (m/z)	334 (M^+).

Digitised by the Department of Library Services in support of open access to information, University of Pretoria, 2021.

UNIVERSITEIT VAN PRETORIA
UNIVERSITY OF PRETORIA
YUNIBESITHI YA PRETORIA

3-Fluoro-4-octyloxy-4'-hydroxybiphenyl (**16**)

Quantities: compound **13** (4.40 g, 0.012 mol), hydrogen peroxide (10%, 16 ml, 0.036 mol).

The experimental procedure was as described for compound **15**.

yield	3.78 g (72%)
mp	126-128°C
^{1}H nmr ($CDCl_3$) δ	7.40 (2H,m), 7.12 (3H,m), 6.88 (2H,m), 4.90 (1H,s), 4.05 (2H,t), 1.83 (2H,m), 1.48 (2H,m), 1.30 (8H,m), 0.88 (3H,t).
ir (KBr) ν_{max} cm^{-1}	3620-3100, 2960, 2924, 2846, 1610, 1512, 1470, 1454, 1315, 1268, 1243, 1147, 835, 807.
ms (m/z)	316(M^+).

2',3-Difluoro-4-octyloxy-4'-hydroxybiphenyl (**17**)

Quantities: compound **14** (2.5 g, 5.5 mmol), hydrogen peroxide (10%, 15 ml, 0.044 mol).

The experimental procedure was as described for compound **15**. The crude product was recrystallised from hexane to give colourless needles.

yield	1.54 g (67%)
mp	82-83°C
^{1}H nmr ($CDCl_3$) δ	7.22 (3H,m), 7.00 (1H,t), 6.66 (2H,m), 5.43 (1H,br), 4.07 (2H,t), 1.83 (2H,pentet), 1.47 (2H,quintet), 1.30 (8H,m), 0.89 (3H,t).
ir (KBr) ν_{max} cm^{-1}	3310 (br), 2951, 2923, 2854, 1626, 1534, 1507, 1470, 1300, 1277, 1236, 1157, 1136, 1113, 1037, 996, 970, 807.
ms (m/z)	334(M^+), 223, 222, 193.

4-Bromo-2-fluoroanisole (**19**)

2-fluoroanisole (10.0 g, 0.079 mol) was dissolved in chloroform (20 ml). To this, bromine (12.53 g, 4.1 ml, 0.079 mol) was added dropwise over 2h. After the addition was complete the solution was stirred at room temperature for 1h whereafter it was gently heated under reflux for another hour. The solution was allowed to cool to room temperature and washed with brine (2×50 ml), 10% sodium hydroxide (2×50 ml) and finally with brine (2×80 ml) before drying over $MgSO_4$. The solvent was removed and the crude product distilled under vacuum.

yield	9.41 g (58%)
bp	54-56°C (0.1 mmHg)
	(lit.[62] 98°C / 20 mmHg)
^{1}H nmr ($CDCl_3$) δ	7.17 (2H,m), 6.81 (1H,at), 3.84 (3H,s).
ms (m/z)	206 (M^+), 204.

Digitised by the Department of Library Services in support of open access to information, University of Pretoria, 2021.

UNIVERSITEIT VAN PRETORIA
UNIVERSITY OF PRETORIA
YUNIBESITHI YA PRETORIA

4-Methoxy-3-fluorobenzonitrile (**20**)

A solution of 4-bromo-2-fluoroanisole (**19**) (9.41 g, 0.046 mol) and anhydrous copper(I) cyanide (4.48 g, 0.050 mol) in DMF (10 ml) was heted under reflux at 180°C for 3h. The dark brown solution which solidified upon cooling was added to a solution of anhydrous iron(III)chloride (8 g) in conc. hydrochloric acid (0.5 ml) and water (80 ml). The mixture was stirred at 50-60°C for 30 min and allowed to cool to room temperature. This was extracted with ether (4×60 ml). The combined ether fractions were washed with brine (2×250 ml) and dried ($MgSO_4$). The crude product was recrystallised from dichloromethane-hexane mixtures to give the pure product as white needles.

yield	4.26 g (62%)
ir (KBr) ν_{max} cm^{-1}	2230 (C≡N), 1285 (lit.[62] 2215, 1285)
^1H nmr ($CDCl_3$) δ	7.41 (1H,dt), 7.34 (1H,dd), 6.99 (1H,at), 3.93 (3H, s).
ms (m/z)	150 (M^+).

3-Fluoro-4-hydroxybenzoic acid (**21**)

A solution of 4-methoxy-3-fluorobenzonitrile (**20**) (4.268 g, 0.028 mol) was refluxed for 14h in a mixture of aqueous hydrobromic acid (60 ml) and acetic acid (30 ml). The solution was left to cool to room temperature, water (30 ml) was added and it was then kept in the refridgerator for 6h. The product was filtered off, washed with a minimum amount of cold water and dried.

yield	3.35 g (77%)
mp	157-158°C (lit.[63] 159°C)
^1H nmr (acetone-d_6) δ	13.28 (1H,br. s), 7.83 (1H,dd), 7.69 (1H,dd), 7.23 (1H,at).
ms (m/z)	156 (M^+)

4-Methoxycarbonyloxybenzoic acid (**25**)

A solution of sodium hydroxide (15 g) in water (400 ml) was chilled to 0°C in ice, after which 4-hydroxybenzoic acid (17.9 g, 0.130 mol) was added. Methylchloroformate (20 g, 0.212 mol) was then added slowly, taking care that the temperature did not exceed 5°C. The reaction mixture was stirred at 0-5°C for 3h during which a white suspension gradually became visible. The pH was adjusted to 4-5 with addition of hydrochloric acid / water (1:1). The voluminous precipitate was then filtered off, washed with water and finally recrystallised from ethanol (200 ml). Another crop of crystals was recovered by concentrating the mother liquor.

yield	23.2 g (91%)
mp	177-178°C, nematic
ir (KBr) ν_{max} cm^{-1}	1746, 1669, 1400, 823.
	(lit.[64] 1740, 1670, 1400, 820)
^1H nmr ($CDCl_3$) δ	7.90 (2H,m), 7.34 (1H,dd), 3.94 (3H, s), -COOH not observed.
ms (m/z)	214 (M^+).

Digitised by the Department of Library Services in support of open access to information, University of Pretoria, 2021.

UNIVERSITEIT VAN PRETORIA
UNIVERSITY OF PRETORIA
YUNIBESITHI YA PRETORIA

3-Fluoro-4-methoxycarbonyloxybenzoic acid (**26**)

Quantities: 3-fluoro-4-hydroxybenzoic acid (**21**) (1.00 g, 6.4 mmol), methylchloroformate (1.212 g, 12.8 mmol).

The experimental procedure was as described for the preparation of compound **25**.

yield	0.918 g (67%)
mp	137-139°C
^{1}H nmr ($CDCl_3$) δ	7.90 (2H,m), 7.34 (1H,dd), 3.94 (3H,s), no obvious COOH.
ir (KBr) ν_{max} cm^{-1}	3200-2600, 1776, 1694, 1598, 1513, 1448, 1285, 1197, 930, 769.

2-Fluoro-4-methoxycarbonyloxybenzoic acid (**27**)

Quantities: 2-fluoro-4-hydroxybenzoic acid (**24**) (0.97 g, 6.23 mmol), methylchloroformate (1.09 g, 11.48 mmol).

The experimental procedure was as described for compound **25**.

yield	1.50 g (89%)
mp	165-166°C
ir (KBr) ν_{max} cm^{-1}	3400-2200, 1580, 1500, 1446, 1330-1190, 1145, 967, 936, 775.

2,3-Difluoro-4-octyloxybiphenyl-4'-yl (4-methoxycarbonyloxy)benzoate (**28**)

To a solution of 4-methoxycarbonyloxybenzoic acid (**25**) (1.50 g, 7.64 mmol) and compound **15** (2.55 g, 7.64 mmol) in THF (60 ml) was added diethylazodicarboxylate (1.329 g, 7.64 mmol) under an atmosphere of dry nitrogen. Triphenylphosphine (2.003 g, 7.64 mmol), dissolved in dry THF (60 ml), was added to the above solution slowly. This solution was stirred at room temperature for 8h. The solvent was removed under reduced pressure and the product purified by flash chromatography [silica gel / petroleum ether (40-60°C) - dichloromethane (1:2)].

yield	3.05 g (78%)
phase transitions	K 76.0°C/99.8°C N 201.9°C Iso
^{1}H nmr ($CDCl_3$) δ	8.27 (2H,m), 7.57 (2H,m), 7.36 (2H,m), 7.28 (2H,m), 7.11 (1H,td), 6.81 (1H,td), 4.08 (2H,t), 3.95 (3H,s), 1.85 (2H,quintet), 1.50 (2H,quintet), 1.33 (8H,m), 0.90 (3H,t).
ir (KBr) ν_{max} cm^{-1}	2925, 2825, 1570, 1530, 1605, 1510, 1475, 1508, 1477, 1270, 1212, 1170, 1085, 940, 800, 766.
ms (m/z)	512(M^+)

Digitised by the Department of Library Services in support of open access to information, University of Pretoria, 2021.

UNIVERSITEIT VAN PRETORIA
UNIVERSITY OF PRETORIA
YUNIBESITHI YA PRETORIA

2,3-Difluoro-4-octyloxybiphenyl-4'-yl 3-fluoro-4-methoxycarbonyloxybenzoate (**29**)

Quantities: compound **15** (0.781 g, 2.3 mmol), 3-fluoro-4-methoxycarbonyloxybenzoic acid (**26**) (0.5 g, 2.3 mmol), diethylazodicarboxylate (0.488g, 2.8 mmol), triphenylphosphine (0.733 g, 2.8 mmol).

The experimental procedure was the same as for compound **28**.

yield	0.526 g (43%)
phase transitions	K 84.0°C/103.8°C N 177.5°C Iso
^{1}H nmr ($CDCl_3$) δ	8.02 (2H,m), 7.54 (2H,m), 7.39 (1H,dd), 7.26 (2H,m), 7.08 (1H,td), 6.79 (1H,td), 4.07 (2H,t), 3.96 (3H,s), 1.83 (2H,quintet), 1.47 (2H,quintet), 1.32 (8H,m), 0.88 (3H,t).
ir (KBr) ν_{max} cm^{-1}	2949, 2922, 2859, 1775, 1743, 1508, 1472, 1438, 1305, 1217, 1192, 1077, 933, 895, 789, 758, 735.
ms (m/z)	530(M^+), 197, 153.

2,3-Difluoro-4-octyloxybiphenyl-4'-yl 2-fluoro-4-methoxycarbonyloxybenzoate (**30**)

Quantities: compound **15** (1.40 g, 4.2 mmol), 2-fluoro-4-methoxycarbonyloxybenzoic acid (**27**) (0.897 g, 4.2 mmol), diethylazodicarboxylate (0.875 g, 5.0 mmol), triphenylphosphine (1.318 g, 5.0 mmol).

The compound was prepared using the same procedure as for the preparation of compound **28**.

yield	1.10 g (49%)
phase transitions	K 60.5°C/117.3°C N 164.7°C Iso
^{1}H nmr ($CDCl_3$) δ	8.14 (1H,t), 7.53 (2H,d), 7.27 (2H,d), 7.30-7.10 (2H,m), 7.08 (1H,td), 6.80 (1H,td), 4.06 (2H,t), 3.94 (3H,s), 1.83 (2H,quintet), 1.47 (2H,quintet), 1.42-1.23 (8H,m), 0.88 (3H,t).
ir (KBr) ν_{max} cm^{-1}	2932, 2853, 1756, 1732, 1615, 1505, 1470, 1447, 1406, 1295, 1247, 1080, 963, 942, 871, 800, 781, 724.
ms (m/z)	530(M^+), 221, 198, 197, 153, 110.

2,3-Difluoro-4-octyloxybiphenyl-4'-yl 4-hydroxybenzoate (**31**)

A suspension of compound **28** (2.7 g, 5.27 mmol) in a mixture of ethanol (60 ml) and ammonia (35%, 60 ml) was stirred at room temperature for 8h or until tlc showed the reaction to be complete. The volatile components were removed on the rotary evaporator (waterbath < 55°C) to give a white powder which was further dried *in vacuo* (P_2O_5).

yield	2.34 g (97%)
mp	145°C
^{1}H nmr ($CDCl_3$) δ	8.13 (2H,m), 7.55 (2H,m), 7.27 (2H,m), 7.09 (1H,td), 6.92 (2H,m), 6.80 (1H,td), 5.04 (1H,s), 4.07 (2H,t), 1.84 (2H,m), 1.48 (2H,m), 1.31 (8H,m), 0.89 (3H,t).

Digitised by the Department of Library Services in support of open access to information, University of Pretoria, 2021.

UNIVERSITEIT VAN PRETORIA
UNIVERSITY OF PRETORIA
YUNIBESITHI YA PRETORIA

ir (KBr) ν_{max} cm^{-1}	3320, 2960, 2930, 2760, 1734, 1705, 1610, 1509, 1475, 1294, 1215, 1200, 1171, 1104, 1082, 800, 765.
ms (m/z)	454(M^+).

2,3-Difluoro-4-octyloxybiphenyl-4'-yl 3-fluoro-4-hydroxybenzoate (**32**)

Compound **29** (0.500 g, 0.94 mmol) was suspended in a mixture of dichloromethane (10 ml), ethanol (20 ml) and ammonia (35%, 10 ml). This was stirred at room temperature until tlc showed the reaction to be complete (~90 min). The solvents were removed under vacuum and the product purified by flash chromatography on a short column [silica gel / petroleum ether (40-60°C) - ethyl acetate (1:1)]. Finally the product was recrystallised from ethyl acetate - hexane mixtures and dried *in vacuo* (P_2O_5).

yield	0.420 g (94%)
mp	135-137°C
^{1}H nmr δ ($CDCl_3$ +10%DMSO-d_6)	7.80 (2H,m), 7.46 (2H,m), 7.18 (2H,m), 7.02 (1H,td), 7.00 (1H,m), 6.73 (1H,td), 4.00 (2H,t), 2.17 (1H,s), 1.76 (2H,quintet), 1.40 (2H,quintet), 1.22 (8H,m), 0.83 (3H,t).
ir (KBr) ν_{max} cm^{-1}	3500-3200, 2951, 2921, 2854, 1730, 1619, 1508, 1470, 1406, 1305, 1229, 1109, 1087, 894, 869, 799, 751.
ms (m/z)	472(M^+), 335, 334, 222, 221, 140, 139.

2,3-Difluoro-4-octyloxybiphenyl-4'-yl 2-fluoro-4-hydroxybenzoate (**33**)

Quantities: compound **30** (1.00 g, 1.9 mmol), ammonia (10-35%, 30 ml).

The experimental procedure was as described for compound **32**.

yield	0.58 g (64%)
mp	179-180°C
^{1}H nmr ($CDCl_3$) δ ($CDCl_3$+20%DMSO-d_6)	7.72 (1H,t), 7.30 (2H,d), 7.01 (2H,d), 6.88 (1H,td), 6.60 (1H,td), 6.50 (1H,dd), 6.42 (1H,dd), 3.85 (2H,t), 2.57 (1H,s), 1.61 (2H,quintet), 1.25 (2H,quintet), 1.20-0.97 (8H,m), 0.66 (3H,t).
ir (KBr) ν_{max} cm^{-1}	3343, 2932, 2885, 2857, 1705, 1617, 1590, 1505, 1470, 1404, 1282, 1199, 1167, 1132, 1070, 971, 899, 860, 795, 767, 676.
ms (m/z)	472(M^+), 335, 334, 223, 222, 221, 193, 139.

(S)-4-n-octyloxy-2,3-difluorobiphenyl-4'-yl 4-(2-fluorooctanoyloxy)benzoate (**34**)

To a solution of compound **31** (0.5 g, 1.1 mmol), (S)-2-fluoro-octanoic acid (0.178 g, 1.1 mmol) and dimethylaminopyridine (0.03 g) in dry dichloromethane (25 ml) was added slowly a solution of

Digitised by the Department of Library Services in support of open access to information, University of Pretoria, 2021.

UNIVERSITEIT VAN PRETORIA
UNIVERSITY OF PRETORIA
YUNIBESITHI YA PRETORIA

dicyclohexylcarbodiimide (DCC) (0.25 g, 1.2 mmol) in dichloromethane (25 ml) under nitrogen. The reaction mixture was stirred at room temperature for 3h. The precipitate (dicyclohexylurea) was filtered off and the solvent removed under reduced pressure. The product was purified by flash chromatography [silica gel / petroleum ether (40-60°C) - dichloromethane (1:2) initially, but gradually increasing the polarity to 1:9 eventually]. This was followed by recrystallization (twice) from dichloromethane - hexane mixtures.

yield	0.39 g (59%)
^{1}H nmr ($CDCl_3$) δ	8.29 (2H,m,Ar-H), 7.57 (2H,m,Ar-H), 7.31 (2H,m,Ar-H), 7.28 (2H,m,Ar-H), 7.11 (1H,td,Ar-H), 6.81 (1H,td,Ar-H), 5.18 (1H,dt, $^2J_{HF}$=48.6 Hz), 4.08 (2H,t), 2.08 (2H,m), 1.84 (2H,m), 1.66-1.22 (18H,m), 0.85 (6H,2×t).
ir (KBr) ν_{max} cm^{-1}	2960, 2938, 2860, 1760, 1735, 1640, 1606, 1510, 1473, 1410, 1290, 1215, 1170, 1084, 802, 750.
ms (m/z)	598(M^+).
$[\alpha]_D^{30}$	insufficient sample

(S)-4-n-octyloxy-2,3-difluorobiphenyl-4'-yl 3-fluoro-4-(2-fluorooctanoyloxy)benzoate (**35**)

Quantities: compound **32** (0.199 g, 0.42 mmol), (S)-2-fluoro-octanoic acid (0.068 g, 0.42 mmol), dimethylaminopyridine (0.013 g), dicyclohexylcarbodiimide (0.104 g, 0.50 mol).

The experimental procedure was as described for compound **34**. The product was purified by flash chromatography [silica gel / petroleum ether (40-60°C) - dichloromethane (1:4)] and recrystallised twice from dichloromethane - hexane mixtures.

yield	0.165 g (64%)
^{1}H nmr ($CDCl_3$) δ	8.04 (2H,m,Ar-H), 7.55 (2H,m,Ar-H), 7.32 (1H,dd,Ar-H), 7.27 (2H,m,Ar-H), 7.08 (1H,td,Ar-H), 6.79 (1H,td,Ar-H), 5.20 (1H,dt, -FCH-, $^2J_{HF}$ = 48.6 Hz), 4.07 (2H,t, -OCH_2-), 2.06 (2H,2×m,-FCH_2CH_2-,$^3J_{HF}$ = 25.3 Hz), 1.83 (2H,pentet,-OCH_2CH_2-), 1.59 (2H,quintet, -$OCH_2CH_2CH_2$-), 1.45 (2H,quintet,-$OCH_2CH_2CH_2CH_2$-), 1.32 (14H,m,alkyl-H), 0.89 (6H,2×t,2×-CH_3).
ir (KBr) ν_{max} cm^{-1}	2951, 2918, 2861, 1769, 1733, 1508, 1469, 1308, 1202, 1108, 1079, 892, 867, 793, 749.
ms (m/z)	616(M^+), 503, 334, 283, 255, 222, 221, 140, 139.
$[\alpha]_D^{30}$	insufficient sample

(S)-4-n-octyloxy-2,3-difluorobiphenyl-4'-yl 2-fluoro-4-(2-fluorooctanoyloxy)benzoate (**36**)

Quantities: compound **33** (0.160 g, 0.3 mmol), (S)-2-fluoro-octanoic acid (0.055 g, 0.3 mmol), dimethylaminopyridine (DMAP) (0.011 g), dicyclohexylcarbodiimide (0.084 g, 0.4 mmol).

Digitised by the Department of Library Services in support of open access to information, University of Pretoria, 2021.

UNIVERSITEIT VAN PRETORIA
UNIVERSITY OF PRETORIA
YUNIBESITHI YA PRETORIA

The compound was prepared using the method described for the preparation of compound **35**.

yield	0.10 g (48%)
^{1}H nmr ($CDCl_3$) δ	8.17 (1H,t,Ar-H), 7.54 (2H,m,Ar-H), 7.28 (2H,m,Ar-H), 7.07 (3H,m,Ar-H), 6.79 (1H,td,Ar-H), 5.14 (1H,dt, -FCH-, $^2J_{HF}$ = 48.7 Hz), 4.06 (2H,t,-OCH_2-), 2.05 (2H,2×m,-FCH_2CH_2-,$^3J_{HF}$ = 24.0 Hz), 1.83 (2H,quintet,-OCH_2CH_2-), 1.69-1.20 (18H,m,alkyl-H), 0.88 (6H,2×t,2×-CH_3).
ir (KBr) ν_{max} cm^{-1}	2955, 2928, 2855, 1760, 1742, 1614, 1506, 1470, 1293, 1254, 1214, 1126,1087, 1062, 976, 877, 800.
ms (m/z)	616(M^+), 515, 471, 455, 333, 283, 221, 193, 189.
$[\alpha]_D^{30}$	+3.1°

(S)-4-n-octyloxy-2,3-difluorobiphenyl-4'-yl 4-(2-fluorooctyloxy)benzoate (**37**)

A solution of compound **31** (0.50 g, 1.1 mmol), (S)-2-fluoro-octanol (0.163 g, 1.1 mmol), diethylazodicarboxylate (0.192 g, 1.1 mmol) was prepared in dry THF (25 ml) under nitrogen. A solution of triphenylphosphine (0.29 g, 1.1 mmol) in THF (10 ml) was added to this slowly. The solution wa stirred overnight at room temperature and the solvent removed under reduced pressure. The residue was purified using flash chromatography [silica gel / petroleum ether (40-60° C) - dichloromethane (1:2)] and recrystallised form hexane - dichloromethane mixtures.

yield	0.31 g (48%)
^{1}H nmr ($CDCl_3$) δ	8.18 (2H,m,Ar-H), 7.56 (2H,m,Ar-H), 7.28 (2H,m,Ar-H), 7.10 (1H,td,Ar-H), 7.02 (2H,m Ar-H), 6.80 (1H,td,Ar-H), 4.87 (1H,2×m, -FCH-, $^2J_{HF}$ = 48.0 Hz), 4.23-4.11 (2H,m,-OCH_2FCH-), 4.08 (2H,t,-OCH_2-), 1.85 (2H,quintet,-OCH_2CH_2-), 1.55-1.20 (20H,m,alkyl-H), 0.90 (6H,2×t,2×-CH_3).
ir (KBr) ν_{max} cm^{-1}	2960, 2940, 2862, 1728, 1610, 1513, 1504, 1472, 1263, 1211, 1172, 1078, 795, 762.
ms (m/z)	584(M^+).
$[\alpha]_D^{30}$	+2.7°

(S)-4-n-octyloxy-2,3-difluorobiphenyl-4'-yl 3-fluoro-4-(2-fluorooctyloxy)benzoate (**38**)

Quantities: compound **32** (0.180 g, 0.38 mmol), (S)-2-fluoro-octanol (0.056 g, 0.38 mmol), diethylazodicarboxylate (0.080 g, 0.46 mmol), triphenylphosphine (0.120 g, 0.46 mmol).

The experimental procedure was as for the preparation of compound **37**.

yield	0.163 g (71%)
^{1}H nmr ($CDCl_3$) δ	7.94 (2H,m,Ar-H), 7.53 (2H,m,Ar-H), 7.24 (2H,m,Ar-H), 7.08 (1H,td,Ar-H), 7.05 (2H,m Ar-H), 6.79 (1H,td,Ar-H), 4.87 (1H,2×m, -FCH-, $^2J_{HF}$ = 48.5 Hz), 4.24 (2H,m,-OCH_2FCH-), 4.06 (2H,t,-OCH_2-), 1.78 (2H,quintet,-OCH_2CH_2-), 1.73 (2H,m,

Digitised by the Department of Library Services in support of open access to information, University of Pretoria, 2021.

UNIVERSITEIT VAN PRETORIA
UNIVERSITY OF PRETORIA
YUNIBESITHI YA PRETORIA

	-FCHC$\underline{H}_2$-), 1.47 (2H,quintet, -OCH$_2$CH$_2$C$\underline{H}_2$-), 1.40-1.18 (16H,m,alkyl-$\underline{H}$), 0.88 (6H,2×t,2×-C$\underline{H}_3$).
ir (KBr) ν_{max} cm$_{-1}$	2952, 2920, 2853, 1727, 1620, 1503, 1470, 1297, 1210, 1076, 794, 754.
ms (m/z)	603(M^+), 270, 269, 249, 222, 221, 140, 139.
$[\alpha]_D^{30}$	insufficient sample

(S)-4-n-octyloxy-2,3-difluorobiphenyl-4'-yl 2-fluoro-4-(2-fluorooctyloxy)benzoate (**39**)

Quantities: compound **33** (0.25 g, 0.53 mmol), (S)-2-fluoro-octanol (0.078 g, 0.53 mmol), diethylazodicarboxylate (0.111 g, 0.64 mmol), triphenylphosphine (0.167 g, 0.64 mmol).

The experimental procedure was as for compound **37**.

yield	0.26 g (82%)
^{1}H nmr ($CDCl_3$) δ	8.06 (1H,t,Ar-$\underline{H}$), 7.53 (2H,m,Ar-$\underline{H}$), 7.26 (2H,m,Ar-$\underline{H}$), 7.07 (1H,td,Ar-$\underline{H}$), 6.80 (2H,m,Ar-$\underline{H}$), 6.71 (1H,dd,Ar-$\underline{H}$), 4.84 (1H,2×m, -FC$\underline{H}$-, $^2J_{HF}$ = 48.4 Hz), 4.14 (2H,dd,-OC$\underline{H}_2$FCH-), 4.06 (2H,t,-OC$\underline{H}_2$-), 1.83 (2H,quintet,-OCH$_2$C$\underline{H}_2$-), 1.69 (2H,m, -FCHC$\underline{H}_2$-), 1.47 (2H,quintet, -OCH$_2$CH$_2$C$\underline{H}_2$-), 1.30 (16H,m,alkyl-$\underline{H}$), 0.89 (6H,2×t,2×-C$\underline{H}_3$).
ir (KBr) ν_{max} cm^{-1}	2958, 2923, 2860, 1743, 1722, 1623, 1581, 1505, 1471, 1436, 1407, 1290, 1275, 1213, 1173, 1139, 1101, 1082, 926, 876, 848, 803, 758, 687.
ms (m/z)	602(M^+), 334, 270, 269, 249, 222, 139.
$[\alpha]_D^{30}$	+1.4°

3-Fluoro-4-octyloxybiphenyl-4'-yl (4-methoxycarbonyloxy)benzoate (**40**)

Quantities: 4-methoxycarbonyloxybenzoic acid (**25**) (0.74 g, 3.79 mmol), compound **16** (1.20 g, 3.79 mmol), diethylazodicarboxylate (0.66 g, 3.79 mmol), triphenylphosphine (0.995 g, 3.79 mmol).

The experimental procedure was as described for the preparation of compound **28**.

yield	1.30 g (69%)
phase transitions	K 88.1°C/112.0°C N 216.2°C Iso
^{1}H nmr ($CDCl_3$) δ	8.26 (2H,m), 7.58 (2H,m), 7.36 (2H,m), 7.28 (2H,m), 7.26 (2H,m), 7.02 (1H,m), 4.07 (2H,t), 3.95 (3H,s), 1.85 (2H,m), 1.49 (2H,m), 1.33 (8H,m), 0.89 (3H,t).
ir (KBr) ν_{max} cm^{-1}	2925, 2860, 1760, 1732, 1605, 1508, 1267, 1215, 1170, 1132, 1090, 800, 770, 720.
ms (m/z)	494(M^+)

Digitised by the Department of Library Services in support of open access to information, University of Pretoria, 2021.

UNIVERSITEIT VAN PRETORIA
UNIVERSITY OF PRETORIA
YUNIBESITHI YA PRETORIA

3-Fluoro-4-octyloxybiphenyl-4'-yl (2-fluoro-4-methoxycarbonyloxy)benzoate (**41**)

Quantities: 2-fluoro-4-methoxycarbonyloxybenzoic acid (**27**) (0.86 g, 4.01 mmol), compound **16** (1.27 g, 4.01 mmol), diethylazodicarboxylate (0.699 g, 4.01 mmol), triphenylphosphine (1.05 g, 4.01 mmol). The experimental procedure was as described for compound **28**.

yield	1.10 g (53%)
phase transitions	K 62.0°C/86.2°C N 192.1°C Iso
^{1}H nmr ($CDCl_3$) δ	8.16 (1H,m), 7.57 (2H,m), 7.36-6.97 (5H,m), 7.27 (2H,m), 4.07 (2H,t), 3.95 (3H,s), 1.84 (2H,m), 1.49 (2H,m), 1.40-1.23 (8H,m), 0.89 (3H,t).
ir (KBr) ν_{max} cm^{-1}	2925, 2830, 1770, 1750, 1731, 1618, 1500, 1285, 1237, 1210, 1125, 965, 811.
ms(m/z)	512(M^+)

2',3-Difluoro-4-octyloxybiphenyl-4'-yl (2-fluoro-4-methoxycarbonyloxy)benzoate (**42**)

Quantities: 2-fluoro-4-methoxycarbonyloxybenzoic acid (**27**) (0.448 g, 2.09 mmol), compound **17** (0.70 g, 2.09 mmol), diethylazodicarboxylate (0.438 g, 2.51 mmol), triphenylphosphine (0.659 g, 2.51 mmol). The experimental procedure was as described for the preparation of compound **28**.

yield	0.78 g (70%)
phase transitions	K 54.3°C/79.0°C N 174.0°C Iso
^{1}H nmr ($CDCl_3$) δ	8.13 (1H,t), 7.43 (1H,t), 7.31-7.06 (6H,m), 7.01 (1H,t), 4.06 (2H,t), 3.94 (3H,s), 1.83 (2H,quintet), 1.47 (2H,quintet), 1.28 (8H,m), 0.88 (3H,t).
ir (KBr) ν_{max} cm^{-1}	2929, 2855, 1772, 1736, 1618, 1500, 1438, 1287, 1263, 1142, 1067, 957, 936, 871, 798, 724.
ms (m/z)	531(M^+).

2',3-Difluoro-4-octyloxybiphenyl-4'-yl (3-fluoro-4-methoxycarbonyloxy)benzoate (**43**)

Quantities: 2-fluoro-4-methoxycarbonyloxybenzoic acid (**26**) (0.458 g, 2.14 mmol), compound **17** (0.715 g, 2.14 mmol), diethylazodicarboxylate (0.447 g, 2.57 mmol), triphenylphosphine (0.674 g, 2.57 mmol). The experimental procedure was as described for the preparation of compound **28**.

yield	0.456 g (40%)
phase transitions	K 74.2°C/100.5°C SmC 105.0°C N 165.1°C Iso
^{1}H nmr ($CDCl_3$) δ	8.00 (2H,m), 7.43 (2H,m), 7.28 (1H,dd), 7.23 (1H,dd), 7.05 (3H,m), 4.06 (2H,t), 3.96 (3H,s), 1.83 (2H,quintet), 1.48 (2H,quintet), 1.36-1.25 (8H,m), 0.87 (3H,t).
ir (KBr) ν_{max} cm^{-1}	2954, 2916, 2853, 1778, 1732, 1592, 1531, 1496, 1434, 1279, 1188, 1132, 1073, 966, 872, 794, 756.
ms (m/z)	531, 530(M^+), 486, 418, 334, 222, 221, 198, 197, 153.

Digitised by the Department of Library Services in support of open access to information, University of Pretoria, 2021.

UNIVERSITEIT VAN PRETORIA
UNIVERSITY OF PRETORIA
YUNIBESITHI YA PRETORIA

3-Fluoro-4-octyloxybiphenyl-4'-yl 4-hydroxybenzoate (**44**)

Quantity: compound **40** (1.30 g, 2.63 mmol).

The compound was prepared using the method described for compound **31**.

yield	0.91 g (79%)
^{1}H nmr ($CDCl_3$) δ	8.13 (2H,m), 7.57 (2H,m), 7.36-6.97 (5H,m), 6.93 (2H,m), 5.51 (1H,s), 4.07 (2H,t), 1.84 (2H,quintet), 1.48 (2H,quintet), 1.34 (8H,m), 0.90 (3H,t).
ir (KBr) ν_{max} cm^{-1}	3680 (br), 2960, 2890, 1722, 1635, 1608, 15118, 1484, 1387, 1284, 1215, 1185, 1146, 1077, 885, 816, 783, 640.
ms (m/z)	436(M^+).

3-Fluoro-4-octyloxybiphenyl-4'-yl 2-fluoro-4-hydroxybenzoate (**45**)

Quantity: compound **41** (1.00 g, 2.0 mmol).

The experimental procedure was as described for the preparation of compound **31**.

yield	0.88 g (99%)
^{1}H nmr (DMSO-d_6) δ	7.96 (1H,t), 7.57 (2H,m), 7.37-6.98 (3H,m), 7.28 (2H,m), 6.70 (2H,m), 4.07 (2H,t), 1.84 (2H,quintet), 1.55-1.15 (10H,m), 0.90 (3H,t).
ir (KBr) ν_{max} cm^{-1}	3380 (br), 2960, 2890, 1723, 1635, 1518, 1485, 1413, 1338, 1284, 1215, 1184, 1147, 1078, 1030, 990, 885, 815, 784, 640, 540.
ms (m/z)	454(M^+)

2',3-Difluoro-4-octyloxybiphenyl-4'-yl 2-fluoro-4-hydroxybenzoate (**46**)

Quantity: compound **42** (0.610 g, 1.15 mmol).

The experimental procedure was as described for the preparation of compound **32**.

yield	0.33 g (61%)
mp	169-170°C
^{1}H nmr ($CDCl_3$) δ	8.00 (1H,t), 7.41 (1H,t), 7.25 (2H,dd), 7.04 (2H,m), 7.00 (1H,t), 6.68 (2H,m), 5.79 (1H,s), 4.06 (2H,t), 1.83 (2H,quintet), 1.47 (2H,quintet), 1.28 (8H,m), 0.87 (3H,t).
ir (KBr) ν_{max} cm^{-1}	3363 (br), 2947, 2855, 1713, 1616, 1591, 1496, 1408, 1323, 1277, 1258, 1135, 1057, 960, 879, 864, 802, 766.
ms (m/z)	472(M^+), 334, 222, 193, 139.

Digitised by the Department of Library Services in support of open access to information, University of Pretoria, 2021.

UNIVERSITEIT VAN PRETORIA
UNIVERSITY OF PRETORIA
YUNIBESITHI YA PRETORIA

2',3-Difluoro-4-octyloxybiphenyl-4'-yl 3-fluoro-4-hydroxybenzoate (**47**)

Quantities: compound **43** (0.410 g, 0.773 mmol), ammonia (10-35%, 6 ml).

The experimental procedure was as for compound **32**, except that the reaction was complete after 45 min.

yield	0.308 g (84%)
mp	134°C
^{1}H nmr δ	7.67 (2H,m), 7.25 (1H,t), 7.08 (2H,2×dd), 6.89 (4H,m),
($CDCl_3$+10%DMSO-d_6)	3.91 (2H,t), 1.67 (2H,quintet), 1.32 (2H,quintet), 1.29-1.10 (8H,m), 0.72 (3H,t).
ir (KBr) ν_{max} cm^{-1}	3303, 3244, 2949, 2925, 2853, 1716, 1597, 1500, 1439, 1405, 1293, 1244, 1208, 1183, 1147, 1116, 1063, 967, 809, 792, 760.
ms (m/z)	472(M^+), 333, 332, 223, 222, 140, 139.

(S)-4-n-octyloxy-3-fluorobiphenyl-4'-yl 4-(2-fluorooctanoyloxy)benzoate (**48**)

Quantities: compound **44** (0.445 g, 1.0 mmol), (S)-2-fluoro-octanoic acid (0.165 g, 1.0 mmol), dicyclohexylcarbodiimide (0.232 g, 1.1 mmol), dimethylaminopyridine (0.03 g).

The experimental procedure was as described for compound **34**.

yield	0.43 g (73%)
^{1}H nmr ($CDCl_3$) δ	8.28 (2H,m,Ar-H), 7.58 (2H,m,Ar-H), 7.36-7.22 (6H,m,Ar-H), 7.03 (1H,m,Ar-H), 5.18 (1H,2×t, -FCH-, $^2J_{HF}$ = 49.4 Hz), 4.07 (2H,t,-OCH_2-), 2.08 (2H,2×m,FCH_2CH_2-,$^3J_{HF}$ = 24.0 Hz), 1.85 (2H,quintet,-OCH_2CH_2-), 1.66-1.23 (18H,m,alkyl-H), 0.90 (6H,2×t,2×-CH_3).
ir (KBr) ν_{max} cm^{-1}	2960, 2930, 2860, 1767, 1740, 1605, 1510, 1290, 1218, 1137, 1085, 800.
ms (m/z)	580(M^+), 316, 265, 203.
$[\alpha]_D^{30}$	insufficient sample

(S)-4-n-octyloxy-3-fluorobiphenyl-4'-yl 2-fluoro-4-(2-fluorooctanoyloxy)benzoate (**49**)

Quantities: compound **45** (0.498 g, 1.1 mmol), (S)-2-fluoro-octanoic acid (0.178 g, 1.1 mmol), dicyclohexylcarbodiimide (0.248 g, 1.2 mmol), dimethylaminopyridine (0.03 g).

The experimental procedure was as described for the preparation of compound **34**.

yield	0.50 g (76%)
^{1}H nmr ($CDCl_3$) δ	8.19 (1H,m,Ar-H), 7.58 (2H,m,Ar-H), 7.28 (2H,m,Ar-H), 7.36-6.97 (5H,m,Ar-H), 5.17 (1H,td, -FCH-, $^2J_{HF}$ = 48.6 Hz), 4.07 (2H,t,-OCH_2-), 2.07 (2H,2×m,FCH_2CH_2-,$^3J_{HF}$ = 24.0 Hz), 1.85 (2H,quintet,-OCH_2CH_2-), 1.64-1.22 (18H,m,alkyl-H), 0.90 (6H,2×t,2×-CH_3).
ir (KBr) ν_{max} cm^{-1}	2960, 2930, 2860, 1770, 1738, 1618, 1510, 1430, 1302, 1137, 870, 803.

Digitised by the Department of Library Services in support of open access to information, University of Pretoria, 2021.

UNIVERSITEIT VAN PRETORIA
UNIVERSITY OF PRETORIA
YUNIBESITHI YA PRETORIA

ms (m/z)	598(M^+), 454, 433, 354, 316, 214.
$[\alpha]_D^{30}$	insufficient sample

(S)-4-n-octyloxy-2',3-difluorobiphenyl-4'-yl 2-fluoro-4-(2-fluorooctanoyloxy)benzoate (**50**)

Quantities: compound **46** (0.201 g, 0.43 mmol), (S)-2-fluoro-octanoic acid (0.069 g, 0.43 mmol), dicyclohexylcarbodiimide (0.105 g, 0.51 mmol), dimethylaminopyridine (0.013 g).

The compound was prepared as was described for compound **34**.

yield	0.150 g (57%)
^{1}H nmr ($CDCl_3$) δ	8.15 (1H,t,Ar-H), 7.43 (1H,t,Ar-H), 7.28 (1H,m,Ar-H), 7.23 (1H,m,Ar-H), 7.08 (4H,m,Ar-H), 7.01 (1H,t,Ar-H), 5.14 (1H,dt, -FCH-, $^2J_{HF}$ = 48.7 Hz), 4.06 (2H,t,-OCH_2-), 2.04 (2H,2×m,-FCH_2CH_2-,$^3J_{HF}$ = 26.4 Hz), 1.83 (2H,quintet,-OCH_2CH_2-), 1.60-1.20 (18H,m,alkyl-H), 0.88 (6H,2×t,2×-CH_3).
ir (KBr) ν_{max} cm^{-1}	2952, 2919, 2856, 1758, 1743, 1618, 1591, 1534, 1500, 1470, 1405, 1288, 1252, 1217, 1439, 1126, 1088, 1063, 963, 878, 802, 761.
ms (m/z)	617 (M^++1), 366, 334, 283, 222, 139.
$[\alpha]_D^{30}$	+1.9°

(S)-4-n-octyloxy-3-fluorobiphenyl-4'-yl 4-(2-fluorooctyloxy)benzoate (**51**)

Quantities: compound **44** (0.450 g, 1.03 mmol), (S)-2-fluoro-octanol (0.153 g, 1.03 mmol), diethylazodicarboxylate (0.179 g, 1.03 mmol), triphenylphosphine (0.270 g, 1.03 mmol).

The experimental procedure was as described for the preparation of compound **37**.

yield	0.25 g (43%)
^{1}H nmr ($CDCl_3$) δ	8.18 (2H,m,Ar-H), 7.57 (2H,m,Ar-H), 7.36-6.97 (3H,m,Ar-H), 7.28 (2H,m,Ar-H), 7.01 (2H,m,Ar-H), 4.87 (1H,2×m,-FCH-, $^2J_{HF}$ = 49.1 Hz), 4.24-4.10 (2H,m,-OCH_2CFH-), 4.07 (2H,t,-OCH_2-), 1.84 (2H,quintet,-OCH_2CH_2-), 1.56-1.22 (20H,m,alkyl-H), 0.90 (6H,2×t,2×-CH_3).
ir (KBr) ν_{max} cm^{-1}	2960, 2925, 2860, 1733, 1612, 1510, 1471, 1272, 1224, 1173, 1147, 1082, 800, 762.
ms (m/z)	566(M^+), 316, 250, 203, 121.
$[\alpha]_D^{30}$	+1.0°

(S)-4-n-octyloxy-3-fluorobiphenyl-4'-yl 2-fluoro-4-(2-fluorooctyloxy)benzoate (**52**)

Quantities: compound **45** (0.450 g, 1.0 mmol), (S)-2-fluoro-octanol (0.147 g, 1.0 mmol), diethylazodicarboxylate (0.172 g, 1.0 mmol), triphenylphosphine (0.260 g, 1.0 mmol).

Digitised by the Department of Library Services in support of open access to information, University of Pretoria, 2021.

UNIVERSITEIT VAN PRETORIA
UNIVERSITY OF PRETORIA
YUNIBESITHI YA PRETORIA

The experimental procedure was as described for the preparation of compound **37**.

yield	0.35 g (60%)
^{1}H nmr ($CDCl_3$) δ	8.08 (1H,t,Ar-H), 7.56 (2H,m,Ar-H), 7.36-6.97 (3H,m,Ar-H), 7.27 (2H,m,Ar-H), 6.78 (2H,m,Ar-H), 4.86 (1H,2×m, -FCH-, $^2J_{HF}$ = 49.7 Hz), 4.21-4.08 (2H,dd,-OCH_2CFH-), 4.07 (2H,t,-OCH_2-), 1.85 (2H,quintet,-OCH_2CH_2-), 1.54-1.22 (20H,m,alkyl-H), 0.90 (6H,2×t,2×-CH_3).
ir (KBr) ν_{max} cm^{-1}	2960, 2925, 2860, 1730, 1626, 1585, 1510, 1472, 1440, 1300, 1272, 1220, 1137, 873, 840, 802, 760.
ms (m/z)	584(M^+), 269, 203, 139.
$[\alpha]_D^{30}$	+2.7°

(S)-4-n-octyloxy-2',3-difluorobiphenyl-4'-yl 2-fluoro-4-(2-fluorooctyloxy)benzoate (**53**)

Quantities: compound **46** (0.220 g, 0.47 mmol), (S)-2-fluoro-octanol (0.069 g, 0.47 mmol), diethylazodicarboxylate (0.097 g, 0.56 mmol), triphenylphosphine (0.147 g, 0.56 mmol).

The experimental procedure was the same as for compound **37**.

yield	0.200 g (71%)
^{1}H nmr ($CDCl_3$) δ	8.07 (1H,t,Ar-H), 7.41 (1H,t,Ar-H), 7.25 (2H,dd,Ar-H), 7.06 (2H,m,Ar-H), 7.00 (1H,t,Ar-H), 6.80 (1H,dd,Ar-H), 6.70 (1H,dd,Ar-H), 4.84 (1H,2×m, -FCH-, $^2J_{HF}$ = 48.6 Hz), 4.14 (2H,dd,-OCH_2CFH-), 4.06 (2H,t,-OCH_2-), 1.83 (2H,quintet,-OCH_2CH_2-), 1.67 (2H,m,-FCH_2CH_2-), 1.47 (2H,quintet, -$OCH_2CH_2CH_2$-), 1.30 (16H,m,alkyl-H), 0.87 (6H,2×t,2×-CH_3).
ir (KBr) ν_{max} cm^{-1}	2952, 2928, 2860, 1743, 1623, 1583, 1501, 1473, 1268, 1242, 1149, 1132, 1108, 1062, 884, 848, 798, 758.
ms (m/z)	602(M^+), 334, 270, 269, 249, 222, 139.
$[\alpha]_D^{30}$	+5.0°

(S)-4-n-octyloxy-2',3-difluorobiphenyl-4'-yl 3-fluoro-4-(2-fluorooctyloxy)benzoate (**54**)

Quantities: compound **47** (0.180 g, 0.38 mmol), (S)-2-fluoro-octanol (0.056 g, 0.38 mmol), diethylazodicarboxylate (0.080 g, 0.46 mmol), triphenylphosphine (0.121 g, 0.46 mmol).

The experimental procedure was the same as for compound **37**.

yield	0.189 g (83%)
^{1}H nmr ($CDCl_3$) δ	7.93 (2H,m,Ar-H), 7.39 (1H,t,Ar-H), 7.25 (2H,2×dd,Ar-H), 7.04 (4H,m,Ar-H), 4.88 (1H,2×m, -FCH-, $^2J_{HF}$ = 48.5 Hz), 4.24 (2H,m,-OCH_2CFH-), 4.06 (2H,t,-OCH_2-), 1.83 (2H,quintet,-OCH_2CH_2-), 1.81-1.54 (2H,m,-FCH_2CH_2-), 1.42 (2H,quintet, -$OCH_2CH_2CH_2$-), 1.40-1.21 (16H,m,alkyl-H), 0.88 (6H,2×t,2×-CH_3).

Digitised by the Department of Library Services in support of open access to information, University of Pretoria, 2021.

UNIVERSITEIT VAN PRETORIA
UNIVERSITY OF PRETORIA
YUNIBESITHI YA PRETORIA

ir (KBr) ν_{max} cm^{-1}	2955, 2924, 2855, 1731, 1618, 1589, 1529, 1499, 1439, 1297, 1236, 1196, 1141, 1108, 800, 753.
ms (m/z)	602(M^+), 334, 271, 222, 221, 140, 139.
$[\alpha]_D^{30}$	insufficient sample

(S)-4-n-octyloxy-2,3-difluorobiphenyl-4-yl 4-(2-chloro-4-methylpentanoyloxy)benzoate (**55**)

Quantities: (S)-2-chloro-4-methylpentanoic acid (0.15 g, 1.0 mmol), compound **31** (0.450 g, 1.0 mmol), dicyclohexylcarbodiimide (0.227 g, 1.1 mmol), dimethylaminopyridine (0.037 g).

The experimental procedure was as described for the preparation of compound **34**.

yield	0.31 g (53%)
^{1}H nmr ($CDCl_3$) δ	8.28 (2H,m,Ar-H), 7.57 (2H,m,Ar-H), 7.29 (4H,m,Ar-H), 7.10 (1H,m,Ar-H), 6.81 (1H,m,Ar-H), 4.57 (1H,t,-CHCl-), 4.08 (2H,t,-OCH_2-), 2.01 (3H,m,-CH_2CH-), 1.84 (2H,quintet,-OCH_2CH_2-), 1.56-1.22 (10H,m,alkyl-H), 1.03 (6H,2×d,2×-CH_3), 0.89 (3H,t,-CH_3).
ir (KBr) ν_{max} cm^{-1}	2965, 2930, 2860, 1770, 1740, 1607, 1510, 1476, 1270, 1210, 1768, 1085, 803.
ms (m/z)	586(M^+), 513, 253, 221, 121.
$[\alpha]_D^{30}$	-11.0°

2,3-Difluoro-4-octyloxybiphenyl 4'-(4-ferrocenyl)benzoate (**56**)

4-Carboxyphenylferrocene (0.101 g, 0.33 mmol), compound **15** (0.110 g, 0.33 mmol) together with a catalytic amount of p-dimethylaminopyridine (DMAP) (0.011 g) were added to dry dichloromethane (20 ml) under nitrogen. Dicyclohexylcarbodiimide (0.085 g, 0.41 mmol) in dichloromethane (3 ml) was added slowly. The solution was stirred overnight at room temperature. After filtration and removal of the solvent under reduced pressure, the residue was purified by flash chromatography [silica gel / petroleum ether (40-60°C) - dichloromethane (1:1)] to give an orange solid which was recrystallised from dichloromethane - hexane mixtures.

yield	0.100 g, (49%)
^{1}H nmr ($CDCl_3$) δ	8.11 (2H,m,Ar-H), 7.55 (4H,m,Ar-H), 7.29 (2H,m,Ar-H), 7.09 (1H,dt,Ar-H), 6.79 (1H,dt,Ar-H), 4.74 (2H,t,-C_5H_4), 4.41 (2H,t,-C_5H_4), 4.07 (2H,t,-OCH_2), 4.05 (5H,s,C_5H_5), 1.83 (2H,quintet,-OCH_2CH_2-), 1.48 (2H,quintet,-$OCH_2CH_2CH_2$-), 1.30 (8H,m,-$(CH_2)_4$-), 0.89 (3H,t,-CH_3).
ir (KBr) ν_{max} cm^{-1}	2922, 2847, 1729, 1603, 1499, 1468, 1401, 1265, 1209, 1172, 1103, 1072, 1012, 889, 855, 824, 767, 694, 521, 481.
ms (m/z)	622(M^+), 290, 289, 262, 261, 120, 55.

Digitised by the Department of Library Services in support of open access to information, University of Pretoria, 2021.

UNIVERSITEIT VAN PRETORIA
UNIVERSITY OF PRETORIA
YUNIBESITHI YA PRETORIA

2.2 Discussion

2.2.1 Scheme 1

Reaction 1C involves linking together two aryl groups by making use of a palladium catalyst. The procedure involves the cross-coupling of an arylboronic acid with an aryl iodide and was developed by Suzuki *et al*[71] and subsequently used with much success in the synthesis of liquid crystals[42,65]. The boronic acid was prepared from the aryllithium reagent by adding tri-isopropylborate (or trimethylborate) in THF at -78°C followed by the hydrolysis of the borate ester with hydrochloric acid. The crucial part in the synthesis of **3** is the lithiation of the position *ortho* to the fluorine atom[42,66]. In the synthesis of **10**, lithiation is forced to take place at the site of the bromo-substituent, but with consequent reduction in yield.

The cross-coupling of the boronic acid with the 1-bromo-4-iodobenzene depends on the fact that the rate of coupling decreases in the order I > Br > Cl > CN >> F, i.e. that coupling will readily occur at the site of the iodo-substituent. The role of the $Pd(PPh_3)_4$ catalyst and its addition to aryl halides has been the subject of an investigation[67]. In an inert solvent such as benzene or 1,2-dimethoxyethane the following is thought to occur[68]:

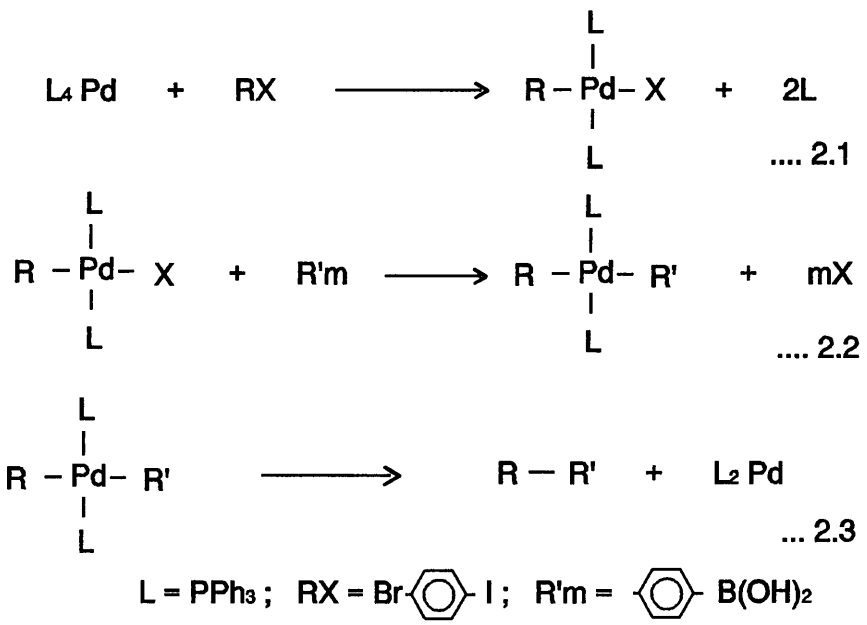

Figure 2.1

Digitised by the Department of Library Services in support of open access to information, University of Pretoria, 2021.

$Pd(PPh_3)_4$ dissociates to give a coordinatively unsaturated species which then undergoes oxidative addition (eq. 2.1). Here the rate determining step (rds) is the cleaving of the C - X bond (eq. 2.4)[67].

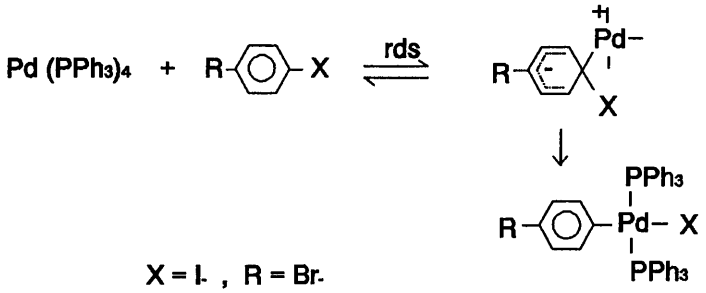

... 2.4

Figure 2.2

This step in turn depends on the extent to which the ring is activated towards substitution, i.e. it depends on the nature of the group R in the *para* position.

Oxidative addition is then followed by transmetallation (eq. 2.2) followed by reductive elimination to give the coupled product (eq. 2.3).

In this work the target compound is the phenol:

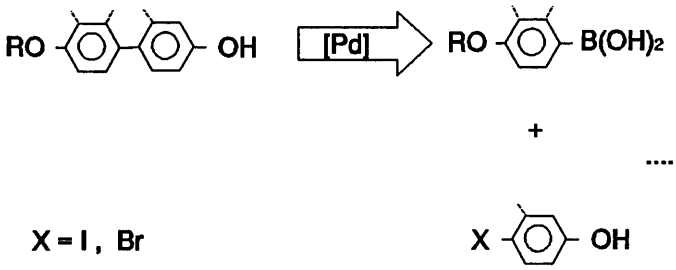

.... 2.5

Figure 2.3

It would therefore have been convenient to prepare the coupled phenol in one step from 4-bromophenol. However, attempts to carry out this coupling reaction in various solvents and even using the more

Digitised by the Department of Library Services in support of open access to information, University of Pretoria, 2021.

UNIVERSITEIT VAN PRETORIA
UNIVERSITY OF PRETORIA
YUNIBESITHI YA PRETORIA

reactive 4-iodophenol were unsuccessful. This failure was thought to be due to the deactivating influence exerted by the hydroxy group which is mildly electron-donating. Hence, it was decided to replace the hydroxy group with a more electron-withdrawing substituent (such as bromine) that could be converted to the hydroxy group in a subsequent step (this will be discussed under *Scheme 2*).

Reaction 1C was carefully monitored with tlc to ensure optimum yield of the biphenyl, but to prevent subsequent coupling of this product (**9**, **10** or **11**) with unreacted boronic acid (which is added in about 10% excess) to give unwanted terphenyl. Even by rigorously excluding air (using degassed solvents) in an attempt to minimise decomposition of the catalyst, a yield of no more than 65% could be obtained for **9** or **10**. The presence of a fluoro-substituent *meta* to the site of reaction (as in **11**) resulted in a decrease in yield.

2.2.2 Scheme 2

Scheme 2 shows the conversion of the bromide to a hydroxy group *via* the boronic acid. Direct nucleophilic displacement of the halogen in an aryl halide by hydrolysis to the corresponding phenol is very difficult unless one or more strongly electron-withdrawing groups are present on the ring. In the case of compounds **9**, **10** and **11**, conversion to the phenol was conveniently done *via* the boronic acid by treating the crude reaction mixture directly with hydrogen peroxide. Although phenols **15** and **16** are quite stable, compound **17** is extremely light sensitive and was difficult to purify.

2.2.3 Scheme 3

4-Methoxy-3-fluorobenzonitrile (**20**) was prepared according to the method published by Kelly[62]. This was then hydrolised in a mixture of aqueous hydrobromic and acetic acid following the method of Nabor *et al*[63].

2.2.4 Schemes 4 and 6

The protection / deprotection of the phenol group of the 4-hydroxybenzoic acid (**22**) or derivatives thereof (**21** and **24**) was done by adapting a method published by Chin and Goodby[64]. The rate of reaction was found to depend on the position of the fluoro-substituent on the aromatic ring.

Esterification of the respective phenols (steps 4B and 6B) was accomplished by employing a Mitsunobu coupling[69]. The reaction conditions (diethylazodicarboxylate (DEAD) and triphenylphosphine in THF) are

Digitised by the Department of Library Services in support of open access to information, University of Pretoria, 2021.

UNIVERSITEIT VAN PRETORIA
UNIVERSITY OF PRETORIA
YUNIBESITHI YA PRETORIA

conducive to the methylcarbonate protecting group remaining intact. Once again, yields varied according to the location of the fluoro-substituent.

2.2.5 Schemes 5, 7 and 8

The respective phenols, **31 - 33** and **44 - 47**, were esterified with (S)-2-fluoro-octanoic acid in the presence of dicyclohexylcarbodiimide (DCC) and N,N-dimethylaminopyridine (DMAP)[70], while their etherification with (S)-2-fluoro-octanol was carried out using the Mitsunobu coupling[69]. The latter method consistently gave good yields (>70%). In contrast to this, the esterification procedure frequently led to average (40-60%) yields and in the extreme case of compound **35** a recovery of only 27%. This is thought to be due to steric hindrance caused by the fluoro-substituent *ortho* to the phenolic OH. Additionally, although the ester-analogue of compound **55** could be prepared in low yield, purification attempts invariably resulted in some degree of saponification, probably for the same reason mentioned before and the compound could not be isolated. Though it was by no means attempted to optimise yields, the method of esterification employed here is clearly not generally adaptable.

---- # ----

Digitised by the Department of Library Services in support of open access to information, University of Pretoria, 2021.

UNIVERSITEIT VAN PRETORIA
UNIVERSITY OF PRETORIA
YUNIBESITHI YA PRETORIA

CHAPTER 3

OPTICAL AND THERMAL PROPERTIES

3.1 Introduction

The properties of liquid crystals are commonly correlated with their molecular structures by way of observing a homologous series of compounds - i.e. the number of carbons in one or both of the terminal chains is increased stepwise (for example see Waugh *et al*[72]). In this work the approach was to keep the length of the chains constant (for reasons mentioned below) and to vary the number and positions of the lateral substituents. Previously, the effect of lateral fluorination on a variety of core systems of achiral compounds was investigated (see section 1.3, page 7), but only more recently have attempts been made to determine the effect of the position and number of fluoro-substituents on the incidence of helical phases and their properties[58,73].

For this work a molecular framework was chosen that would be conducive to the formation of a smectic C^* phase:

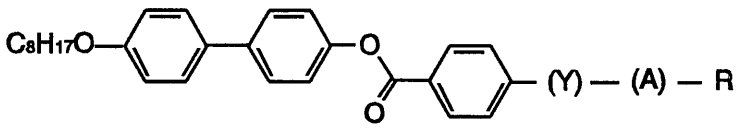

R = C_6H_{13}- (or -$CH_2CH(CH_3)_2$)

Y = -OCH_2- or -OOC-

A = -HC*F- (or -HC*Cl-)

Here, a biphenyl-ester-phenyl core system is combined with two terminal chains of intermediate, but nearly equal length. This was then combined with the following:

(i) two different groups Y (approximately equal in length but differing in rigidity) linking the core with the chiral center;

Digitised by the Department of Library Services in support of open access to information, University of Pretoria, 2021.

UNIVERSITEIT VAN PRETORIA
UNIVERSITY OF PRETORIA
YUNIBESITHI YA PRETORIA

(ii) a fluoro (or in one case chloro)-substituent at the chiral center which serves the dual purpose of being useful for nmr experiments and of introducing a dipole onto the chiral center;

(iii) lateral fluoro-substituents which were used in various combinations of the positions indicated - this was done in a manner that would facilitate the study of the molecules by ^{19}F nmr spectroscopy.

This chapter concerns the identification of liquid crystalline phases, the determination of phase transition temperatures as well as the measurement of selected electro-optical experiments.

Mesophases are in the first instance identified by optical microscopy - each type of mesophase shows a characteristic texture when a film of material on a microscope slide is viewed through crossed polarisers. The different textures displayed by the chiral nematic or cholesteric (Ch) and smectic A (SmA) phases (both of which commonly occur in liquid crystals prepared for this work) are well-documented[74,75]. The chiral smectic C (SmC^*) phase can display a variety of textures[75]. These depend to a large extent on the texture of the preceding phase as well as on the thickness of the observed sample and some examples will be discussed in section 3.2. Some of the compounds exhibit frustrated phases: (i) the chiral smectic A (TGB_{A^*}) phase and (ii) one or more blue phases (BP). The occurrence and identification of these phases are discussed.

Phases transitions are accomplished by a change in enthalpy which can be measured using differential scanning calorimetry (DSC). DSC therefore cannot be used to identify a phase, but the magnitude of the enthalpy change often reveals whether a transition is first or second order. Whereas first order transitions are commonly associated with SmA - Ch or SmC^* - Ch transitions, The SmC^* - SmA transition is usually second order. However, in this work some exceptions were found where the SmC^* - SmA transition sometimes tends towards being weakly first order and the SmA - Ch transition is second order.

Finally, as most of the compounds possess a ferroelectric SmC^* phase some of their electro-optical properties were measured. These are discussed in section 3.4.

To summarise, attempts are made to relate macroscopic properties (occurrence of liquid crystalline phases, tilt angle, polarisation, pitch length) to the molecular structure of the compounds. Some of the liquid crystals were additionally investigated on the molecular level using nmr spectroscopy. These compounds are included in this chapter for the purpose of comparison, but they will be discussed more extensively in chapters 5, 6 and 7.

Digitised by the Department of Library Services in support of open access to information, University of Pretoria, 2021.

UNIVERSITEIT VAN PRETORIA
UNIVERSITY OF PRETORIA
YUNIBESITHI YA PRETORIA

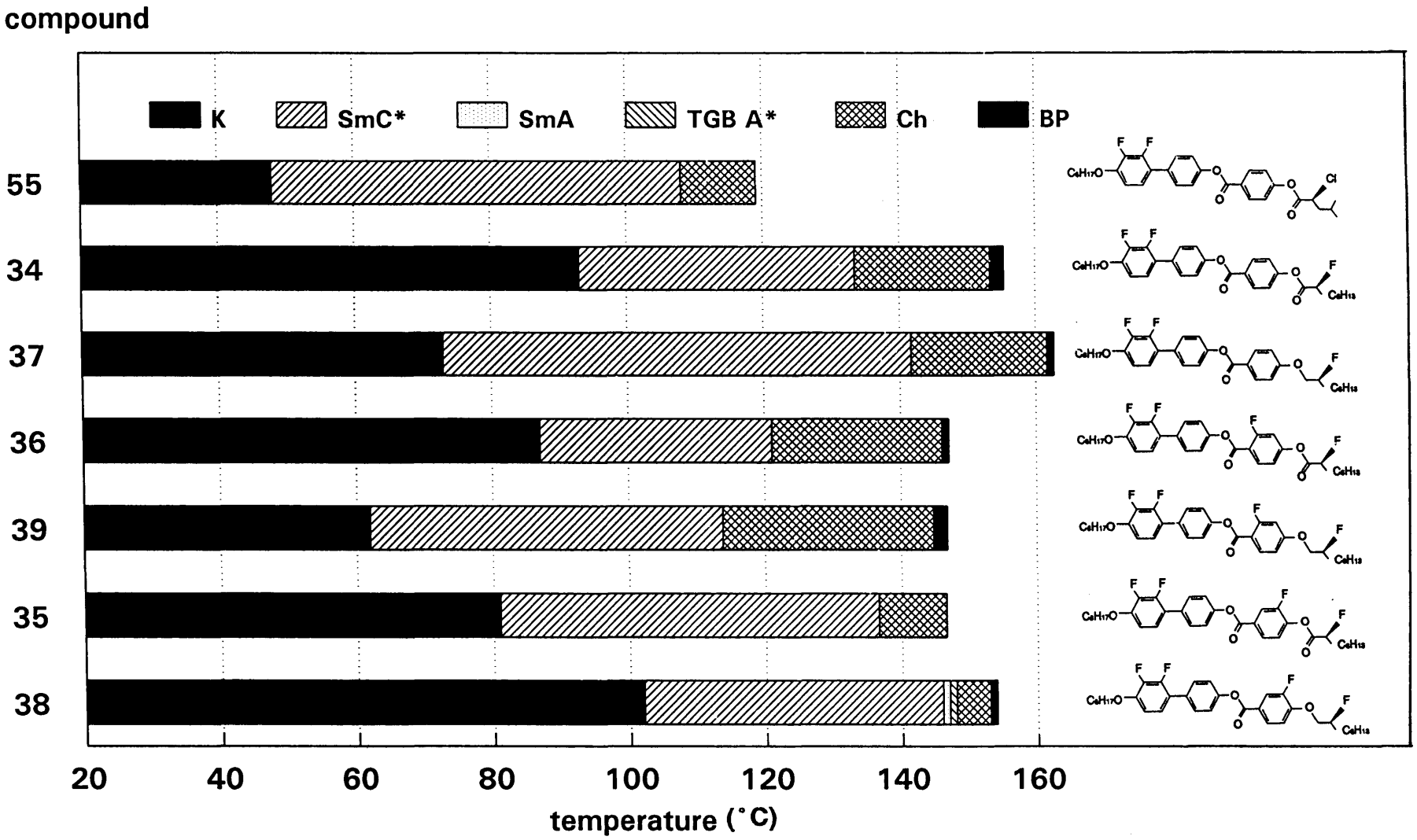

Figure 3.1 Transition temperatures (°C) of compounds containing a 2,3-difluorophenyl unit.

Digitised by the Department of Library Services in support of open access to information, University of Pretoria, 2021.

UNIVERSITEIT VAN PRETORIA
UNIVERSITY OF PRETORIA
YUNIBESITHI YA PRETORIA

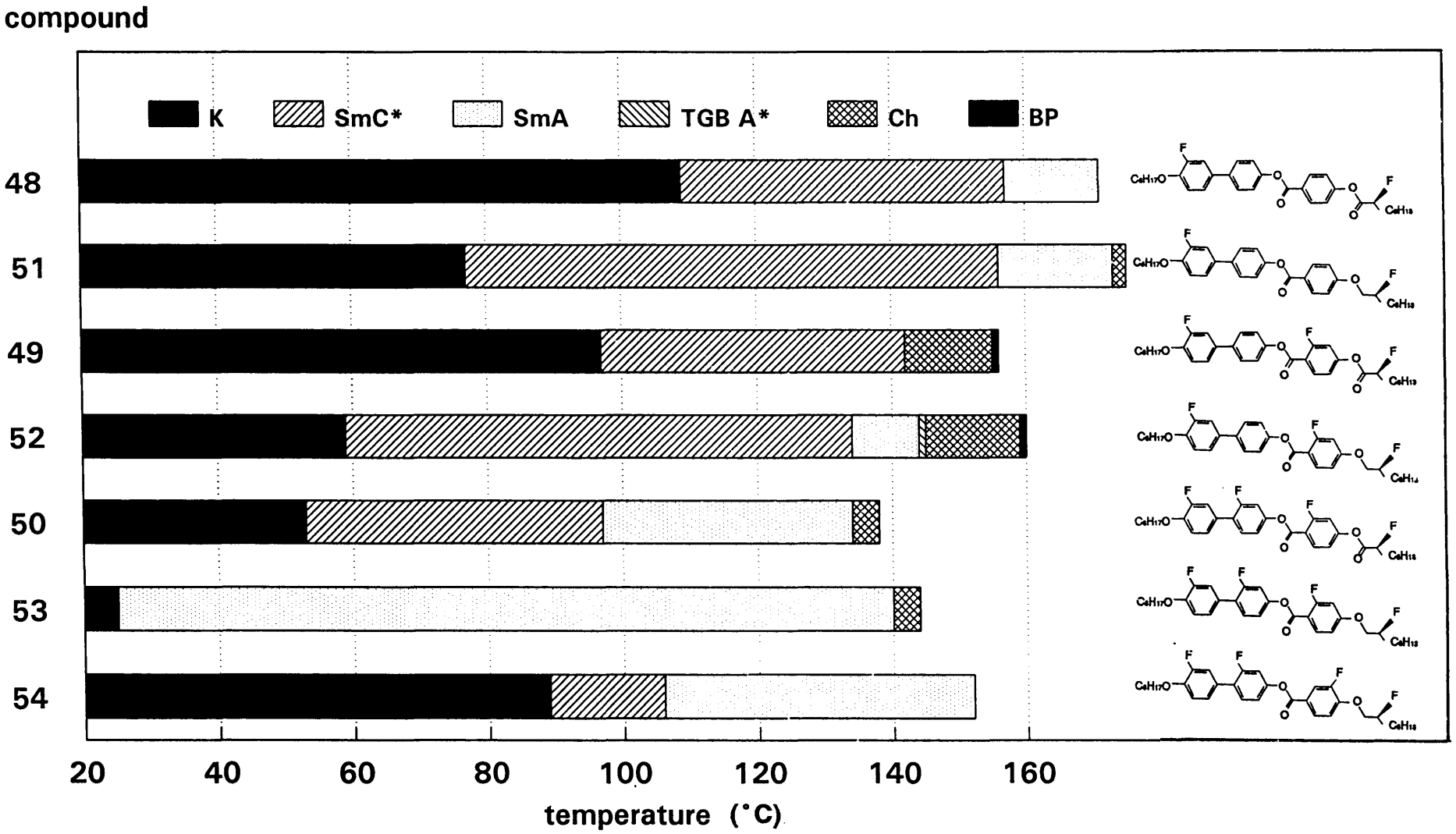

Figure 3.2 Transition temperatures (°C) of compounds without a 2,3-difluorophenyl unit.

Digitised by the Department of Library Services in support of open access to information, University of Pretoria, 2021.

UNIVERSITEIT VAN PRETORIA
UNIVERSITY OF PRETORIA
YUNIBESITHI YA PRETORIA

Table 3.1 Transition temperatures (°C) and enthalpy of phase changes (ΔH / kJ.mol^{-1}).

Compound	mp		SmC*		SmA		TGBA*		Ch		BPI		BPII		Iso
55	●	69	●					108.1 d	●					119.3	●
		[28.76]						[2.25]						[0.69]	
34	●	98 d[a]	●					133.4	●	153.3	●	154.2	●	155.5	●
		[29.52][b]						[1.66]						[1.49][c]	
37	●	93 ℓ	●					141.7	●	162.0	●	162.7	●	163.3	●
		[25.02]						[1.29]						[1.51][c]	
36	●	93 d	●					121.1 ℓ	●	146.8	●			146.9	●
		[31.24]						[2.24]						[1.04][c]	
39	●	84 ℓ	●					113.8 ℓ	●	145.5	●			147.2	●
		[29.40]						[1.40]						[1.37][c]	
35	●	86 d	●					137.0[e] ℓ	●					147.0	●
		[32.91]						[1.02]						[1.26]	
38	●	118 ℓ	●	146.0	●	146.0	●	146.0	●	152.9	●	152.9	●	153.8	●
		[43.23]		[0][d]		[0][d]		[1.39]						[1.57][c]	

a. d = *dextrorotatory* ("left-handed" helix) ; ℓ = *laevorotatory* ("right-handed" helix)
b. [ ] enthalpy change for the transition in kJ.mol^{-1}.
c. value is the combined total enthalpy change for BPs - Iso transitions
d. [0] too small to measure.
e. Ch phase is preceded by a nematic phase which forms at 136.6°C (see text).

Digitised by the Department of Library Services in support of open access to information, University of Pretoria, 2021.

UNIVERSITEIT VAN PRETORIA
UNIVERSITY OF PRETORIA
YUNIBESITHI YA PRETORIA

Table 3.2 Transition temperatures (°C) and enthalpy of phase changes (ΔH / kJ.mol^{-1}) of compounds without the 2,3-difluorophenyl group.

Compound	mp		SmC*		SmA		TGBA*		Ch		BPI		BPII		Iso
48	●	124 d	●	157.4	●									171.1	●
		[32.35]		[0.13]										[4.88]	
51	●	104 ℓ[a]	●	156.6	●			173.7	●					175.5	●
		[30.72][b]		[0.04]										[5.58][c]	
49	●	105 d	●					141.9	●	155.5	●	155.6	●	155.6	●
		[32.57]						[1.10]						[1.50][c]	
52	●	77 ℓ	●	134.5	●	144.4	●	145.3	●	159.5	●			160.2	●
		[26.12]		[0.09]				[0.43]						[1.72][c]	
50	●	73 ℓ→d	●	97.2	●			133.9 ℓ	●					137.7	●
		[53.57]		[0.03]				[0.88]						[1.38]	
53	●			38	●			140.5	●					144.2	●
				[20.67]				[1.42]						[1.64]	
54	●	104 ℓ	●	106.5	●									152.2	●
		[45.20]		[0]										[6.62]	

a. d = *dextrorotatory* ("left-handed" helix); ℓ = *laevorotatory* ("right-handed" helix).
b. [ ] enthalpy change for the transition in kJ.mol^{-1}.
c. value is the combined total enthalpy change for BPs - Iso transitions.
d. [0] too small to measure.

Digitised by the Department of Library Services in support of open access to information, University of Pretoria, 2021.

UNIVERSITEIT VAN PRETORIA
UNIVERSITY OF PRETORIA
YUNIBESITHI YA PRETORIA

3.2 Optical microscopy studies

3.2.1 Experimental

Phase textures were observed and transition temperatures measured using a Zeiss Universal polarizing microscope in conjunction with a Mettler FP82 hot stage and FP80 control unit. Photographs were taken on a Leitz Laborlux microscope equipped with polarisers and a Leitz Wild MPS52 camera, using Fujicolor ASA 100 film. Magnification shown is 125×.

3.2.2 Results

For the purpose of discussion the compounds are conveniently divided into two groups:

(i) compounds containing a 1,2-difluorophenyl unit (figure 3.1) and

(ii) compounds without this unit (figure 3.2).

Transition temperatures and enthalpy changes of compounds of type (i) are listed in table 3.1. All these compounds exhibit a wide SmC* phase (27°C < Δ_{SmC*} < 50°C), a Ch phase and one or more blue phases. Only one of the compounds (**35**) does not exhibit any blue phases. This is due to the long pitch of the Ch phase of this compound, which is evident from the existence of a nematic phase below the Ch phase - the Ch pitch increases rapidly with decreasing temperature to eventually become infinite. Although this phenomenon is not unknown, it remains unusual and is discussed in greater detail in chapter 4.

None of these compounds exhibit a SmA phase, except compound **38** where a very short range SmA phase (< 0.1°C) together with a TGB_{A*} phase is observed. This compound also exhibits two blue phases: cooling from the isotropic liquid reveals BPII which is visible as blue platelets on a blue background, while evidence of BPI can only be seen as platelets within the Ch phase just below the transition.

The SmC* phase of compound **39** displays the *schlieren* texture which brightens from orange-brown to blueish-yellow as the temperature is lowered as a result of the pitch length of the helix becoming shorter (as the pitch is dependent on the tilt angle of the molecules, this means that the tilt angle is increasing). In contrast, the overlying Ch phase changes in colour from red to blue as the temperature increases, with transition to the isotropic melt occurring *via* a BPI (fig. 3.3). The helix is classified as "right-handed" in both the SmC* and Ch phases.

In a similar manner, the Ch phase of **36** reflects visible light that changes from blue to red with decreasing temperature. The ensuing SmC* phase initially appears black just below the transition, but as the length of the pitch approaches the wavelength of visible light it becomes iridescent. The

Digitised by the Department of Library Services in support of open access to information, University of Pretoria, 2021.

UNIVERSITEIT VAN PRETORIA
UNIVERSITY OF PRETORIA
YUNIBESITHI YA PRETORIA

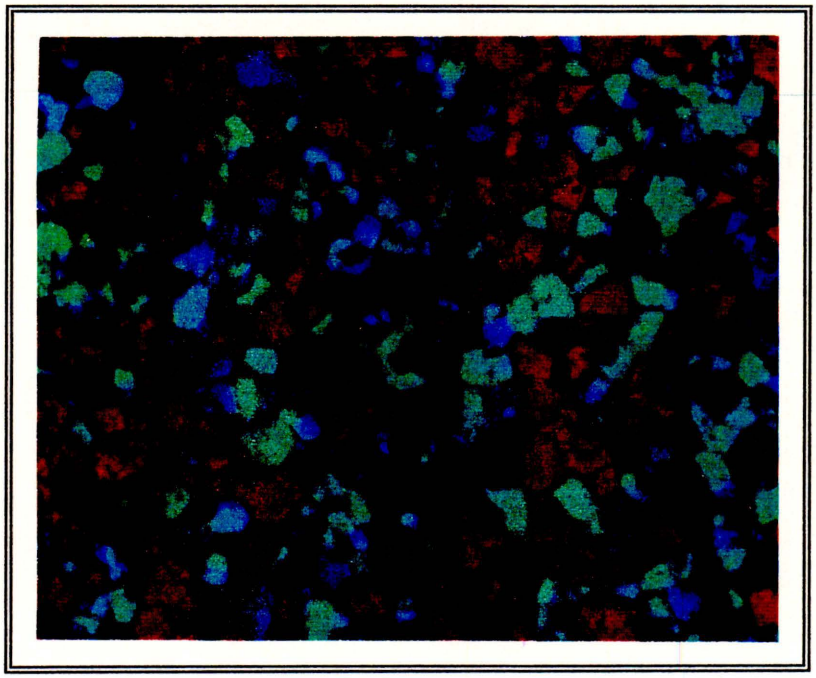

Figure 3.3 The platelet texture of BPI of compound **39**.

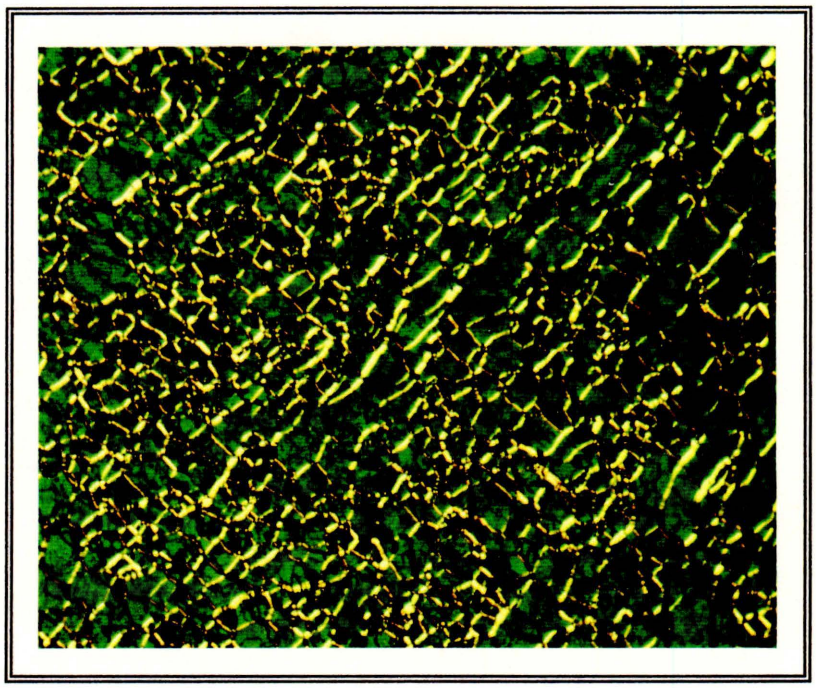

Figure 3.4 The Grandjean plane ("oily streak") texture of the Ch phase as displayed by compound **55**.

Digitised by the Department of Library Services in support of open access to information, University of Pretoria, 2021.

UNIVERSITEIT VAN PRETORIA
UNIVERSITY OF PRETORIA
YUNIBESITHI YA PRETORIA

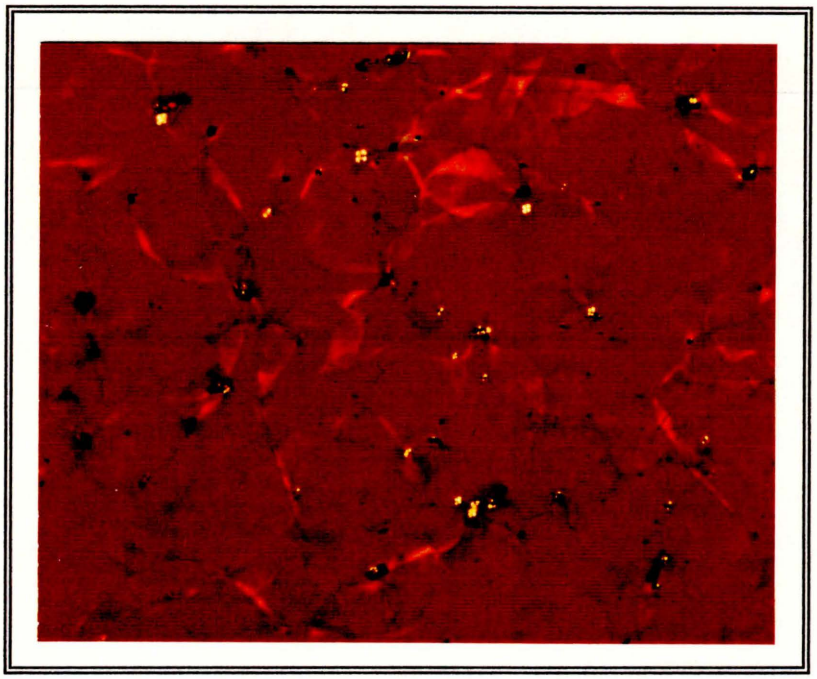

Figure 3.5 The petal texture of the SmC* phase of compound **36**.

petal texture is displayed, which changes in colour from red (see fig. 3.5) through to yellow before crystallizing. In contrast with **39**, the helices of the SmC* and Ch phases of **36** have an opposite twist sense - the helix in the Ch phase is "right-handed" and that in the SmC* phase is "left-handed". This phenomenon has been observed before for binary mixtures[77] as well as for pure liquid crystals[76].

Compounds of type (ii), i.e. those without a 1,2-difluorophenyl unit, are shown in fig. 3.2 and their transition temperatures and enthalpy changes are given in table 3.2. Five of the compounds have a wide SmC* range ($40°C < \Delta_{SmC*} < 80°C$), but **54** only has a narrow SmC* phase and **53** has no such phase at all. The Ch phase exhibited by all the compounds of type (i) (see fig. 3.1) is supplanted to a great extent by the SmA phase in compounds of type (ii) (an example is shown in the sequence in fig. 3.6), except for compound **49** (which has no SmA phase) and compound **52** (which only has a small SmA phase). The sequence shown in fig. 3.6 shows the formation of the typical focal-conic fan texture of the SmA phase as well as its subsequent transformation into the SmC* phase. Compounds **49** and **52** are the only ones of type (ii) displaying one or more blue phases. Also, a TGB_{A*} phase is observed for compound **52**. When this compound is heated, the TGB_{A*} phase makes its appearance from the homeotropic SmA texture in the form of thin detached threads which quickly grow longer to form a network of filaments (fig. 3.7(a)). The network rapidly becomes more dense as it is transformed into the planar Ch texture, which undergoes a colour change from red through to blue upon further heating. The somewhat different texture displayed by the TGB_{A*} phase during the cooling cycle is shown in fig.

Digitised by the Department of Library Services in support of open access to information, University of Pretoria, 2021.

UNIVERSITEIT VAN PRETORIA
UNIVERSITY OF PRETORIA
YUNIBESITHI YA PRETORIA

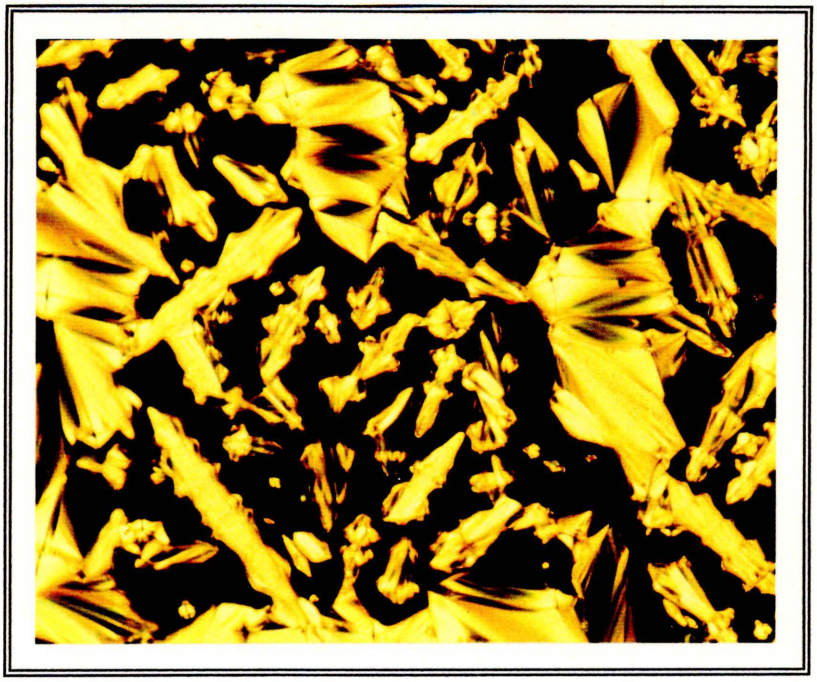

Figure 3.6(a) The formation of SmA batonnets when cooling the isotropic phase of **48**.

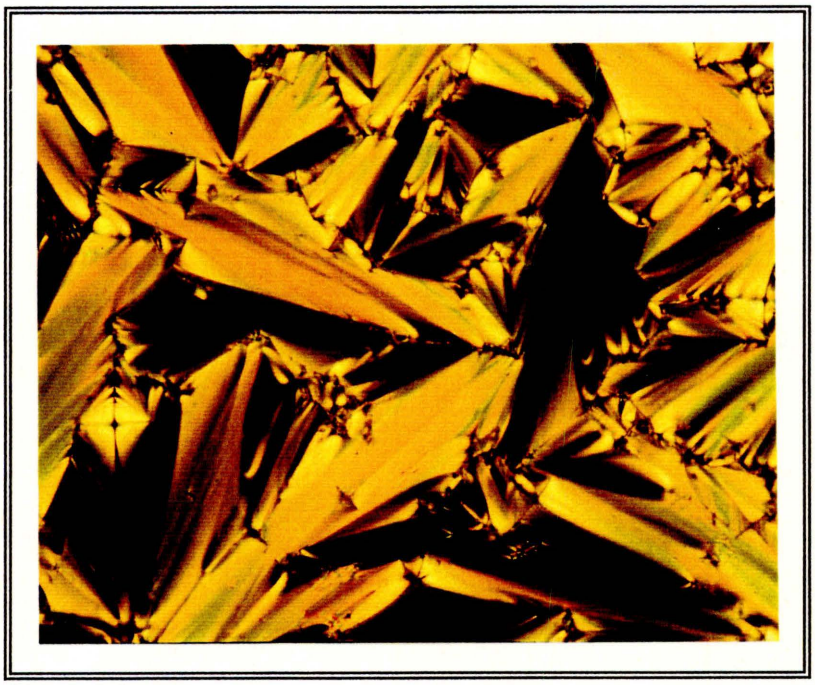

Figure 3.6(b) The focal conic fan texture of the SmA phase of **48**.

Digitised by the Department of Library Services in support of open access to information, University of Pretoria, 2021.

UNIVERSITEIT VAN PRETORIA
UNIVERSITY OF PRETORIA
YUNIBESITHI YA PRETORIA

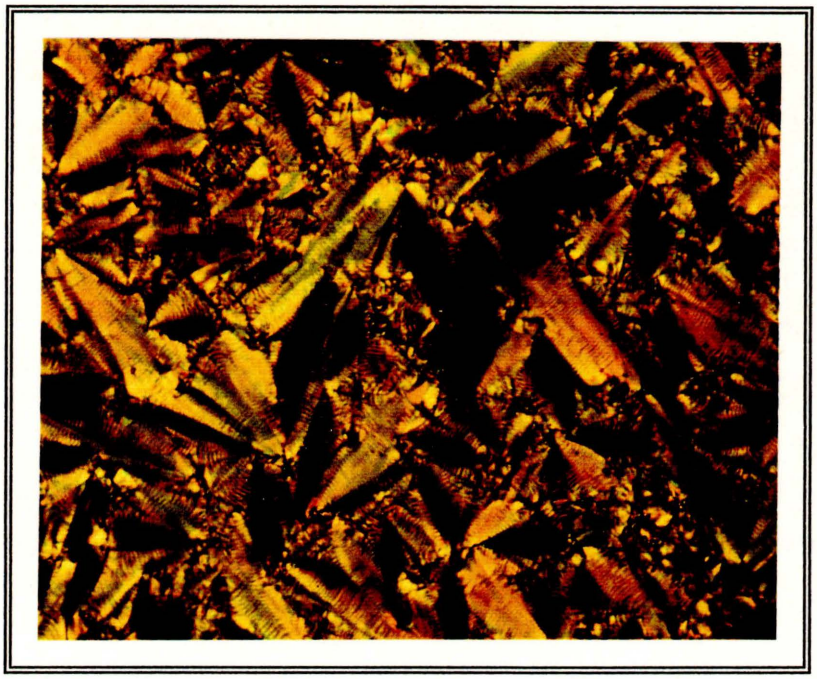

Figure 3.6(c) The paramorphotic broken focal-conic fan texture of the SmC* phase of **48** obtained when cooling the SmA phase, showing pitch lines.

3.7(b). The textures displayed by the SmC* phase of compound **50** are shown in the sequence in fig. 3.8 (a-c). The SmA phase preceding the SmC* phase is homeotropic and therefore appears black. This situation continues to prevail immediately below the SmA - SmC* transition (the average direction of the helical axes now perpendicular to the smectic layers), but is gradually replaced by a schlieren texture that brightens as the temperature decreases (fig. 3.8 (a)). Further cooling results in rapid transformation to the texture shown in fig. 3.8 (b) at 64°C - a texture which appears to flow when subjected to mechanical stress. Reducing the temperature even further leads to the rigid texture shown in fig. 3.8 (c). These observations can be explained as follows: initially the direction of the pitch of the helix is perpendicular to the smectic layers, which are in turn parallel to the surfaces of the glass slides, causing the "pseudohomeotropic" texture to be observed. As the temperature is lowered, the pitch decreases as a result of the tilt angle becoming larger, until it becomes of the order of the wavelength of visible light. The point at which the material is fluid-like is thought to coincide with an inversion of direction of twist of the helix, followed by an increase in pitch as the helix winds itself up in the opposite direction. The lower temperature region (i.e. below 64°C) was determined by rotation of the polars of the microscope to have the opposite twist sense to the higher temperature region. This is discussed further in the following section 3.2.3 as well as in chapter 7.

Digitised by the Department of Library Services in support of open access to information, University of Pretoria, 2021.

UNIVERSITEIT VAN PRETORIA
UNIVERSITY OF PRETORIA
YUNIBESITHI YA PRETORIA

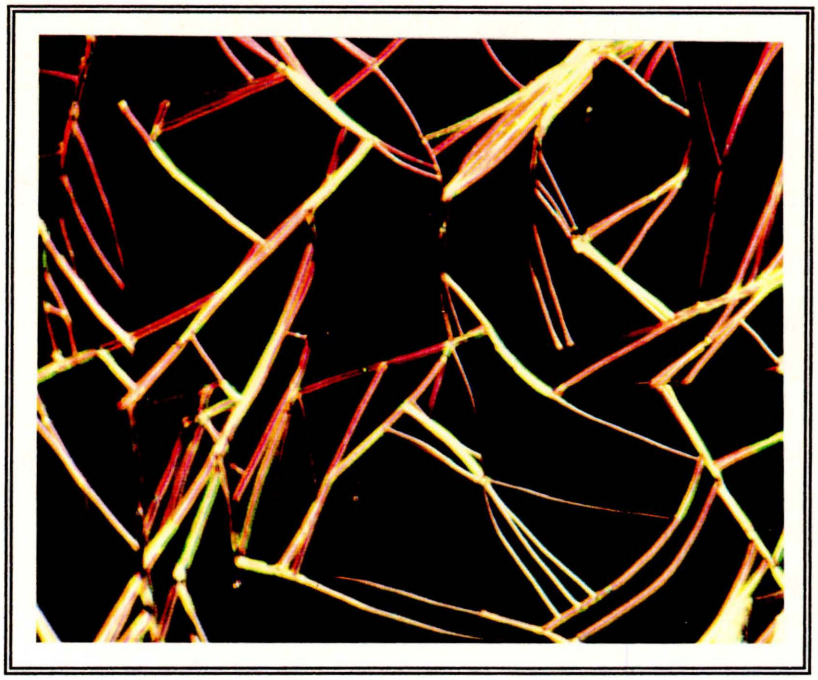

Figure 3.7 (a) The filament texture of the TGB_{A*} phase observed at 148°C when heating compound **52**.

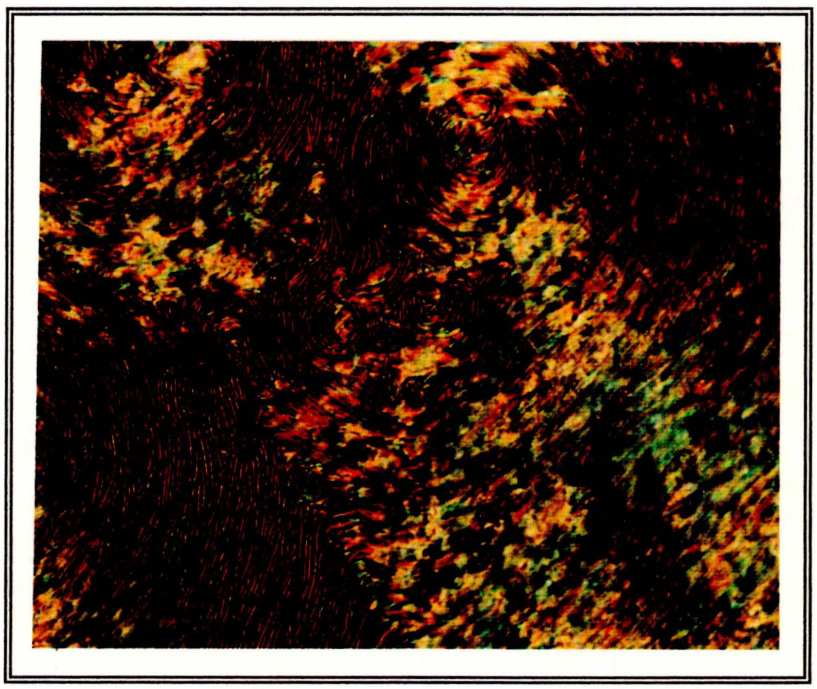

Figure 3.7 (b) The texture observed for the TGB_{A*} phase at 148°C upon cooling from the Ch phase (compound **52**).

Digitised by the Department of Library Services in support of open access to information, University of Pretoria, 2021.

UNIVERSITEIT VAN PRETORIA
UNIVERSITY OF PRETORIA
YUNIBESITHI YA PRETORIA

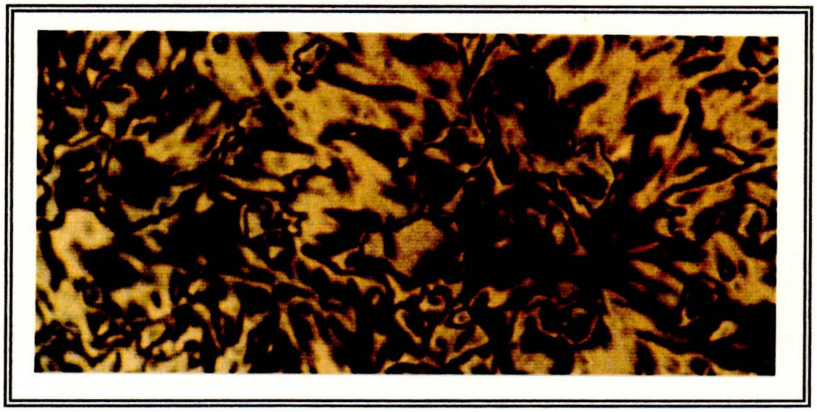

(a)

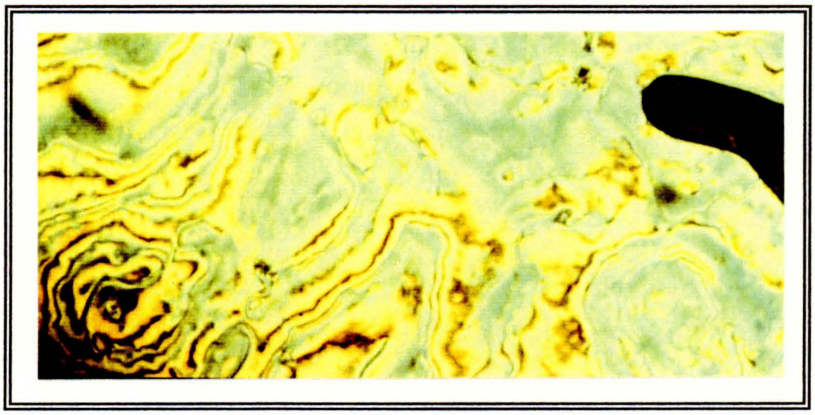

(b)

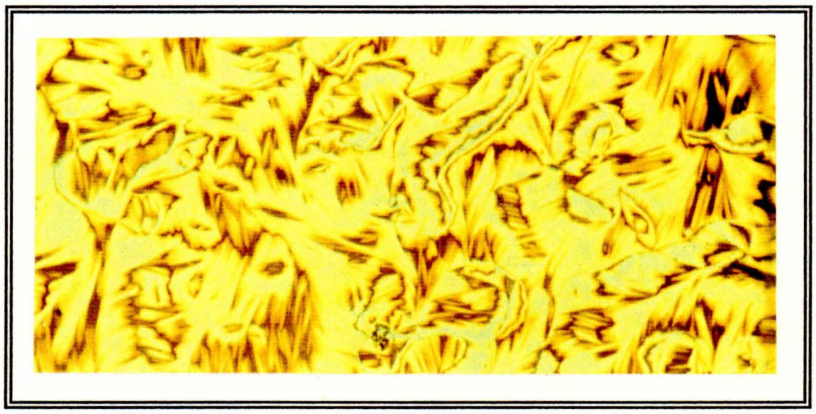

(c)

Figure 3.8 Sequence showing the texture exhibited by compound **50** (a) before, (b) during, at 64°C and (c) after the twist inversion of the helix.

Digitised by the Department of Library Services in support of open access to information, University of Pretoria, 2021.

UNIVERSITEIT VAN PRETORIA
UNIVERSITY OF PRETORIA
YUNIBESITHI YA PRETORIA

3.2.3 Discussion

2,3 - difluorophenyl unit vs. 3 - fluorophenyl unit

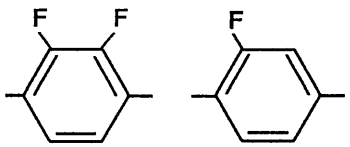

type (i) type (ii)

Compounds belonging to both of these types exhibit the desired wide smectic C^* phase, while higher order smectic phases are completely suppressed. The compounds clearly fall into one of two groups (types (i) and (ii) shown above) distinguishable by the following features:

1. The clearing points of compounds of type (i) are on average 10-20°C lower than their monofluoro analogues;
2. the 2,3 - difluorophenyl unit stabilises the Ch phase, but suppresses the formation of a SmA phase all together - the 3 - fluorophenyl unit tends to do the opposite;
3. compounds of type (i) show a greater tendency towards the formation of blue phases.

The question of whether these phenomena are of common occurrence now arises. The literature revealed that compounds with a similar molecular framework (but achiral) were prepared by Chambers *et al*[78], a typical example of which is given below for the purpose of comparison:

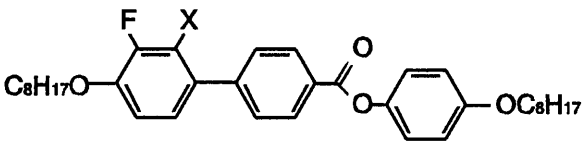

A: X = F (i.e. belonging to type (i))

K 83.8°C SmC 151.7°C SmA 154.9°C N 165.4°C Iso

B: X = H (i.e. belonging to type (ii))

K 93°C SmC 167.5° SmA 182.4°C Iso

Digitised by the Department of Library Services in support of open access to information, University of Pretoria, 2021.

UNIVERSITEIT VAN PRETORIA
UNIVERSITY OF PRETORIA
YUNIBESITHI YA PRETORIA

Both of these compounds have a wide SmC* range, while **A** has a very narrow SmA phase and **B** has no nematic phase at all. Furthermore, the clearing point of **A** is lower than that of **B**. These features seem to be common to a range of liquid crystals prepared by these authors and are in agreement with the observations made in this work.

Fluorination of the biphenyl unit

An interesting observation can be made when compounds containing the 2',3 - difluorobiphenyl unit (compounds **50**, **53** and **54**) are compared with compounds not containing this unit (see figure 3.2). Compounds with this unit have a wide SmA phase (**50**: Δ_{SmA} = 36.7°C; **53**: Δ_{SmA} = 102.5°C; Δ_{SmA} = 45.7°C), two of them (**50** and **53**) have a very narrow Ch phase and two of them (**50** and **54**) a narrow SmC* phase (fig. 3.9). It therefore seems that the 2',3-disubstituted biphenyl unit encourages formation of a SmA phase while at the same time it impedes the formation of Ch or SmC* phases. This means that this unit favours an orthogonal arrangement of the molecules and that it discourages and sometimes even prevents the formation of helical structures.

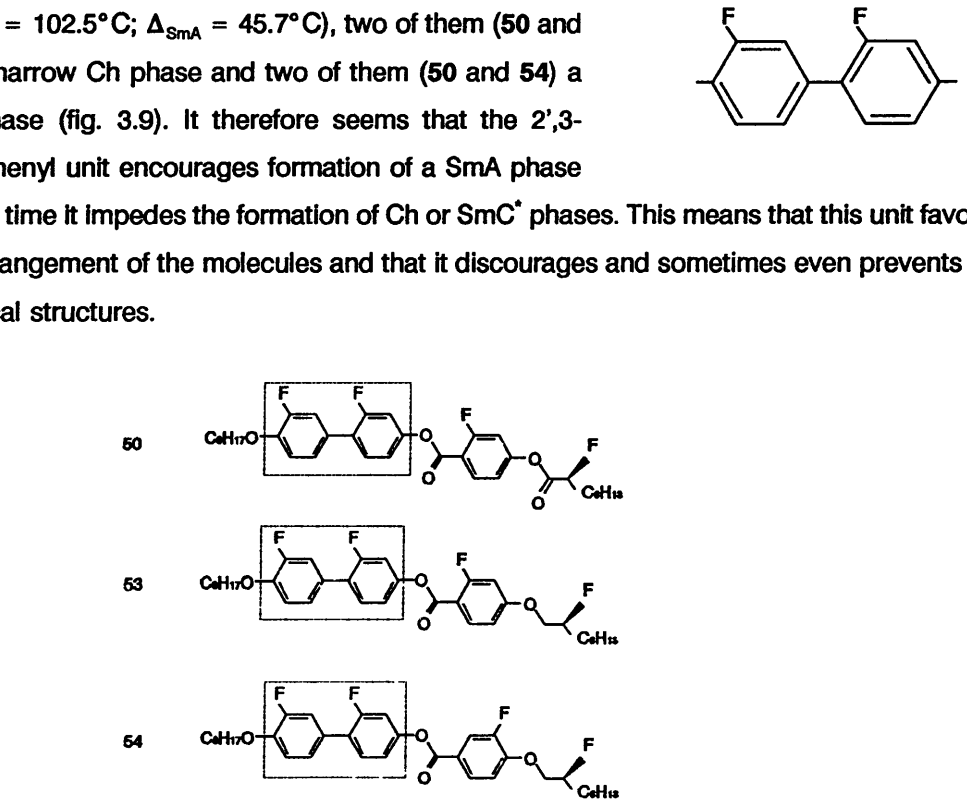

Figure 3.9 Phases and transition temperatures of compounds with the 2',3-biphenyl unit.

Digitised by the Department of Library Services in support of open access to information, University of Pretoria, 2021.

UNIVERSITEIT VAN PRETORIA
UNIVERSITY OF PRETORIA
YUNIBESITHI YA PRETORIA

These observations suggest that the introduction of a fluoro-substituent on one of the four inner positions of the biphenyl unit plays an important role, which in turn points towards the involvement of the inter-ring dihedral angle. However, these are not the only compounds containing a single fluoro-substituent on one of the inner positions of the biphenyl group. Compounds with the 2,3-difluorobiphenyl group (compounds **34 - 39**) fall within the same category, but in contrast, they do not exhibit the SmA phase. The difference is obvious from the example shown in fig.3.10.

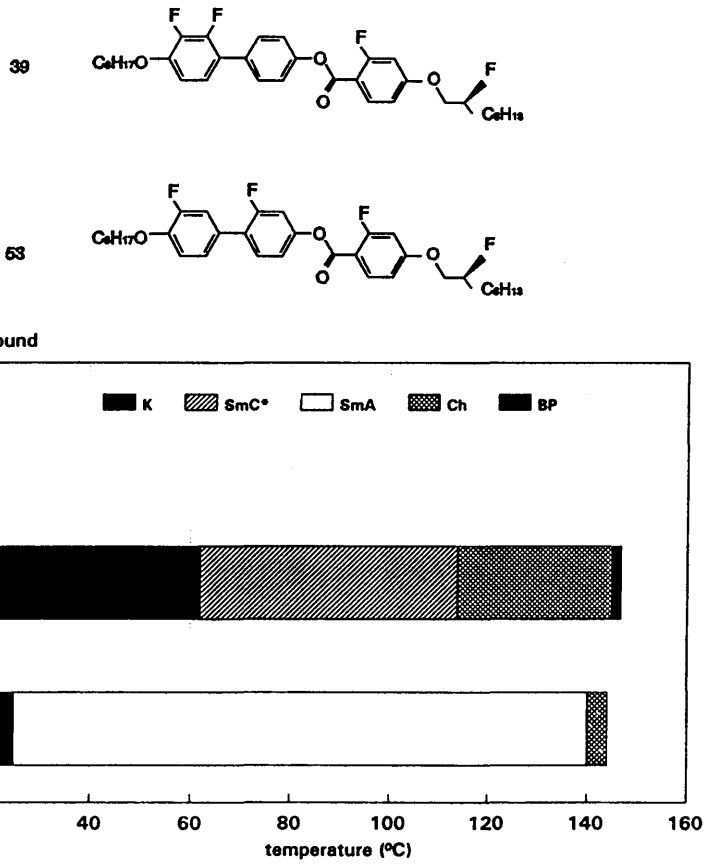

Figure 3.10 Phases and transition temperatures of compounds with a single substituent on an inner position of the biphenyl unit.

It is clear that a 2',3-disubstituted biphenyl group does disrupt the molecular packing to a greater extent than any of the other patterns of substitution and that apart from that, it appears to have a detrimental effect on the chirality of a compound. It is possible that the tendency to prevent the formation of helical structures could possibly be a driving force behind the unwinding / rewinding of the SmC* helix of compound **50**. Two of the compounds containing the 2',3-difluorobiphenyl unit were investigated further using ^{19}F nmr spectroscopy and the results are presented in chapter 7.

Fluorination of the phenyl ring

Fluorination of the phenyl ring in the 2-position (*meta* to the chiral chain) has a very small influence on the incidence or temperature range of phases (compare esters **34** and **36**; ethers **37** and **39** in fig.3.1)

Digitised by the Department of Library Services in support of open access to information, University of Pretoria, 2021.

UNIVERSITEIT VAN PRETORIA
UNIVERSITY OF PRETORIA
YUNIBESITHI YA PRETORIA

in the presence of the 2,3-difluorophenyl unit. In the absence of this unit the SmA phase of **48** is completely replaced by a Ch phase upon fluorination at the 2-position (**49**), while the stabilities of both the Ch and SmC* phases are enhanced (fig.3.2). Fluorination *ortho* to the chain (3-position) has the effect of reducing the overall mesophase stability (particularly that of the Ch phase) and of raising the clearing temperature somewhat as shown in fig.3.11 for three of the ethers.

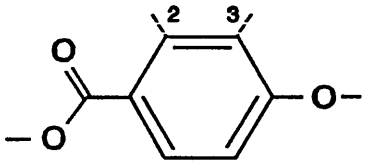

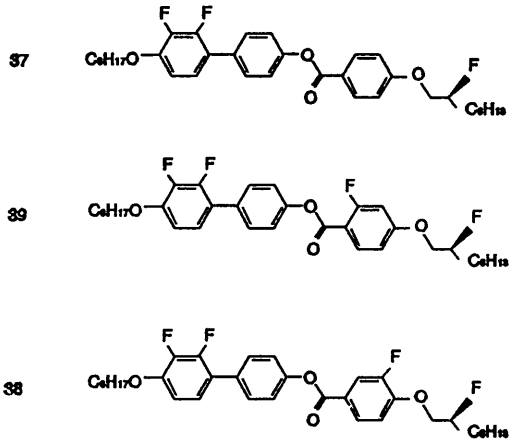

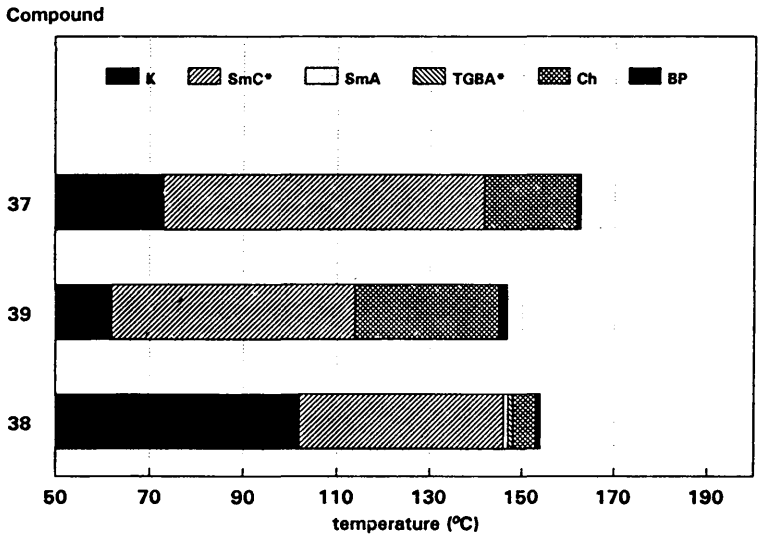

Figure 3.11 Phases and transition temperatures showing the effect of fluorination of the phenyl ring.

Digitised by the Department of Library Services in support of open access to information, University of Pretoria, 2021.

UNIVERSITEIT VAN PRETORIA
UNIVERSITY OF PRETORIA
YUNIBESITHI YA PRETORIA

Number of fluoro-substituents

Although the position of the lateral substituents is clearly important, it is possible to lower the clearing point (and sometimes the melting point) of a liquid crystal by merely adding additional fluoro-substituents. This point is illustrated in figures 3.12 and 3.13 - addition of a third substituent resulted in a substantial decrease in both melting and clearing point.

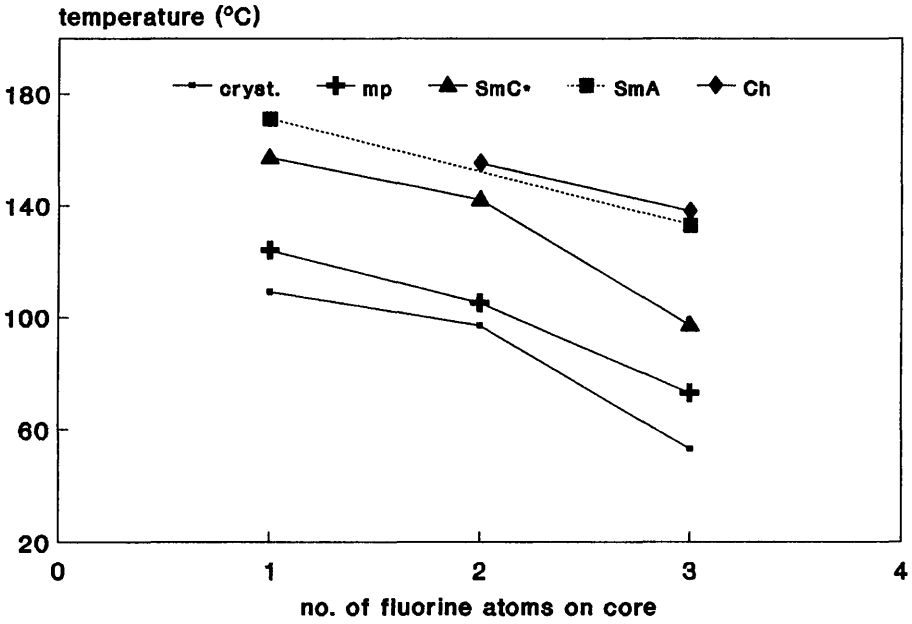

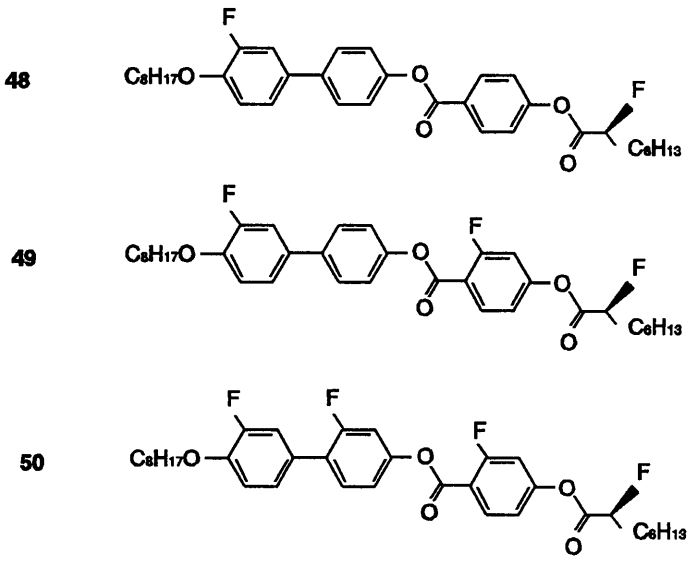

Figure 3.12 The transition temperatures of three of the esters as a function of the number of monosubstituted phenyl rings.

Digitised by the Department of Library Services in support of open access to information, University of Pretoria, 2021.

UNIVERSITEIT VAN PRETORIA
UNIVERSITY OF PRETORIA
YUNIBESITHI YA PRETORIA

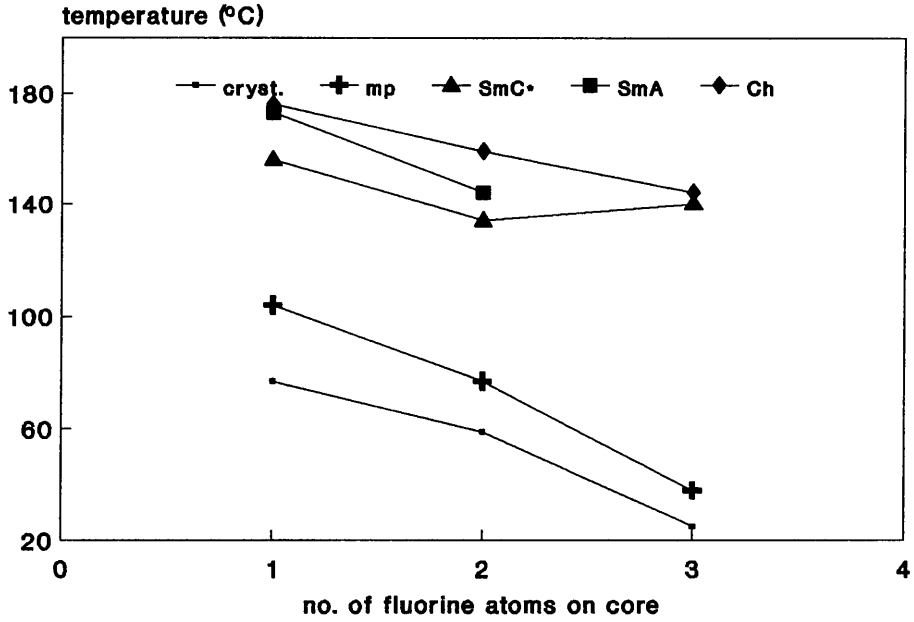

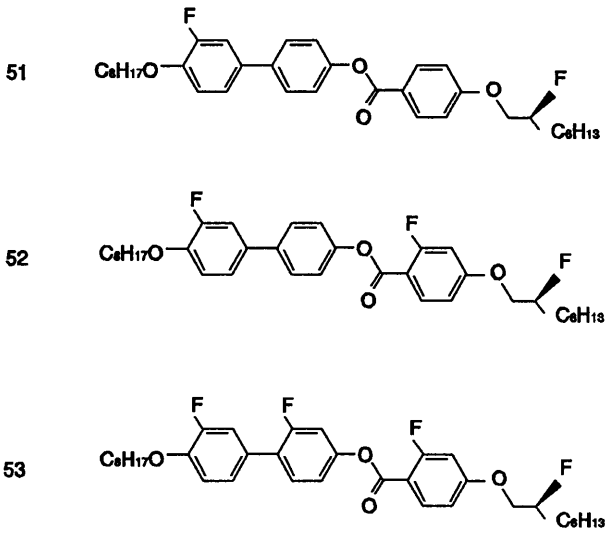

Figure 3.13 The transition temperatures of three of the ethers as a function of the number of fluoro-substituents.

Chirality

The term "chirality" arises from the fact that a chiral phase possesses twofold optical activity:

1. molecular optical activity - the phase is composed of optically active molecules;
2. macromolecular optical activity - a result of the helical twist induced by the chiral molecules in the bulk of the phase.

Digitised by the Department of Library Services in support of open access to information, University of Pretoria, 2021.

UNIVERSITEIT VAN PRETORIA
UNIVERSITY OF PRETORIA
YUNIBESITHI YA PRETORIA

The chirality of a liquid crystal molecule is therefore a term used to describe its ability to induce helical phases in the macromolecular sense. The thermal stability of frustrated phases (such as TGB_{A^*}[83] or BP[84,85]) depends to a large degree on this macromolecular chirality: blue phases commonly occur for compounds in which the pitch of the cholesteric phase is short (i.e. < 500 nm)[79]. The factors influencing the incidence and the range of the TGB_{A^*} phase have only been investigated more recently[76]. However, not much is known about the effect of lateral fluorination on the chirality of a compound, although the position of the fluoro-substituent has been found to play a role in determining the incidence of TGB_{A^*} phases[58].

Of the compounds prepared for this work, **52** and **38** both posess one or more blue phase as well as a TGB_{A^*} phase. In the case of **52** the TGB_{A^*} phase is generated to facilitate transition of the short pitch Ch phase into the short range SmA phase. Keeping this in mind one would expect to find a TGB_{A^*} phase at the Ch - SmA transition of compound **51**, but no such phase could be detected. The Ch - SmC^* transition of **38** is similarly facilitated by a TGB_{A^*} phase accompanied by a very short range SmA phase.

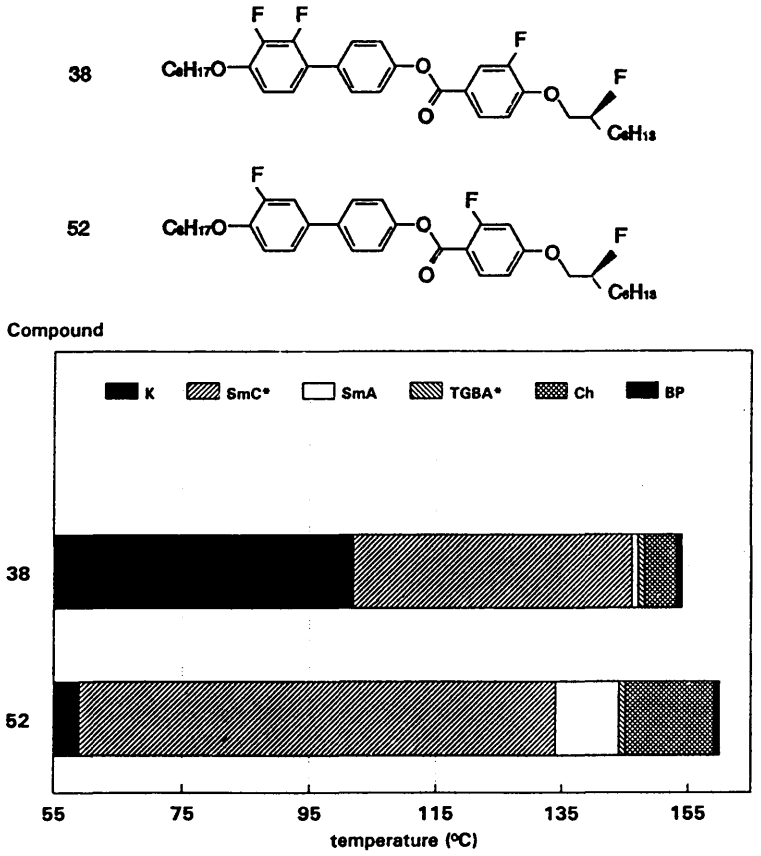

Figure 3.14 The incidence of TGB_{A^*} phases.

Compounds **52** and **38** can therefore be classified as having a high chirality. From a structural point of view these compounds have little in common with the exception that both of them contain ether linking groups (fig. 3.14). The ether link does in fact seem to enhance the chirality as demonstrated by all

Digitised by the Department of Library Services in support of open access to information, University of Pretoria, 2021.

UNIVERSITEIT VAN PRETORIA
UNIVERSITY OF PRETORIA
YUNIBESITHI YA PRETORIA

compounds containing this link. On the other hand, compounds containing the 2',3-difluorobiphenyl group (**50**, **53** and **54**) are of low chirality as they are not conducive to the formation of helical structures.

To conclude: it would appear that the number / position of fluoro-substituents does not influence the chirality in any systematic way.

3.3 Calorimetric studies

3.3.1 Experimental

Transition temperatures and the change in enthalpy for each phase transition were measured using a Perkin-Elmer DSC7 instrument equipped with a data station. The instrumental accuracy was calibrated against an indium standard and was found to be close to the value reported in the literature (28.45 $J.g^{-1}$). The thermal properties of the materials were investigated under a variety of heating and cooling rates (2°, 5° and 10° C min^{-1}) in aluminium pans.

3.3.2 Results

Transition temperatures and enthalpy changes are given in tables 3.1 and 3.2.
The SmC^*-Ch transitions are measured to have ΔH values in the range 1.1 - 2.3 $kJ.mol^{-1}$. An exception to this is the SmC^*-Ch transition of **35** of which the value falls below this range and can therefore be described as being only weakly first order.

The magnitude of the enthalpy change measured for the various SmA-Ch transitions varies considerably, from 1.42 $kJ.mol^{-1}$ for compound **53** (which has an extremely wide and stable SmA phase) to 0.43 $kJ.mol^{-1}$ in the case of **52** (which has a less stable SmA phase accompanied by a TGB_{A^*} phase).

The SmC^*-SmA transitions of compounds **50** and **51** are extremely weak, while that of **54** cannot even be detected. These transitions are second order events. The SmC^* - SmA transitions of **52** and **48** take place with a somewhat larger change of enthalpy and can perhaps be regarded to be very weakly first order.

Digitised by the Department of Library Services in support of open access to information, University of Pretoria, 2021.

UNIVERSITEIT VAN PRETORIA
UNIVERSITY OF PRETORIA
YUNIBESITHI YA PRETORIA

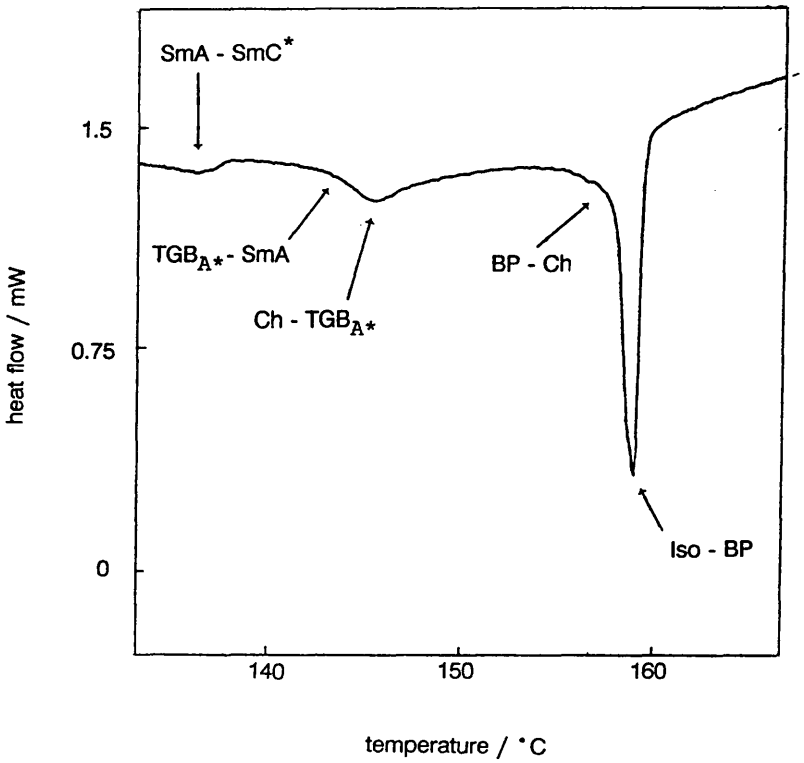

Figure 3.15 The DSC thermogram of the high temperature region of the cooling cycle of **52**. The cooling rate was 5°C min^{-1}.

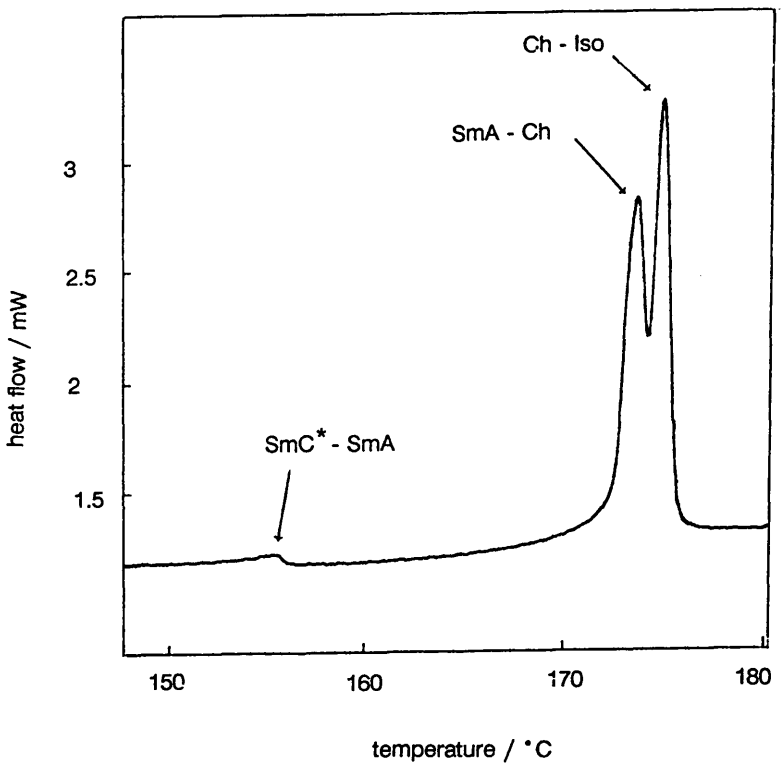

Figure 3.16 The DSC thermogram of the high temperature region of the heating cycle of **51**. The heating rate was 5°C min^{-1}.

Digitised by the Department of Library Services in support of open access to information, University of Pretoria, 2021.

UNIVERSITEIT VAN PRETORIA
UNIVERSITY OF PRETORIA
YUNIBESITHI YA PRETORIA

3.3.3 *Discussion*

The SmC* - SmA phase transition is generally observed to be second order, but some exceptions are known[79,80]. As compounds **48** and **52** (fig.3.15) have SmC* - SmA transitions with slightly larger transition energies, it is interesting to compare their structures. Structurally they have nothing in common: **48** is an ester while **52** is an ether; **48** has one lateral fluoro-substituent and **52** has two. Both of these compounds exhibit short range SmA phases (**48**: Δ_{SmA} = 14°C; **52**: Δ_{SmA} = 10°C) which could be anticipated to stem from transitions approaching first order owing to their lower stability. However, compound **51** (Δ_{SmA} = 17°C) should then also have a SmC* - SmA transition with a larger change in enthalpy, but it has not (fig.3.16). A previous attempt to rationalise the order of the phase transition in terms of the range of the SmA phase was unsuccessful[81], but more recently new evidence was obtained that for very narrow SmA phases the SmC* - SmA transition can be first order[82].

Compound **50** displays an unusually large enthalpy change at the K - SmC* transition. This could be a possible consequence of the unwinding / rewinding of the helix which occurs monotropically. The point at which helix inversion takes place does not coincide with a measurable change in enthalpy on the cooling cycle. The SmC* - SmA transition is second order, but the subsequent SmA - Ch transition is only weakly first order. This is unusual and is suggestive of a weakening of the layer ordering in the SmA phase which could result in a comparatively long Ch pitch (hence the absence of any blue phases). This phenomenon is even more pronounced for compound **52**, the first cooling cycle of the thermogram of which is shown in fig.3.15.

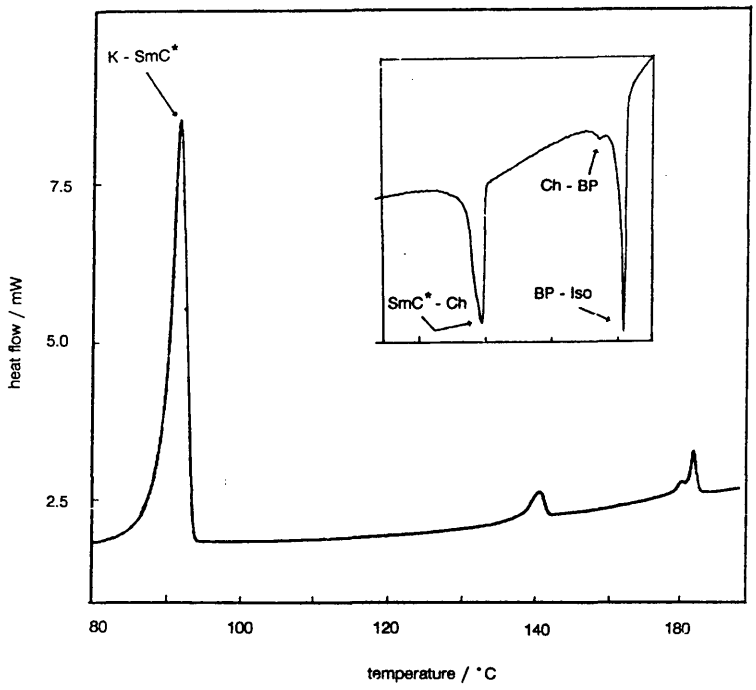

Figure 3.17 The DSC thermogram of **37**. Shown is the heating cycle (5°C min^{-1}). The insert shows the high temperature region of the cooling cycle.

Digitised by the Department of Library Services in support of open access to information, University of Pretoria, 2021.

UNIVERSITEIT VAN PRETORIA
UNIVERSITY OF PRETORIA
YUNIBESITHI YA PRETORIA

Figure 3.17 shows DSC thermograms of **37** and show that the blue phases occur reversibly. Only the Ch - BPI transition is distinguishable as the BPI - BPII transition is concealed by the much larger BPII - Iso transition peak. The BPII - Iso transition is first order, but the Ch - BPI transition is only weakly so.

These observations are in agreement with what is known to date: Thoen[86] showed conclusively that the Ch - BPI, BPI - BPII and BP - Iso transitions are first order using adiabatic scanning calorimetry, although prior to that second order status was claimed for the Ch - BP transition by Demus *et al*[87].

3.4 Electro-optical properties

3.4.1 Experimental

Measurements were done in parallel buffed polyimide coated 0.25 cm^2 indium-tin-oxide cells of varying thickness (2.5 - 4 μm). The compound was introduced into the cell by way of capillary action at a temperature approximately 5°C above the clearing point. It was then slowly cooled (-3°C / min) to the SmA phase or to 0.5°C below the SmC^* - Ch transition when the SmA phase is not present. Generally a good alignment of the molecules in the SmC^* phase was obtained in this manner, but in the absence of a SmA phase, it was sometimes necessary to employ an ac electric field to aid the alignment.

The tilt angle was determined by rotating the sample to obtain optical extinction between crossed polariser and analyser on application of a dc field of opposite polarity[88]. (The tilt angle obtained in this manner is the optical tilt angle - i.e. the angle between the position of the cores of the molecules and the normal to the smectic layers).

The value of the spontaneous polarisation was measured in 0.25 cm^{-2} indium-tin-oxide coated cells obtained from Electronics Chemicals High Technology Group, Japan. The cells were coated with polyimide and buffed unidirectionally as above. AC fields were applied using an Advance Electronics AF signal generator J2C in a sine-wave mode. The hysteresis loop was observed on a Dartron Instruments dual trace oscilloscope D17 and the spontaneous polarisation was determined using a Diamant bridge[89].

Both tilt angle (θ) and spontaneous polarisation (Ps) measurements were carried out as a function of temperature.

3.4.2 Results and discussion

Optical tilt angle

The tilt angle measurements for **48** and **51** respectively are presented graphically in fig. 3.18 as a function of temperature. For both of the compounds, the tilt angle increases rapidly as the temperature

Digitised by the Department of Library Services in support of open access to information, University of Pretoria, 2021.

UNIVERSITEIT VAN PRETORIA
UNIVERSITY OF PRETORIA
YUNIBESITHI YA PRETORIA

decreases to saturate at approximately 35°. A temperature dependency of this nature is usually associated with a second order SmC* - SmA transition, which would merely involve a tilting of the already layered molecules. However, the tilt angle is larger than zero at the transition for both **48** and **51**, particularly so for **48**. Its tilt angle increases from 14.7° (at T_C - T = 0.5°C) to 33° immediately prior to crystallization. This behaviour is intermediary to what would normally result from first order (a fairly constant tilt that may approach 45°) or second order transitions (a smaller tilt increasing from 0° at T_C - T = 0°C to seldom more than 25°C). The transition can therefore not be regarded to be purely second order - this is supported by the DSC analysis. As mentioned before (section 3.3.3) each of these compounds possess only a short range SmA phase, which could be a possible cause for the abovementioned effects.

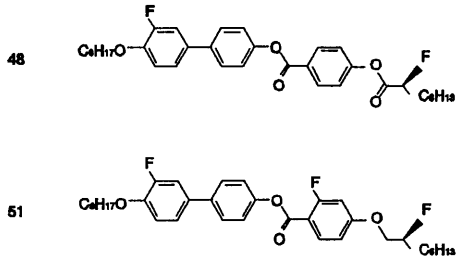

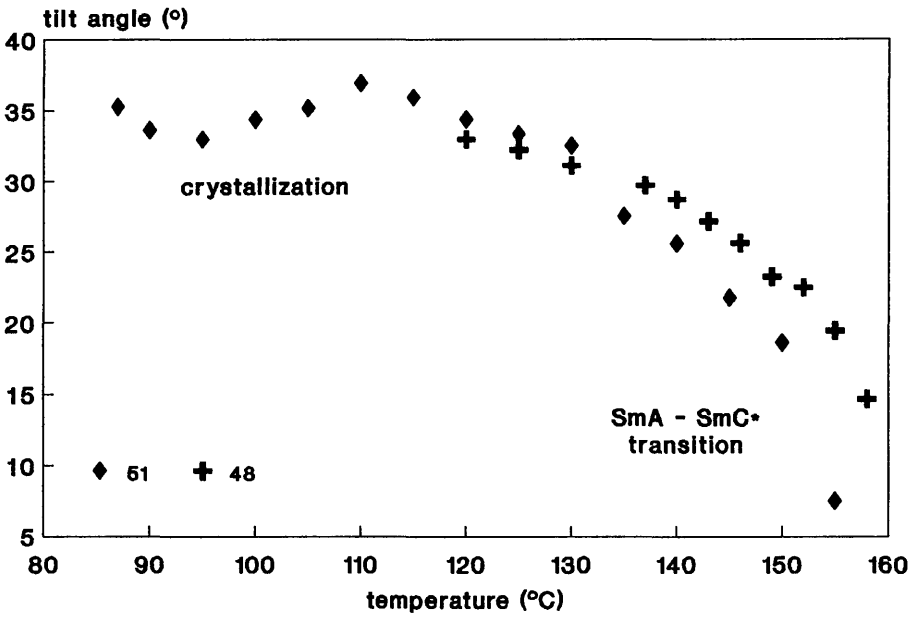

Figure 3.18 Tilt angle, θ, as a function of temperature of **48** (+) and **51** (♦). The applied voltage was 15V and the cell spacing 5μm in both cases.

Tilt angle measurements were also performed on compounds **35, 38, 50** and **54** and these will be

Digitised by the Department of Library Services in support of open access to information, University of Pretoria, 2021.

UNIVERSITEIT VAN PRETORIA
UNIVERSITY OF PRETORIA
YUNIBESITHI YA PRETORIA

discussed in context in other chapters as well (**35**: chapter 4; **50**: chapter 6; **38** and **54**: chapter 7). For the purpose of comparison and to be able to appreciate the influence of changes in the structure of the core on tilt angle measurements, some discussion is presented here.

The structures of compounds **50** and **54** differ by way of the position of the fluoro-substituent on the lone phenyl ring and the group linking the chiral center with the core. Both compounds have a SmA phase as well as a SmC* phase. Attempts to obtain even a reasonable alignment for **50** were unsuccessful. The tilt angle is very small and increases from approximately 1° to just over 5° at 60°C below which temperature no switching appears to occur. This point coincides with the temperature at which the helix was observed to invert (section 3.2.2; fig. 3.8)

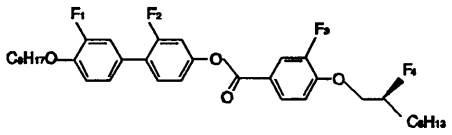

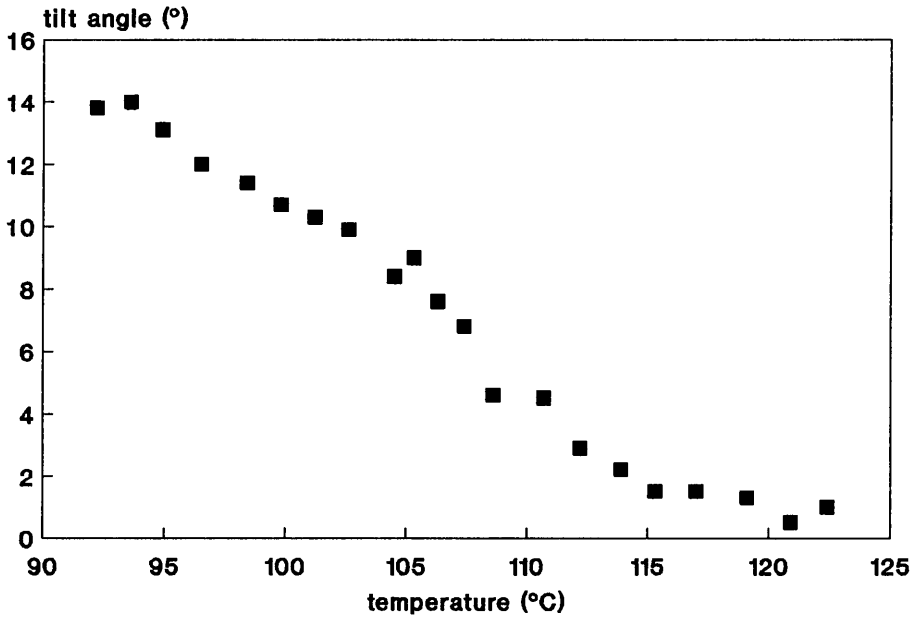

Figure 3.19 The tilt angle as a function of temperature of **54** (applied voltage 10V). The cell spacing was 3μm.

The tilt angle of **54** (fig.3.19, see also chapter 6) increases with decreasing temperature from 8°at the SmC* - SmA transition to 14°. The behaviour of the tilt angle as a function of temperature of both **50** and **54** is typical of compounds with a second order SmC* - SmA transition. In addition, in compound **54** a tilt of the molecules is induced by the dc electric field in the SmA phase. This phenomenon is

Digitised by the Department of Library Services in support of open access to information, University of Pretoria, 2021.

UNIVERSITEIT VAN PRETORIA
UNIVERSITY OF PRETORIA
YUNIBESITHI YA PRETORIA

known as the electroclinic effect[90] and the amount of the induced tilt is, except for temperatures close to the SmC* - SmA transition, proportional to the applied field strength[91].

The variation of the tilt angle of compounds **35** and **38** (fig. 3.20) with temperature is remarkably similar. In both cases the tilt angle decreases with decreasing temperature, from approximately 20° just below the Ch - SmC* transition to 10° immediately prior to crystallization. Structurally, the only difference between these two compounds is that **35** is an ester whereas **38** is an ether, but their core structures are the same. Their behaviour is contrary to what has been observed to date by other workers - usually the tilt angle increases with decreasing temperature. Here the pitch of the SmC* helix becomes longer as the temperature decreases. The tilt angle behaviour of compound **35** is discussed in more detail in chapter 4 which is devoted to this compound.

In conclusion: even the slightest change in the structure of the core has a significant influence on the behaviour of the tilt angle of these compounds. This supports the observation made by Goodby[59], who suggested that the tilt is stabilised by intermolecular core - core interactions.

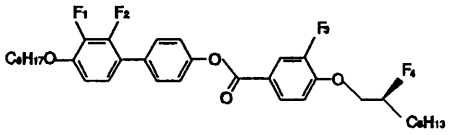

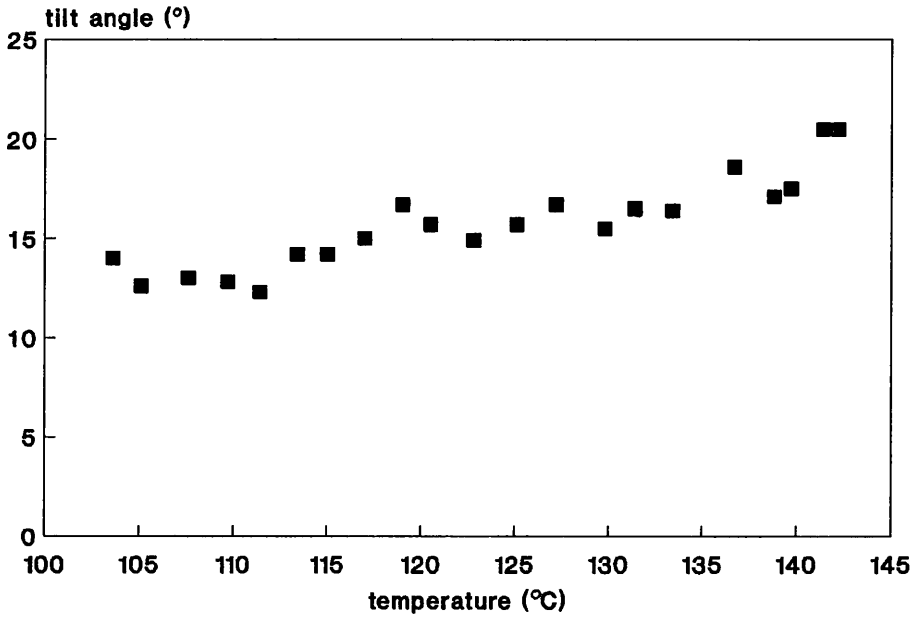

Figure 3.20 Tilt angle as a function of temperature for compound **38**. (applied voltage 8V, cell spacing 3μm).

Digitised by the Department of Library Services in support of open access to information, University of Pretoria, 2021.

UNIVERSITEIT VAN PRETORIA
UNIVERSITY OF PRETORIA
YUNIBESITHI YA PRETORIA

3.5 Summary and conclusions

1. All the compounds (except **53**) have the desired smectic C* phase and higher ordered smectic phases are completely suppressed.

2. Most of the compounds, with the exception of **34, 37, 48, 51** and **52**, have clearing temperatures sufficiently low for nmr study.

3. The number and position of lateral fluoro-substituents greatly influence the incidence and range of phases of the liquid crystals, in particular the presence of the 2,3-difluorophenyl or 2',3-difluorobiphenyl unit.

4. The 2',3-difluorobiphenyl group appears to discourage the formation of helical structures and favours an orthogonal arrangement of the molecules. The presence of this group could possibly be the driving force behind the inversion of the direction of the helix in the ferroelectric smectic C* phase.

5. A helix inversion occurs in the cholesteric phase of one of the compounds.

6. The number of fluoro-substituents does not appear to influence the chirality of the compounds in any systematic way, but the 2',3-difluorobiphenyl group acts detrimentally.

7. The range of the SmA phase appears to influence the nature of the SmC^* - SmA transition.

8. Some of the compounds exhibit second order or weakly first order SmA - Ch transitions.

9. The structure of the core critically influences the behaviour of the tilt angle with temperature. Two of the compounds exhibit unusual ferroelectric properties - the tilt angle decreases with decreasing temperature.

----- # -----

Digitised by the Department of Library Services in support of open access to information, University of Pretoria, 2021.

UNIVERSITEIT VAN PRETORIA
UNIVERSITY OF PRETORIA
YUNIBESITHI YA PRETORIA

CHAPTER 4

A HELIX INVERSION IN THE CHOLESTERIC PHASE OF THE LIQUID CRYSTAL (S)-4-n-OCTYLOXY-2,3-DIFLUOROBIPHENYL-4'-YL 3-FLUORO-4-(2-FLUOROOCTANOYLOXY)BENZOATE

4.1 Introduction

Several chiral systems, where an inversion in the chiral properties with respect to temperature has been observed, have been investigated. Some examples are shown in fig. 4.1. The first compound[92], (S)-2-methylbutyl 4'-n-nonoyloxybiphenyl-4-carboxylate, **A**, exhibits a smectic A and a ferroelectric smectic C* phase. Upon cooling into the ferroelectric phase a spontaneous polarisation develops along the C_2 axis of the phase, with its value reaching a maximum before falling again[93]. The magnitude of the polarisation reaches zero before surprisingly increasing again.

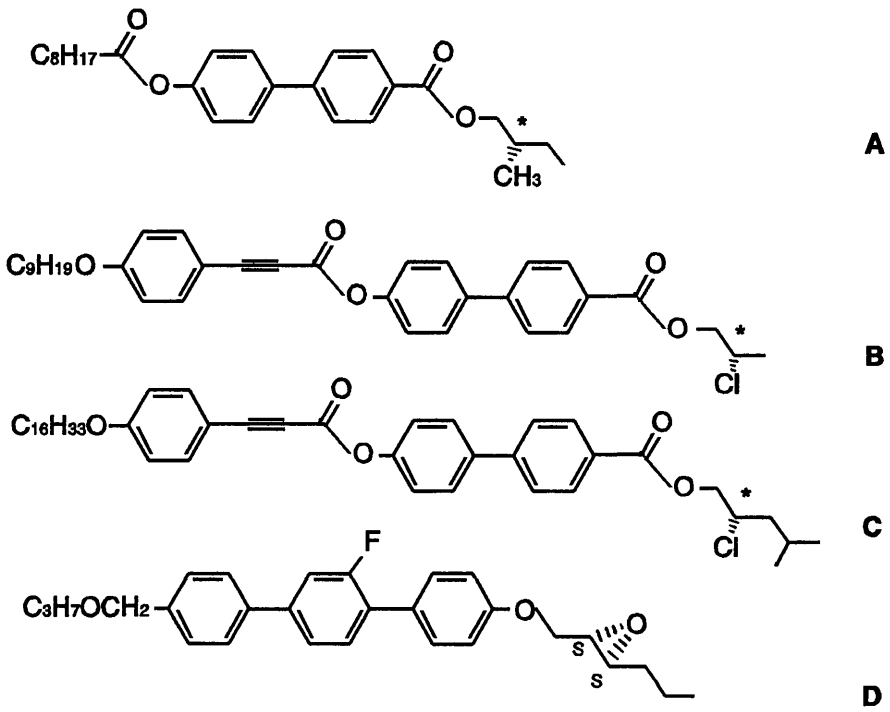

Figure 4.1

Digitised by the Department of Library Services in support of open access to information, University of Pretoria, 2021.

UNIVERSITEIT VAN PRETORIA
UNIVERSITY OF PRETORIA
YUNIBESITHI YA PRETORIA

Initially, at higher temperatures in the ferroelectric phase, the spontaneous polarisation is defined as being negative[59], Ps(-), but as the temperature falls the polarisation direction inverts and has the opposite sign, Ps(+). The second compound, (S)-2-chloropropyl 4'-(4-n-nonyloxyphenylpropioloyloxy) biphenyl-4-carboxylate[94], **B**, exhibits cholesteric and smectic A phases, and on cooling from the isotropic liquid the cholesteric helix unwinds and then rewinds. Thus, at higher temperatures in the cholesteric phase this material possesses a left-handed helix, but as the temperature is lowered the helix unwinds through a cholesteric phase that has an infinite pitch to give a cholesteric phase that has a right-handed helix. Compound **C**, (S)-2-chloro-4-methylpentyl 4'-(4-n-hexadecyloxyphenyl propioloyloxy)biphenyl-4-carboxylate, behaves somewhat similarly to compound **B**, except that the helical inversion takes place in the helical ferroelectric smectic C* phase[95]. However, in this case the direction of the spontaneous polarisation does not invert with temperature. Compound **D** is quite remarkable in that it has helical inversions in both the cholesteric and smectic C* phases, and accompanying the helix transposition in the smectic C* phase the direction of the spontaneous polarisation also crosses over[96]. An inversion of the helix was also found to occur in the cholesteric phase of another compound containing the S,S-epoxy chiral moiety, but with an entirely different core structure, namely 4-[(S,S)-2,3-epoxyhexyloxy]-phenyl-4-(decyloxy)-benzoate[97]. The handedness of the helix changes from right (upper temperature region) to left (region below the nematic region).

These effects were interpreted in terms of a model of interconverting, but competing, species whose concentrations are temperature dependent. The interconverting species were then related to changes in the conformational structures of the molecules[93-96].

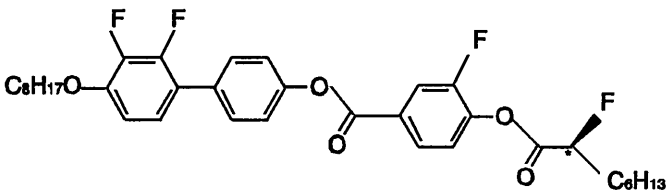

K 86°C SmC* 137.0°C Ch 147.0°C Iso

Figure 4.2 Structure and phase transitions of **35**.

In this chapter, the liquid crystalline properties of compound **35**, (S)-4-n-octyloxy-2,3-difluorobiphenyl-4'-yl 3-fluoro-4-(2-fluorooctanoyloxy)benzoate (fig. 4.2), are examined. In the following sections its physical properties, together with results that clearly show that this material undergoes an inversion in its cholesteric phase are presented[98].

Digitised by the Department of Library Services in support of open access to information, University of Pretoria, 2021.

UNIVERSITEIT VAN PRETORIA
UNIVERSITY OF PRETORIA
YUNIBESITHI YA PRETORIA

4.2 Experimental

The synthesis and characterization of compound **35** is described in chapter 2. Liquid-crystalline phases and phase transition temperatures were determined using thermal optical microscopy and differential scanning calorimetry as described in chapter 3.

The pitch in the cholesteric phase was measured by determining the distance between the dechiralization lines in the fingerprint texture of the phase using a calibrated Filar eyepiece attached to the polarizing microscope. The Filar eyepiece was calibrated against a graduated one millimetre microscope scale (10 μm spacing).

Tilt angle measurements and determination of the spontaneous polarisation were carried out as described in section 3.4.1.

4.3 Results

4.3.1 Optical microscopy

Studies on the pure material

The transition temperatures determined from polarising microscopy are given in figure 4.2 and are also given in table 3.1. The cholesteric phase was identified from its Grandjean planar and fingerprint textures, and on cooling to just above the cholesteric to smectic C* transition (137°C) an interesting phenomenon was observed. The helical structure of the cholesteric phase was found to unwind so that the mesophase became totally untwisted, and then upon further cooling a helical structure reformed, but with the helix now twisted in the opposite direction. This is clearly seen for the cholesteric phase (Ch) at the point where the fingerprint texture gives way to the homeotropic texture of the nematic phase (Ch_u), as shown in fig. 4.4(a). This figure shows the crossover point in the helical twist sense. In the black region of the photomicrograph the molecules are essentially ordered so that the direction of observation is along the optic axis of the phase, whereas in the fingerprint region a helical structure exists. As the preparation is cooled further, the fingerprints return over the whole of the area shown and eventually a Grandjean plane texture reforms. However, it should be noted that the lower temperature cholesteric phase has a fleeting existence and it quickly gives way to the formation of a ferroelectric smectic C* phase. Rotation of the upper polarizer of the microscope, above and below the point where the helix is unwound, reveals that the sign of the helix inverts with temperature. This showed that the upper temperature cholesteric phase is right-handed (ℓ) whereas the lower phase is left-handed (d). This process of unwinding of the helix just before the

Digitised by the Department of Library Services in support of open access to information, University of Pretoria, 2021.

UNIVERSITEIT VAN PRETORIA
UNIVERSITY OF PRETORIA
YUNIBESITHI YA PRETORIA

transition to the smectic C* phase leads directly to the ferroelectric phase being formed with relatively good alignment, which is very unusual for a material exhibiting a cholesteric to smectic C transition.

For the smectic C* phase normal pseudohomeotropic and *schlieren* defect textures are observed. Rotation of the upper polariser confirms that the structure is left-handed (*d*), which is in agreement with the proposed rules linking twist sense and spontaneous polarization direction[99,100].

Contact studies

Various contact preparations of materials of known helical twist sense were studied in order to confirm the presence of a helix inversion in compound **35** and to determine the helical twist direction with respect to temperature. The first contact to be investigated was that between the test material **35** and the standard **E**[99]. Compound **E** (fig 4.3(a)) has been reported to exhibit a right-handed helix in its cholesteric phase. The contact region between the two compounds shows no discontinuity between the two cholesteric phases.

(a)

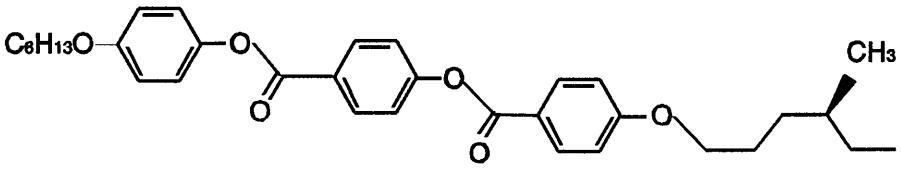

E

K 78.5°C SmC* 115.0°C Ch 175.3°C Iso

(b)

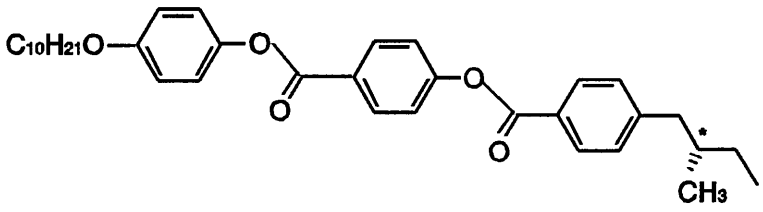

F

K 83.3°C Ch 149.0°C Iso

Figure 4.3 Structures of standard materials used in contact miscibility studies with compound **35**.

Figure 4.4 (b) shows the texture of a typical region that includes the contact boundary at 147°C. The green colour appears fairly uniform across the photomicrograph indicating that the two phases have roughly similar pitch lengths in their cholesteric phases. The selective reflection of green light

Digitised by the Department of Library Services in support of open access to information, University of Pretoria, 2021.

UNIVERSITEIT VAN PRETORIA
UNIVERSITY OF PRETORIA
YUNIBESITHI YA PRETORIA

(a)

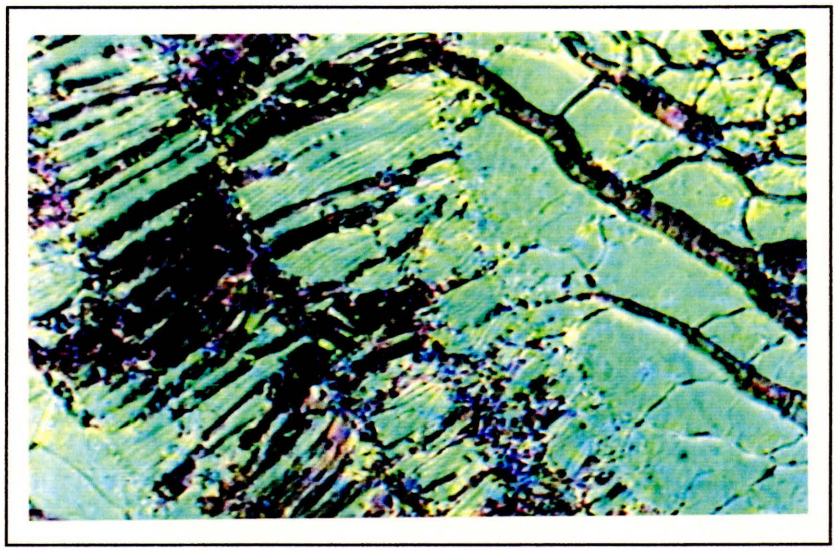

(b)

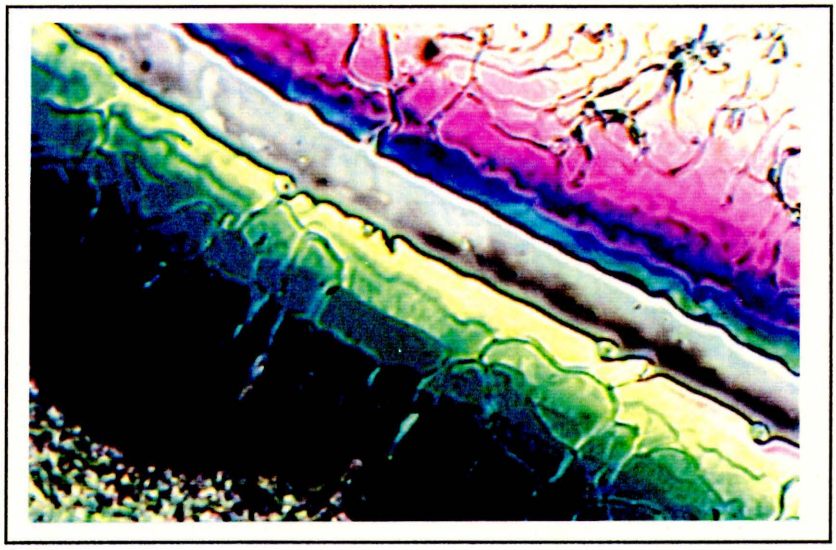

(c)

Figure 4.4 Microscopic defect textures of (a) the point at which the helix of **35** inverts; (b) and (c) contact regions between **35** and standard materials (see text). Magnification ×100.

Digitised by the Department of Library Services in support of open access to information, University of Pretoria, 2021.

UNIVERSITEIT VAN PRETORIA
UNIVERSITY OF PRETORIA
YUNIBESITHI YA PRETORIA

indicates that the pitch length is approximately 0.7 μm. This contact therefore confirms that for the upper temperature region of the cholesteric phase the helix has a right-handed twist.

A second contact preparation was made between compound **35** and ester **F**[101]. The standard material, **F**, has been shown to have a left-handed helix. Therefore the two materials should form a nematic phase where the pitch diverges at the contact boundary as the two helical structures compensate. Figure 4.4(c) shows the contact boundary of the two materials at a temperature of 141.6°C. It can be seen from the rivulet of nematic phase (grey area) running across the preparation that there is a divergence in the pitch. The strong variation in colour across the sample also indicates that the pitch length of the mesophase is changing sharply with concentration. The divergence in the pitch confirms that the upper temperature cholesteric phase does not possess a left-handed helix. When the preparation is cooled down to below the crossover point for the helix inversion in compound **35**, the contact boundary shows no discontinuity confirming that the lower temperature cholesteric phase has a left-handed helical structure.

4.3.2 Differential scanning calorimetry

The phase transitions of **35** were also investigated by differential scanning calorimetry as shown in fig. 4.5. The main figure shows the first heating cycle for the compound and it can be seen from the thermogram that the change in enthalpy of the clearing point and smectic C* to cholesteric

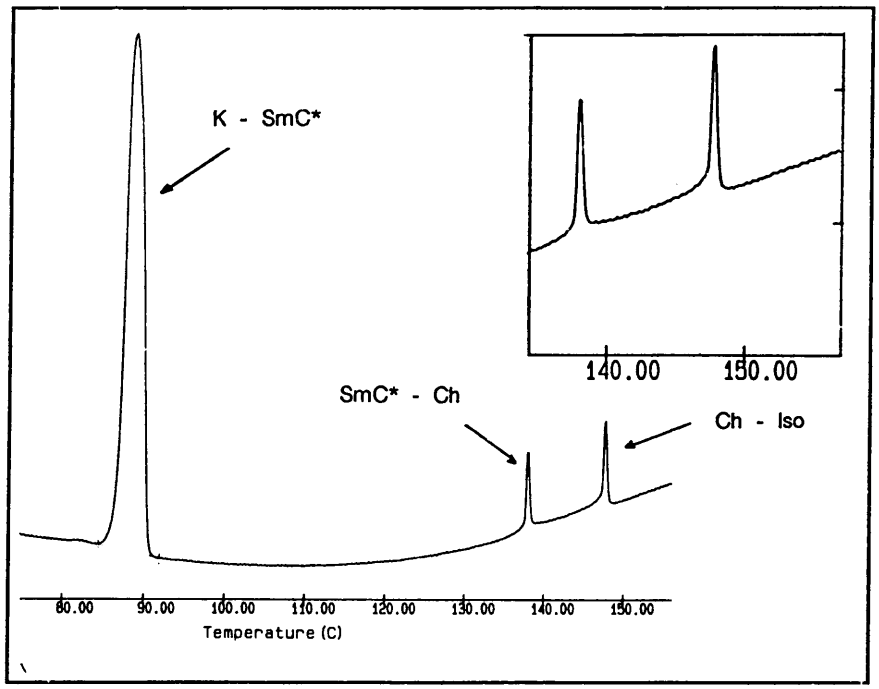

Figure 4.5 The DSC heating cycle of compound **35**. The heating rate was 10°C.min^{-1}. The insert shows an enlargement of the higher temperature region.

Digitised by the Department of Library Services in support of open access to information, University of Pretoria, 2021.

UNIVERSITEIT VAN PRETORIA
UNIVERSITY OF PRETORIA
YUNIBESITHI YA PRETORIA

transitions are relatively small and that the peak shapes are broad suggesting that the phase transitions are weakly first order in nature. It is also interesting to note from the enlargement of the higher temperature region, shown in the inset, that there are accompanying shoulders on both the Ch - Iso and SmC* - Ch transitions. The two shoulders are on opposite sides of the peaks to one another, indicating that these events are not artefacts of the experimental technique but are real. The cooling cycle shows that these two events in the thermogram become better resolved, but the shoulder at the Ch - SmC* transition does not correspond in temperature to the inversion point in the cholesteric phase. Presently, there is no explanation for these shoulders.

4.3.3 Pitch measurements

The pitch of the helix in the cholesteric phase of compound **35** was measured as a function of temperature from a point near to the clearing transition down to a temperature close to the phase change to the smectic C* phase. The pitch was found to diverge as the temperature was reduced. After the inversion in the sign of the helix had taken place, the temperature range preceeding the formation of the smectic C* phase was too short for accurate measurements to be made. Therefore, table 4.1 gives the pitch (μm) measured up to the point of inversion and the values are plotted as a function of temperature in fig. 4.6.

Table 4.1 Pitch length of **35** in the cholesteric phase.

Temperature / °C	Pitch / μm
136.4	8.5
137.6	6.2
138.1	5.6
140.2	4.4
141.5	3.6
143.2	1.8

Digitised by the Department of Library Services in support of open access to information, University of Pretoria, 2021.

UNIVERSITEIT VAN PRETORIA
UNIVERSITY OF PRETORIA
YUNIBESITHI YA PRETORIA

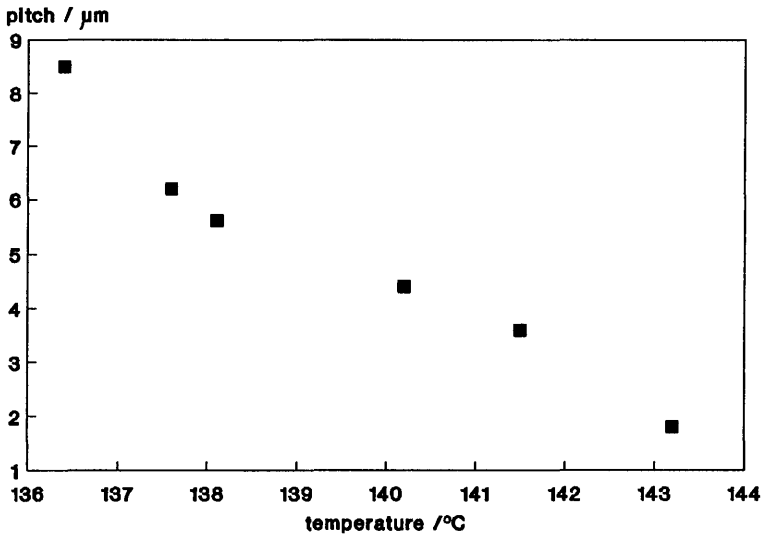

Figure 4.6 The pitch of the helix of **35** in the cholesteric phase as a function of temperature.

Digitised by the Department of Library Services in support of open access to information, University of Pretoria, 2021.

UNIVERSITEIT VAN PRETORIA
UNIVERSITY OF PRETORIA
YUNIBESITHI YA PRETORIA

4.3.4 Spontaneous polarisation measurements

The spontaneous polarisation was measured as a function of temperature in the smectic C* phase of compound **35**. The results obtained for three consecutive cooling runs are superimposed in fig. 4.7. It can be seen from this graph that the spontaneous polarisation increases almost linearly with the decreasing temperature which is somewhat unexpected for a material that exhibits a direct cholesteric to ferroelectric smectic C* transition. For a first order phase change of this type it is to be expected that the spontaneous polarisation would show a sharp jump at the phase transition before levelling off rapidly as the temperature is reduced. This more gradual rise in the polarisation might be due to the fact that the Ch - SmC* transition is relatively weakly first order as shown by differential scanning calorimetry.

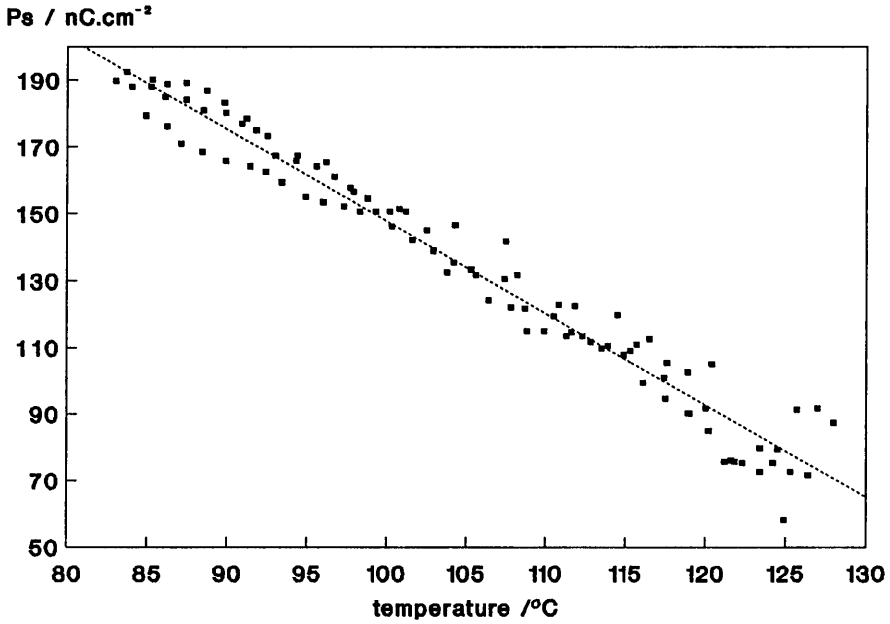

Figure 4.7 The spontaneous polarisation in the ferroelectric smectic C* phase of compound **35** measured as a function of temperature. The polarization was measured in a cell with 3 μm spacing at a frequency of 60 Hz and 10 V peak-to-peak ac to effect switching.

The direction of the spontaneous polarisation in the smectic C* phase was determined according to standard procedures[93] by poling the material which was held in an electro-optic cell (see also section 3.4.1). Throughout the whole temperature range of the phase only a positive spontaneous polarisation, Ps(+), was observed, confirming that there is no polarisation inversion occuring.

Digitised by the Department of Library Services in support of open access to information, University of Pretoria, 2021.

UNIVERSITEIT VAN PRETORIA
UNIVERSITY OF PRETORIA
YUNIBESITHI YA PRETORIA

The maximum value obtained for the polarisation is of the order of 200 nC.cm^{-2}. This is thought to be the result of an increase in the effective dipole at the chiral centre as a result of the proximity of the fluoro-substituent on the core and is discussed in more detail in chapter 6.

4.3.5 Tilt angle measurements

In the process of measuring the spontaneous polarisation, the optical tilt angle was also determined as a function of temperature. The results obtained are shown in fig. 4.8. The variation of the optical tilt angle with temperature is quite surprising. Initially, at the Ch - SmC* transition, a jump in the value of the tilt angle was found as expected for a first order phase transition. However, instead of the tilt angle levelling off with the reduction in temperature, it started to fall slowly, almost halving its value over a 50°C temperature range. This behaviour is not due to a falling value of the spontaneous polarization as the latter steadily increases over the same temperature range. In addition to this, the tilt angle is relatively small for a material that exhibits a Ch - SmC* transition, for which tilt angles of the order of 45° are not uncommon.

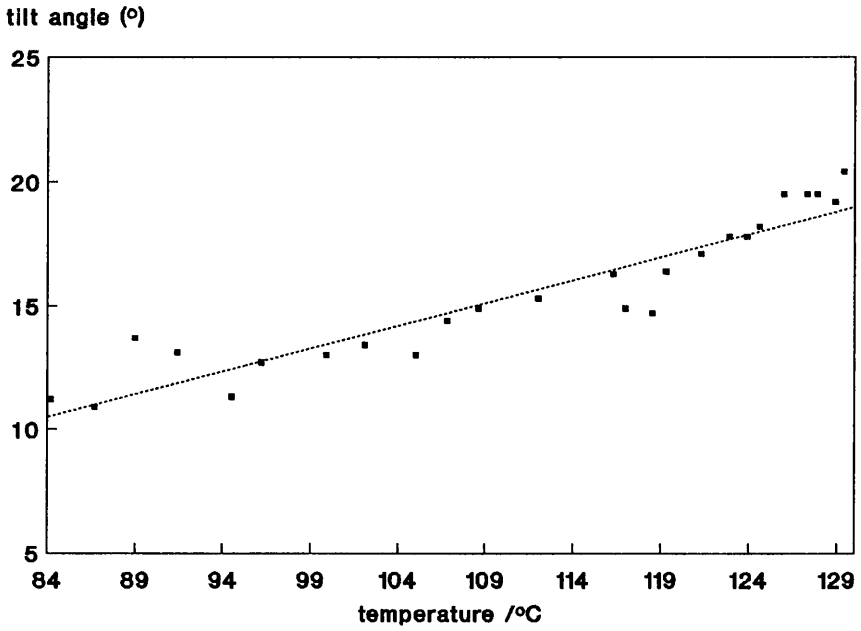

Figure 4.8 Optical tilt angle (°) of **35** plotted as a function of temperature.

As the optical tilt angle is closely related to the positions that the transition moments of the molecules make with respect to the layers, these results appear to indicate that the angle which the aromatic core forms with the layer normal decreases with reduced temperature, i.e. the molecules stand up as the sample is cooled. This is the reverse of the normally expected behaviour.

Digitised by the Department of Library Services in support of open access to information, University of Pretoria, 2021.

UNIVERSITEIT VAN PRETORIA
UNIVERSITY OF PRETORIA
YUNIBESITHI YA PRETORIA

The results suggest that the parallel core-core interactions (low tilt) in this particular system are relatively strong in comparison to the situation where they are only partially overlapping (high tilt). This is supported by the fact that the phase transition from the cholesteric phase is only weakly first order, whereas typically for the Ch - SmC* phase change it is strongly first order.

4.4 Discussion

The results obtained show that there is an inversion in the helical twist direction in the cholesteric phase of compound **35**. However, in the smectic C* phase there is no such inversion and polarisation and tilt angle studies show that the direction of the spontaneous polarisation remains constant with respect to temperature.

In previous investigations of inversion phenomena[94] it was suggested that conformational structures play an important role in determining both the twist and polarization directions. In compound **35** the structural architecture is very different to that of other compounds that show inversions. In particular, the chiral centre in **35** is closer to the core than in other "inversion" materials which have chiral centres usually removed from the aromatic core by at least two atoms, thereby allowing some degree of free rotation about the chiral centre itself[102]. Similarly, the peripheral aliphatic chain is longer in compound **35** than in compounds **A** to **D** (fig. 4.1). It has been suggested in the past that a longer peripheral chain has the effect of rotationally damping the motion of the chiral centre, consequently leading to higher spontaneous polarisations[103]. The rotational damping, therefore, should lead to one principal conformational structure being present, thereby negating the possibility of inversions occurring in chirality dependent properties. This can be seen to be clearly the case when the conformational structures of compound **35** are considered. The conformers related to structural changes about the chiral centre are shown together in fig. 4.9 in their most extended forms. These give the molecule an overall gross zigzag shape which is conducive to the formation of smectic C* phases[104]. Structures **G** and **H** have the carbonyl group and the aromatic fluoro-substituent on opposite sides of the molecule, whereas for structures **I** and **J** they are on the same side. It is expected that the latter will be of much higher energy than the former, because of the increased steric hindrance and strong repulsive polar effects.

In all four structures, assuming that the peripheral aliphatic chain attached to the chiral centre is fully extended and, for reasons of packing constraints, the material retains an overall zigzag molecular shape, then the steric and polar properties about the chiral centre will be similar for each conformer. The steric bulk and dipole associated with the chiral centre will be on the same side of the molecule in all four conformers. If this is the case the four conformers will have the same associated twist and polarization directions, and therefore there will be no competition between conformers to

Digitised by the Department of Library Services in support of open access to information, University of Pretoria, 2021.

UNIVERSITEIT VAN PRETORIA
UNIVERSITY OF PRETORIA
YUNIBESITHI YA PRETORIA

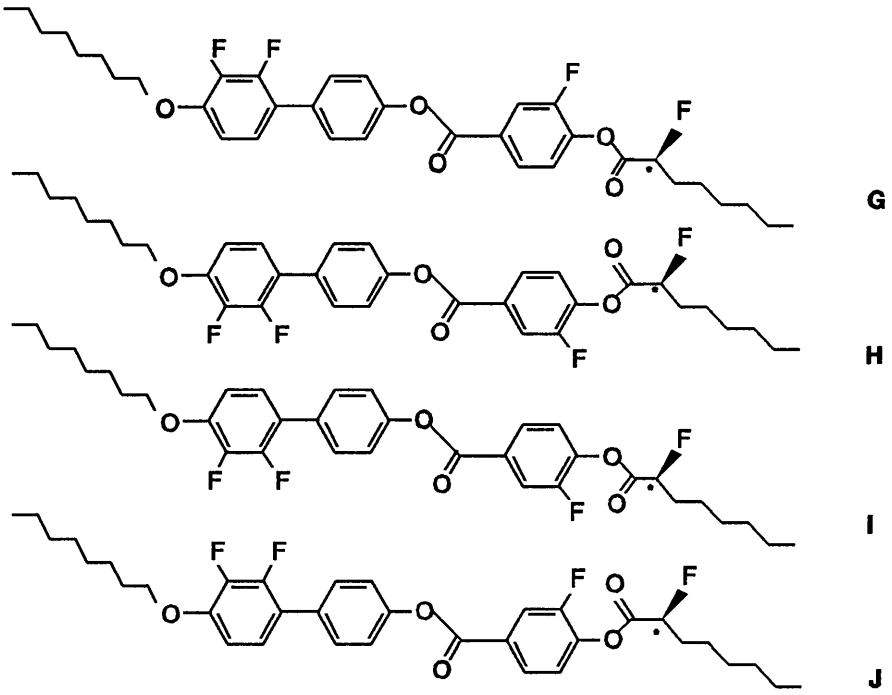

Figure 4.9 Zigzag shaped conformer structures of **35**.

drive the inversion phenomena. However, it is known[105] in a variety of difluoro-substituted systems that the fluoro-substituents prefer to be located in close proximity to one another. Similar to related compounds where the carbonyl group is replaced by a methylene group (see chapter 6) and where the two fluorine atoms are also in close proximity, the following can be said with respect to the steric and dipolar properties about the chiral centre of these conformers. Figure 4.10 shows the structures of two possible conformers in the vicinity of the aromatic ring that carries the chiral chain. The fluoro-substituents on the chiral centre and the aromatic ring have been brought in close approximation so that the fluorine atom lies to the right of the ring in structure **K** and to the left in **L**. It can be seen from the stereochemistry about the chiral centre in **K** that the peripheral chain lies closer to the long axis of the molecule than it does in structure **L**. Thus it might be expected that structure **K** is more

Digitised by the Department of Library Services in support of open access to information, University of Pretoria, 2021.

UNIVERSITEIT VAN PRETORIA
UNIVERSITY OF PRETORIA
YUNIBESITHI YA PRETORIA

conducive to forming liquid crystalline phases because of its lath-like shape, and therefore it may be preferred over structure **L**. Nevertheless, the two structures will have different polar and steric properties, and more importantly when the two conformers are compared it can be seen that the two effects will operate from opposing sides of the molecular structure. The opposing effects for the related fluoro-substituents, carbonyl groups and the terminal aliphatic chains will put the two conformers into competition.

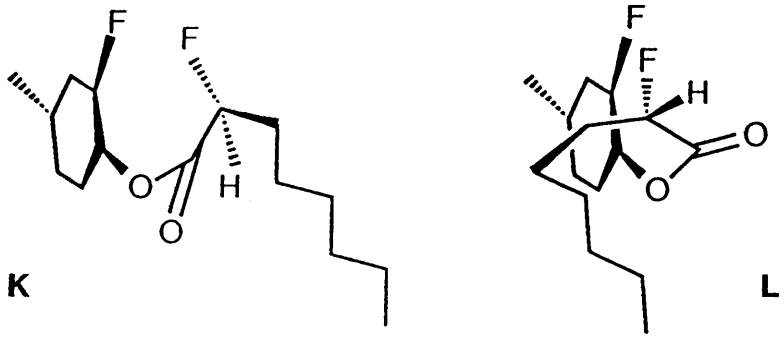

Figure 4.10 Structures of two conformers where the fluoro-substituents are brought in close proximity.

It is possible that the concentrations of the two competing conformer species are temperature dependent and that they are interconvertible *via* a small energy barrier. At a given temperature one species will then dominate over the other and when this is reversed at another temperature, an inversion in chiral properties will occur as was suggested previously[93-96].

4.5 Conclusion

In this chapter it was demonstrated that compound **35** exhibits a twist inversion in the helix of its cholesteric phase. It was shown that a conventional model of competing conformer species cannot be used to explain this phenomenon and therefore it was speculated that the competing species can be created through the interactions of the fluoro-substituents on the aromatic core and the chiral centre. Compound **35** is also shown to possess unusual tilt angle and thermodynamic properties.

---- # ----

Digitised by the Department of Library Services in support of open access to information, University of Pretoria, 2021.

CHAPTER 5

(S)-4-n-OCTYLOXY-2,3-DIFLUOROBIPHENYL-4'-YL 4-(2-CHLORO-4-METHYLPENTANOYLOXY)BENZOATE: A FLUORINE-19 NMR STUDY.

5.1 Introduction

In this chapter the use of a new experimental technique for obtaining proton-decoupled ^{19}F nmr spectra of liquid crystals is discussed. The technique is used to investigate the orientational order of the liquid crystal, (S)-4-n-octyloxy-2,3-difluorobiphenyl-4'-yl 4-(2-chloro-4-methylpentanoyloxy)-benzoate **55** which contains a 2,3-difluorophenyl unit. The study culminates in the calculation of the order parameter as a function of temperature, which makes it possible to make conclusions about the molecular motion in each mesophase. An attempt is also made to draw a comparison between this work and the only other published fluorine-19 nmr investigation of a liquid crystal.
The work presented in this chapter has appeared in print[106].

5.2 The problem of proton-decoupling.

The major problem associated with the acquisition of ^{19}F nmr spectra of liquid crystalline samples is the achievement of good proton-decoupling. Owing to the small difference between the Larmor frequencies of ^{1}H and ^{19}F and also the large magnitude of the heteronuclear ^{1}H - ^{19}F dipolar coupling, this can be extremely difficult.

The classical approach to decoupling is to subject the protons to a strong irradiation that is spread across the whole proton chemical shift range, so-called broad-band decoupling. However, there are two major problems associated with this approach. The first is that of providing an effective decoupling field across the entire proton chemical shift range. At 300 MHz a typical proton spectrum spreads over about 3000 Hz. In a sample consisting of an oriented phase such as a liquid crystal, this spread can increase to 25 kHz as a consequence of the large dipolar coupling between protons. As the required decoupling power increases in proportion to the square of the frequency spread, much more power is needed. The second problem, in effect a result of the first one, is that of radio-

Digitised by the Department of Library Services in support of open access to information, University of Pretoria, 2021.

UNIVERSITEIT VAN PRETORIA
UNIVERSITY OF PRETORIA
YUNIBESITHI YA PRETORIA

frequency heating. Some of the power used for decoupling is absorbed by the sample, causing undesired heating. This constitutes a serious problem when spectra of liquid crystals are obtained, where uncontrolled heating could lead to a phase transition, or to the observation of a mixture of two phases[107].

In order to overcome these problems, Avent *et al*[33] employed the spin echo technique to effect proton-decoupling when obtaining ^{19}F nmr spectra of a liquid crystal. This technique relies on the selective suppression of broad lines, thereby causing only sharp lines to be observed, a technique well suited to the study of liquid crystals. A major disadvantage of the spin echo technique is the long recording time necessary for a spectrum (± 8 h).

More recently, Shaka described a new scheme for low-power broadband heteronuclear decoupling[108]. It is based on the use of a composite radiofrequency pulse sequence and is now generally referred to as the WALTZ-sequence. The fact that it relies on less power in order to achieve the same decoupling (which, by implication, means less undesired heating) means that a much wider proton frequency region can be covered. This prompted us to investigate its usefulness towards obtaining sufficiently decoupled ^{19}F nmr spectra of fluorinated liquid crystals.

5.3 Experimental

In order to achieve optimum efficiency during removal of ^{1}H - ^{19}F dipolar coupling, the following experiment was employed:

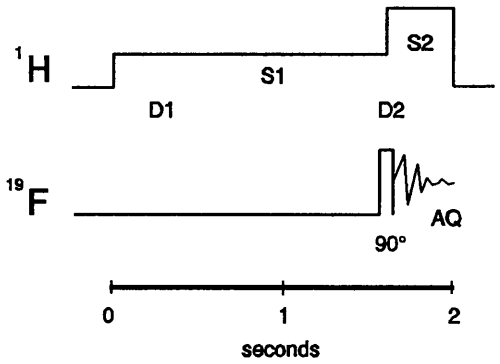

1. S1 = low-power broadband decoupling (γB_2 = 2.5 kHz) during delay time D1 = 1.5 s.
2. S2 = switch to higher decoupling power (γB_2 = 9.26 kHz) only during acquisition time of 0.19s.

Figure 5.1 The experiment used to obtain decoupled ^{19}F nmr spectra.

Digitised by the Department of Library Services in support of open access to information, University of Pretoria, 2021.

UNIVERSITEIT VAN PRETORIA
UNIVERSITY OF PRETORIA
YUNIBESITHI YA PRETORIA

By employing the higher decoupling power for a limited time of 0.19 s during the total cycling time of 1.7 s, radiofrequency overheating was kept to a minimum. Total decoupling was assumed when a further decrease in linewidth was not obtained on increasing the decoupling power. The advantage of this method lies in the fact that although ^{1}H - ^{19}F coupling is efficiently removed, homonuclear ^{19}F - ^{19}F dipolar interactions are left intact#. This means that it can be used to obtain ^{19}F - ^{19}F dipolar coupling constants and other useful information such as order parameters.

^{19}F nmr spectra were obtained using a Bruker AC 300 spectrometer equipped with a QNP probehead and a variable temperature control unit. The liquid crystal was contained in a coaxial insert (Wilmad Glass Co., USA) with an outer diameter of 2 mm. This was inserted into a standard 5 mm nmr tube containing dimethylsulfoxide-d_6 which served the dual purpose of providing a lock signal as well as to minimise temperature gradients in the sample.

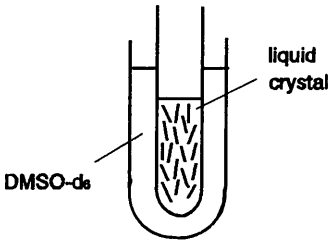

Spectra were acquired after slowly cooling the compound from the isotropic melt (1°C / min) in the magnetic field to ensure good alignment. Under these conditions a satisfactory spectrum could be obtained in 5 min (Iso), 30 min (nematic or Ch) and 2 - 3 h (smectic).

Spectra were analysed and δ_{F1} and δ_{F2} obtained using the method of Diehl and Khetrapal[110]

$$\delta_{F1F2}^{2} = [(x - y) - (J_{FF} - D_{FF})^{2}] \quad \ldots 5.1$$

where x and y are obtained from the experimental spectra as follows:

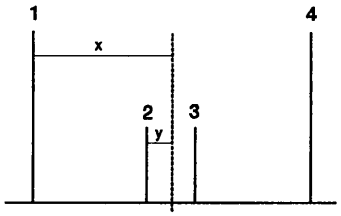

for a fixed x (say line 4), y can be the distance from either line 2 or 3 to the center

#Homonuclear dipolar interactions between fluorines are in fact quite difficult to remove and would require spinning speeds in excess of 30 kHz (together with MAS), as linewidths are only reduced proportionally to the inverse spinning rate[109].

Digitised by the Department of Library Services in support of open access to information, University of Pretoria, 2021.

UNIVERSITEIT VAN PRETORIA
UNIVERSITY OF PRETORIA
YUNIBESITHI YA PRETORIA

Analysis of the AB spin system according to this method yields the dipolar coupling constant at a given temperature:

$$D_{FF} = ½ (x + y - J_{FF}) \qquad ...5.2$$

5.4 Results

The compound, together with its phases and transition temperatures (as determined by nmr), is shown in fig. 5.2.

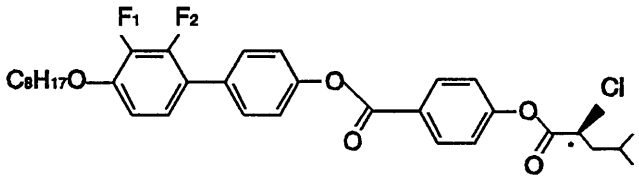

55

K 48°C / 74°C SmC* 107°C Ch 117°C Iso

Figure 5.2 Structure and phase transitions of **55**.

^{19}F nmr spectra were obtained at a range of temperatures and a spectrum representative of each phase is shown in fig. 5.3. The isotropic melt (fig. 5.3(a)) has the expected two doublets (AX spin system, $^{3}J_{FF}$ = 17.5 Hz) of which the low field one was assigned to F_1**. Cooling of the compound to below its clearing point results in a dramatic change in chemical shift and a spectrum of which the pattern, upon closer inspection, corresponds to that of an AB spin system (fig. 5.3(b)). Chemical shifts are listed in table 5.1 and are presented graphically in fig. 5.4. The Ch - SmC* transition is characterised by a sudden jump in chemical shift. The different degree to which δ_{F1} and δ_{F2} respond to a change in temperature is illustrated by the graph. It is obvious that F_1 is much more susceptible to a small change in temperature, particularly in the Ch phase, but that temperature has little effect on the chemical shift of both F_1 and F_2 throughout the SmC* phase.

**For assignment of chemical shifts, see appendix A.

Digitised by the Department of Library Services in support of open access to information, University of Pretoria, 2021.

UNIVERSITEIT VAN PRETORIA
UNIVERSITY OF PRETORIA
YUNIBESITHI YA PRETORIA

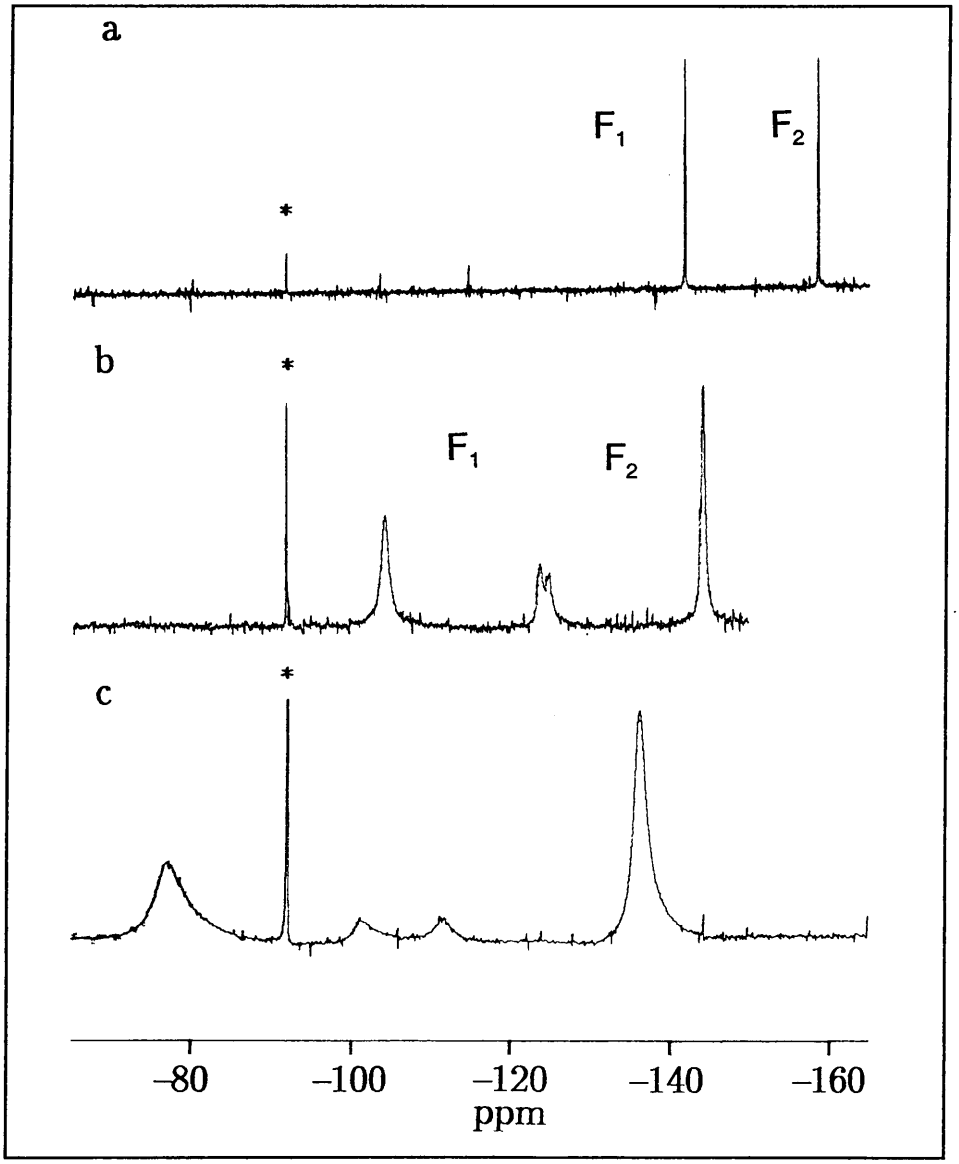

Figure 5.3 Proton-decoupled ^{19}F nmr spectra of **55**: (a) Iso (118°C), (b) Ch (116°C) and (c) SmC* (66°C). 1-Bromo-3-fluoro-4-iodobenzene was used as external reference (- 91 ppm rel. $CFCl_3$) and is indicated by *.

Digitised by the Department of Library Services in support of open access to information, University of Pretoria, 2021.

UNIVERSITEIT VAN PRETORIA
UNIVERSITY OF PRETORIA
YUNIBESITHI YA PRETORIA

Table 5.1 Experimental ^{19}F - ^{19}F dipolar coupling constants (D_{FF}), chemical shift values and calculated order parameters (S_{FF}) of **55** at a range of temperatures.

Phase/ transition	t (°C)	D_{FF} (Hz)	$\delta(F_1)$ ppm	$\delta(F_2)$ ppm	S_{FF}
Iso	120	-	-141.8	-158.6	-
	118	-	-141.5	-158.3	-
Iso - Ch	117	2670	-123.1	-136.1	0.453
Ch	116	2940	-117.7	-132.3	0.499
	115	3110	-116.5	-131.0	0.527
	114	3090	-114.2	-130.4	0.524
	113	3200	-112.9	-129.6	0.542
	112	3270	-112.0	-128.8	0.555
	111	3350	-111.2	-128.0	0.568
	109	3460	-110.6	-127.2	0.587
	108	3520	-110.6	-126.8	0.597
Ch - SmC*	107	3580	-110.1	-126.5	0.607
SmC*	105	4540	-101.1	-117.8	0.770
	101	4630	-99.8	-116.9	0.785
	96	4720	-99.1	-116.3	0.801
	92	4740	-98.4	-115.8	0.804
	88	4790	-98.0	-115.9	0.812
	83	4830	-97.8	-115.4	0.819
	79	4900	-97.8	-114.9	0.831
	75	4950	-97.6	-114.3	0.840
	66	4960	-96.6	-114.4	0.841

Digitised by the Department of Library Services in support of open access to information, University of Pretoria, 2021.

UNIVERSITEIT VAN PRETORIA
UNIVERSITY OF PRETORIA
YUNIBESITHI YA PRETORIA

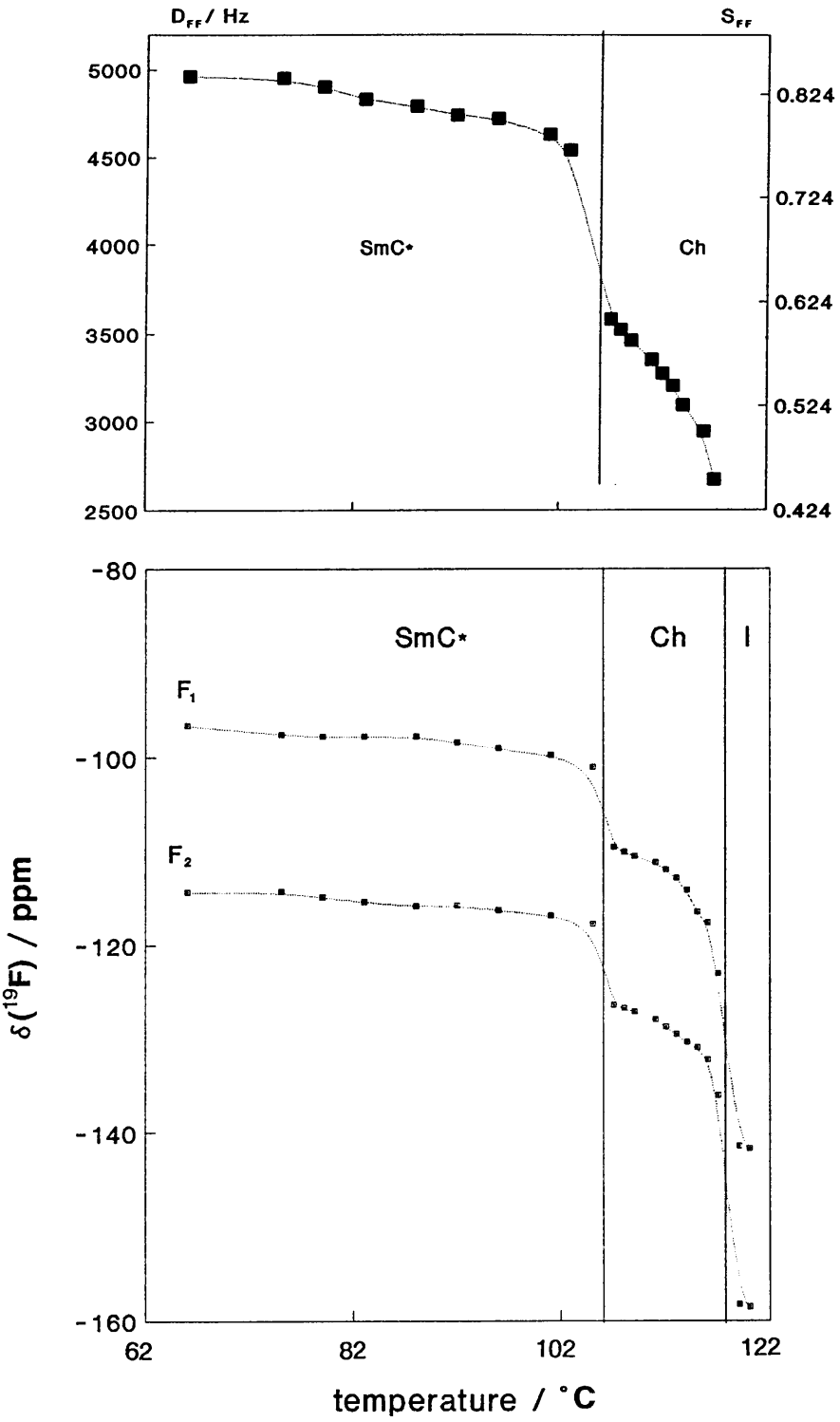

Figure 5.4 ^{19}F chemical shifts, dipolar coupling constants (D_{FF}) and the order parameter (S_{FF}) plotted as a function of temperature.

Digitised by the Department of Library Services in support of open access to information, University of Pretoria, 2021.

UNIVERSITEIT VAN PRETORIA
UNIVERSITY OF PRETORIA
YUNIBESITHI YA PRETORIA

Spectra were also analysed to obtain the ^{19}F - ^{19}F dipolar coupling constant D_{FF} - the values obtained are given in table 5.1. D_{FF} increases quite rapidly as the temperature is lowered throughout the Ch phase, with the Ch - SmC* transition once again marked by a sudden change - an increase of approximately 1000 Hz.

5.5 Discussion

5.5.1 Helical structure

The resolution of the spectra obtained throughout show that the helical structure of the Ch phase is destroyed by the magnetic field (7.04 T) and that the phase then becomes nematic-like. The directors of the molecules remain parallel to the external field as the temperature is lowered and the helix is prevented from forming in the SmC* phase. This occurs because the magnetic susceptibility anisotropy, $\Delta\epsilon$, for this material is most likely to be positive, as is the case with most thermotropic liquid crystals.

5.5.2 Line broadening

In the Ch phase the linewidth of F_1 is larger than that of F_2, an effect which becomes more pronounced as the temperature is lowered. There are two possible causes of such significant broadening. The first is that of chemical shift anisotropy, $\Delta_{\sigma F}$. The chemical shift of a particular nucleus arises from its shielding by surrounding electrons, but this shielding critically depends on the orientation of the molecule in the magnetic field as a factor of $(3\cos^2\theta-1)$. This is even more significant for aromatic molecules, as the benzene ring has a highly anisotropic electron distribution. In an oriented environment such as the liquid crystalline state, molecules rotate rapidly around their long molecular axes. This means that the chemical shift of the fluoro-substituents can vary by a few hundred ppm as the molecule rotates in the field, a problem that becomes worse as rotation slows due to a decrease in temperature. The large chemical shift range of ^{19}F is another factor that contributes to the chemical shift anisotropy.

The two fluoro-substituents do not exhibit the same $\Delta_{\sigma F}$. The location of F_1 at the end of the aromatic core could make it more susceptible to movement caused by the flexible chain, producing a changing electronic environment and hence an increase in $\Delta_{\sigma F}$. Furthermore, the $-OCH_2-$ protons could, also as a result of movement of the chain, cause a varying amount of ^1H - ^{19}F interaction, which would lead to an increased broadening of the resonance of F_1.

Digitised by the Department of Library Services in support of open access to information, University of Pretoria, 2021.

UNIVERSITEIT VAN PRETORIA
UNIVERSITY OF PRETORIA
YUNIBESITHI YA PRETORIA

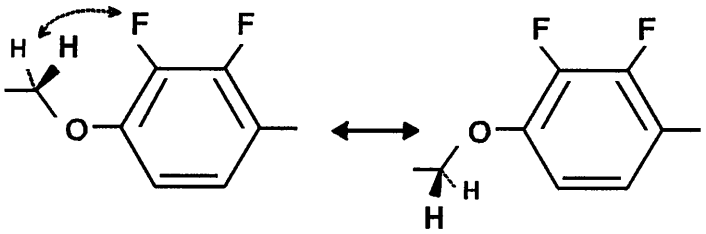

Figure 5.5 Possible ^{1}H - ^{19}F interaction as a cause of an increase in linewidth.

The second possible, but less important reason for the broadening observed is heteronuclear dipole-dipole interaction, which also depends on molecular orientation in the magnetic field. The two protons on the aromatic ring containing the fluoro-substituents as well as nearby ^{1}H nuclei on the octyl chain can interact with the ^{19}F nuclei in this manner.

Both the abovementioned causes greatly depend on the degree of order in the molecular environment - hence the observed increased broadening in the more densely packed SmC* phase. The combined effects of chemical shift anisotropy, $\Delta_{\sigma F}$, (which broadens peaks asymmetrically) together with dipolar coupling, D_{FF}, (which broadens the two peaks in a dipolar split doublet by equal amounts) would thereby give a differential broadening of the kind observed.

5.5.3 Dipolar coupling, D_{FF}.

D_{FF} values obtained from the spectra are given in table 5.1. It is important to note that D_{FF} may contain a contribution J_{FF}^{aniso} from the anisotropy of the indirect spin-spin coupling such that

$$D_{FF} = D_{FF}^{dir} + J_{FF}^{aniso} \qquad ....5.3$$

The latter has the same directional dependence as D_{FF}^{dir}. (i.e. the measured value depends on the orientation in the magnetic field). Sometimes it is therefore referred to as "pseudo dipolar coupling"[110]. When the interacting nuclei are fluorines, these anisotropic interactions can be significant, as was found for 1,2-difluoroethane dissolved in a nematic solvent[111]. The magnitude of J_{FF}^{aniso} has been determined for a number of fluorobenzenes in nematic solvents[112,113]. From these it was concluded that J_{FF}^{aniso} (*ortho*) is usually negligible, but that J_{FF}^{aniso} (*meta*) and J_{FF}^{aniso} (*para*) can be of the order of a few hertz. In this work J_{F1F2}^{aniso} was taken to be zero as the two fluoro-substituents are in an *ortho*-arrangement, therefore

Digitised by the Department of Library Services in support of open access to information, University of Pretoria, 2021.

UNIVERSITEIT VAN PRETORIA
UNIVERSITY OF PRETORIA
YUNIBESITHI YA PRETORIA

$$D_{FF} = D_{FF}^{dir} \text{ (measured)} \qquad ....5.4$$

Selected measurements were verified using computational iterative calculations (PANIC-software) while keeping $^3J_{FF}$ constant. Values obtained in this manner were found to be in excellent agreement with those obtained experimentally.

The only published ^{19}F nmr study of a liquid crystal (referred to in section 5.2) yielded dipolar coupling constants at selected temperatures. A brief comparison will be made between their results and the results obtained in this work.

Table 5.2 A comparison between a published study[33] and this work.

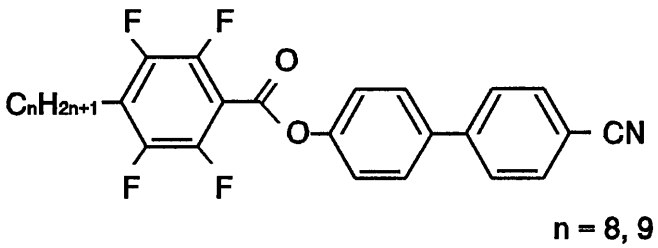

n = 8, 9

Compound	n = 8[a]		n = 9[a]	55[b]	
Phase	nematic	SmA	SmA	Ch	SmC*
t / °C	127 (T_{NI} - 45)	80 (T_{SmA-N} - 40.5)	91 (T_{SmA-N} - 48.5)	107 -117	66 - 105
D_{FF} (ortho)	3646.5±23.2	3988±10.8	3861±29.8	2670 - 3580	4540 - 4960
S_{FF}	0.675	0.738	0.715	0.453 - 0.607	0.770 -0.841

a. Reference 33. Measurements were obtained at selected temperatures only.
b. This work. Measurements were obtained at a range of temperatures.

Unfortunately the published compounds were only examined at selected temperatures and they do not have SmC phases. D_{FF} values obtained in this work for the Ch phase are slightly lower, but of

Digitised by the Department of Library Services in support of open access to information, University of Pretoria, 2021.

UNIVERSITEIT VAN PRETORIA
UNIVERSITY OF PRETORIA
YUNIBESITHI YA PRETORIA

comparable magnitude to those of the published work, while D_{FF} (SmA phase) falls in-between the range of values of the Ch and SmC* phases.

5.5.4 Order parameter

The dipolar coupling is defined by[6]

$$D_{FF} = -\frac{h\gamma_F^2}{4\pi^2} \cdot \frac{1}{2}\left(\frac{3\cos^2\theta - 1}{r_{FF}^3}\right) \qquad 5.5$$

where h: Planck's constant

γ_F: magnetogyric ratio for $^{19}F = 25.1665 \times 10^7\ T^{-1}.s^{-1}$

θ: the angle between the internuclear vector F_1 - F_2 and the direction of the magnetic field

r_{FF}: internuclear distance $F_1...F_2 = 2.622$ Å [114].

For ^{19}F the value of $(h\gamma_F^2 / 4\pi^2)$ is 1.063×10^5 Å^3.s^{-1}.

As F_1 and F_2 are attached to the same rigid part of the molecule and the directors of the molecules are aligned with the field, eq. 5.5 can be written as

$$D_{FF} = -1.063 \times 10^5 \cdot S_{FF} \cdot r_{FF}^{-3} \qquad 5.6$$

where S_{FF} (the order parameter) is the degree of orientation of the internuclear vector, F_1 - F_2:

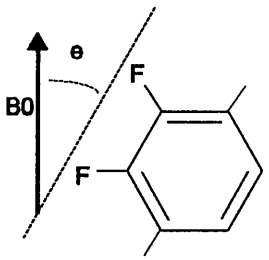

Digitised by the Department of Library Services in support of open access to information, University of Pretoria, 2021.

UNIVERSITEIT VAN PRETORIA
UNIVERSITY OF PRETORIA
YUNIBESITHI YA PRETORIA

The range of S_{FF} is defined as $-0.5 \leq S_{FF} \leq +1$, which means that at $S_{FF} = +1.0$ the $F_1 - F_2$ vector (and therefore the core of the molecule) would be parallel to B_0 and at $S_{FF} = -0.5$ perpendicular to it.

Values calculated for S_{FF} are given in table 5.1 and are presented graphically in fig. 5.4 (top). Lowering the temperature causes the molecular movement in the Ch phase to become more restricted, resulting in an increase in the order parameter which in turn causes D_{FF} to increase. In the SmC* phase the order parameter (and therefore D_{FF}) does not change appreciably with temperature and is close to its theoretical maximum. This indicates that the molecular directors, rather than the normals to the smectic planes, are aligned with the field as illustrated in fig. 5.6.

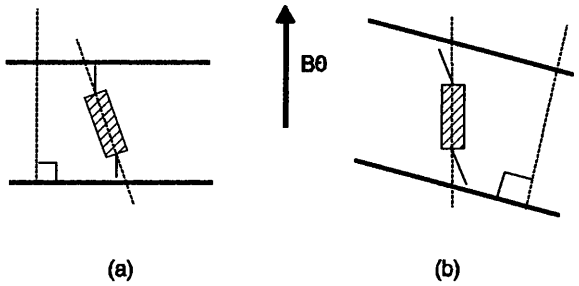

Figure 5.6 The two possible orientations of a molecule in the magnetic field in the SmC* phase.
(a) molecular directors tilted: expected decrease in S_{FF},
(b) smectic planes tilted: expected increase in S_{FF}

5.5.5 Nmr vs microscopy and calorimetry

At the Ch - SmC* transition (here in effect a nematic - SmC transition as the helical structure of both phases is destroyed) the molecules take on a layered arrangement. However, in this case the molecules do not tilt over in the smectic phase; instead the smectic planes tilt while the molecular directors remain aligned with the magnetic field. The point at which tilting of the layers occurs is reflected as a sharp discontinuity on both the chemical shift and order parameter graphs - this is indicative of a first order transition. The first order character of the Ch - SmC* transition was initially revealed by DSC analysis, a result that is clearly supported by the nmr experiments. The usefulness of employing a molecular technique (such as nmr) in conjunction with microscopy and calorimetry (which are macromolecular techniques) is obvious.

Digitised by the Department of Library Services in support of open access to information, University of Pretoria, 2021.

UNIVERSITEIT VAN PRETORIA
UNIVERSITY OF PRETORIA
YUNIBESITHI YA PRETORIA

5.6 Conclusion

The selective fluorination of liquid crystals provides a simple yet powerful method by which molecular behaviour in a particular liquid crystalline phase can be observed. It was shown that well-resolved spectra can be obtained in a short time without elaborate equipment using a conventional high-resolution probe and that the simplicity of the spectra allows for instant recognition of phases and phase transitions. In addition to this, information concerning the molecular orientation is obtained which in turn can support calorimetric and electro-optical measurements.

These encouraging results prompted the investigation of other fluorinated liquid crystals using the technique described in this chapter. These are presented in the following two chapters.

---- # ----

Digitised by the Department of Library Services in support of open access to information, University of Pretoria, 2021.

CHAPTER 6

COUPLING BETWEEN DIPOLES ON THE CORE AND AT THE STEREOCENTRE OF THE CHAIN: A COMPARATIVE STUDY OF TWO LIQUID CRYSTALS.

6.1 Introduction

The size and electronegativity of a substituent at the chiral centre, the nature of the group linking the stereocentre with the core and the nature and position of lateral substituents on the core are known to contribute to the ferroelectric properties of a liquid crystal. In 1988 it was shown that substitution on the end-ring of the core with a polar substituent (such as cyano) *ortho* to the chiral chain could cause an increase in the spontaneous polarisation[56].

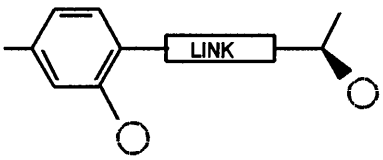

Subsequently it was established that the presence of an *ortho* fluoro-substituent on the end-ring together with an electronegative substituent on the chiral centre could lead to as much as a threefold increase in polarisation[57]. The uncertainty in possible reasons for these observations prompted the work presented in this chapter. Two liquid crystals were synthesised for the purpose of this work, with both of them containing the molecular unit shown below.

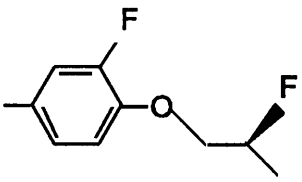

Digitised by the Department of Library Services in support of open access to information, University of Pretoria, 2021.

UNIVERSITEIT VAN PRETORIA
UNIVERSITY OF PRETORIA
YUNIBESITHI YA PRETORIA

The two compounds were subjected to ^{19}F nmr analysis in their various liquid-crystalline phases using the technique described in chapter 5 in an attempt to answer the question: "Does any direct interaction exist between the fluoro-substituents on the aromatic core and at the chiral centre?". In addition, compound **38** contains a 2,3-difluorophenyl unit, which has its two substituents conformationally fixed with respect to one another. This unit is intended to act as a probe of the molecular orientational order so as to provide a basis for the discussion concerning interaction between the core and the chiral centre.

The nmr experiments provided evidence that there is indeed an interaction between the core and the chiral centre. Further support for these results was obtained by subjecting the particular molecular subunit to conformational analysis. Differential scanning calorimetry (DSC) and optical tilt angle measurements complete the study of these two compounds.

6.2 Experimental

Nmr experiments were conducted using the technique described in section 5.3.1. Chemical shift values and dipolar coupling constants were obtained from the spectra. Selected values were verified by computational iterative calculations using Bruker software (PANIC) by varying coupling constants and linewidths until a close fit is obtained between the computer-generated and experimental spectra.

Molecular mechanics calculations were performed using the SYBYL software package (version 5.41, Tripos Associates) on a DEC VAX 3400 computer. The standard Tripos force field[115] was used in all energy calculations. The potential functions included energies arising from bond stretching, angle bending, out-of-plane bending, torsional deviations, Van der Waals interactions and electrostatic interactions. For the latter contribution, charges were calculated using the method of Gasteiger and Marsili[116]. Energy minimizations were executed with Maximin 2. Systematic conformational searching[117] was performed with energy calculations using the search algorithm (CSEARCH) of SYBYL's Advanced Computational Module. The search program checks for Van der Waals contacts among the non-bonded atoms by scanning all possible torsional angles around the rotatable bonds.

Five rotatable bonds were defined as in fig. 6.7 and were independently rotated with an angle increment of 30° through a range of 360°. All different local minima were identified and used for energy minimization. The two most important torsional angles, C - O - C - C(F) and O - C - C(F) -C were given particular attention.

DSC and tilt angle measurements were conducted as described in sections 3.3 and 3.4 respectively.

Digitised by the Department of Library Services in support of open access to information, University of Pretoria, 2021.

UNIVERSITEIT VAN PRETORIA
UNIVERSITY OF PRETORIA
YUNIBESITHI YA PRETORIA

6.3 Results

The two compounds discussed in this chapter, together with their phases and transition temperatures are shown in fig.6.1.

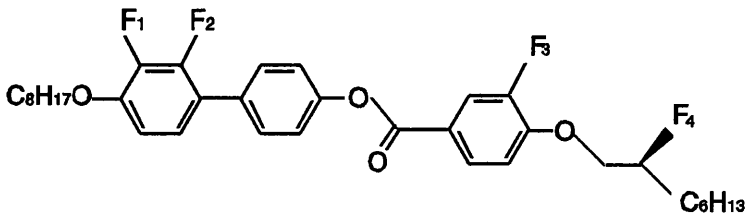

38: K 102°C / 118°C SmC* 146.0°C Ch 152.9°C BP 153.8°C Iso

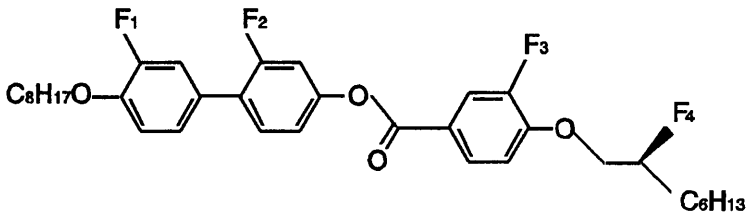

54: K 89°C / 103°C SmC* 106.5°C SmA 152.2° Iso

Figure 6.1 Structures and phase transition temperatures of the compounds.

The only structural difference between these two compounds is the position of a single fluoro-substituent on the core, yet their polymorphism differs markedly. Compound **38** has a wide smectic C* phase together with a cholesteric phase. It also has two blue phases ,BPI and BPII, here simply denoted as BP. Compound **54**, in contrast, has a wide smectic A phase and an underlying smectic C* phase, with no cholesteric phase.

6.3.1 ^{19}F nmr: chemical shifts and appearance of spectra.

The ^{19}F chemical shifts of compounds **38** and **54** are given in tables 6.1 and 6.2 respectively and are presented graphically in figures 6.13 and 6.14. Selected spectra are shown in figures 6.2 and 6.3 in order to illustrate the descriptions provided in the following paragraphs.

Digitised by the Department of Library Services in support of open access to information, University of Pretoria, 2021.

UNIVERSITEIT VAN PRETORIA
UNIVERSITY OF PRETORIA
YUNIBESITHI YA PRETORIA

The spectrum of the isotropic state (fig. 6.2, top) of compound **38** consists of four peaks, the high field one of which was assigned to the fluoro-substituent on the chiral centre (F_4) and the three occurring at lower field to the aromatic fluorines as indicated on the spectrum. The blue phase is readily distinguished from both the isotropic state and the cholesteric phase by its unique spectrum: the peaks of the aromatic fluorines are of similar chemical shift, but slightly broadened compared to those in the isotropic state. The peak of F_4, in contrast, remains sharp compared to those of the aromatic fluorines throughout the blue and cholesteric phases. The cholesteric phase is additionally characterised by further broadening of F_1, F_2 and F_3, an effect which is more pronounced for the most deshielded nucleus (F_3). The Ch - SmC* transition is marked by a sharp increase in $\delta(^{19}F)$ for the aromatic fluoro-substituents (fig. 6.2 and graphically illustrated in fig. 6.13) as opposed to the resonance of the fluorine on the chiral centre which does not undergo any shift. The SmC* phase is characterised by well-resolved peaks. F_1 and F_2, which are in close proximity on the molecule, form an AB spin system from which the dipolar coupling constant can be extracted (section 6.3.2). Furthermore, the peak of F_3 is resolved into a doublet. This can only be due to its coupling with F_4, as is clear from fig. 6.5 where the individual components of the spectrum are shown. The resonance of F_4 is of low intensity and severely broadened and is unresolved. This situation continues for approximately 5°C below the Ch - SmC* transition, below which the gradual increase in linewidth has a detrimental effect on the resolution. It should be noted that there is no significant change in the chemical shift of any of the fluorines throughout the SmC* phase. As the solid state is approached (fig. 6.2, bottom) the spectrum becomes distorted possibly as a result of the large chemical shift anisotropy and intermolecular effects.

Digitised by the Department of Library Services in support of open access to information, University of Pretoria, 2021.

UNIVERSITEIT VAN PRETORIA
UNIVERSITY OF PRETORIA
YUNIBESITHI YA PRETORIA

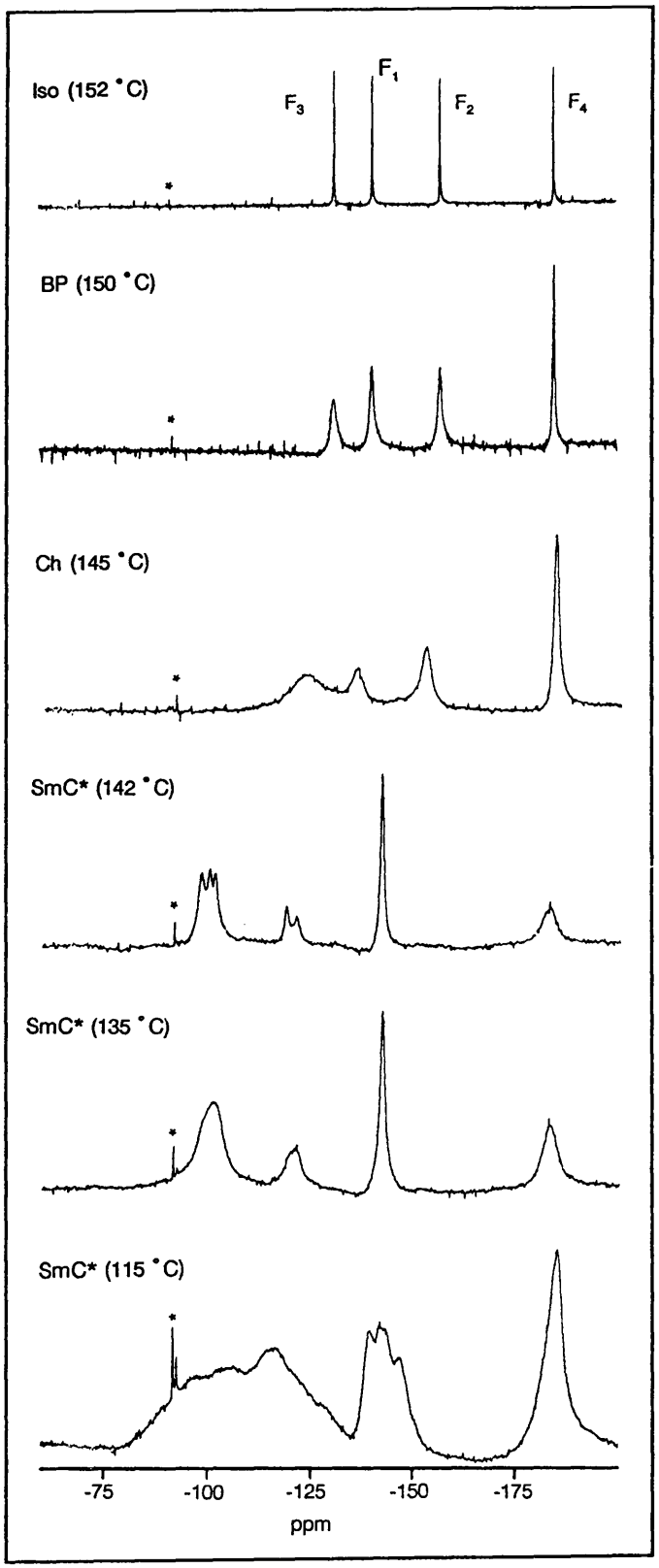

Figure 6.2 Proton-decoupled ^{19}F nmr spectra of **38** at a range of temperatures. 1-Bromo-3-fluoro-4-iodobenzene was used as external reference (-91 ppm rel. $CFCl_3$) and is indicated by *.

Digitised by the Department of Library Services in support of open access to information, University of Pretoria, 2021.

UNIVERSITEIT VAN PRETORIA
UNIVERSITY OF PRETORIA
YUNIBESITHI YA PRETORIA

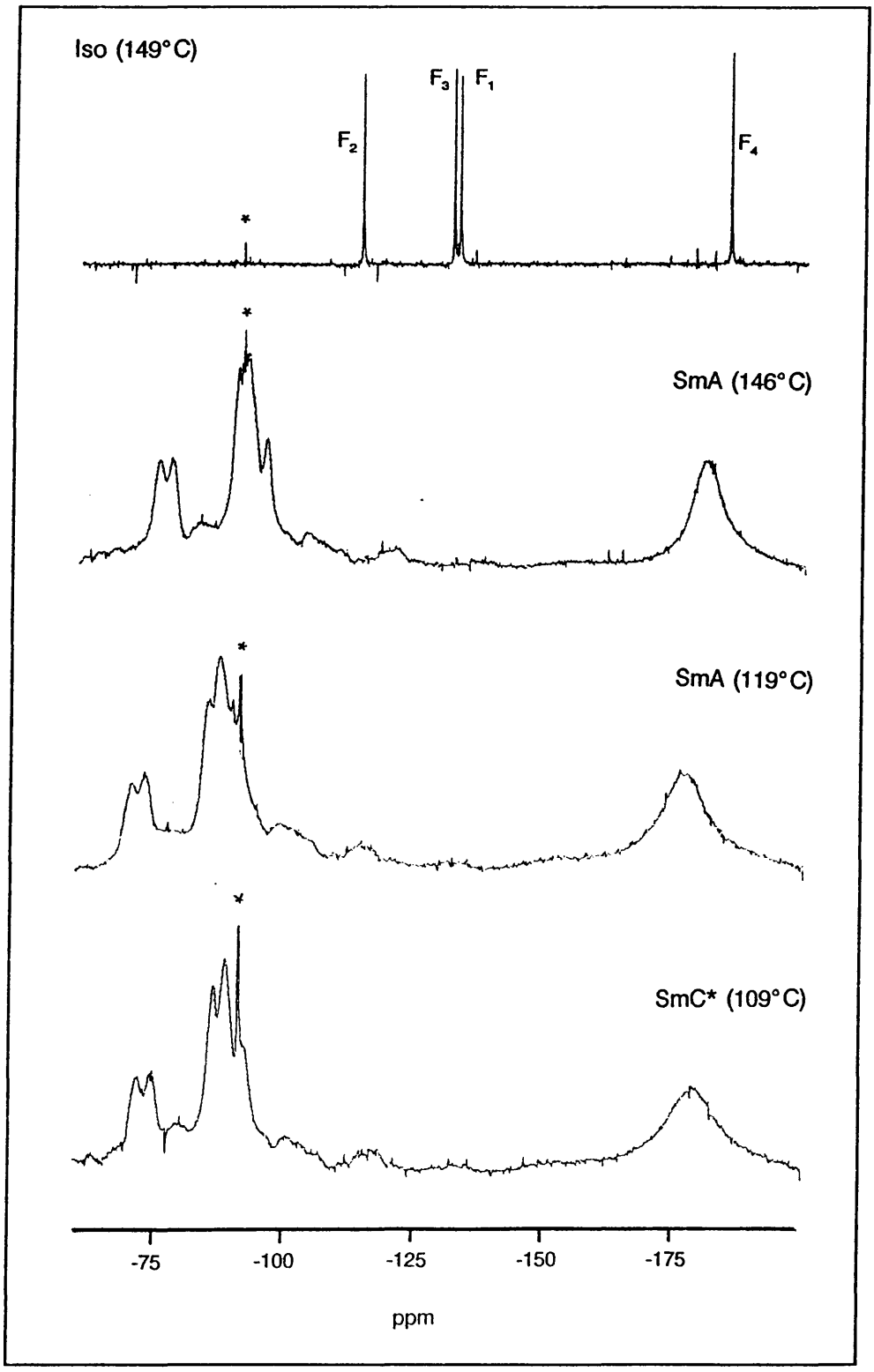

Figure 6. 3 Proton-decoupled ^{19}F nmr spectra of **54** at a range of temperatures. 1-Bromo-3-fluoro-4-iodobenzene was used as external reference (-91 ppm rel. $CFCl_3$) and is indicated by *.

Digitised by the Department of Library Services in support of open access to information, University of Pretoria, 2021.

UNIVERSITEIT VAN PRETORIA
UNIVERSITY OF PRETORIA
YUNIBESITHI YA PRETORIA

Table 6.1 ^{19}F nmr chemical shift values of **38** at a range of temperatures.

Phase	t / °C	δ(^{19}F) / ppm			
		F_1	F_2	F_3	F_4
Iso	152	-139.8	-156.5	-130.5	-184.2
BP	150	-139.6	-156.5	-130.0	-184.4
Ch	149	-135.7	-152.6	-123.6	-183.5
	147	-135.3	-152.0	-122.7	-183.4
	145	-134.9	-151.8	-122.2	-183.4
	144	-134.4	-151.1	-120.3	-183.3
SmC*	142	-111.9	-129.0	-100.1	-182.4
	141	-111.4	-128.7	-100.5	-182.3
	140	-111.2	-128.5	-100.8	-182.7
	139	-111.3	-128.1	-99.5	-182.4
	137	-110.7	-127.7	-99.2	-182.5

Table 6.2 ^{19}F nmr chemical shift values of **54** at a range of temperatures.

Phase	t / °C	δ(^{19}F) / ppm			
		F_1	F_2	F_3	F_4
Iso	149	-132.7	-113.9	-131.5	-185.3
SmA	147	-95.2	-76.9	-92.5	-181.0
	145	-94.3	-76.3	-91.8	-181.3
	139	-91.5	-73.7	-89.1	-178.0
	134	-91.1	-73.0	-87.6	-177.0
	129	-90.7	-72.1	-87.0	-177.4
	124	-90.1	-71.9	-86.3	-177.5
	119	-88.5	-71.8	-86.2	-177.6
SmC*	109	-87.9	-71.4	-85.6	-177.7

Digitised by the Department of Library Services in support of open access to information, University of Pretoria, 2021.

UNIVERSITEIT VAN PRETORIA
UNIVERSITY OF PRETORIA
YUNIBESITHI YA PRETORIA

The ^{19}F nmr spectrum of the isotropic state of compound **54** is shown in fig. 6.3 (top). The high field resonance at -185.3 ppm was assigned to the fluorine at the chiral centre (F_4) and the low field resonance to the fluoro-substituent on the central aromatic ring (F_2). Unfortunately the other two fluorines (F_1 and F_3) have very similar chemical shifts and this complicated matters somewhat. Nevertheless, after comparison with the spectrum of compound **38**, the peak occurring at lower chemical shift was assigned to F_1, as is indicated on the spectrum. The Iso- SmA transition is characterised by a large down field shift of the aromatic fluorines and an increase in the linewidth of all the peaks, but this is more pronounced for F_4. The SmA - SmC* transition does not coincide with any significant change in the appearance of the spectrum - in fact, it is not possible to determine the point of transition by observing the nmr spectra.

6.3.2 ^{19}F nmr: dipolar coupling and order parameter

The fluoro-substituents on the 2,3-difluorophenyl unit of compound **38** (F_1 and F_2) give rise to two doublets with a vicinal coupling of $^3J_{F1F2}$ = 20 Hz (obtained from the spectrum of the isotropic phase, but not resolved in fig. 6.2). No coupling of F_1 with F_2 is resolved in the blue or cholesteric phases. In the upper temperature region of the smectic C* phase two sets of doublets, which together form an AB spin system, are observed for F_1 and F_2. Coupling constants (table 6.3) were obtained directly from the spectra by using the method of Diehl and Khetrapal (section 5.3.1). Computational iterative calculations were then employed to confirm these.

Table 6.3 ^{19}F dipolar coupling constants, D_{F1F2}, and order parameters, S_{F1F2}.

t / °C	D_{F1F2}	S_{F1F2}
142	3260	0.552
141	3200	0.543
140	3160	0.536
139	3130	0.531
137	3110	0.527

D_{F1F2} has a maximum value immediately below the Ch - SmC* transition after which it decreases gradually as the temperature is lowered (see fig. 6.4). As the distance $F_1...F_2$ is known, the order parameter for each temperature can be calculated using equation 5.6. Values are given in table 6.3 and shown graphically in fig. 6.4.

Digitised by the Department of Library Services in support of open access to information, University of Pretoria, 2021.

UNIVERSITEIT VAN PRETORIA
UNIVERSITY OF PRETORIA
YUNIBESITHI YA PRETORIA

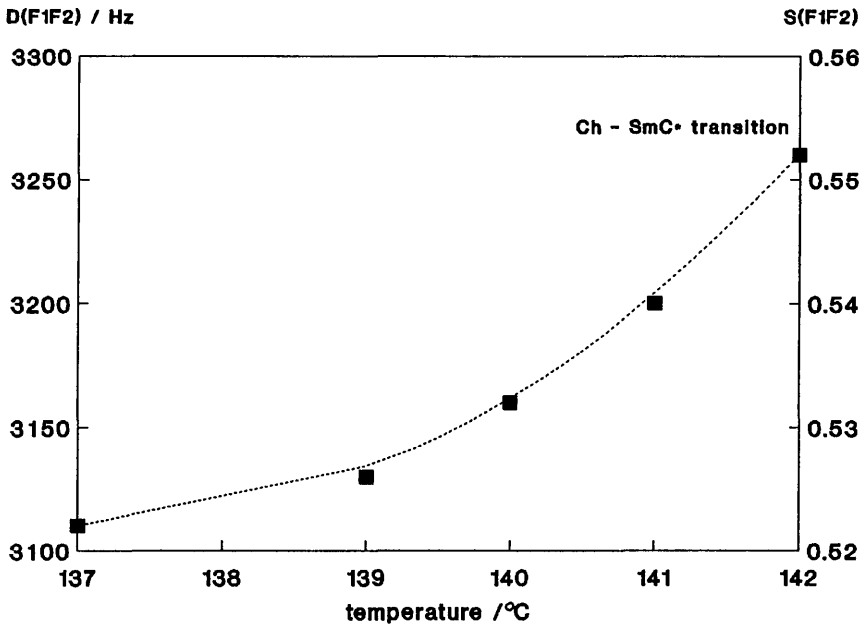

Figure 6.4 ^{19}F dipolar coupling constants and calculated order parameters of the upper temperature region of the SmC* phase of **38** plotted as a function of temperature.

Direct coupling of F_3 with F_4 is observed as a splitting of the F_3-resonance into a doublet located slightly upfield from the fourth line of the AB spin system (fig. 6.2). This can clearly be seen in fig. 6.5 (c) where the computer-generated components of the spectrum are shown. The resolution of the spectra immediately below the Ch - SmC* transition permitted the extraction of the coupling constant: at 142°C, D_{F3F4} = 350 Hz and at 141°C, D_{F3F4} = 390 Hz. Below 141°C, the F_3 doublet is insufficiently resolved to obtain the magnitude of the coupling. In contrast to F_3, the peak of the fluorine on the chiral centre (F_4) is broad and unresolved. Using the computer-generated spectrum (fig. 6.5(b)), it could be estimated from the shape of the peaks that D_{F2F3} does not exceed 20 Hz.

The ^{19}F nmr spectra of compound **54** are shown in fig. 6.3. From the spectrum of the smectic A phase it is possible to extract the important coupling constants. The F_2 resonance occurs as a doublet as a result of its direct coupling with F_1 and the magnitude of the coupling is measured to be 660 Hz. This value remains constant throughout the SmA and into the SmC* phase and appears to be temperature-independent. From the group of peaks situated at -88 ppm it is clear that a significant dipolar interaction between F_3 and F_4 does exist, but that it would have to be resolved with the aid of spectral simulation. Thus, it was determined that D_{F3F4} = 520 Hz at 146°C (immediately below the Iso - SmA transition) and increasing to 630 Hz at 109°C (below the SmA - SmC* transition)

Digitised by the Department of Library Services in support of open access to information, University of Pretoria, 2021.

UNIVERSITEIT VAN PRETORIA
UNIVERSITY OF PRETORIA
YUNIBESITHI YA PRETORIA

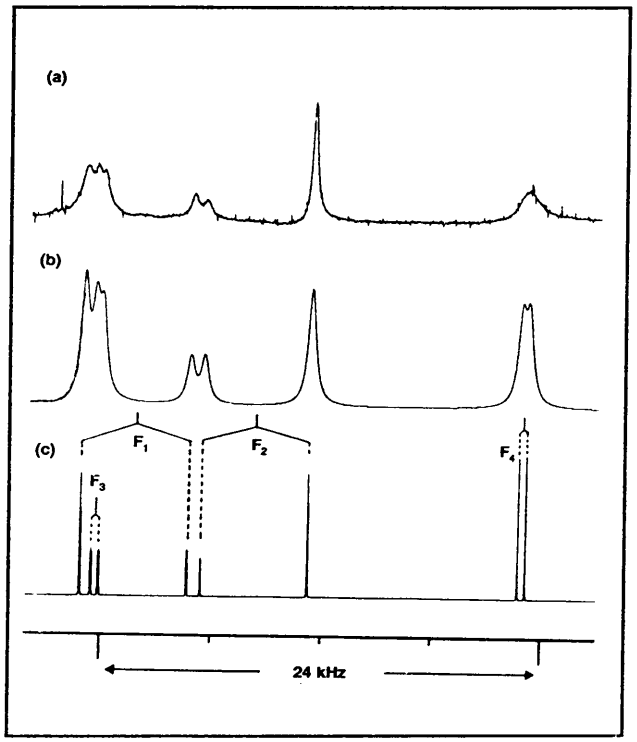

Figure 6.5 ^{19}F nmr spectra of **38**: (a) experimental spectrum at 142°C (SmC* phase); (b) simulated spectrum plotted with a linewidth of 500 Hz; (c) components of the spectrum.

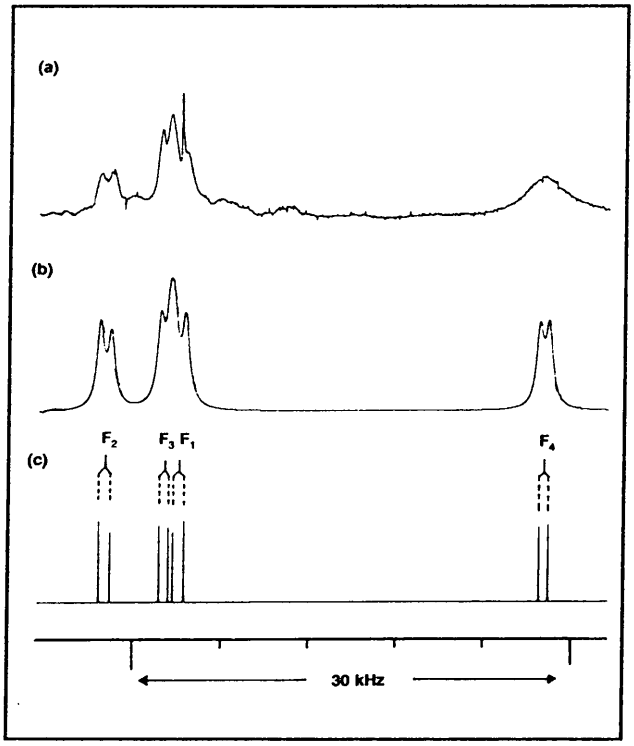

Figure 6.6 ^{19}F nmr spectra of **54**: (a) experimental spectrum at 109°C (SmC* phase); (b) simulated spectrum plotted with a linewidth of 500 Hz; (c) components of the spectrum.

Digitised by the Department of Library Services in support of open access to information, University of Pretoria, 2021.

UNIVERSITEIT VAN PRETORIA
UNIVERSITY OF PRETORIA
YUNIBESITHI YA PRETORIA

as shown in fig. 6.6. D_{F2F3} can be estimated to be not greater than 70 Hz from the linewidth of the peaks and this value does not appear to change with temperature.

6.3.3 Molecular mechanics

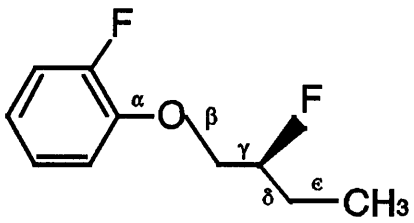

Figure 6.7 The molecular subunit of **38** and **54** which was submitted to conformational analysis showing the five bonds which were rotated.

The systematic conformational search involving the stepwise rotation of the five bonds defined in fig. 6.7 yielded 67 conformations with a total energy within 16 kJ.mol^{-1} of the lowest energy conformation. For eight of these the energy was within 7.5 kJ.mol^{-1}. The two lowest energy conformations (I and II) were identified (see table 6.4) and retrieved for energy minimization.

Table 6.4 Dihedral angles (°) and energies for the two lowest energy conformations resulting from the initial systematic search.

Rotatable bond	I	II
α	-90	90
β	180	180
γ	-60	-60
δ	180	180
ε	-[b]	-[b]
E[a]	0.00	0.09

a. Energy difference from minimum energy conformation (in kJ.mol^{-1}).

b. Rotation of this bond involves rotation of the methyl group and there is no preferred orientation.

Digitised by the Department of Library Services in support of open access to information, University of Pretoria, 2021.

UNIVERSITEIT VAN PRETORIA
UNIVERSITY OF PRETORIA
YUNIBESITHI YA PRETORIA

The results show that the O-CH_2 bond protrudes almost perpendicular to the plane of the aromatic ring, but that it does not matter whether it protrudes above or below the plane (i.e. +90° or -90°). As the ultimate aim of this part of the work is to establish the conformation of the molecular segment in which the chiral centre finds itself, the most important rotatable bonds are β and γ. The reason for this is that when γ is known, the value of the O - C - C - F angle would simultaneously be known and hence the preferred position of the fluorine on the chiral centre relative to that of the fluorine on the core.

Therefore, while keeping the other four rotatable bonds fixed in their positions determined in the search routine (table 6.4), γ was allowed to rotate freely in order to establish which one of the conformers shown in fig. 6.8 has the lowest energy. The result of the minimization is shown in table 6.5 where the results for the three lowest energy conformations (I, II and III) are listed.

Table 6.5 Dihedral angles (°), energies and interfluorine distances for the three lowest energy conformations.

Rotatable bond	I	II	III
α	-68	-69	-68
β	179	180	180
γ	-60	-180	60
δ	177	177	177
ε	-64	-64	-64
E[a]	0.00	7.58	9.34
F•••F[b]	4.980	5.178	4.108

a. Energy difference from minimum energy conformation (in $kJ.mol^{-1}$).

b. Distance (Å) between the fluorine on the chiral centre and the fluorine on the aromatic ring.

These values were subsequently confirmed by carrying out an additional minimization, where γ was kept at -60° and β was allowed to rotate freely. The results correspond to conformer C in fig. 6.8. The oxygen atom and C1 on the chain prefer a *gauche* arrangement, which in turn implies that the

Digitised by the Department of Library Services in support of open access to information, University of Pretoria, 2021.

UNIVERSITEIT VAN PRETORIA
UNIVERSITY OF PRETORIA
YUNIBESITHI YA PRETORIA

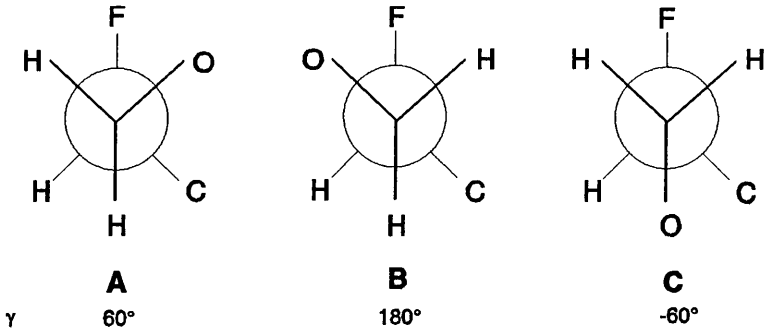

Figure 6.8 Projections of the three possible rotational conformations around γ.

oxygen and the fluorine atom on the chiral carbon are *antiperiplanar*. Therefore, concerning the distance between the two fluorine atoms it is clear that they prefer to be neither at the longest nor the shortest possible distance from each other, but at an intermediary distance of 4.980 Å (see table 6.5). The chain is in an extended conformation as shown in fig. 6.9.

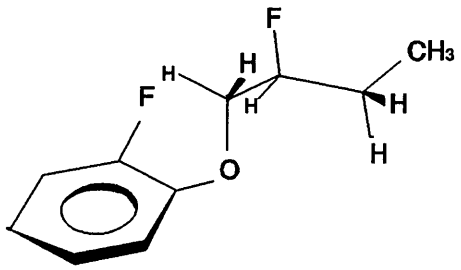

Figure 6.9 Schematic representation of the minimum energy conformation of the molecular subunit containing the chiral centre of **38** and **54**.

The minimum energy conformation is also shown in fig. 6.10 (a) where the Van der Waals volumes of the atoms are represented as spheres of a different colour for each kind of atom: hydrogen (blue-green), fluorine (green) and oxygen (red). In fig. 6.10 (b) two orthogonal views of the Van der Waals volumes of the atoms are shown, this time coloured according to electrostatic potential at the surface of the Van der Waals distance (red = electron deficient, green = neutral, blue = electron rich). Figures 6.10 (c) and (d) respectively depict two different perspectives of the contours of the

Digitised by the Department of Library Services in support of open access to information, University of Pretoria, 2021.

UNIVERSITEIT VAN PRETORIA
UNIVERSITY OF PRETORIA
YUNIBESITHI YA PRETORIA

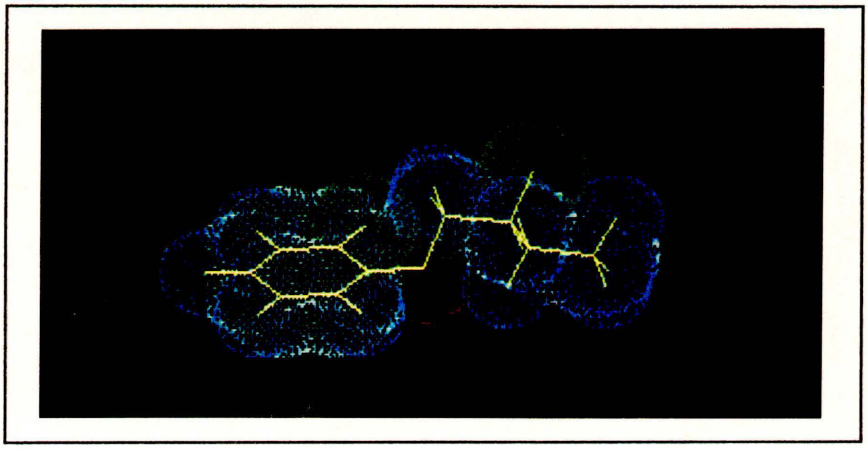

(a)

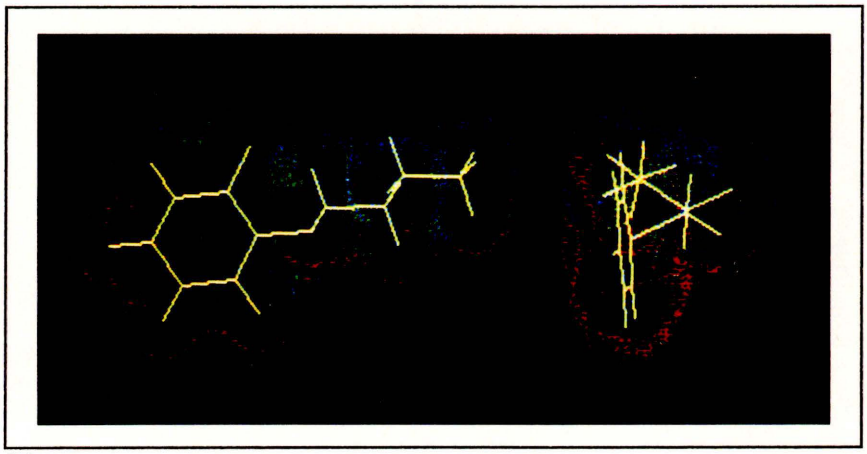

(b)

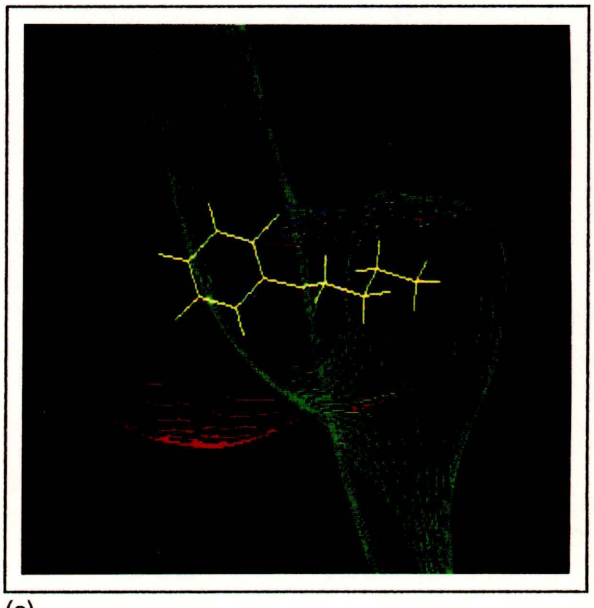

(c)

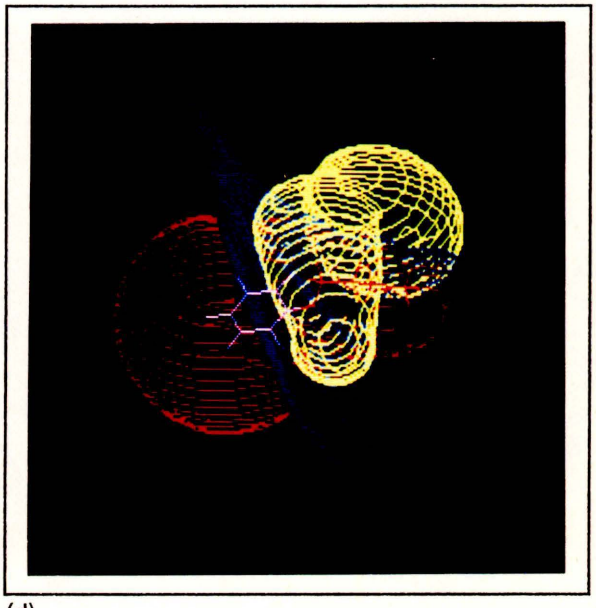

(d)

Figure 6.10 Minimum energy conformation of the molecular subunit (see text).

Digitised by the Department of Library Services in support of open access to information, University of Pretoria, 2021.

UNIVERSITEIT VAN PRETORIA
UNIVERSITY OF PRETORIA
YUNIBESITHI YA PRETORIA

electrostatic potential surrounding the subunit of the molecule. In (c): red = electron deficient, green = neutral, blue = electron rich and in (d): red = electron deficient, blue = neutral and yellow = electron rich. The location of the two electronegative fluorine atoms can clearly be seen in (c) blue and (d) yellow. The overall picture that emerges is one of the existence of a strong electrostatic gradient perpendicularly across the long axis of the molecule.

6.3.4 Optical, thermal and electro-optical properties.

The optical properties of compound **38** have been discussed in section 3.2.2. The compound has two blue phases followed by a cholesteric phase of which the pitch length is short and varies from approximately 500 nm to 600 nm just above the Ch - SmC* transition. The blue phases are visible on both the heating and cooling traces of the DSC thermogram as shoulders of the larger BP - Iso transition peak. The enthalpy change involving the Ch - SmC* transition (fig. 6.11) is evidential of a first order transition. The optical tilt angle, measured as a function of temperature, is plotted in fig. 3.21. As is to be expected from a compound with a first-order Ch - SmC* transition, the tilt angle of **38** is fairly large (20°) at the transition. However, it then decreases gradually with temperature. This behaviour is unusual and is contrary to what has been observed to date.

Compound **54** differs structurally from compound **38** in that it has a 2',3-difluorobiphenyl unit (fig. 6.1) which tends to favour an orthogonal arrangement of the molecules (see discussion in section 3.2.3) - it has a wide SmA phase followed by a short range SmC* phase. Optically the SmA - SmC* transition is difficult to pinpoint as both phases appear black due to a homeotropic arrangement of the molecules. The SmC* phase is nevertheless characterised by small areas of broken focal conic fans. This suggests that the SmA - SmC* transition is second-order and this is confirmed by the DSC thermogram which has no measurable evidence of a transition at 106.5°C (fig. 6.12). The behaviour of the optical tilt angle as a function of temperature of compound **54** is shown in fig. 3.20(b). It is typical for a compound with a second order SmA - SmC* transition (typically such compounds have a small value at the transition which then increases gradually with decreasing temperature) and in addition it exhibits electroclinic behaviour: the tilt angle increases gradually to 8° at the phase transition and then to 14° prior to crystallization.

Digitised by the Department of Library Services in support of open access to information, University of Pretoria, 2021.

UNIVERSITEIT VAN PRETORIA
UNIVERSITY OF PRETORIA
YUNIBESITHI YA PRETORIA

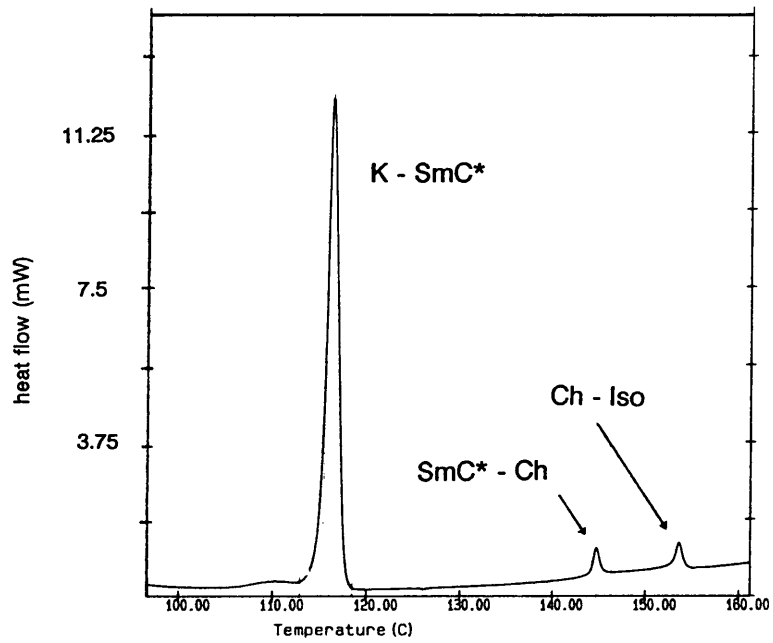

Figure 6.11 DSC thermogram of compound **38**.

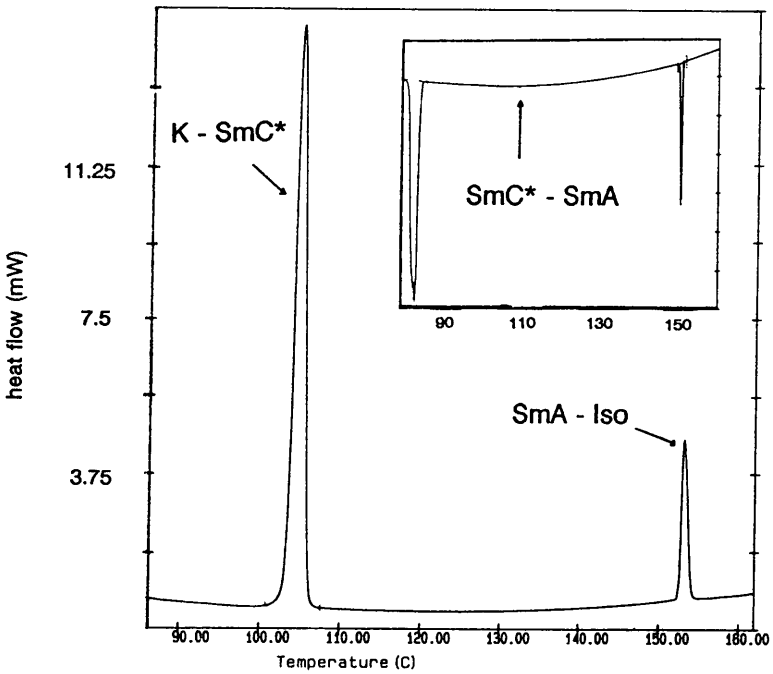

Figure 6.12 DSC thermogram of compound **54**.

Digitised by the Department of Library Services in support of open access to information, University of Pretoria, 2021.

UNIVERSITEIT VAN PRETORIA
UNIVERSITY OF PRETORIA
YUNIBESITHI YA PRETORIA

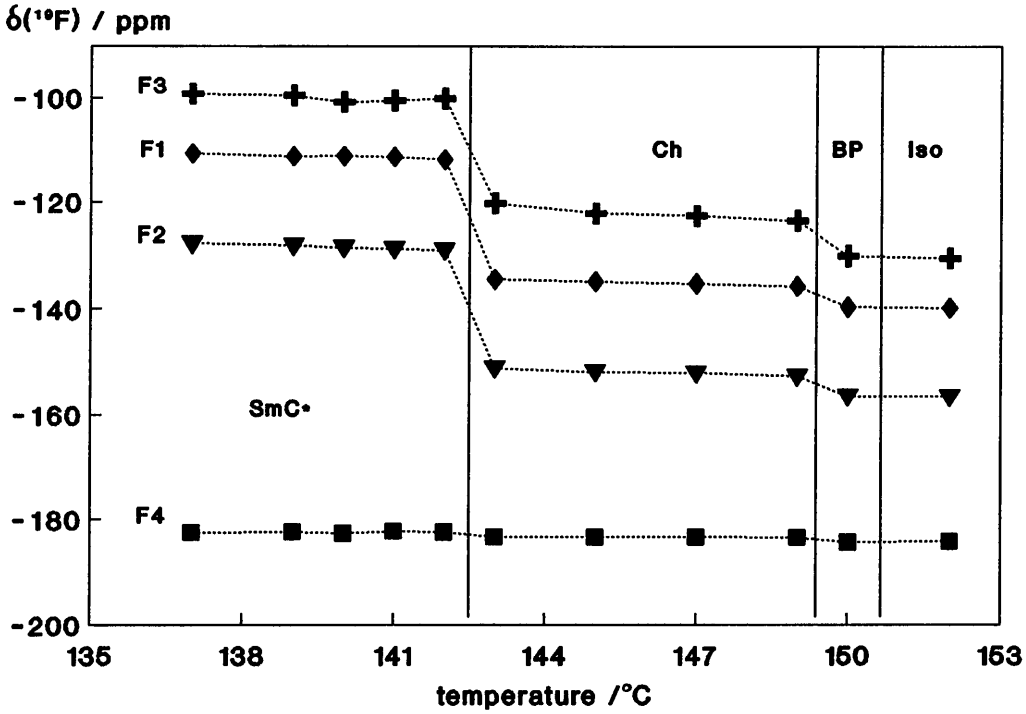

Figure 6.13 ^{19}F nmr chemical shifts of **38** plotted as a function of temperature.

6.4 Discussion

6.4.1 ^{19}F nmr chemical shift and DSC: a comparison

In figures 6.13 and 6.14 respectively the ^{19}F chemical shift of each of the four fluoro-substituents of **38** and **54** is plotted as a function of temperature. The SmC* - Ch and Ch - BP transitions of **38** which are classified as first-order as a result of the change of enthalpy involved (DSC), are characterised by a large change in chemical shift of the core fluorines, F_1, F_2 and F_3 (fig. 6.13). The first-order nature of the Iso - SmA transition of **54** is reflected similarly. In contrast to this, the SmC* - SmA transition is not accompanied by any change in chemical shift. The chemical shift of the fluorine on the chiral centre, F_4, is temperature-independent.

These results are similar to those found for the other compounds (chapters 5 and 7) and demonstrate that ^{19}F nmr can provide useful information concerning the nature of the transition.

Digitised by the Department of Library Services in support of open access to information, University of Pretoria, 2021.

UNIVERSITEIT VAN PRETORIA
UNIVERSITY OF PRETORIA
YUNIBESITHI YA PRETORIA

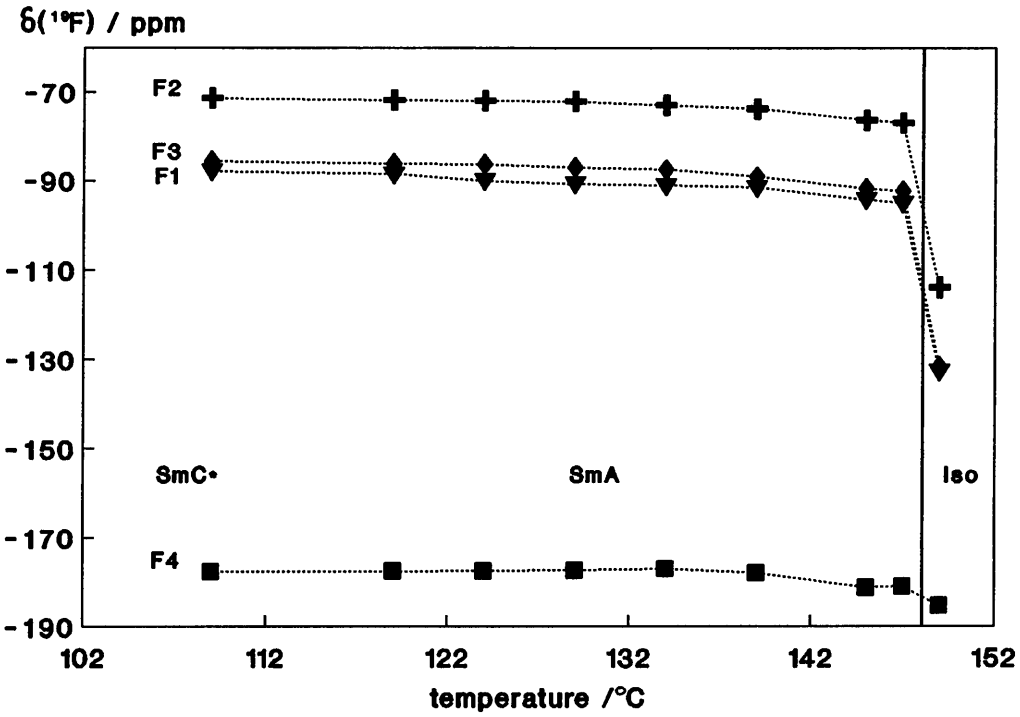

Figure 6.14 ^{19}F nmr chemical shifts of **54** plotted as a function of temperature.

6.4.2 Orientational order

The nmr spectral resolution obtained for **38** and **54** is due to unwound helices in both the Ch and SmC* phases in the presence of the magnetic field. Although it was initially believed that the helical structure of the SmC* phase is preserved[23,24], it was since found that a magnetic field of 7.05 T is sufficient to prevent the formation of the helix[26,27] as is found for compound **55** (section 5.4.1) as well as those discussed in this chapter.

Direct coupling between F_1 and F_2 of the 2,3-difluorophenyl unit of **38** provides useful information concerning the orientational order. In the SmC* phase the direct coupling reaches a maximum of 3260 Hz at the Ch - SmC* transition below which it decreases, initially fast but then levelling off at around 3000 Hz (fig. 6.4). Consequently similar behaviour is shown by the order parameter of the core, S_{FF}, (the F_1 - F_2 vector is parallel to the 1,4 axes of the biphenyl group) which, interestingly, is quite low for a SmC* phase - it does not exceed 0.552. Furthermore, in contrast to work done by other groups on compounds with a SmC* phase[27,118], here the order parameter of the core decreases with temperature. This result also contrasts that found for compound **55** (section 5.4.4 and fig. 5.4). In the case of **55** the increase in S_{FF} can be accounted for by considering the molecular directors

Digitised by the Department of Library Services in support of open access to information, University of Pretoria, 2021.

UNIVERSITEIT VAN PRETORIA
UNIVERSITY OF PRETORIA
YUNIBESITHI YA PRETORIA

aligned with the magnetic field and the smectic layers tilted as shown in fig. 5.6. This conclusion is based on the assumption that the compound exhibits "normal" tilt angle behaviour, i.e. that the tilt angle increases with decreasing temperature. The tilt angle (θ) of **38** does not change with temperature in the "normal" way as can be seen in fig. 3.21. Therefore the orientation of the molecules cannot be explained in terms of the diagram in fig. 6.15 which although it does account for a decrease in S_{FF}, does not account for a simultaneous decrease in θ.

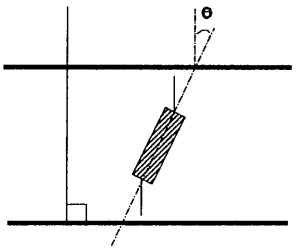

Figure 6.15

Based on the available evidence a likely explanation that would account for the observed behaviour of the order parameter in the SmC* phase is presented in fig.6.16. Immediately below the Ch - SmC* transition a tilting of the smectic layer planes occurs as in fig 6.16 (a). The molecules are tilted in the layers with a tilt angle θ_1 with respect to the layer normal (support for this is obtained by simply substituting the value of D_{F1F2} = 3260 Hz into equation 5.5, which gives θ = 33° which means that the core is tilted at an angle of 33° with respect to the direction of the magnetic field). As the temperature decreases, the layer planes tilt even further with respect to the magnetic field, B_0, but the molecules do not tilt over at the same rate. This would have a decrease in tilt,θ_2, of the molecules as result ($\theta_2 < \theta_1$ as in fig. 6.16(b)).

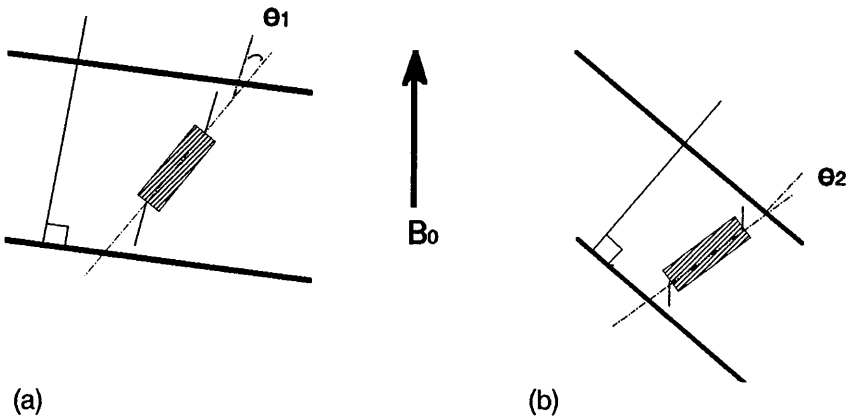

Figure 6.16 Orientation of **38** in the magnetic field.

Digitised by the Department of Library Services in support of open access to information, University of Pretoria, 2021.

UNIVERSITEIT VAN PRETORIA
UNIVERSITY OF PRETORIA
YUNIBESITHI YA PRETORIA

At the same time it would account for a decrease in the order parameter due to the molecular directors now being less aligned with the magnetic field. The latter would also explain why the well-resolved spectra in the upper region of the SmC* phase give way to broader unresolved peaks.

In the case of compound **54**, D_{F1F2} does not change significantly throughout the SmA phase. This, together with the fact that the spectra remain well-resolved throughout the phase, suggests that in this case the molecular directors and consequently the smectic layer normals are aligned with the magnetic field. At the SmA - SmC* transition (and even before as there is an electroclinic effect) there is no significant change in linewidth of the peaks or in the spectral resolution. This very gradual change reflects the second order nature of the transition. The fact that the peaks remain well-resolved in the SmC* phase is an indication that the molecular directors are on average still aligned with the magnetic field and this means that the smectic layer planes are tilting, but only very gradually.

6.4.3 Tilt angle

The reason for the unusual behaviour of the tilt angle in the ferroelectric phase of compound **38** is not obvious. Although the tilt angle of compound **35** shows a similar tendency, this compound and **38** stand in complete contrast to what is observed for **54** (section 6.3.4). Keeping in mind that even though **35** is an ester and **38** an ether, the core structures of these two compounds are similar (both contain the 2,3-difluorophenyl unit together with a 3-fluorophenyl unit), whereas the core of **54** differs in that it contains the 2',3-difluorobiphenyl unit. In view of the fact that the 2,3-difluorophenyl unit has its two lateral substituents fixed to the same side of the molecule at any given time, it is possible that these two compounds possess an unusually high negative dielectric anisotropy (i.e. $\epsilon_{\perp} >> \epsilon_{\parallel}$ relative to the long molecular axis). It would also explain the fact that for compound **38**, the molecular directors seem to tilt away from and for **54** are aligned with the magnetic field. A dielectric anisotropy of this nature could, together with the overall shape of the core (i.e. the positions of lateral substituents), result in strong core-core interactions which would be associated with the observed low tilt behaviour (as is suggested in chapter 4).

6.4.4 Coupling between the core and the chiral centre.

An interpretation of the observed coupling between F_3 (on the core) and F_4 (at the chiral centre) in both **38** and **54** is complicated by the fact that the two nuclei are not conformationally fixed with respect to one another. The two are separated by six bonds, three of which are independently rotatable. Here it is necessary to rely on the concept of average molecular conformation[119] and to keep in mind that overall rotation of the molecule must be coupled to individual rotation of cores and chains in order to retain the overall average conformation[22,120]. As the average orientation of the cores

Digitised by the Department of Library Services in support of open access to information, University of Pretoria, 2021.

UNIVERSITEIT VAN PRETORIA
UNIVERSITY OF PRETORIA
YUNIBESITHI YA PRETORIA

of the molecules is known from observing D_{F1F2}, some conclusions can be drawn. In the SmC* phase of **38**, D_{F3F4} increases with decreasing temperature as opposed to D_{F1F2}. Although impossible to quantify, this suggests that for compound **38** the chains are less tilted than the cores as this would result in an increasing order parameter along a F_3 - F_4 vector. For compound **54** D_{F3F4} is also found to increase with decreasing temperature (section 6.3.2). However, it is important to note that the magnitude of D_{FF} not only depends on the orientation of the F...F vector with respect to the direction of the magnetic field, but also on the F...F distance. A change in F_3...F_4 of 1Å would lead to a change of approximately 750 Hz in D_{FF}. The observed increase in D_{F3F4} for both **38** and **54** could therefore also be a consequence of a decrease in the average F_3...F_4 distance due to small conformational changes in the form of the rotation about bonds β or γ (see fig. 6.7). This could be indicative of a slowing down of the molecular motion at the chiral centre and is supported by the fact that the F_4 resonance broadens as the temperature decreases.

The direct interaction between F_3 (on the core) and F_4 (at the chiral centre) as observed with nmr spectroscopy is supported by the results of the conformational analysis. The lowest energy conformation of the molecular subunit containing the chiral centre, shows a definite overlap of the electrostatic potentials of the two fluoro-substituents, which serves to create a transverse electrostatic gradient across that part of the molecule.

6.5 Summary and conclusion

Two liquid crystals, both with a ferroelectric smectic C* phase, were synthesised. By placing a fluoro-substituent on the aromatic core, in the *ortho* position with respect to the chiral chain, it was possible to observe its interaction with a fluoro-substituent placed on the chiral centre. This was done by employing an nmr technique developed for this work, which involves observing ^{19}F - ^{19}F dipolar interaction. Conformational analysis of the molecular subunit containing the chiral centre confirmed that a fluorine - fluorine interaction would indeed exist if the preferred conformation in the smectic C* phase coincides with the lowest energy conformation calculated. This is the first time that it could be shown by way of experiment that a dipole - dipole ("through space") interaction of this kind does occur.

^{19}F nmr additionally provided information concerning the orientation of the molecules in the smectic C* phase of both the compounds. The suggested orientation of the molecular cores appears to be in agreement with the information obtained from optical tilt angle measurements, which revealed an unusual behaviour for one of the compounds in its ferroelectric phase.

---- # ----

Digitised by the Department of Library Services in support of open access to information, University of Pretoria, 2021.

CHAPTER 7

PROPERTIES OF LIQUID CRYSTALS CONTAINING THE 2',3 - DIFLUOROBIPHENYL UNIT

7.1 Introduction

A comparison of various laterally fluorinated liquid crystals in chapter 3 of this dissertation showed that compounds containing a 2',3-difluorobiphenyl group (fig.7.1) tend to have a wide smectic A phase. Furthermore, this group is found to discourage or even prevent the formation of helical structures, particularly the smectic C* phase, as it seems to favour an orthogonal arrangement of the molecules. The properties conferred by the two monofluorinated phenyl rings linked together as shown below appear to markedly contrast the properties resulting from only one of the biphenyl rings being monofluorinated, such as in compounds **49** and **52**. The latter compound (where F_2 in **53** is replaced by H) is highly chiral and apart from a wide smectic C* phase and a cholesteric phase, it exhibits a chiral smectic A (or TGB_{A^*}) and blue phase.

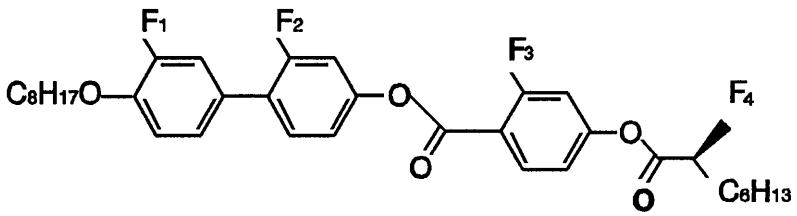

50: K 73°C SmC* 97.2°C SmA 133.9°C Ch 137.7°C Iso

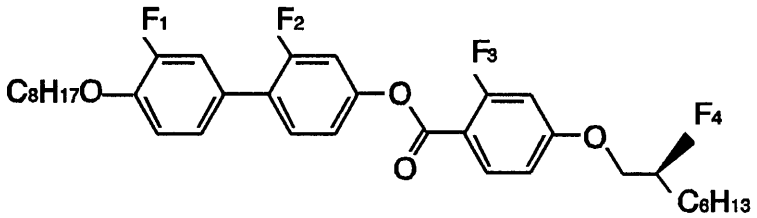

53: K 38°C SmA 140.5°C Ch 144.2°C Iso

Figure 7.1 Structure, phases and phase transition temperatures of compounds **50** and **53**.

Digitised by the Department of Library Services in support of open access to information, University of Pretoria, 2021.

UNIVERSITEIT VAN PRETORIA
UNIVERSITY OF PRETORIA
YUNIBESITHI YA PRETORIA

Likely causes for these observations, as suggested in chapter 3, are

(i) the additional substituent F_2 could result in variations in the inter-ring dihedral angle, due to its location at one of the inner positions of the biphenyl group;

(ii) the respective locations of F_1 and F_2, which need not be on the same side of the molecule, could result in a wider molecule and subsequently a less dense molecular packing as suggested by Osman[121].

These observations prompted a more extensive investigation. In this chapter the results of a study of two liquid crystals containing the 2',3-difluorobiphenyl group are presented. This includes ^{19}F nmr as well as optical, thermal and electro-optical measurements. An attempt is also made to explain the unusual ferroelectric behaviour displayed by compound **50** in terms of structural features. These two compounds are compared with the structurally related compound **54** (chapter 6).

The 2',3-difluorobiphenyl unit has not found common use in the synthesis of liquid crystals, but the properties conferred by some related fluorinated substructures are discussed.

7.2 Experimental

The syntheses of compounds **50** and **53** are described in section 2.2.

Optical microscopy studies, thermal analysis and electro-optical measurements were conducted as described in sections 3.2.1, 3.3.1 and 3.4.1 respectively.

^{19}F nuclear magnetic resonance spectra were acquired of the compounds in their isotropic state and in their various liquid crystalline phases using the technique described in section 5.3.1. Dipolar coupling constants were verified (or in some cases estimated) using the commercial PANIC-software supplied by Bruker.

7.3 Results

7.3.1 Optical, thermal and electro-optical measurements

The liquid crystalline phases and phase transition temperatures of compounds **50** and **53** are given in fig. 7.1 together with their structures. Enthalpy changes of the phase transitions are listed in table 3.2. Both compounds have three lateral fluoro-substituents attached to the core and this includes the 2',3-difluorobiphenyl group. Therefore the only structural difference between them concerns the group

Digitised by the Department of Library Services in support of open access to information, University of Pretoria, 2021.

UNIVERSITEIT VAN PRETORIA
UNIVERSITY OF PRETORIA
YUNIBESITHI YA PRETORIA

linking the core with the chiral centre: **50** has an ester link, while **53** has an ether link. Both of the compounds have a cholesteric phase that is readily characterised by its Grandjean planar texture. In the case of compound **53** this is followed by an extremely wide smectic A phase (Δ_{SmA} = 102.5°C) which exhibits the typical focal conic fan texture. Compound **50** has, in addition to a smectic A phase that appears black due to a homeotropic arrangement of the molecules, a smectic C* phase. The phase is chiral (a helical structure exists) and initially, just below the SmA - SmC* transition, the helical axes are orientated perpendicularly to the smectic layers. This results in a "pseudohomeotropic" situation which has a black appearance. A *schlieren* texture gradually appears and brightens as the temperature is lowered. The textural changes observed throughout the smectic C* phase of **50** are shown in the series of photographs in fig. 3.8 in chapter 3 and are described in the accompanying text. It was concluded that the observed changes coincide with a change in the direction of the helix. The helix (left-handed in the upper temperature region) unwinds with decreasing temperature and at a certain temperature the pitch of the helix becomes infinite, similar to what was found to occur in the cholesteric phase of compound **35** (chapter 4). Further cooling causes the helix to wind up again, but in the opposite direction (right-handed), as was confirmed by rotation of the polars of the microscope. At the point in temperature at which the helix is unwound a fluid blueish-yellow texture, partly *schlieren* with black areas dispersed therein, is observed. As would be expected, the continuity and gradualness with which the unwinding and rewinding of the helix occurs does not take place with a measurable change in enthalpy. The DSC thermogram of compound **50** is shown in fig. 7.2 and the point of inversion is marked with an arrow. The SmC* - SmA transition is second-order, but the SmA - Ch transition is only weakly first-order (see section 3.3.3).

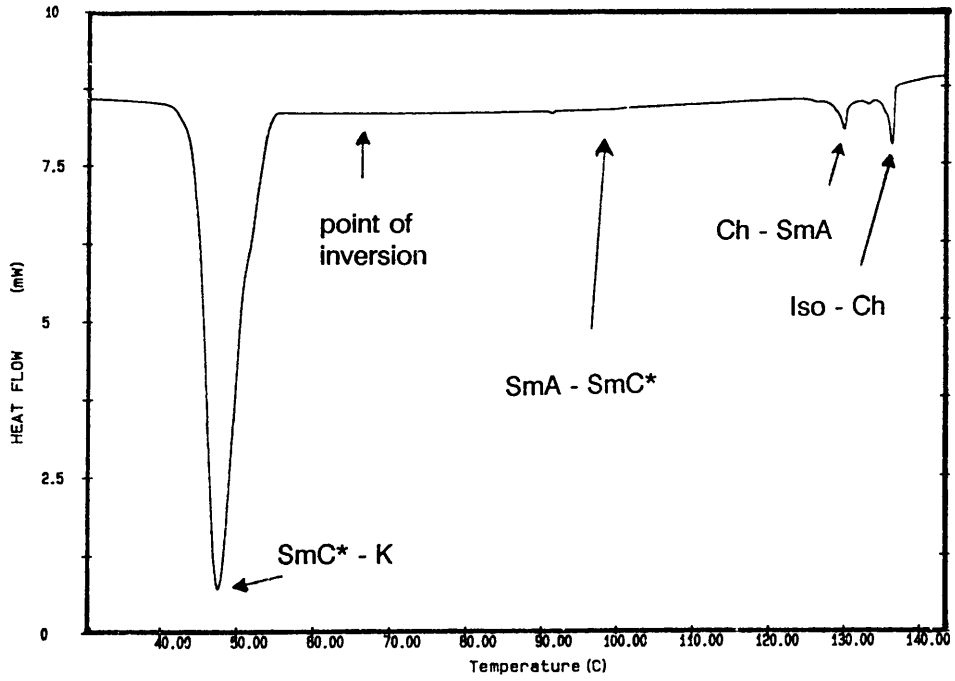

Figure 7.2 DSC thermogram of compound **50**. Shown is the cooling cycle (-10°C.min^{-1}).

Digitised by the Department of Library Services in support of open access to information, University of Pretoria, 2021.

UNIVERSITEIT VAN PRETORIA
UNIVERSITY OF PRETORIA
YUNIBESITHI YA PRETORIA

Electro-optic measurements in the ferroelectric smectic C* phase of compound **50** were hampered by the extremely poor alignment characteristics of this compound. Nevertheless, the optical tilt angle was measured as a function of temperature in the upper region of the phase and is shown graphically in fig. 7.3 (the wide distribution of points is due to the poor alignment). The tilt angle is very small and increases from approximately 1° to just over 5° at 60°C, below which temperature no switching appears to occur. Therefore, it would appear that switching does not occur below the temperature at which the helix inverts. The small tilt angle is an indication that the pitch of the helix is long.

Owing to the poor alignment of the molecules, no attempt was made to measure the spontaneous polarisation.

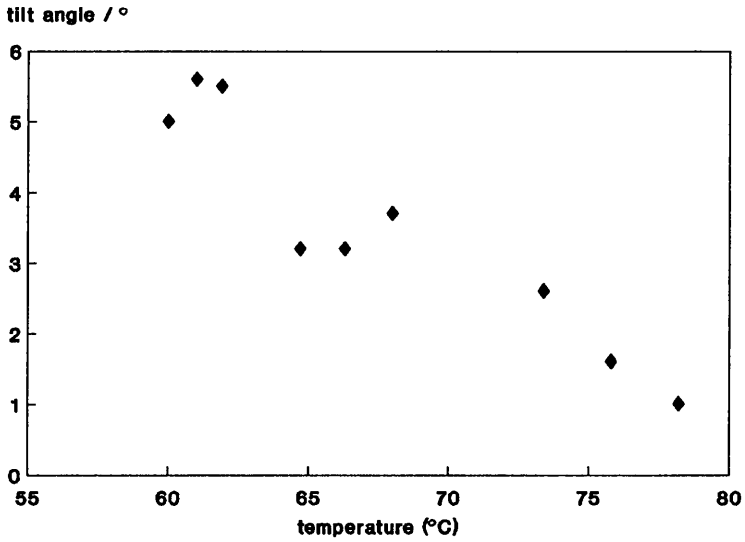

Figure 7.3 The tilt angle of **50** plotted as a function of temperature (applied voltage 16V).

7.3.2 ^{19}F nmr: chemical shift

Selected proton-decoupled ^{19}F nmr spectra of the isotropic liquid and the various liquid crystalline phases of compounds **50** and **53** are shown in figures 7.4 and 7.5. Graphic representations of the chemical shift as a function of temperature are given in figures 7.6 and 7.7 respectively.

Digitised by the Department of Library Services in support of open access to information, University of Pretoria, 2021.

UNIVERSITEIT VAN PRETORIA
UNIVERSITY OF PRETORIA
YUNIBESITHI YA PRETORIA

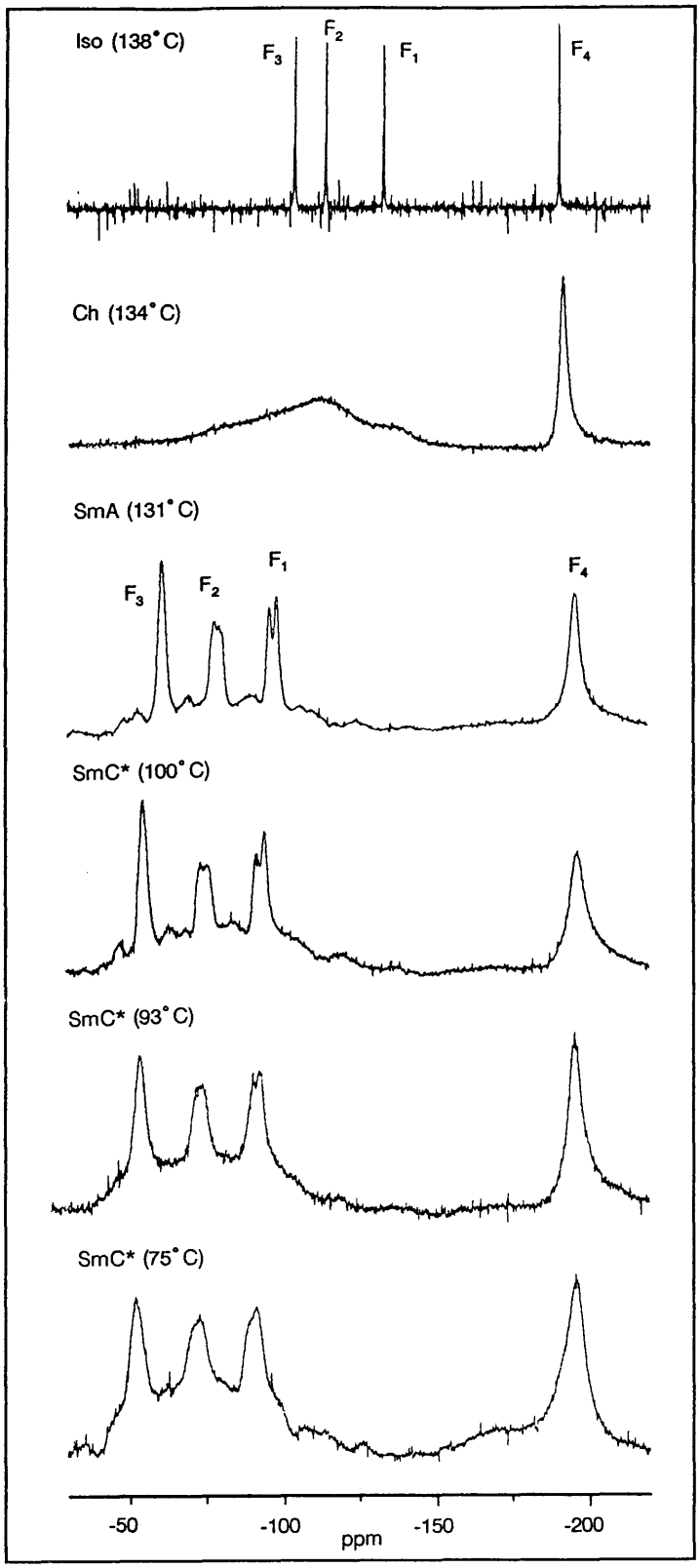

Figure 7.4 Proton-decoupled ^{19}F nmr spectra of the isotropic liquid at 138 °C and of the various liquid crystalline phases of compound **50** at the temperatures indicated.

Digitised by the Department of Library Services in support of open access to information, University of Pretoria, 2021.

UNIVERSITEIT VAN PRETORIA
UNIVERSITY OF PRETORIA
YUNIBESITHI YA PRETORIA

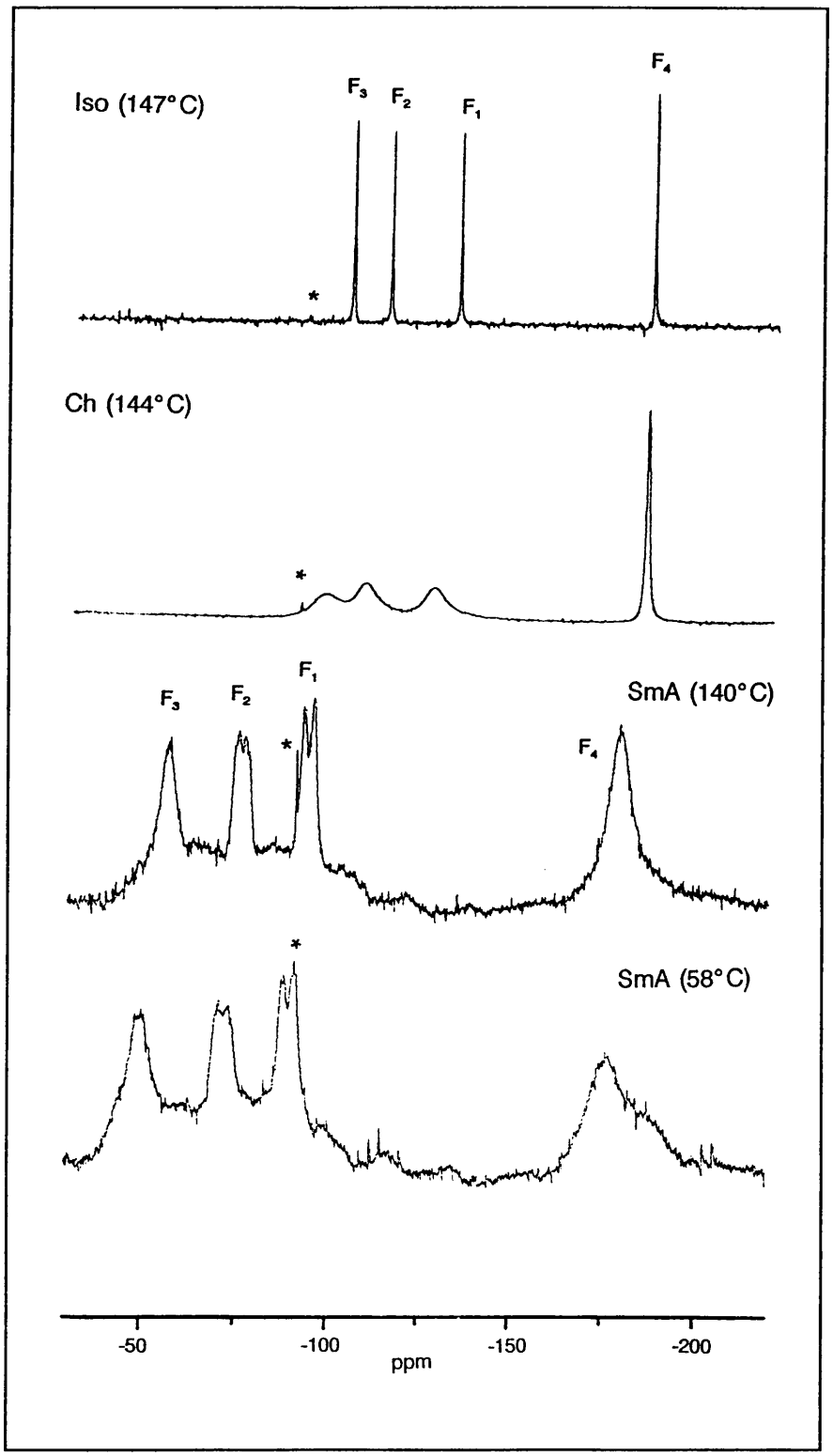

Figure 7.5 Proton-decoupled ^{19}F nmr spectra of the isotropic liquid at 147 °C and of the various liquid crystalline phases of compound **53** at the temperatures indicated.

Digitised by the Department of Library Services in support of open access to information, University of Pretoria, 2021.

UNIVERSITEIT VAN PRETORIA
UNIVERSITY OF PRETORIA
YUNIBESITHI YA PRETORIA

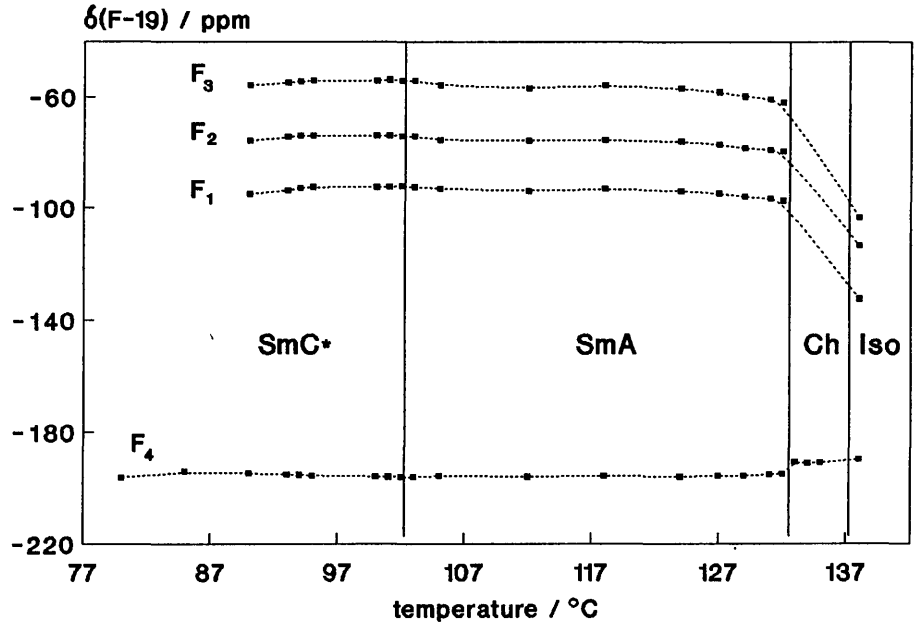

Figure 7.6 ^{19}F nmr chemical shift of compound **50** shown graphically as a function of temperature.

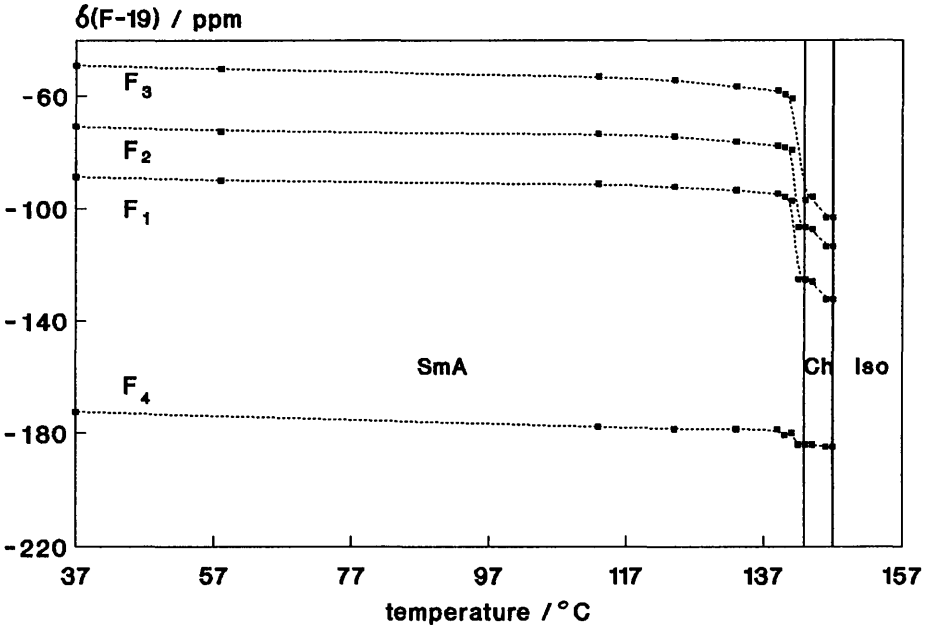

Figure 7.7 ^{19}F nmr chemical shift of compound **53** plotted as a function of temperature.

Digitised by the Department of Library Services in support of open access to information, University of Pretoria, 2021.

UNIVERSITEIT VAN PRETORIA
UNIVERSITY OF PRETORIA
YUNIBESITHI YA PRETORIA

In the isotropic state the chemical shifts of the aromatic fluorines (F_1, F_2 and F_3) of the two compounds are very similar[$]. The fluorine on the chiral centre of compound **50**, F_4, is shifted upfield by approximately 4 ppm with respect to F_4 of **53** due to the presence of the carbonyl group in the former.

The cholesteric phase of **50** and **53** is characterised by broad, featureless peaks in the aromatic region, while the peak of the fluorine on the chiral centre remains relatively sharp. With reference to the isotropic liquid, the aromatic fluorines of **53** undergo a slight downfield shift in the cholesteric phase, but are severely broadened. Once again the peak of the fluorine on the chiral centre remains sharp relative to those of the others.

The Ch - SmA transition is marked by a jump in the chemical shift of the aromatic fluorines of both of the compounds. In fact, the respective aromatic regions of the spectra of both **50** and **53** recorded at 1°C below their Ch - SmA transitions are remarkably similar in appearance (i.e. with respect to linewidth and chemical shift). The aromatic fluorines of **50** occur at slightly higher chemical shifts compared to those of **53**, with F_3 shifted most. This could indicate that intermolecular effects are more prominent in the case of compound **50**. The spectrum of **53** does not change much throughout the smectic A phase as is obvious when comparing the spectrum recorded at 58°C with the one recorded at 140°C. However, the linewidth of the fluorine on the chiral centre increases considerably with decreasing temperature. This is similar to what is observed for the smectic A phase of **50** for which such segmental motional behaviour is also found.

The SmA - SmC* transition does not coincide with any significant change in the appearance of the spectrum. As is the case for compound **38** (chapter 6) it is not possible to determine the temperature at which the phase transition occurs by observing the nmr spectra. This is indicative of a very gradual change in the molecular order and orientation as could be expected from a second-order event. In contrast to what is observed in the lower temperature region of the smectic A phase of **53**, the spectral resolution becomes worse as the temperature is lowered in the smectic C* phase of **50** and the peaks become broad. These features serve to distinguish the smectic C* phase of **50** (at 75°C for example) from the smectic A phase of **53** at the same temperature. They show that the observed spectral changes are not merely brought about by changes due to a decrease in molecular movement at lower temperatures, but by the existence of a different phase. At the same time it should be kept in mind that intermolecular effects seem to play a greater role in the case of **50**.

[$]For the assignment of ^{19}F chemical shifts see appendix A.

Digitised by the Department of Library Services in support of open access to information, University of Pretoria, 2021.

UNIVERSITEIT VAN PRETORIA
UNIVERSITY OF PRETORIA
YUNIBESITHI YA PRETORIA

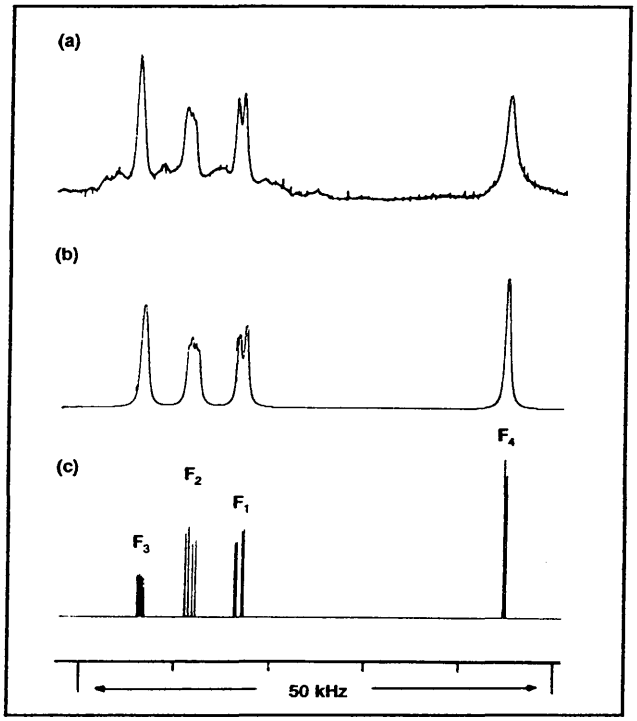

Figure 7.8 Proton-decoupled ^{19}F nmr spectra of **50**: (a) experimental spectrum at 131°C (SmA phase); (b) simulated spectrum plotted with a linewidth of 500 Hz; (c) components of the spectrum.

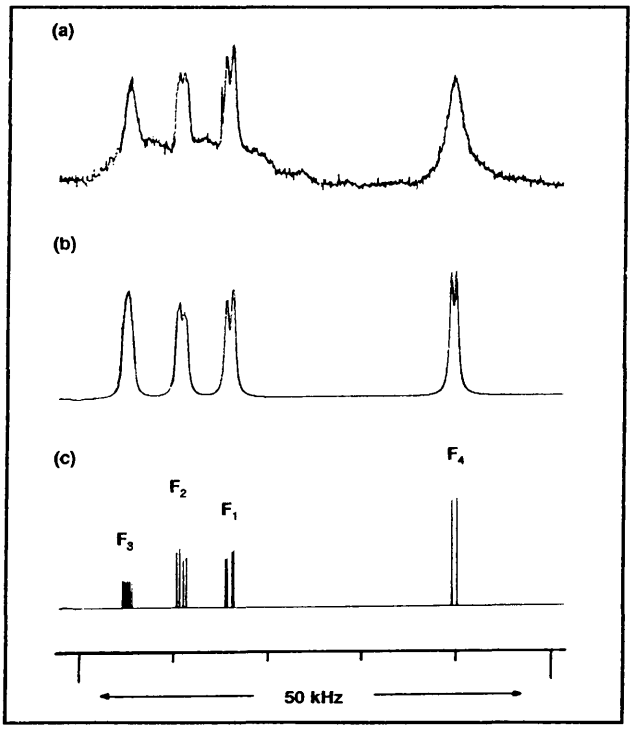

Figure 7.9 Proton-decoupled ^{19}F nmr spectra of 53: (a) experimental spectrum at 141°C (SmA phase); (b) simulated spectrum plotted with a linewidth of 500 Hz; (c) components of the spectrum.

Digitised by the Department of Library Services in support of open access to information, University of Pretoria, 2021.

UNIVERSITEIT VAN PRETORIA
UNIVERSITY OF PRETORIA
YUNIBESITHI YA PRETORIA

Attempts to record spectra below 75°C for compound **50** were abandoned due to the long acquisition times (at least 8h) that would have been necessary in order to obtain satisfactory spectra.

The resolution of the spectra of the smectic A phase of both **50** and **53** suggests that the molecular directors are aligned with the magnetic field.

7.3.3 ^{19}F - ^{19}F dipolar coupling

In the smectic A phase of compound **53** and in both the smectic A and C* phases of compound **50** the spectral resolution permits the extraction of the larger coupling constants (see figures 7.4 and 7.5). Smaller coupling constants were estimated by computational adjustment of the peak shapes.

For compound **50** the F_1 resonance appears as a doublet due to its direct coupling with F_2. The dipolar coupling constant is 365 Hz and seems to be temperature-independent. F_2 is observed as a doublet of doublets, albeit broad, but with the aid of spectral simulation it could be established that the smaller of the two coupling constants involved has a value of 170 Hz (D_{F2F3}).

Table 7.1 ^{19}F - ^{19}F dipolar coupling constants for compounds **50** and **53**.

D_{FF}	Dipolar coupling constant D_{FF} / Hz[a]	
	50	**53**
F_1F_2	365	350
F_1F_3	90[d]	70[d]
F_1F_4	-[b]	-[b]
F_2F_3	170	150
F_2F_4	-[b]	-[b]
F_3F_4	110[d]	270[c]

a. The error is estimated to be 10%.
b. Too small to obtain.
c. See text.
c and d. Values were not obtained directly from the spectrum, but were estimated with the aid of spectral simulation.

Digitised by the Department of Library Services in support of open access to information, University of Pretoria, 2021.

UNIVERSITEIT VAN PRETORIA
UNIVERSITY OF PRETORIA
YUNIBESITHI YA PRETORIA

The components of the spectrum are shown in fig. 7.8 (c). In fig. 7.8 (b) the simulated spectrum, adjusted for linewidth, is shown. The direct coupling constants of compound **50** are given in table 7.1 together with those of compound **53**. The magnitude of the direct coupling D_{F3F4} between F_3 on the core and F_4 on the chiral centre cannot be obtained directly from the spectrum, but is estimated to be 110 Hz. The dipolar coupling constants of compound **53** are of a comparable magnitude to those of **50** with the exception of D_{F3F4}. This difference can be ascribed to a difference in the average $F_3...F_4$ distance of the two compounds. That is, the larger value measured for **53** implies that the average $F_3...F_4$ distance for this compound is shorter than it is for **50**. However, not only would this distance differ as a result of structural differences between the two compounds, but a larger dipolar coupling could also signify a decreased average distance due to a slowing down of rotational movement. Such an effect would be temperature-dependent - unfortunately the coupling constant is too small to determine whether this is true.

Order parameters were not calculated for either of these two compounds. All four of the fluorine nuclei are rotationally independent which would necessitate the use of a combination of order parameters in order to describe the vector between the two nuclei[122].

7.3.4 The interannular dihedral angle

In order to determine the influence of a single fluoro-substituent located at one of the "inner" positions of a biphenyl group (such as in **50** or **53**) on the dihedral angle, a crystal structure determination was carried out. Numerous attempts to obtain suitable single crystals of either **50** or **53** were unsuccessful, so it was decided to modify one of the liquid crystals by way of attachment of a group that would increase its ability to crystallise. This led to the preparation of the compound 2,3-difluoro-4-octyloxy-biphenyl-4'-(4-ferrocenyl)benzoate, **56**, and the determination of its X-ray crystal structure (fig. 7.10 - synthetic details of this compound are provided in section 2.2 and particulars of the determination of its structure appear elsewhere[114]).

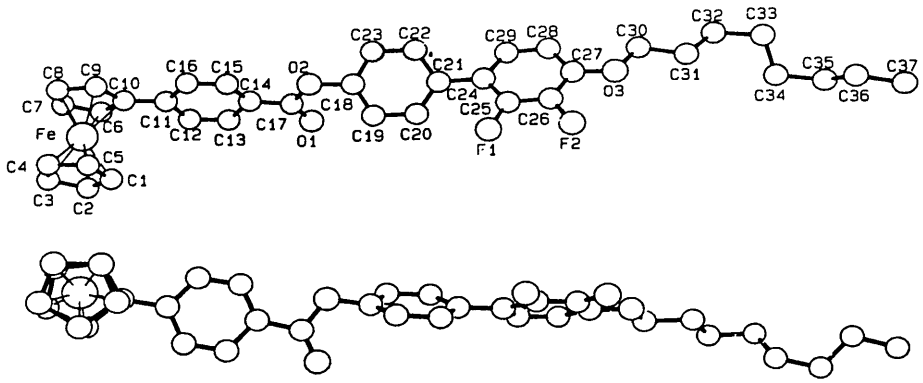

Figure 7.10 Two perspective views of **56** prepared with ORTEP[134].

Digitised by the Department of Library Services in support of open access to information, University of Pretoria, 2021.

UNIVERSITEIT VAN PRETORIA
UNIVERSITY OF PRETORIA
YUNIBESITHI YA PRETORIA

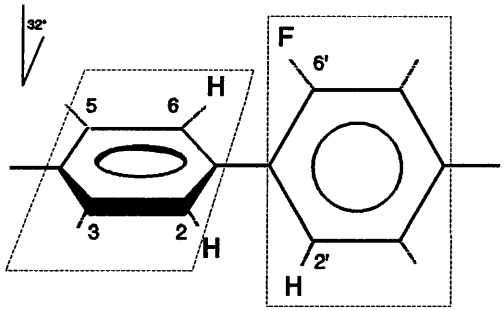

Figure 7.11

It was found that, in the crystal, the unsubstituted ring of the biphenyl unit is tilted by 32° relative to the fluorinated ring (shown schematically in fig. 7.11).

7.4 Discussion

7.4.1 The biphenyl unit

The minimum number of directly interacting nuclei required for the calculation of the complete structural geometry of part of a molecule is four. As the study of the biphenyl unit of compounds containing the 2',3-difluorobiphenyl group involves observing the interaction between only two nuclei, a detailed structural analysis is not possible.

The conformation of biphenyl has been unambigously determined to be planar in the solid state by means of X-ray diffraction[123]. More recently d'Annibale *et al* showed that biphenyl unsubstituted on the four inner positions is twisted with an angle of 34°[124]. This was achieved by measuring the dipolar couplings (D_{HH}) obtained when dissolving the biphenyl in a nematic solvent. For the 2',3-difluorinated biphenyls, such as in compounds **50**, **53** and also **54** (chapter 6), the lateral substituents can be located either on the "same" side of the molecule (as in fig. 7.12(a)) or on "opposite" sides of the molecule as in fig. 7.12(b). For both cases (a) and (b) the dihedral angle can be expected to be the same as only a single fluoro-substituent is situated on one of the four inner positions. This is also true for situation (c) for which the dihedral angle was measured to be 32° in the solid state (section 7.3.4). Work done by Field and Sternhell[125] showed that the dihedral angle is influenced by the Van der Waals radii of the four substituents on the inner positions of biphenyl. Their analysis of 2,6-difluoro-4,4'-disubstituted biphenyls dissolved in a nematic solvent showed that even the small fluorine atom could cause a significant increase in the dihedral angle. However, the large difference

Digitised by the Department of Library Services in support of open access to information, University of Pretoria, 2021.

UNIVERSITEIT VAN PRETORIA
UNIVERSITY OF PRETORIA
YUNIBESITHI YA PRETORIA

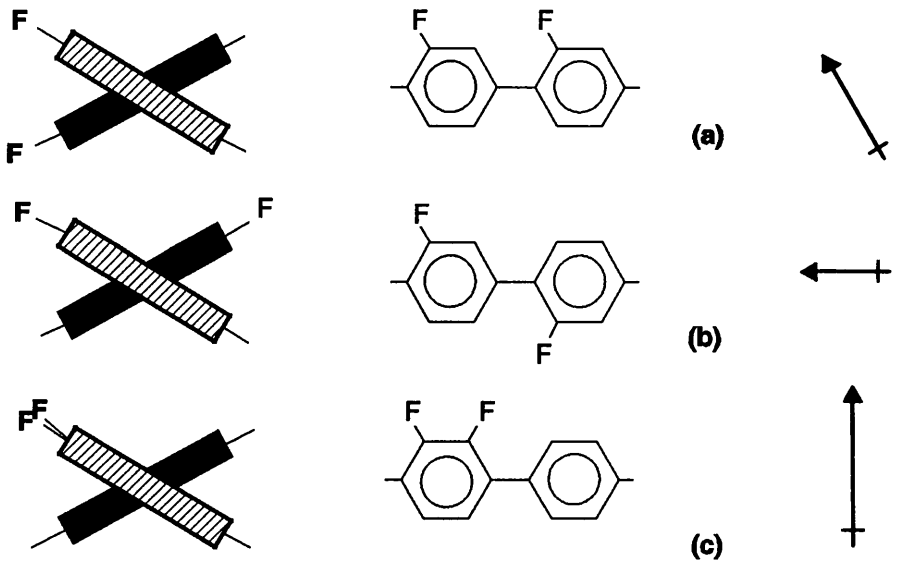

Figure 7.12 Possible different locations of the fluoro-substituents on the biphenyl group (centre), also showing the projection along the aryl-aryl bond (left) and the direction of the nett dipole (right).

between the value of 47.8° they measured for the difluorinated biphenyl and the value of 32° obtained in this work is unrealistic and cannot merely be explained in terms of one of them being in the solid state and the other in liquid crystalline solution. It must therefore be assumed that the presence of the second fluoro-substituent on one of the inner positions in their compounds leads to a further increase in the dihedral angle. For the purpose of the discussion given below, a dihedral angle of 32° in the liquid crystalline state was assumed.

Before the dipolar coupling measured between F_1 and F_2 in this work can be discussed, it is necessary to establish whether there is rotation about the aryl-aryl bond in the biphenyl group. D'Annibale *et al*[124] found this not to be the case - a result supported by those of Field and Sternhell[7] who found that not only can the possibility of free rotation be excluded, but a fixed dihedral angle is maintained independently of temperature. Subsequently it was shown by Celebre *et al*[135] that this dihedral angle does not change appreciably on changing phase or when changing from the solid to the liquid crystalline state. For all of compounds **50**, **53** and **54** the dipolar coupling D_{F1F2} (table 7.2) was found to be temperature-independent and this is also indicative of the absence of rotation about the aryl-aryl bond.

In the smectic A phase, although the molecules are aligned with their directors on average parallel with the direction of the magnetic field, the vector connecting F_1 with F_2 will form an angle with the

Digitised by the Department of Library Services in support of open access to information, University of Pretoria, 2021.

UNIVERSITEIT VAN PRETORIA
UNIVERSITY OF PRETORIA
YUNIBESITHI YA PRETORIA

field. The magnitude of D_{F1F2} will therefore depend not only on the distance $F_1...F_2$ but also on the the angle the vector forms with the magnetic field.

Table 7.2 A comparison of the ^{19}F - ^{19}F dipolar coupling constants in the smectic A phase.

Compound	D_{F1F2}
50	365
53	350
54	660

If F_1 and F_2 are located on the "same" side of the molecule (fig. 7.12 (a)) the distance between them would be 4.4Å (maximum possible D_{F1F2} = 1250 Hz); if not (fig. 7.12(b)) the distance would be 5.9Å[##] (maximum possible D_{F1F2} = 520 Hz). Substitution of these values into equation 5.6 gives the maximum theoretically attainable dipolar coupling constant for both of these cases (this would be the dipolar coupling measured had the F_1 - F_2 vector been aligned with the magnetic field - values are shown in parentheses above). In practice, however, these values are not attainable as the molecules would then have to be tilted in the smectic A phase. Nevertheless, for compound **54** D_{F1F2} = 660 Hz (table 7.2 and chapter 6), a value that clearly exceeds the maximum allowable value for a distance between the two nuclei of 5.9Å. This means that the possibility of the two fluoro-substituents occurring on "opposite" sides of the molecule can be ruled out. Unfortunately, for both **50** and **53** D_{F1F2} is much smaller than either of the theoretically attainable values, so no conclusions can be drawn. For these compounds it is therefore also possible that the two fluoro-substituents in question are located on "opposite" sides of the molecule, and by doing so disturbing the degree of order in the phase and leading to the measurement of a smaller dipolar coupling constant.

The situation described in the preceding paragraphs would also hold for the smectic C* phase of compounds **50** and **54**, except that the molecular directors would undergo a gradual tilt with a concommitant decrease in the observed dipolar coupling. Owing to poor spectral resolution these measurements are not available.

[##] $F_1...F_2$ distances were obtained from the X-ray crystal structure by substituting the appropriate hydrogen atoms with fluorine.

Digitised by the Department of Library Services in support of open access to information, University of Pretoria, 2021.

UNIVERSITEIT VAN PRETORIA
UNIVERSITY OF PRETORIA
YUNIBESITHI YA PRETORIA

7.4.2 The helical order in the smectic C phase.*

Compound **50** exhibits an inversion in the helical twist direction in its smectic C* phase. Although unusual, this phenomenon has been observed previously for other compounds. Their structures are shown in fig. 4.1 (compounds **C**[95] and **D**[96]) and the helix inversion is explained in terms of the dominance of a particular conformational structure over another at a given temperature. The fluorinated compounds prepared in this work have important structural differences from **C** and **D** and in chapter 4 the helix inversion in the cholesteric phase of compound **35** is explained in terms of different orientations of the polar groups (carbonyl and C - F) in the vicinity of the chiral centre at different temperatures. This also offers an explanation of why compounds with a related structure do not exhibit this phenomenon.

In chapter 3 a comparison of the mesomorphic properties of fluorinated liquid crystals revealed that compounds containing the 2',3-difluorobiphenyl unit (**50, 53** and **54**) seem to prefer an orthogonal arrangement of the molecules (i.e. they only exhibit small helical phases or no such phases at all). This is in agreement with the work of Vauchier *et al*[126]. They studied the effect of 2',6-difluoro substitution on chiral molecules and found that the wide smectic C* phase of the non-fluorinated molecules is completely suppressed and that the cholesteric phase becomes much destabilised upon 2',6-difluorination.

Although the helix inversion observed for compound **50** could possibly be explained in terms of the predominance of conformers involving the chiral centre at certain temperatures, this would not explain why compounds with a similar structural environment about their chiral centres (**36** and **49**) do not display this tendency. For **50**, the origin of the inversion could lie within the structure of the biphenyl unit. Two possible structures are shown in fig. 7.12 (a,b). It is clear that a different net dipole would exist across the biphenyl group for each of these two cases (indicated with the arrows). In addition to this, the effective size of each of these molecular subunits would differ (b >> a). Keeping in mind that the intermolecular repulsive or attractive forces (caused by the number and position of lateral substituents) can influence the packing density of the molecules[127], (a) and (b) could result in the formation of different types of mesophases. Taking this even further, it is possible that in the same phase one of the structures will predominate at a certain temperature. As the temperature changes, the other structure becomes the dominant one (possibly *via* "ring-flip"of one of the rings[128,129]) which will result in a change in the positions of the lateral fluoro-substituents. Consequently, a change in the nett dipole will occur. As the location and direction of the transverse dipole can affect the polarity and spontaneous polarization of a molecule[130], it is possible that these competing dipoles could be the driving force behind the observed helix inversion. However, it has been suggested[131] that it is the size and the overall shape of the core that contribute to the

Digitised by the Department of Library Services in support of open access to information, University of Pretoria, 2021.

UNIVERSITEIT VAN PRETORIA
UNIVERSITY OF PRETORIA
YUNIBESITHI YA PRETORIA

ferroelectric properties of a liquid crystal rather than the transverse dipole moment across the core, which is of lesser importance. Unfortunately, due to reasons mentioned before (section 7.3) it was not possible to obtain ^{19}F nmr spectra throughout the smectic C* phase of compound **50**. Measurement of the spontaneous polarisation in order to determine whether a change in the sign of Ps occurs was not possible due to the poor alignment characteristics of the compound.

7.4.3 Coupling between the core and the chiral centre.

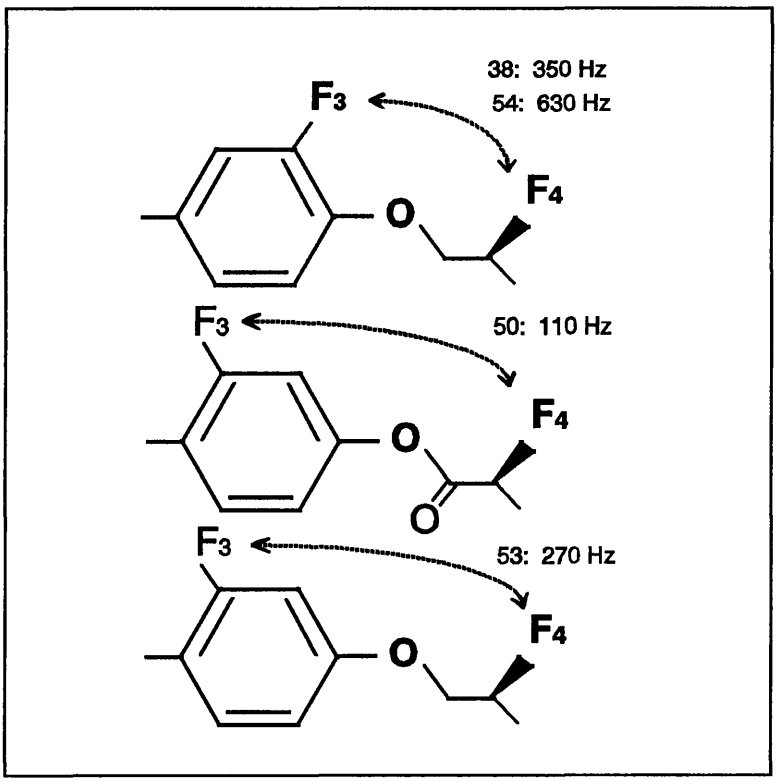

Figure 7.13 Dipolar interaction between the core and the chiral centre in terms of D_{F3F4} for **53** (SmA phase) and **38, 50** and **54** (SmC* phase, 1°C below the SmA - SmC* transition).

The observed (or simulated) interaction between F_3 (on the core) and F_4 (at the chiral centre) of compounds **50** and **53** (D_{F3F4}) is given in fig. 7.13 where it is compared with D_{F3F4} for compounds **38** and **54**. The magnitudes of these coupling constants clearly reflect the fact that the $F_3...F_4$ distance is larger in **50** and **53** and is an indication of the greater influence exerted by the lateral substituent in the position *ortho* to the chiral chain.

Digitised by the Department of Library Services in support of open access to information, University of Pretoria, 2021.

UNIVERSITEIT VAN PRETORIA
UNIVERSITY OF PRETORIA
YUNIBESITHI YA PRETORIA

The influence that dipole(s) on the core seem to have on dipole(s) at the chiral centre was first noticed by workers at the Chisso Corporation in Japan[132]. Their conclusions concerning this influence of the substituent *ortho* to the chiral chain (initially methyl but later extended to cyano and halides) are based on the fact that such a lateral group will sterically force the group at the chiral centre into a specific orientation (referred to by them as "steric coupling")[56]. This argument was extended by Wand *et al*[57] who attempted to predict the conformation of the molecular subunit containing the chiral centre by considering the most probable conformation of the entire molecule in the smectic C* phase (the so-called "binding site" approach). The predictions are then justified by way of assuming a "steric coupling" between a lateral substituent on the core and one on the chiral centre along the lines of the work by the Japanese workers. Other workers suggested that the introduction of a hydroxyl substituent *ortho* to the chiral chain could engage in hydrogen bonding with eg. a carbonyl group in the chain, which could have the same effect[13]. However, care has to be exercised when assuming that the conformation that appears to be the most likely for the section containing the chiral centre, is the predominant one, simply in order to justify the magnitude of the spontaneous polarisation.

In this work, for the first time, a significant dipole - dipole interaction is shown to exist between the core and the chiral centre of compound **38** (chapter 6) by way of experiment. More specifically, in this chapter it is shown that when the two nuclei concerned are fluorines, such a dipolar interaction also appears to exist between *meta* - F_3 on the core and F_4, although it is significantly smaller than the measured interaction between *ortho* - F_3 and F_4. The interaction is observed in both the smectic A and smectic C* phases.

7.4.4 ^{19}F nmr linewidths

In the cholesteric phases of both compounds **50** and **53** a slow exchange (on the nmr time scale) takes place between different "sites", which causes the observation of broad peaks for F_1, F_2 and F_3. The peak of F_4 remains sharp due a larger degree of movement of the chain and the resulting rapid exchange between different possible environments. In the smectic A phase of both **50** and **53** and the smectic C* phase of **50** the aromatic core finds itself in a fairly uniform and stable environment. The chains become motionally restricted (a slower exchange between different "sites") as is obvious from the gradual broadening of the peak of F_4. In the smectic A phase of **53** the F_4 resonance becomes very broad and a slow exchange situation is reached at 331 K.

It would only be possible to obtain further information in this regard by recording the spectra at different field strengths.

Digitised by the Department of Library Services in support of open access to information, University of Pretoria, 2021.

UNIVERSITEIT VAN PRETORIA
UNIVERSITY OF PRETORIA
YUNIBESITHI YA PRETORIA

7.5 Summary and conclusion

The properties of two liquid crystals with identical core structures, but different chiral chains, were investigated. ^{19}F nmr spectra were obtained of the compounds in their isotropic and liquid crystalline states. The 2',3 - difluorobiphenyl unit, which appears to be instrumental in the conferment of the mesomorphic properties of these compounds, was studied more closely. An attempt was made to explain the apparent ability of this unit to discourage or even prevent the formation of helical structures and thereby to justify the helix inversion observed in the smectic C* phase of one of the compounds. Some comparisons are drawn between these compounds and published compounds with related structures.

The apparent dipolar interaction between *meta* - F_3 on the core and F_4 as well as that between *ortho* - F_3 and F_4 (chapter 6) are discussed in terms of earlier suggestions by other workers that such an interaction does exist and that it appears to be the reason for an increase in the spontaneous polarization of ferroelectric compounds.

---- # ----

Digitised by the Department of Library Services in support of open access to information, University of Pretoria, 2021.

UNIVERSITEIT VAN PRETORIA
UNIVERSITY OF PRETORIA
YUNIBESITHI YA PRETORIA

CHAPTER 8

CONCLUDING REMARKS

Several of the initial objectives of the project were achieved and it was particularly rewarding to use a combination of widely differing techniques to this effect. The most significant aspects are summarised here.

(1) All the new liquid crystals, with a single exception, have the desired thermally stable smectic C* phase.

(2) The number and position of the lateral aromatic fluoro-substituents is found to greatly influence the incidence and range of the liquid crystalline phases. In particular, the presence of the 2,3 - difluorophenyl unit leads to stabilisation of the cholesteric phase, but at the same time suppresses the formation of the smectic A phase. In contrast to this, the 2',3 - difluorobiphenyl unit seems to discourage the formation of helical structures.

(3) One of the compounds undergoes an inversion of its cholesteric helix. This phenomenon could not be explained in terms of the conventional model of competing conformer species due to significant structural differences between this compound and those for which the phenomenon had previously been observed. Instead it is suggested that the competing conformer species are created through an interaction between fluoro-substituents on the core and at the chiral centre.

(4) Of particular interest is the influence exerted by the lateral fluoro-substituents on the ferroelectric properties. Two of the compounds exhibit unusual tilt angle behaviour in the smectic C* phase - the tilt angle decreases with decreasing temperature and is the reverse of the normally expected behaviour. A helix inversion takes place in the smectic C* phase of one of the esters. It is thought to be a consequence of the presence of the 2', 3 - difluorobiphenyl unit which seems to have a disruptive influence on helical structures.

(5) Particularly challenging was the development of an instrumental technique in order to be able to measure ^{19}F nmr spectra of liquid crystals. It became clear that ^{19}F nmr is a powerful technique with which to study liquid crystals as it is considerably more sensitive to changes in the molecular environment than ^{13}C nmr.

Digitised by the Department of Library Services in support of open access to information, University of Pretoria, 2021.

(6) The importance of achieving a good alignment of the molecules when attempting the acquisition of nmr spectra manifested itself throughout. In this regard a precedent cholesteric phase seems to be crucial in order to obtain satisfactory spectra of the smectic phases.

(7) ^{19}F nmr was found useful for the determination of the orientational order of a liquid crystal, by way of observing the dipolar coupling as a function of temperature.

(8) The apparent phenomenon of steric interaction between a proximate lateral dipole on the core and at the chiral centre was probed using nmr. For the first time it could be shown, by measurement of the dipolar coupling between two fluoro-substituents using ^{19}F nmr, that such an interaction does exist. Support for this result was obtained from conformational analysis of the molecular subunit containing the chiral centre, which also revealed the existence of a transverse electrostatic gradient across this subunit.

In short, the work carried out for this project furthers the understanding of the orientational behaviour of liquid crystals and it supplements the available data concerning the relationship between molecular structure and liquid crystalline properties. Possibly for the first time a combination of microscopic and macroscopic techniques was used to investigate these properties. In addition it is possible that some of the compounds can prove useful for conveying certain properties to mixtures for use in ferroelectric display devices.

---- # ----

Digitised by the Department of Library Services in support of open access to information, University of Pretoria, 2021.

UNIVERSITEIT VAN PRETORIA
UNIVERSITY OF PRETORIA
YUNIBESITHI YA PRETORIA

APPENDIX A

FLUORINE-19 CHEMICAL SHIFTS AND COUPLING CONSTANTS

Listed in this appendix are the solution chemical shifts and scalar coupling constants of the ^{19}F nuclei of selected fluorinated precursory compounds and liquid crystals prepared in this work.

^{19}F chemical shifts and ^{19}F - ^{19}F coupling constants (especially aromatic) have been studied extensively and the work has been summarised in two volumes[136,137]. The ^{19}F nucleus has a wide chemical shift range of over 1000 ppm and is consequently extremely sensitive to its molecular environment. This is quite obvious from the results shown below. The aromatic fluorines resonate in the range -100 to -170 ppm depending on the proximity of other ^{19}F nuclei. Also given is the vicinal coupling constant originating from the 2,3-difluorophenyl group. The fluorine on the chiral chain resonates between -185 and -197 ppm depending on whether the chiral centre is linked to the core *via* an ester or an ether group and also on whether the lone phenyl ring is fluorinated or not.

Experimentally the spectra of the compounds were obtained in isotropic solution (approx. 10 mg / ml $CDCl_3$) and are externally referenced against $CFCl_3$. Some of the phenols (indicated by *) have a low solubility in chloroform and they were measured in DMSO-d_6.

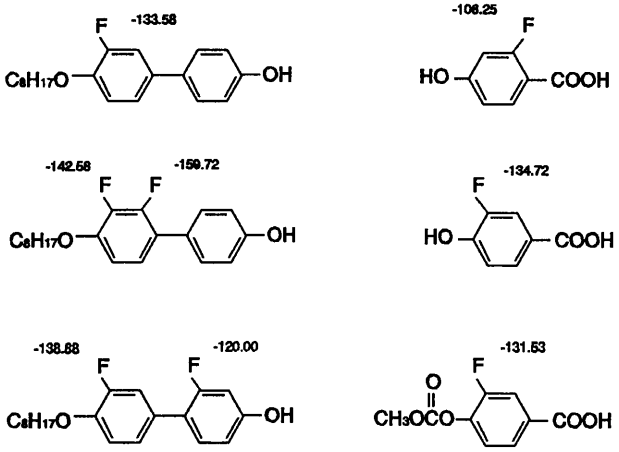

Digitised by the Department of Library Services in support of open access to information, University of Pretoria, 2021.

UNIVERSITEIT VAN PRETORIA
UNIVERSITY OF PRETORIA
YUNIBESITHI YA PRETORIA

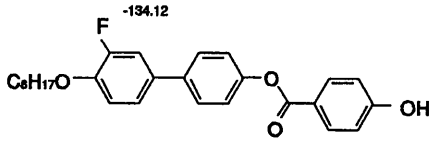

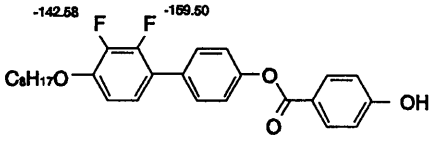

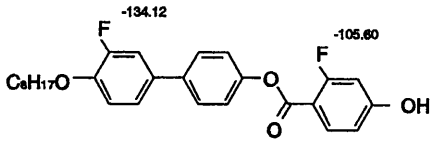

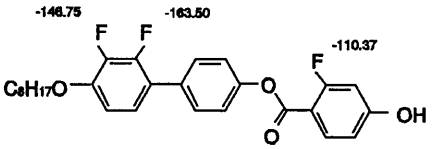

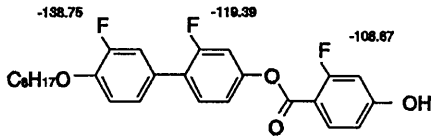

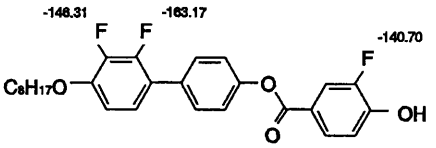

*

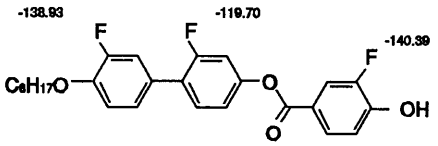

*

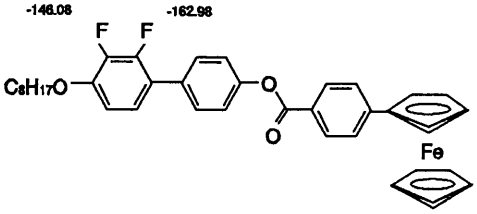

Digitised by the Department of Library Services in support of open access to information, University of Pretoria, 2021.

UNIVERSITEIT VAN PRETORIA
UNIVERSITY OF PRETORIA
YUNIBESITHI YA PRETORIA

34 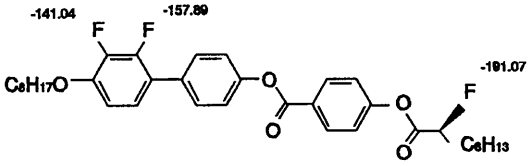

J = 19.8 Hz

35 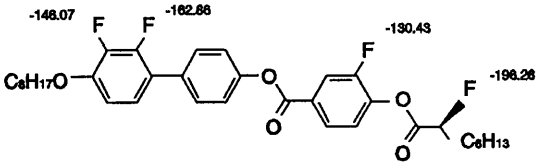

J = 16.9 Hz

36 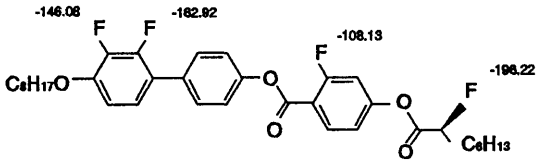

J = 19.6 Hz

37 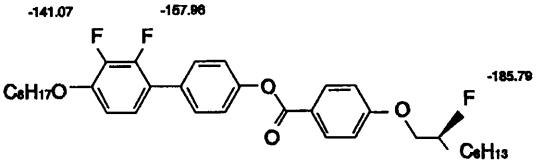

J = 19.4 Hz

38 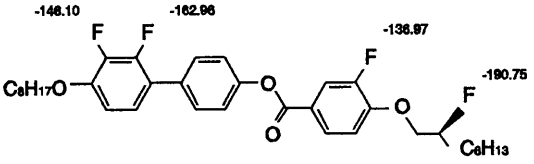

J = 20.1 Hz

39 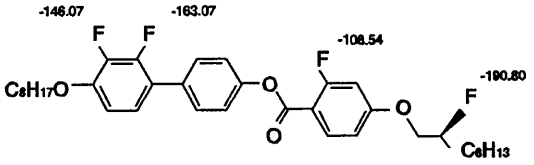

J = 20.3 Hz

48 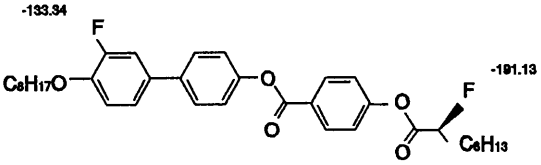

49 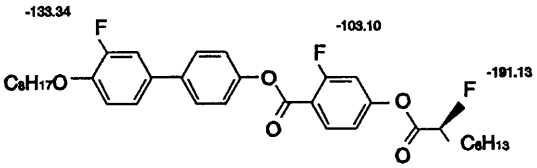

50 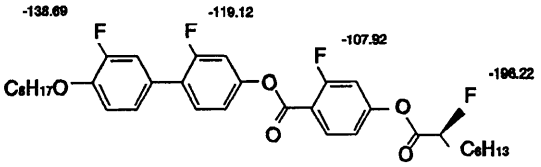

Digitised by the Department of Library Services in support of open access to information, University of Pretoria, 2021.

UNIVERSITEIT VAN PRETORIA
UNIVERSITY OF PRETORIA
YUNIBESITHI YA PRETORIA

51 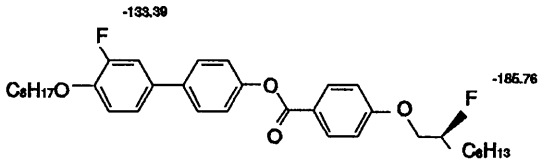

52 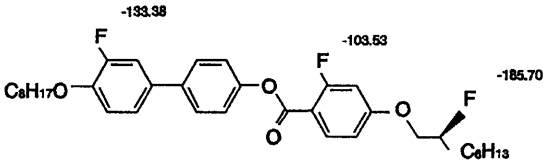

53 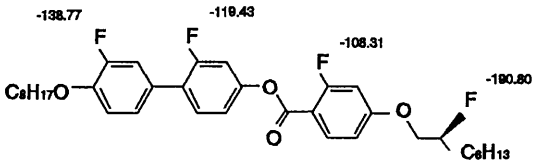

54 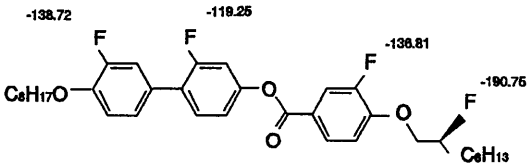

55 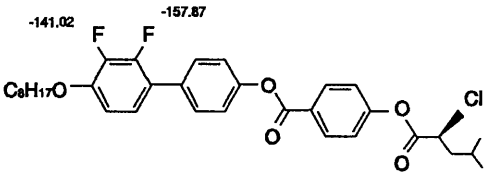

J = 18.7 Hz

---- # ----

Digitised by the Department of Library Services in support of open access to information, University of Pretoria, 2021.

UNIVERSITEIT VAN PRETORIA
UNIVERSITY OF PRETORIA
YUNIBESITHI YA PRETORIA

REFERENCES

1. R.B. Meyer, L.Liebert, L. Strzelecki and P. Keller; *J. Phys. Lett. (Paris)* **36** (1975) 69.
2. N.A. Clark and S.T. Lagerwall; *Appl. Phys. Lett.* **36** (1980) 899.
3. J.W. Goodby; *Science* **231** (1986) 350.
4. J.W. Goodby and J.S. Patel; *Proc. SPIE* **684** (1986) 52.
5. G.R. Luckhurst; *Quat. Rev.* **22** (1968) 179.
6. J.W. Emsley and J.C. Lindon; *Nmr Spectroscopy Using Liquid Crystal Solvents* (Pergamon, Oxford, 1975).
7. R.D. Spence, H.A Moses and P.L. Jain; *J. Chem. Phys.* **21** (1953) 380.
8. W.D. Phillips, J.C. Rowell and L.R. Melby; *J. Chem. Phys.* **41** (1964) 2551.
9. J.C. Rowell, W.D. Phillips, L.R. Melby and M. Panar; *J. Chem. Phys.* **43** (1965) 3442.
10. A.D. Buckingham and K.A. McLauchlan; *Progr. NMR Spectrosc.* **2** (1967) 63.
11. A.G. Avent, J.W. Emsley and D.L. Turner; *J. Magn. Res.* **52** (1983) 57.
12. D. Catalano, C. Gandolfo, G.N. Shilstone and C.A. Veracini; *Liq. Cryst.* **11** (1992) 151.
13. R. Teeäär, M. Alla and E. Lippmaa; *Org. Magn. Res.* **19** (1982) 134.
14. B.M. Fung and M. Gangoda; *J. Chem. Phys.* **83** (1985) 3285.
15. P. Forster and B.M. Fung; *J. Chem. Soc. Faraday Trans. II* **84** (1988) 1083.
16. C.-D. Poon, C.M. Wooldridge and B.M. Fung; *Mol. Cryst. Liq. Cryst.* **157** (1988) 303.
17. J.S. Lewis, E. Tomchuk and E. Bock; *Mol. Cryst. Liq. Cryst.* **198** (1991) 191 and refs. therein.
18. W. Guo and B.M. Fung; *J. Chem. Phys.* **95** (1991) 3917.
19. C.J.R. Counsell, J.W.Emsley, G.R.Luckhurst and H.S. Sachdev; *Mol. Phys.* **63** (1988) 33.
20. D.J. Photinos, E.T. Samulski and H. Toriumi; *J. Chem. Phys.* **94** (1991) 2758.
21. J. Bozek, H.M. Hutton, J.S. Lewis, E. Tomchuk and E. Bock; *Mol. Cryst. Liq. Cryst.* **122** (1985) 191.
22. R.F. Bryan, A.J. Leadbetter, A.I. Mehta and P.A. Tucker; *Mol. Cryst. Liq. Cryst.* **104** (1984) 257.
23. M. Luzar, V. Rutar, J. Seliger, M. Burgar and R. Blinc; *Ferroelectrics* **24** (1980) 215.
24. M. Luzar, V. Rutar, J. Seliger and R. Blinc; *Ferroelectrics* **58** (1984) 115.
25. C.-D. Poon and B.M. Fung; *Liq. Cryst.* **5** (1989) 1159.
26. C.-D. Poon and B.M. Fung; *J. Chem. Phys.* **91** (1989) 7392.
27. W. Richter, D. Reimer, B.M. Fung, R.J. Twieg and K. Betterton; *Liq. Cryst.* **8** (1990) 687.
28. M.S. Ho, B.M. Fung, M. Wand R.T. Vohra; *Ferroelectrics* **138** (1993) 51.
29. A. Yoshizawa, H. Kikuzaki, T. Hirai and M. Yamane; *Jpn. J. Appl. Phys.* **28** (1989) L1988.
30. A. Yoshizawa, H. Kikuzaki, T. Hirai and M. Yamane; *Jpn. J. Appl. Phys.* **29** (1990) L1153.
31. A. Yoshizawa, I. Nishiyama, H. Kikuzaki and N. Ise; *Jpn. J. Appl. Phys.* **31** (1992) L860.
32. A. Yoshizawa, A. Yokoyama, H. Kikuzaki and T. Hirai; *Liq. Cryst.* **14** (1993) 513.

Digitised by the Department of Library Services in support of open access to information, University of Pretoria, 2021.

UNIVERSITEIT VAN PRETORIA
UNIVERSITY OF PRETORIA
YUNIBESITHI YA PRETORIA

33. A.G. Avent, J.W. Emsley and G.R. Luckhurst; *Mol. Phys.* **49** (1983) 737.
34. G.W. Gray; *Mol. Cryst. Liq. Cryst.* **1** (1966) 333.
35. J. Mann; *Chem. Soc. Rev.* **16** (1987) 381.
36. M.R.C. Gerstenberger and A. Haas; *Angew. Chem. Int. Ed. Eng.* **20** (1981) 647.
37. P. Balkwill, D. Bishop, A. Pearson and I. Sage; *Mol. Cryst. Liq. Cryst.* **123** (1985) 57.
38. S.M. Kelly and Hp. Schad; Helv. Chim. Acta **68** (1985) 1444.
39. R. Eidenschink; *Mol. Cryst. Liq. Cryst.* **123** (1985) 57.
40. L.K.M. Chan, G.W. Gray, D. Lacey and K.J. Toyne; *Mol. Cryst. Liq. Cryst.* **158B** (1988) 209.
41. K.J. Toyne in *Thermotropic Liquid Crystals*, ed. G.W. Gray (Wiley, Chichester, 1987).
42. G.W. Gray, M. Hird, D. Lacey and K.J. Toyne; *J. Chem. Soc. Perkin Trans. 2* (1989) 2041.
43. G.W. Gray, M.Hird and K.J. Toyne; *Mol. Cryst. Liq. Cryst.* **195** (1991) 221.
44. M. Hird, G.W. Gray and K.J. Toyne; *Liq. Cryst.* **11** (1992) 531.
45. G.W. Gray, M. Hird and K.J. Toyne; *Mol. Cryst. Liq. Cryst.* **204** (1991) 43.
46. D.M. Walba and N.A. Clark; *Ferroelectrics* **84** (1988) 65.
47. K. Yoshino, M. Ozaki, H. Taniguchi, M. Ito, K. Satoh, N. Yamasaki and T. Kitazume; *Jpn. J. Appl. Phys.* **26** (1987) L77.
48. J. Bömelburg, G. Heppke and A. Ranft; *Z. Naturforsch.* **44B** (1989) 1127.
49. N. Shiratori, I. Nishiyama, A. Yoshizawa and T. Hirai; *Jpn. J. Appl. Phys.* **29** (1990) L2086.
50. N. Shiratori, A. Yoshizawa, I. Nishiyama, M. Fukumasa, A. Yokoyama, T. Hirai and M. Yamane; *Mol. Cryst. Liq. Cryst.* **199** (1991) 129.
51. D.M. Walba, H.A. Razavi, A. Horiuchi, K.F. Eidman, B. Otterholm, R.C. Haltiwanger, N.A. Clark, R. Shao, D.S. Parmar, M.D. Wand and R.T. Vohra; *Ferroelectrics* **113** (1991) 21.
52. R. Buchecker, S.M. Kelly, J. Fünfschilling; *Liq. Cryst.* **8** (1990) 217.
53. H. Nohira, S. Nakamura and M. Kamei; *Mol. Cryst. Liq. Cryst.* **180B** (1990) 379.
54. S. Nakamura and H. Nohira; *Mol. Cryst. Liq. Cryst.* **185** (1990) 199.
55. H. Nohira; *J. Syn. Org. Chem. Jpn.* **49** (1991) 467.
56. K. Furakawa, K. Terashima, M. Ichihashi, S. Saitoh, K. Miyazawa and T. Inukai; *Ferroelectrics* **85** (1988) 451.
57. M.D. Wand, R.T. Vohra, D.M. Walba, N.A. Clark and R. Shao; *Mol. Cryst. Liq. Cryst.* **202** (1991) 183.
58. C.J. Booth; Lecture O2 presented at the British Liquid Crystal Society Annual Conference, Manchester 29 - 31 March 1993.
59. J.W. Goodby, R. Blinc, N.A. Clark, S.T. Lagerwall, M.A. Osipov, S.A. Pikin, T. Sakurai, K. Yoshino and B. Zeks; *Ferroelectric Liquid Crystals* (Gordon and Breach, Philadelphia, 1991).
60. F. Tournilhac, L.M. Blinov, J. Simon and S.V. Yablonsky; *Nature* **359** (1992) 621.
61. D.R. Coulson; *Inorg. Synth.* **13** (1972) 121.
62. S.M. Kelly; *Helv. Chim. Acta* **67** (1984) 1578.

Digitised by the Department of Library Services in support of open access to information, University of Pretoria, 2021.

UNIVERSITEIT VAN PRETORIA
UNIVERSITY OF PRETORIA
YUNIBESITHI YA PRETORIA

63. M.F. Nabor, H.T. Nguyen, C. Destrade, J.P. Marcerou and R.J. Twieg; *Liq. Cryst.* **10** (1991) 785.
64. E. Chin and J.W. Goodby; *Mol. Cryst. Liq. Cryst.* **141** (1986) 311.
65. V. Reiffenrath, J. Krause, H.J. Plach and G. Weber; *Liq. Cryst.* **5** (1989) 159.
66. H. Gilman and T.S. Soddy; *J. Org. Chem.* **22** (1957) 1715.
67. P. Fitton and E.A. Rick; *J. Organomet. Chem.* **28** (1971) 287.
68. A. Gillie and J.K. Stille; *J. Am. Chem. Soc.* **102** (1980) 4933.
69. O. Mitsunobu; *Synthesis* (1981) 1.
70. B. Neises and W. Steglich; *Angew. Chem. Int. Ed. Eng.* **17** (1978) 522.
71. H. Suzuki, A. Kondo, M. Inouye and T. Ogawa; *Synthesis* (1986) 121.
72. M.A. Waugh, S.M. Stein, E.Chin and J.W. Goodby; *Liq. Cryst.* **11** (1992) 135.
73. A. Bouchta, H.T. Nguyen, M.F. Achard, F. Hardouin, C. Destrade, R.J. Twieg, A. Maaroufi and N. Isaert; *Liq. Cryst.* **12** (1992) 575.
74. H. Sackmann and D. Demus; *Mol. Cryst. Liq. Cryst.* **2** (1966) 81.
75. G.W. Gray and J.W. Goodby; *Smectic Liquid Crystals* (Leonard Hill, Glasgow, 1984).
76. A.J. Slaney; PhD dissertation, University of Hull (UK), 1992.
77. Ch. Bahr, C. Escher, D. Fliegner, G. Heppke and H. Molsen; *Ber. Bunsenges. Phys. Chem.* **95** (1991) 1233.
78. M. Chambers, R. Clemitson, D. Coates, S. Greenfield, J.A. Jenner and I.C. Sage; *Liq. Cryst.* **5** (1989) 153.
79. Ch. Bahr and G. Heppke; *Mol. Cryst. Liq. Cryst.* **4** (1986) 31.
80. D.S. Parmar, N.A. Clark, D.M. Walba and M.D. Wand; *Phys. Rev. Lett.* **62** (1989) 2136.
81. G. Heppke, D. Lötzch and R. Shashidhar; *Liq. Cryst.* **3** (1988) 489.
82. J. Suermann and U.Finkenzeller; Poster FM - 1 presented at the *European Conference on Liquid Crystal Science and Technology* , **ECLC 93**, Flims, Switzerland, March 1993.
83. J.W. Goodby, M.A. Waugh, S.M. Stein, E. Chin, R. Pindak and J.S. Patel; *Nature* **337** (1989) 449.
84. P.P. Crooker; *Liq. Cryst.* **5** (1989) 751.
85. T. Seideman; *Rep. Prog. Phys.* **53** (1990) 659.
86. J. Thoen; *Phys. Rev. A* **37** (1988) 1754.
87. D. Demus, H.G. Hahn and F. Kuschel; *Mol. Cryst. Liq. Cryst.* **44** (1978) 61.
88. J.S. Patel and J.W. Goodby; *Mol. Cryst. Liq. Cryst.* **144** (1987) 117.
89. H. Diamant, K. Drenck and R. Pepinsky; *Rev. Sci. Instr.* **28** (1957) 30.
90. S. Garoff and R.B. Meyer; *Phys. Rev. Lett.* **38** (1977) 848.
91. Ch. Bahr, G. Heppke and U. Klemke; *Ber. Bunsenges. Phys. Chem.* **95** (1991) 761.
92. J.W. Goodby, E. Chin, J.M. Geary, J.S. Patel and P.L. Finn; *J. Chem. Soc. Faraday Trans. I* **83** (1987) 3429.

Digitised by the Department of Library Services in support of open access to information, University of Pretoria, 2021.

UNIVERSITEIT VAN PRETORIA
UNIVERSITY OF PRETORIA
YUNIBESITHI YA PRETORIA

93. J.S. Patel and J.W. Goodby; *Phil. Mag. Lett.* **55** (1987) 283.

94. A.J. Slaney, I. Nishiyama, P. Styring and J.W. Goodby; *J. Mater. Chem.* **2** (1992) 805.

95. A.J. Slaney, unpublished results.

96. P. Styring, J.D. Vuijk, I. Nishiyama, A.J. Slaney and J.W. Goodby; *J. Mater. Chem.* **3** (1993) 399.

97. I. Dierking, F. Giesselmann, P. Zugenmaier, W. Kuczynski, S.T. Lagerwall and B. Stebler; *Liq. Cryst.* **13** (1993) 45.

98. C. Loubser, P.L. Wessels, P. Styring and J.W. Goodby; *J. Mater. Chem.*, accepted for publication.

99. J.W. Goodby, E. Chin, T.M. Leslie, J.M. Geary and J.S. Patel; *J. Am. Chem. Soc.* **108** (1986) 4729.

100. J.W. Goodby and T.M. Leslie; *Mol. Cryst. Liq. Cryst.* **110** (1984) 175.

101. J.W. Goodby and T.M. Leslie in *Liquid Crystals and Ordered Fluids*, vol. 4, eds. A.C. Griffin and J.F. Johnson (Plennum, New York, 1984).

102. K. Yoshino, M. Ozaki, T. Sakurai, M. Honma and K. Sakamoto; *Jpn. J. Appl. Phys.* **23** (1984) L175.

103. J.W. Goodby, J.S.Patel and E.Chin; *J. Phys. Chem. Lett.* **91** (1987) 5838.

104. R. Bartolino, J. Doucet and G. Durand; *Ann. Phys.* **3** (1978) 389.

105. E.L. Eliel; *Stereochemistry of Carbon Compounds* (McGraw-Hill, New York, 1962).

106. C. Loubser, P.L. Wessels, J.W. Goodby and P. Styring; *Liq. Cryst.* **15** (1993), in press.

107. B.M. Fung; *J. Magn. Res.* **86** (1990) 160.

108. A.J. Shaka, J. Keeler and R. Freeman; *J. Magn. Res.* **53** (1983) 313.

109. R.K. Harris and P.Jackson; *Chem. Rev.* **91** (1991) 1427.

110. P. Diehl and C.L. Khetrapal in *Nmr. Basic Principles and Progress,* vol. 1 (Springer Verlag, Berlin, 1969).

111. G.J. den Otter and C. Maclean; *Chem. Phys.* **3** (1974) 119.

112. G.J. den Otter, W. Heijser and C. Maclean; *J. Magn. Res.* **11** (1974) 13.

113. G.J. den Otter and C. Maclean; *J. Mol. Struct.* **31** (1976) 57.

114. C. Loubser, C. Imrie and P.H. van Rooyen*; Adv. Mater.* **5** (1993) 45.

115. M. Clark, R.D. Cramer III and Van Opdenbosch; *J. Comput. Chem.* **10** (1989) 982.

116. J. Gasteiger and M. Marsili; *Tetrahedron* **36** (1980) 3219.

117. D. Mayer, C.B. Naylor, I. Motoc and G.R. Marshall; *J. Computer-aided Mol. Design* **1** (1987) 3.

118. R. Blinc, M. Čopič, I. Drevenšek, A. Levstik, I. Muševič and B. Žekš; *Ferroelectrics* **113** (1991) 59.

119. Z. Luz and Y.S. Meiboom; *J. Chem. Phys.* **59** (1973) 275.

120. J.W. Emsley and G.R. Luckhurst; *Mol. Phys.* **41** (1980) 19.

Digitised by the Department of Library Services in support of open access to information, University of Pretoria, 2021.

UNIVERSITEIT VAN PRETORIA
UNIVERSITY OF PRETORIA
YUNIBESITHI YA PRETORIA

121. M.A. Osman; *Mol. Cryst. Liq. Cryst.* **128** (1985) 45.

122. G.R. Luckhurst; Personal communication, 9 March 1993.

123. A. Hargreaves and S. Hasan - Rizvi; *Acta Cryst.* **15** (1962) 365.

124. A. d' Annibale, L. Lunazzi, A.C. Boicelli and D. Macciantelli; *J. Chem. Soc. Perkin Trans. II (1973) 1396.*

125. L.D. Field and S. Sternhell; J. Am. Chem. Soc. **103** (1981) 738.

126. C. Vauchier, F. Vinet and N. Maiser; *Liq. Cryst.* **5** (1989) 141.

127. M.A. Osman; *Z. Naturforschung* **38A** (1983) 693.

128. S.J. Heyes, C.M. Dobson, J.E. Taguchi, D.W. Bruce and R. Dhillon; Lecture **O18** presented at the Annual Conference of the British Liquid Crystal Society, Manchester, 29 - 31 March 1993.

129. H.W. Spiess; *Chem. Rev.* **91** (1991) 1320.

130. B. Linström, H. Kresse, D. Demus, C. Tschierske and D. Joachimi; *Ferroelectrics* **120** (1991) 225.

131. N. Shiratori, A. Yoshizawa, I. Nishiyama, M. Fukumasa, A. Yokoyama, T. Hirai and M. Yamane; *Mol. Cryst. Liq. Cryst.* **199** (1991) 129.

132. T. Inukai, S. Saitoh, H. Inoue, K. Miyazawa, K. Terashima and K. Furukawa; *Mol. Cryst. Liq. Cryst.* **141** (1986) 251.

133. K. Yoshino, H. Taniguchi, M. Ozaki; *Ferroelectrics* **91** (1989) 267.

134. C.K. Johnson, ORTEP. Report ORNL - 3794. Oak Ridge National Laboratory, 1965.

135. G. Celebre, M. Longeri, E. Cicilia and J.W. Emsley; *Liq. Cryst.* **7** (1990) 731.

136. J.W. Emsley and L. Phillips; *Progr. NMR Spectrosc.* **7** (1971) 1.

137. J.W. Emsley, L. Phillips and V. Wray; *Progr. NMR Spectrosc.* **10** (1976) 83.

Digitised by the Department of Library Services in support of open access to information, University of Pretoria, 2021.